

# **Isolation and characterization of a novel *Shigella* bacteriophage by electron microscopy**

**Thesis submitted for the degree of  
Doctor of Philosophy (Science)  
at  
Department of Life Science and Bio-technology  
Jadavpur University  
2023**



**Bani Mallick, M.Sc.**

**Index No: 117/19/Life Sc./26**

**Registration No: SLSBT1211719**

**Division of Electron Microscopy  
ICMR-National Institute of Cholera and Enteric Diseases  
P-33 C.I.T. Road, Scheme-XM,  
Beliaghata, Kolkata-700010**



**icmr**  
INDIAN COUNCIL OF  
MEDICAL RESEARCH

**NICED**  
NATIONAL INSTITUTE OF  
CHOLERA AND ENTERIC DISEASES

आई. सी. एम. आर. – राष्ट्रीय कॉलरा और आंत्र रोग संस्थान  
ICMR - NATIONAL INSTITUTE OF CHOLERA AND ENTERIC DISEASES  
स्वास्थ्य अनुसंधान विभाग, स्वास्थ्य और परिवार कल्याण मंत्रालय, भारत सरकार  
Department of Health Research, Ministry of Health and Family Welfare, Govt. of India

WHO COLLABORATING CENTRE FOR RESEARCH AND TRAINING ON DIARRHOEAL DISEASES

## CERTIFICATE FROM THE SUPERVISOR

This is to certify that the thesis entitled “**Isolation and characterization of a novel *Shigella* bacteriophage by electron microscopy**” submitted by **Smt. Bani Mallick** who got her name registered on 17.10.2019 for the award of **Ph.D. (Science)** degree of **Jadavpur University**, is absolutely based upon her own work under the supervision of **Dr. Moumita Dutta** and that neither this thesis nor any part of it has been submitted for either any degree/diploma or any other academic award anywhere before.

*Moumita Dutta* 18-08-2023

(Signature of the Supervisor date with official seal)

डा. मोमिता दत्ता / Dr. Moumita Dutta  
वैज्ञानिक-सी / Scientist-C  
आईसीएमआर-राष्ट्रीय कॉलरा और आंत्र रोग संस्थान  
ICMR-National Institute of Cholera and Enteric Diseases  
कोलकाता-700 010 / Kolkata-700 010

पी-३३, सी.आई.टी. रोड, स्किम - १०एम, बेलियाघाटा, कोलकाता - ७०००१०, भारत

P-33, C.I.T. Road, Scheme - XM, Beliaghata, Kolkata - 700010, India

निदेशक/ Director : 91-33-2363 3373, 2370 1176, पि.बि.एक्स / PBX : 91-33-2353 7469 / 7470, 2370 5533 / 4478 / 0448

फैक्स / Fax : 91-33-2363 2398, 2370-5066, वेब / Website : www.niced.org.in

## Declaration

I hereby declare that the research work embodied in the thesis entitled as “**Isolation and characterization of a novel *Shigella* bacteriophage by electron microscopy**” is carried out by me at **ICMR- National Institute of Cholera and Enteric Diseases, Kolkata, India** under the supervision of **Dr. Moumita Dutta, Scientist-D, Division of Electron Microscopy**. This work is original and not submitted in part or full for any degree or diploma to this or any other university. All ideas and references are duly acknowledged.

Date 18.08.2023

Bani Mallick

Bani Mallick



**THIS THESIS IS DEDICATED TO  
MY BELOVED PARENTS**

**Who taught me the value of humanity, empathy, and kindness**



## ACKNOWLEDGMENTS

*As I stand on the doorstep of completing my doctoral work, I take this special moment to express my sincere appreciation for all those people who have contributed substantially in making this dissertation take its present shape and have made it an unforgettable experience for me.*

*At the very outset, I would like to express my deepest gratitude to Dr. Moumita Dutta, my research supervisor for giving me the opportunity to pursue my Ph.D. career and giving me the required freedom to think and implement my ideas. Her patience, flexibility, genuine caring, concern, and faith in my ability inspired and motivated me. I revere her as a scientist and take pride in being associated with such a wonderful person during this phase of my career from whom I learned a lot not only about science but also the way of life. She has provided me with all her support and encouragement whenever needed and has taught me the intricacies of research life with great patience, guiding me always to keep focus. For this, I cannot thank her enough. I forever remain grateful to her.*

*I deeply acknowledge Dr. Shanta Dutta, Director of ICMR-National Institute of Cholera and Enteric Diseases for granting me the privilege to continue my work in this esteemed institute.*

*My sincere thank goes to Dr. Amar Nath Ghosh, Retired Scientist, Division of Electron Microscopy, ICMR-NICED, Kolkata for his valuable suggestions for my work.*

*I gratefully acknowledge Dr. Hemanta Koley, Scientist- F, ICMR- NICED, Kolkata, and Dr. Asish Kumar Mukhopadhyay Scientist- F, ICMR-NICED, Kolkata for providing bacterial strains for my work.*

*I wish to acknowledge Dr. Somnath Dutta, Associate Professor of the Molecular Biophysics Unit, IISC, Bangalore for his immense help in the structural work of my thesis through data collection in their national facility.*

*I would like to thank Dr. Jayati Sengupta, Senior Principal Scientist, IICB, Kolkata, for her valuable advice throughout my thesis work.*

*I also want to thank Dr. Parimal Karmakar, Head of Department (HOD), Department of Life Science and Biotechnology, Jadavpur University, for allowing my Ph.D. registration in the*

*department. I would also like to thank other faculty members of Jadavpur University for their useful lectures and advice throughout my Ph.D. coursework.*

*This work also bears the support and constant help of my seniors, friends, and other members of the EM division, NICED. Among them, I express my heartfelt thanks to departmental senior Dr. Sayani Das, and my lab mates Ms. Payel Mondal and Mr. Aninda Dutta. Words cannot be expressed to convey my heartiest appreciation for having a friend like Payel. Right from the beginning of my research carrier, she has been helping me in every possible aspect, cheering me up in every odd and enjoying with me for every success. I also want to thank staff members of the EM division Mrs. Arpita Sarbjna, TO-C and Mr. Bivash Ranjan Mallick, Lab attendant-2 for their continuous help and support.*

*I am also thankful to many other research fellows at NICED mainly Mrs. Suparna Chakraborty, Mr. Sanjib Kumar Sardar, Mr. Bipul Chandra Karmakar, Dr. Suhrid Maiti, Dr. Suman Das, Dr. Debjyoti Bhakat, Indranil Mondal, Dr. Mainak Chakraborty, Dr. Deotima Sarkar, Ms. Sangita Paul, Ms. Puja Bose, Ms. Ajanta Ghosal, Mr. Tapas Haldar, Mr. Prolay Halder, Mr. Soumalya Banerjee, Mr. Sanjib Das, Mrs. Amrita Bhattacharjee, Mr. Gourab Halder, Ms. Sunayana Saren, Ms. Priyanka Basak, Mrs. Priya Verma, Mr. Sagnik Bakshi, Ms. Raina Das, Ms. Upasana Baskey, Ms. Risha Haldar, Mr. Niraj Nag, Ms. Uzma Khan for their selfless encouragement and support which helped to overcome the tough times during my work.*

*I would like to thank the University Grant Commission, Govt of India for granting me a research fellowship and I am also thankful to the Indian Council of Medical Research and NICED for the support with institutional funding of my thesis project.*

*It is very difficult to express my heartiest thanks to my parents in words. Their unconditional love, care, advice, faith, and indescribable support to me throughout during my professional journey so far are invaluable. My father Mr. Rathin Mallick always supported me in all my decisions and my mother Mrs. Ranjita Mallick always encouraged me to choose research as my career and always supported me emotionally in my tough times. I am very grateful for their understanding, positive stimulation, and trust in me during pursuing my doctoral thesis work. I am deeply thankful to my brother Mr. Pradip Mallick for all his love and support. I am also thankful to all my other family members for always believing in me.*

*This last word of acknowledgment I have saved for two of my very good friends Dr. Pritha Ghosh and Ms. Ankita Mukherjee. Without their constant help, encouragement, support, and patience I would have not been able to complete my doctoral study.*

*I would like to thank all my teachers in school, college, and university who have allowed me to grow and learn with them.*

*Undoubtedly no task can be accomplished without the blessing of “God” the Almighty. Whatever I am today it is all because of ‘His’ blessings.*

*Finally, I would like to thank many others who were important to the successful realization of my Ph.D. thesis, as well as express my apology that I could not mention them personally.*

*Thank you all once again!!!!*

*Bani Mallick*

**Index No.:** 117/19/Life Sc./26

**Thesis Title:** Isolation and characterization of a novel *Shigella* bacteriophage by electron microscopy

---

---

### ABSTRACT

Enteric disease such as Shigellosis is one of the leading causes of morbidity and mortality worldwide. The increased prevalence of multidrug-resistant *Shigella* spp. has revived the importance of bacteriophages as an alternative therapy to antibiotics. Based on the bactericidal properties of lytic bacteriophages, they are considered potential biocontrol and therapeutic agents. Therefore, phage research involving isolation, characterization, and applications has recently significantly increased.

In this study, a *Shigella* bacteriophage Sfk20 was isolated from the lake water of the diarrheal outbreak area of Kolkata and found to be a novel lytic phage with promising potential against the host bacteria *Shigella flexneri* 2a. The morphological study (transmission electron microscopy and scanning electron microscopy) revealed that the bacteriophage had a prolate head and a long contractile tail indicating a member of the *Myoviridae* family. Phage Sfk20 showed infectivity against *Shigella flexneri*, *Shigella sonnei*, *Shigella dysenteriae* 1, and two non-typhoidal *Salmonella* strains. The one-step growth curve study of Sfk20 revealed a latent period (20 mins) and large burst size (123 pfu per infected cell). Phage Sfk20 showed high stability at a 4-37°C temperature range and a pH range of 7-9. A study on phage stability conducted at different salinity revealed phage Sfk20 remains active within 0-5% salt concentration. A study on understanding the nature of the phage Sfk20 host receptor suggested that the outer membrane LPS of the *Shigella flexneri* 2a acts as a receptor for the phage Sfk20. The bacteriolytic activity of phage Sfk20 study at various MOI showed that the growth of the host bacteria became restricted at high MOI. The whole-genome sequencing study revealed that the bacteriophage Sfk20 contains a linear double-stranded genome consisting of 164878 bp, 35.62% G+C content 241 ORF, and ten tRNA. The genomic analysis also confirmed the presence of lytic genes and the absence of lysogeny, virulent genes, and toxic genes. The comparative genomic study and phylogenetic analysis suggested that phage Sfk20 belongs to the family of *Myoviridae*. Using the LC-MS/MS technique in proteomic analysis, around 40 Sfk20 phage proteins were detected and identified, which helped to understand the structural landscape of phage Sfk20. The structural characterization of the phage Sfk20 was carried out using single-particle cryo-electron microscopy and image processing and the structure of the phage proteins was predicted using deep learning and homology-based approaches. The structural characterization of phage and its proteins further expands our knowledge of phage biology. The attachment of the phage particle to its host and subsequent intracellular development of phage and host cell lysis were visualized in a time-dependent experiment using thin-section transmission electron microscopy (FEI Tecnai 12 BioTwin) and scanning electron microscopy (FEI Quanta 200). This study further confirmed the lytic cycle of phage Sfk20. Bacteriophage Sfk20 showed antibiofilm activity against *Shigella* bacteria alone and in combination with ampicillin. The synergistic effect of Sfk20 and ampicillin on the removal of biofilm was observed by scanning electron microscopy. The efficiency of the phage cocktail was confirmed based on the ability to remove the biofilm. The result of this study implies that Sfk20 has the potential to work as a biocontrol agent and phage therapy candidate.

Bani Mallik 18.08.2023  
Signature of Candidate

Moumita Dutta 18-08-2023  
Signature of Supervisor

डॉ: मोमिता दत्ता / Dr. Moumita Dutta  
वैज्ञानिक-सी / Scientist-C  
आईसिएमआर-राष्ट्रीय कोलरा और आंत्र रोग संस्थान  
ICMR-National Institute of Cholera and Enteric Diseases  
कोलकाता-700 010 / Kolkata-700 010

---

# TABLE OF CONTENTS

---

Preface	i-ii
Symbols and abbreviations	iii-iv
List of figures	v-ix
List of tables	x
 <b>CHAPTER 1: Introduction</b>	 1-3
 <b>CHAPTER 2: Review of Literature</b>	 4-48
2.1 Shigellosis	5
2.2 <i>Shigella</i> -the pathogen	5-6
2.3 Pathogenesis of <i>Shigella</i>	6-9
2.4 Shigellosis and epidemiology	9-11
2.5 Immunity development of <i>Shigella</i> infection	11-12
2.6 Treatments for shigellosis	12-16
2.6.1 Regular treatment of shigellosis	12-13
2.6.2 Current scenario of antimicrobial resistance among <i>Shigella</i> spp.	13-15
2.6.3 Development of vaccines	15-16
2.6.4 Importance of searching for an alternative treatment	16
2.7 General introduction of bacteriophages	17-21
2.7.1 Biology of bacteriophages	17
2.7.2 History of bacteriophages	18-19
2.7.3 Origin of bacteriophages	19
2.7.4 Life cycle of bacteriophages	20-21
2.8 The classification of bacteriophages	22-26
2.8.1 Morphological and structural diversity	22
2.8.2 Tailed phages	22-24
2.8.3 Membrane containing phages	25

2.8.4	Bacteriophages with small icosahedral capsids	25-26
2.8.5	Phages with filamentous morphology	26
2.9	Basic characterization of bacteriophages	26-29
2.9.1	Host specificity	26
2.9.2	Determination of lytic and virulent nature	27
2.9.3	Safety and toxicity	27
2.9.4	Antibiofilm activity	27-28
2.9.5	External factors affecting bacteriophages	28-29
2.9.5.1	Temperature	28
2.9.5.2	pH factor	28-29
2.9.5.3	Salinity	29
2.10	Bacteriophage genomics	29-33
2.10.1	Background study	29-30
2.10.2	Genomic diversity of bacteriophage	30-31
2.10.3	Metagenomics of bacteriophage	32
2.10.4	Evolution of bacteriophage	32-33
2.11	Contribution of electron microscopy in the study of bacteriophages	33-37
2.11.1	Importance of electron microscopy	33
2.11.2	Use of negative staining to study bacteriophages	34
2.11.3	Use of cryo-electron microscopy to study the structure of bacteriophages	35-36
2.11.4	Use of scanning electron microscopy to study bacteriophages	37
2.12	Structural studies of bacteriophages	37-40
2.12.1	Overview of bacteriophage structure	37-38
2.12.2	Importance of bacteriophage structure determination	38
2.12.3	Three-dimensional structure determination by single particle analysis	38-40
2.13	Application of bacteriophages for therapeutic purpose	40-45
2.13.1	Early history of phage therapy	40-41
2.13.2	Current status of phage treatment	42-43
2.13.3	Advantages and limitations of phage therapy	44-45



2.14	Bacteriophages against <i>Shigella</i> bacteria	45-48
2.14.1	<i>Shigella</i> bacteriophages	45-46
2.14.2	Phage-based control to <i>Shigella</i> infection	46-48

## **CHAPTER 3: Objectives** 49-50

## **CHAPTER 4: Materials & Methods** 51-89

4.1	List of chemicals	52-53
4.2	List of equipment	53-54
4.3	Preparation of the media	55-56
4.4	Preparation of buffers	56-59
4.5	Preparation of various reagents	60-66
4.6	Bacterial strains	66
4.7	Colony forming unit (CFU) calculation	66
4.8	Growth curve of bacteria	67
4.9	Isolation, propagation, enrichment, and purification of the phage sample	67-68
4.10	Plaque assay	68
4.11	Methods involved to determine morphology using transmission electron microscopy	68-70
4.11.1	Carbon coating of the grids	68-69
4.11.2	Glow-discharge of the carbon-coated grids	69
4.11.3	Negative staining of the samples	69-70
4.11.4	Transmission electron microscopy of the samples	70
4.12	Host range analysis and efficiency of plating calculation of phage Sfk0	70-71
4.13	One-step growth curve and adsorption kinetics	71-72
4.14	Phage stability assay under various physiological conditions	72
4.14.1	Stability of phage Sfk20 under various temperatures	72
4.14.2	Phage sensitivity at various pH	72
4.14.3	Phage stability under ultraviolet irradiation	72
4.14.4	Stability of phage virion at different saline conditions	72



4.15 Phage Sfk20 receptor identification	73
4.15.1 Proteinase K treatment	73
4.15.2 Periodate treatment	73
4.16 The bacteriolytic activity of phage Sfk20	73
4.17 Genomic characterization of the phage Sfk20	73-76
4.17.1 Isolation of the genomic DNA of phage Sfk20	73-74
4.17.2 Restriction digestion of the DNA and separation using DNA gel electrophoresis	74-75
4.17.3 Genome sequencing and analysis	75-76
4.17.4 Phylogenetic analysis	76
4.18 Proteomic characterization phage Sfk20	76-78
4.18.1 Isolation of phage Sfk20 proteins	76
4.18.2 Protein profile analysis by running SDS-PAGE	76-77
4.18.3 Phage proteomic analysis using LC-MS/MS	77-78
4.18.3.1 In-solution tryptic digestion	77
4.18.3.2 LC-MS/MS analysis	77-78
4.19 Structural characterization of phage Sfk20	78-83
4.19.1 Sample preparation for cryo-electron microscopy	78
4.19.2 Cryo-EM data collection	78
4.19.3 Cryo-EM data processing	79-83
4.19.3.1 Computational processing of Sfk20 capsid structure	79-80
4.19.3.2 Processing of phage Sfk20 head-to-tail connector structure	81
4.19.3.3 Processing of the tail part of phage Sfk20	81-82
4.19.3.4 Processing of the baseplate part of phage Sfk20	82-83
4.19.4 UCSF- Chimera	83
4.20 Structure prediction of phage Sfk20 proteins using neural network-based and homology modeling-based methods	83-85
4.21 Study of phage Sfk20 life cycle by electron microscopy	86-87
4.21.1 Phage-host interaction study by TEM	86
4.21.2 Phage-host interaction study by SEM	86-87

4.22 <i>Shigella</i> biofilm formation and degradation study by phage Sfk20	87-89
4.22.1 Biofilm degradation assay using phage Sfk20 and ampicillin	87-88
4.22.1.1 Biofilm degradation assay study by scanning electron Microscopy	87
4.22.1.2 Quantitative assay of biofilm degradation	87-88
4.22.2 Biofilm degradation assay using phage cocktail	88-89
4.22.2.1 Preliminary characterization of the other cocktail member phage Sfk23	88
4.22.2.2 Preparation of phage cocktail of phage Sfk20 and Sfk23	88
4.22.2.3 Biofilm formation and degradation in microtiter plate	88-89
4.22.3 Statistical analysis	89

## **CHAPTER 5: Morphological and biological characterization of a lytic *Shigella* phage Sfk20**

5.1 Introduction	91-92
5.2 Results	93-107
5.3 Discussion	108-111

## **CHAPTER 6: Genomic and proteomic characterization of *Shigella* phage Sfk20**

6.1 Introduction	113-114
6.2 Results	115-139
6.3 Discussion	140-142

## **CHAPTER 7: Structural characterization of *Shigella* phage Sfk20 using single-particle cryo-electron microscopy and image processing**

7.1 Introduction	144-145
7.2 Results	146-158
7.3 Discussion	159-161

<b>CHAPTER 8: Prediction of phage Sfk20 proteins using structure prediction-based approaches</b>	162-180
8.1 Introduction	163-164
8.2 Results	165-178
8.3 Discussion	179-180
<b>CHAPTER 9: <i>In vitro</i> phage -host interaction study by electron microscopy</b>	181-193
9.1 Introduction	182-183
9.2 Results	184-191
9.3 Discussion	192-193
<b>CHAPTER 10: Antibiofilm activity of <i>Shigella</i> phage Sfk20 against host bacteria</b>	194-208
10.1 Introduction	195-196
10.2 Results	197-205
10.3 Discussion	206-208
<b>CHAPTER 11: General Discussion</b>	209-214
<b>CHAPTER 12: Conclusion, Significance &amp; Future prospects</b>	215-217
<b>CHAPTER 13 Bibliography</b>	218-260
<b>CHAPTER 14 Publications &amp; Conferences</b>	261-263

## PREFACE

Shigellosis is a significant public health issue in low- and middle-income countries and a significant source of morbidity in developed nations. Though severe cramps and mucosal bleeding are not unusual, the diarrheal disease often has a self-limiting duration of up to 10 days. Sepsis, encephalopathy, hemolytic uremic syndrome, and, in rare cases, intestinal perforation also occur during shigellosis (Khan, Griffiths, and Bennish 2013). *Shigella* is extremely contagious, has an extremely low infectious dose, and is effectively transmitted by contaminated food, drink, and fomites as well as through the fecal-oral route. salads, chicken, milk and dairy products, fish, veggies, and other common foods are examples of sources. Additionally implicated as a mechanical vector is *Musca domestica*, a common housefly with a preference for human feces.

Maternal immunity may prevent *Shigella* infections in humans during the first six months of life before immunity develops and becomes protective (Mani, Wierzba, and Walker 2016). However, repeated infections are not rare because immunity is quite specific and infection can be caused by numerous serotypes. This is especially problematic in impoverished nations during the summer and the rainy season, where overcrowding and poor hygiene are frequent (Puzari, Sharma, and Chetia 2017). To date, the most popular therapeutic agent against dysentery has been antibiotics. However, as drug-resistant *Shigella* has slowly emerged, concerns about the long-term effectiveness of treatments have grown. Since the 1940s, *Shigella*'s drug-resistance traits have been known and during the past few decades, more and more multidrug-resistant strains have emerged. It takes time, effort, and money to develop new antibiotics to tackle these novel strains. Additionally, there is currently no vaccine available to effectively prevent shigellosis, making it a significant medical and societal issue on a global scale. Therefore, alternative approaches for reducing the incidence and severity of shigellosis are urgently needed. One possible approach is to use bacteriophages for the treatment in place of conventional antibiotics.

Bacteriophages are bacterial viruses that are arguably the oldest and most ubiquitous organisms on Earth. Phages contain a genome (DNA or RNA) surrounded by a protein coating (capsid) and can infect bacteria (Clark and March 2006). These bacterial viruses are found remarkably in a variety of environments. Lytic phages, in contrast to antibiotics, are quite selective, typically only attacking a subset of strains within a single bacterial species or among closely

related species. The use of "phage therapy" to treat numerous bacterial human diseases was made possible by their outstanding antibacterial activity. Phage therapy was first developed a century ago, nearly ten years before antibiotic therapy. It has however never outperformed the latter due to the development of antibiotics. However, due to the rate at which bacteria evolve resistance to antibiotics nowadays, phage therapy gained attention. Therefore, the interest is continuously growing to isolate and characterize novel bacteriophages. Effective phages are relatively easily isolated, including from environmental water sources during dysentery outbreaks and there is a rich history of phage therapy for shigellosis, with large and successful interventions reported since the 1930s.

The thesis contains 10 Chapters. Chapter 1 presents a brief background of the present study. Chapter 2 reviews the available literature on the effect of *Shigella* infection on human health, the regular treatment of shigellosis, the multidrug-resistant *Shigella* strains, the importance of alternative treatment, Phage therapy as well as phage biology. Chapter 3 describes the objectives of the present work. Chapter 4 describes the material methods used to carry out the present work. Chapter 5 describes the morphological and biological characterization of the lytic *Shigella* bacteriophage used in this study. Chapter 6 reported the genomic and proteomic characterization of the lytic bacteriophage. Chapter 7 showed the structural characterization of bacteriophage using single-particle cryo-electron microscopy and image processing. Chapter 8 deals with the characterization of the phage structural proteins using deep learning and homology-based approaches. Chapter 9 depicts the *in vitro* study of phage-host interaction. Chapter 10 describes the antibiofilm activity of the novel bacteriophage. Chapter 11 deals with a general discussion. Chapter 12 deals with the conclusion, significance, and future prospects of the present work. Chapter 13 deals with the bibliography of the current study. Finally, Chapter 14 provides a list of publications and conferences.

---

# SYMBOLS AND ABBREVIATION

---

Å	Angstrom
aa	Amino acid
ADP	Adenosine diphosphate
APS	Ammonium persulfate
atm	atmosphere
ATP	Adenosine triphosphate
bp	Base pair(s)
BSA	Bovine serum albumin
CFU	Colony forming unit
cm	Centimeter
Cryo-EM	Cryo-electron microscopy
CTF	Contrast Transfer Function
(k)Da	(kilo)Dalton
DNA	Deoxyribonucleic acid
ds	Double-stranded
EM	Electron microscopy
EDTA	Ethylene diamine tetra acetic acid
ESI-MS	Electrospray ionization mass spectrometry
FSC	Fourier Shell Correlation
FEG	Field emission gun
gms	Grams
gp(s)	Gene product(s)
h	Hour
ICTV	International Committeon Taxonomy of Viruses
Kb	Kilo basepair

kDa	Kilo Dalton
kV	Kilo Volt
LPS	Lipopolysaccharide
M	Molar
mA	Milli Ampere
µg	Microgram
µl	Microlitre
µm	Micrometer
ml	Mililitre
ICTV	International Committee on the Taxonomy of Viruses
MDR	multi-drug resistant
MOI	multiplicity of infection
MS	mass spectrometry
MS/MS	tandem mass spectrometry
ORF(s)	open reading frame(s)
SDS-PAGE	sodium dodecyl sulphate polyacrylamide electrophoresis
TAE	Tris acetate EDTA
TEMED	N,N,N,'N' tetramethylethylenediamine
Tris	Tris (hydroxymethyl) aminoethane
UA	Uranyl acetate
UV	Ultraviolet



# List of figures

Figure No.		Page No.
<b>Figure 2.1</b>	Schematic diagram of the gram-negative <i>Shigella</i> bacteria.	6
<b>Figure 2.2</b>	Mechanism of cellular pathogenesis of <i>Shigella</i> spp.	9
<b>Figure 2.3</b>	Worldwide distribution of Shigellosis.	11
<b>Figure 2.4</b>	Structure of T4-like bacteriophage.	17
<b>Figure 2.5</b>	Schematic diagram of the DNA injection mechanism of T4 bacteriophage.	20
<b>Figure 2.6</b>	Lytic and lysogenic life cycle of bacteriophage.	21
<b>Figure 2.7</b>	The basic morphology of tailed bacteriophages belongs to the <i>Caudovirale</i> family.	24
<b>Figure 2.8</b>	Number of complete genomes and genome size distribution in phage families.	31
<b>Figure 2.9</b>	Schematic diagram of the negative staining and visualization using transmission electron microscopy.	34
<b>Figure 2.10</b>	A step-by-step workflow of single particle cryo-electron microscopy imaging and data processing.	36
<b>Figure 2.11</b>	Milestones of bacteriophage research.	41
<b>Figure 2.12</b>	List of some FDA-approved phage-based products.	43
<b>Figure 4.1</b>	Restriction digestion of genomic DNA.	75
<b>Figure 4.2</b>	Processing of the DDD movie files into micrograph using EMAN 2.9.	80
<b>Figure 4.3</b>	Particle picking of the bacteriophage capsid.	80
<b>Figure 4.4</b>	Helical reconstruction of the phage Sfk20 tail part.	82
<b>Figure 4.5</b>	User-friendly interface for AlphaFold2 available through Jupyter Notebooks in Google Colaboratory.	84

<b>Figure 4.6</b>	User-friendly interface for ESMFold available through Jupyter Notebooks in Google Colaboratory.	84
<b>Figure 4.7</b>	Homology modeling software Phyre 2.	85
<b>Figure 4.8</b>	Structural homolog was identified using DALI server.	85
<b>Figure 5.1</b>	Electron micrograph of <i>Shigella flexneri 2a</i> bacteria: (A) scanning electron micrograph and (B) ultrathin section of <i>Shigella flexneri 2a</i> bacteria.	93
<b>Figure 5.2</b>	The growth curve of <i>Shigella flexneri 2a</i> , 2457T bacteria.	94
<b>Figure 5.3</b>	A visible clear zone of lysis in the middle of the plate.	95
<b>Figure 5.4</b>	Phage Sfk20 plaques are formed in the double-layered agar plate.	95
<b>Figure 5.5</b>	Transmission electron micrograph of phage Sfk20: (A) negatively stained image of phage Sfk20 has a prolate-shaped head and a long contractile tail and (B) phage Sfk20 interacting with an OMV particle.	96
<b>Figure 5.6</b>	Scanning electron micrograph of phage Sfk20.	97
<b>Figure 5.7</b>	Growth characteristics of <i>Shigella</i> phage Sfk20.	100
<b>Figure 5.8</b>	Adsorption kinetics of <i>Shigella</i> phage Sfk20.	101
<b>Figure 5.9</b>	Stability of phage Sfk20 was tested at various temperature conditions (4°C to 70°C).	102
<b>Figure 5.10</b>	Sfk20 stability at pH ranging from 3-13.	103
<b>Figure 5.11</b>	Sfk20 stability under ultra-violet light for 20 seconds.	104
<b>Figure 5.12</b>	Survival of the phage Sfk20 virions suspended in the double distilled water adjusted with 0-20% NaCl concentration.	105
<b>Figure 5.13</b>	Effects of Proteinase K and periodate treatment in adsorption of Sfk20 bacteriophage to <i>Shigella flexneri 2a</i> strain.	106
<b>Figure 5.14</b>	The bacteriolytic activity of phage Sfk20 against <i>Shigella flexneri 2a</i> .	107
<b>Figure 6.1</b>	Phage genomic DNA was digested with different restriction enzymes.	115
<b>Figure 6.2</b>	The genome sequence data was deposited in GenBank and the NCBI accession number is MW341595.	117

<b>Figure 6.3</b>	Easyfig schematic alignment of phage Sfk20 genome with five closely related phages using BLASTn program.	120
<b>Figure 6.4</b>	Schematic map of phage Sfk20 genome prepared using CGView.	123
<b>Figure 6.5</b>	Phylogenetic trees of Sfk20 were constructed based on: (A) the baseplate wedge subunit and (B) the terminase large subunit (TerL) using “ONE CLICK” at Phylogeny.fr.	125
<b>Figure 6.6</b>	Protein profile of bacteriophage Sfk20.	136
<b>Figure 7.1</b>	Cryo-electron micrograph of full Sfk20 bacteriophage particles: (A) native non-contracted tail conformation and (B) in the contracted tail state.	146
<b>Figure 7.2</b>	Set of good 2D class averages of the phage Sfk20 capsid.	147
<b>Figure 7.3</b>	Projection images of the 3D initial model of phage Sfk20 capsid.	148
<b>Figure 7.4</b>	The density map of Sfk20 capsid: (A) the side view showed elevated 5-fold symmetry and a depressed 3-fold symmetry, (B) the top view of the capsid and (C) the bottom view of the capsid	149
<b>Figure 7.5</b>	Good 2D class averages of the phage Sfk20 connector, used for further reconstruction purposes.	150
<b>Figure 7.6</b>	Projection images of the 3D initial model of the phage Sfk20 connector.	151
<b>Figure 7.7</b>	The density map of the phage Sfk20 head-to-tail connector: (A) capsid to connector junction, (B) top view of the connector, (C) bottom view of the connector and (D) the central section view of the connector part.	152
<b>Figure 7.8</b>	The tail particles of phage Sfk20.	154
<b>Figure 7.9</b>	Few 2D class averages of the phage Sfk20 tail part, used for further reconstruction.	154
<b>Figure 7.10</b>	The density map of the phage Sfk20 tail. The helical tail sheath is quite prominent.	154
<b>Figure 7.11</b>	Good 2D class averages of the phage Sfk20 baseplate, used for further reconstruction purposes.	155
<b>Figure 7.12</b>	Projection images of the 3D initial model of the phage Sfk20 baseplate.	156
<b>Figure 7.13</b>	The density map of the baseplate of the Sfk20 bacteriophage:	157

(A) the side view of the baseplate structure. The long piercing device was also visible, (B) the top view of the baseplate showed 6-fold symmetry, (C) the bottom view of the phage baseplate and (D) the baseplate (marked in blue) is attached to the tail part (in green).

<b>Figure 7.14</b>	The three-dimensional reconstruction of intact phage Sfk20 structure with capsid, the portal vertex connector, tail, and baseplate complex.	158
<b>Figure 8.1</b>	The structure of major capsid protein (ORF-207) was predicted using AlphaFold2, ESMFold, and Phyre2 and aligned with the experimental structure.	167
<b>Figure 8.2</b>	The structure of putative neck protein (ORF-195) was predicted using AlphaFold2, ESMFold, and Phyre2 and aligned with the experimental structure.	168
<b>Figure 8.3</b>	The structure of tail sheath protein (ORF-200) was predicted using AlphaFold2, ESMFold, and Phyre2 and aligned with the experimental structure.	170
<b>Figure 8.4</b>	The structure of tail tube protein (ORF-201). was predicted using AlphaFold2, ESMFold, and Phyre2 and aligned with the experimental structure.	171
<b>Figure 8.5</b>	The structure of baseplate wedge protein (ORF-188). was predicted using AlphaFold2, ESMFold, and Phyre2 and aligned with the experimental structure.	173
<b>Figure 8.6</b>	The structure of the baseplate wedge completion tail fiber socket was predicted using AlphaFold2, ESMFold, and Phyre2 and aligned with the experimental structure.	174
<b>Figure 8.7</b>	An average TM-score graph for all models predicted using AlphaFold2, ESMFold, and Phyre2.	176
<b>Figure 8.8</b>	Box plots of RMSD values of AlphaFold2, ESMFold, and Phyre2 are shown from left to right, respectively.	176
<b>Figure 9.1</b>	Thin-section electron micrograph of control <i>Shigella flexneri</i> 2a bacteria without treatment of phage.	184
<b>Figure 9.2</b>	TEM images of the ultrathin section of <i>Shigella flexneri</i> 2a infected with isolated host-specific phage Sfk20 at a 15 minutes time point.	185
<b>Figure 9.3</b>	TEM images of the ultrathin section of <i>Shigella flexneri</i> 2a infected with isolated host-specific phage Sfk20 at 30 minutes points: (A) TEM image of 30 minutes showed intracellular phage	187

development started, **(B)** the cytoplasmic material of the host cell was disorganized and **(C)** intracellular fully developed phage, loss of internal material and membrane disorganization are visible.

<b>Figure 9.4</b>	TEM images of the ultrathin section of <i>Shigella flexneri 2a</i> infected with isolated host-specific phage Sfk20 at 60 minutes time point.	188
<b>Figure 9.5</b>	Scanning electron micrograph of the Sfk20 bacteriophage.	189
<b>Figure 9.6</b>	Scanning electron micrograph of the infected bacterial cell with phage Sfk20 at the early phase.	190
<b>Figure 9.7</b>	Scanning electron micrograph of the infected bacterial cell with phage Sfk20 at the mid-phase.	191
<b>Figure 9.8</b>	Scanning electron micrograph of the infected bacterial cell with phage Sfk20 at the late phase.	191
<b>Figure 10.1</b>	Scanning electron micrograph of the 24-hour biofilm formation and degradation assay: <b>(A)</b> 24-hour untreated control, <b>(B)</b> biofilm treated with antibiotic ampicillin, <b>(C)</b> biofilm treated with phage Sfk20 and <b>(D)</b> biofilm treated with the combination of Sfk20 and ampicillin.	198
<b>Figure 10.2</b>	Scanning electron micrograph of the 48-hour biofilm formation and degradation assay: <b>(A)</b> 48-hour untreated control, <b>(B)</b> biofilm treated with antibiotic ampicillin, <b>(C)</b> biofilm treated with phage Sfk20 and <b>(D)</b> biofilm treated with the combination of Sfk20 and ampicillin.	200
<b>Figure 10.3</b>	Percentage of biofilm removal with phage Sfk20, antibiotic ampicillin, and the combination of both with respect to untreated control.	201
<b>Figure 10.4</b>	Scanning electron micrograph of biofilm formation and degradation assay: <b>(A)</b> 48-hour control biofilm, <b>(B)</b> biofilm treated with Ampicillin, <b>(C)</b> Biofilm treated with phage Sfk20 and <b>(D)</b> biofilm treated with the combination of Sfk20 and ampicillin.	202
<b>Figure 10.5</b>	Transmission electron micrograph of the bacteriophage Sfk23.	203
<b>Figure 10.6</b>	Percentage of biofilm removal with phage Sfk20, Sfk23, and the combination of both with respect to untreated control.	205

---

## List of tables

---

Figure No.		Page No.
<b>Table 2.1</b>	Activity and the center of phage therapy	43
<b>Table 4.1</b>	Bacterial strains used for the host range analysis	71
<b>Table 5.1</b>	Host range analysis of phage Sfk20	98
<b>Table 5.2</b>	Efficiency of plating of phage Sfk20	99
<b>Table 6.1</b>	Comparison of genomic properties of phage Sfk20 with closely related <i>Myoviridae</i> phages	118
<b>Table 6.2</b>	Comparison of some recently published <i>Shigella</i> phages based on biological properties	119
<b>Table 6.3</b>	All predicted ORFs, Their positions in the Sfk20 phage genome, strand, their function and their role in the phage life cycle	126-135
<b>Table 6.4</b>	Detection and identification of phage Sfk20 proteins by LC-MS/MS	138-139
<b>Table 8.1</b>	TM-score of all the predicted models	175
<b>Table 8.2</b>	RMSD values of all the predicted models	177
<b>Table 8.3</b>	pLDDT score-based coloring of AlphaFold2 and ESMFold predicted models	177-178
<b>Table 10.1</b>	Host range analysis of phage Sfk23	204



# CHAPTER 1

## Introduction





### 1.1. INTRODUCTION

Shigellosis is one of the major public health problems in developing and underdeveloped countries caused by the invasion of rectal, colonic, and distal ileal epithelium by rod-shaped *Shigella* spp. It mainly affects children below five years old and also the civilian and military travelers who visit many endemic areas (Olson et al. 2019; Steffen, Hill, and DuPont 2015). Annually 188 million cases of Shigellosis and 164000 deaths occur worldwide due to shigellosis (Kotloff et al., 2018). The symptoms of shigellosis include bloody watery diarrhea, fever, nausea, tenesmus, etc. A very low infectious dose (10-100 no. of cells) is sufficient for the infection to occur (HL 2010). Various contaminated food products such as salads, milk, soft cheese, deli meats, fresh fruits, and vegetables (Morgan et al. 2006; Okame et al. 2012) are usually responsible for Shigellosis outbreaks. There are also some indirect routes of transmission including ingestion of contaminated foods and drinks, via some regularly used contaminated objects, and also by various house-fly vectors which can physically carry the infected feces.

Antibiotics are considered common therapeutic agents for the treatment of dysentery to date. The drug-resistance features of *Shigella* have been reported since the 1940s and thereafter the multi-drug resistant species has steadily increased in the last few decades. The development of new antibiotics is time-consuming as well as expensive and laborious. Moreover, no effective vaccine is available yet to combat this disease (Magiorakos et al. 2012). Increasing multi-drug resistance to *Shigella* spp. and the lack of the development of new antibiotics cause significant challenges in the treatment of shigellosis. Therefore, some novel solutions are needed urgently to multidrug-resistant *Shigella* spp. Nowadays phage therapy is getting attention as an alternative mode of treatment.

Bacteriophages are viruses and the most abundant biological entity within the ecosystem (Clokier et al. 2011a). These viruses are very much host specific and able to inhibit various foodborne pathogens including *Shigella* without disturbing beneficial microflora. Bacteriophages, use the host replication machinery to replicate inside the bacterial cell by hijacking its cellular components and releasing mature phage particles by lysing the host cell (Ofir and Sorek 2018). The virulence effect of the phages is higher within the human body than when applied to bacteria grown in a laboratory environment (Shan et al. 2018). Lytic phages can effectively destroy their host within a very short period of time. Therefore, lytic phages are

used as potential biocontrol agents and for treatment purposes where conventional antibiotics failed. (Nagel, Chan, De Vos, El-Shibiny, Kang'ethe, Makumi, and J.-P. Pirnay 2016).

Twort (Twort 1915) and Felix d'Herelle (D'Herelle 1961) independently and around the same time discovered the existence of bacteriophages. Immediately after the discovery, d'Herelle used a phage for the treatment of *Shigella dysenteriae* infection in children(. d'Herelle F 1931). The research of bacteriophage was started almost ten years earlier than the discovery of antibiotics. Antibiotics discovery has garnered much attention from scientists in the past few decades. As a result, phage-based research was greatly overshadowed. Thankfully, some experts from Eastern Europe explored phage therapy and carried out a sizable number of phage therapy studies and treatments. (Williams Smith and Huggins 1983). A new hope has emerged as a result of the advancements made in phage-based research in Eastern Europe over the years for investigating the use of phage therapy against multidrug-resistant bacteria. In addition to long-standing programs in the Republic of Georgia and in Poland, established phage therapy programs are now available in the United States, Belgium, France, and Sweden. Collaboration efforts in Europe and Australia were effective in creating standardized phage therapy regimens to enable therapeutic uses (Khatami et al. 2022; Onsea et al. 2021). Some well-known medical institutes involved in phage-based research are the Eliava Institute in Tbilisi, Georgia, and the Hirsfeld Institute in Wroclaw, Poland. Nowadays lytic bacteriophages have not only been used for therapeutic purposes but also used as effective biocontrol agents in various fields and created new hope for scientists.



# CHAPTER 2

## **Review of Literature**



### 2.1 Shigellosis:

Shigellosis is commonly known as acute bacillary dysentery caused by the ingestion of *Shigella* spp. present in contaminated food and drinks, primarily linked to difficulty in accessing safe water and proper sanitation. The low infectious dose of bacteria is sufficient to provide a high rate of infection. However, the pathogen can survive poorly in the environment. Sometimes the common house fly *Musca domestica* may serve as a vector for *Shigella* transmission (Reviews et al. 2016). The most common symptoms of shigellosis are the passing of loose stools mixed with blood and mucous accompanied by abdominal cramps, tenesmus, and fever. Sometimes it may be asymptomatic but, in some cases, it may produce mild to moderate dysentery with fever, severe abdominal cramps, and rectal pain. *Shigella* mainly affects children below five years old so high fever and rectal prolapse are common symptoms for children and later malnutrition can also be developed. Sometimes mild to severe life-threatening conditions can occur due to shigellosis. Some patients also complained about arthritis and arthralgia. Leukemoid reactions and hemolytic uraemic syndrome are seen in *Shigella dysenteriae* 1 infection and may be fatal.

### 2.2 *Shigella*- the pathogen:

*Shigella* spp. are Gram-negative, non-motile, rod-shaped, non-spore-forming, and facultative anaerobic bacteria (**Figure 2.1**). Their cells are 0.4-0.6 µm across by 1-3µm long. It was first discovered by a Japanese scientist, Kiyoshi Shiga in 1897 (Trofa et al. 1999). The first discovered *Shigella* species was *Shigella dysenteriae*. Soon in 1899 *Shigella flexneri* (The, Medical, and Sep 2017), *Shigella sonnei* in 1906, and in 1921 *Shigella boydii* were discovered ((SHIGA 1936). Based on the type-specific antigens of the four *Shigella* species, various serotypes have been identified. *Shigella flexneri* is the main cause of endemic shigellosis in low- and middle-income countries particularly sub-Saharan Africa and Asia. On the other hand, *Shigella sonnei* is the most common pathogen for shigellosis to occur in high-income countries.

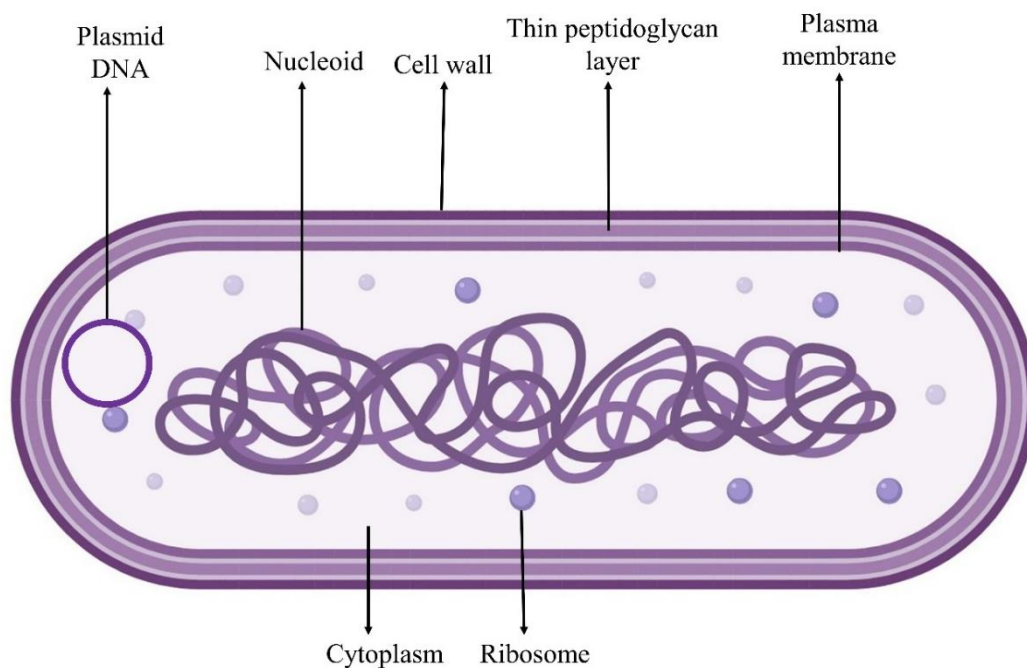


**Figure 2.1:** Schematic diagram of the gram-negative *Shigella* bacteria

### 2.3 Pathogenesis of *Shigella*:

*Shigella* bacteria entered the body by ingestion of contaminated foods and drink. A low infectious (10- 100 cells) dose is required for the infection to occur (HL et al. 1989). After entering into the body this small group of bacteria passes through the stomach surviving in the acidic environment of the stomach. It was reported that some antibacterial effectors are continuously released from intestinal mucosa when the bacteria entered the intestinal tract and *Shigella* spp. successfully downregulate the expressions of those antibacterial peptides (Islam et al. 2001) in the stomach. After passing through the stomach and small intestine, bacteria entered the large intestine and establish the infection. *Shigella* infection mainly occurs in the intestinal mucosa.

The knowledge of the *Shigella* pathogenesis mechanism is obtained from the study of *Shigella flexneri*. The infection mechanism is a complex and multistep process involving a cytotoxic diarrhoeal prodrome, cytokine-mediated inflammation of the colon, and necrosis of the colonic epithelium (**Figure 2.2**). The process is divided into four major steps i) invasion of the bacterial cell ii) intracellular multiplication iii) intracellular and intercellular spread of *Shigella* iv) host cell killing.

## CHAPTER 2

---

To reach the intestinal mucosa cells bacterial cells first crosses the intestinal epithelium which protects the human body against pathogenic bacteria (Sansonetti 2004) Initially, *Shigella flexneri* cannot penetrate into the epithelial cells from the apical sides but it enters into the microfold cells (M cells) and reaches into the epithelial cell via transcytosis (Sansonetti et al. 1996; Wassef, Keren, and Mailloux 1989). M cells are special types of epithelial cells that continuously collect various particles from the gut lumen and deliver them to intestinal mucosal tissue where the immune response can be started.

*Shigella flexneri* is released into the intraepithelial pocket after the transcytosis and the bacteria come across the macrophages in the intraepithelial pocket that engulf and destroy the incoming pathogen. *Shigella flexneri* can survive within the macrophage and induce the apoptosis of macrophages (Islam et al. 1997; Zychlinsky et al. 1996; Zychlinsky, Prevost, and Sansonetti 1992). After the death of the macrophages two proinflammatory cytokines IL-1 $\beta$  and IL-18 are released (Sansonetti et al. 2000; Zychlinsky et al. 1994). Both cytokines are involved to produce an acute and massive inflammatory response. IL-1 $\beta$  is responsible for the strong inflammation of the intestine which is one of the major symptoms of shigellosis whereas natural killer cells (NK cells) are produced by IL-18. This IL-18 help in the production of gamma interferon (IFN- $\gamma$ ) thus increasing the innate immune response (Sansonetti et al. 1995, 2000; Way et al. 1998).

After the release from the dead macrophage cells *Shigella flexneri* enters into the epithelial cells from the basolateral side to hide themselves from the phagosome and start replicating inside the cytoplasm (Sansonetti et al. 1986). The cytoplasmic bacterial cells then move and spread into adjacent epithelial cells by actin polymerization and also avoid the host immune defense components (Bernardini et al. 1989; Monack and Theriot 2001; Stevens, Galyov, and Stevens 2006). A strong inflammatory response is created when the *Shigella flexneri* invade the epithelial cells. Next, an intracellular surveillance system that is mediated by Nod-1 can recognize the release of bacterial peptidoglycan fragments and activate nuclear factor  $\kappa$ B or NF- $\kappa$ B. Nuclear factor (NF- $\kappa$ B) is responsible for the upregulation and secretion of IL-8 (Girardin et al. 2003; Pédrón, Thibault, and Sansonetti 2003; Philpott et al. 2000; Sansonetti et al. 1999) and IL-8 helps to enter the polymorphonuclear neutrophil leukocyte (PMN) in the site of infection (Sansonetti et al. 1999; Singer and Sansonetti 2004). In some recent studies, it was shown that some effector proteins are secreted by *Shigella flexneri* which promote the migration of polymorphonuclear neutrophil leukocytes by affecting the transcriptional

response of infected epithelial cells(McCormick, Siber, and Maurelli 1998; Zurawski et al. 2006).

The integrity of the epithelial cell lining is disrupted by the PMN cells thus more bacteria are able to cross the submucosa cells without the need of M cells (O. J. J. Perdomo et al. 1994; J. J. Perdomo, Gounon, and Sansonetti 1994). *Shigella flexneri* bacteria also weaken the tight junction of the EC layer by changing the composition of the proteins(Sakaguchi et al. 2002). Therefore, the destruction of the macrophages, the influx of the PMN cells, and the rapid disruption of the epithelial cells increase the load of bacteria in the tissue. Therefore, all these processes are involved in the development of diarrhoea (Laohachai et al. 2003) which is the primary symptom of shigellosis. Severe tissue destruction occurs in shigellosis which results in impaired adsorption of the water, solutes, nutrients, and blood in the stool. As the membrane transport process is damaged severely, the electrolyte imbalance occurs in the shigellosis. *Shigella* enterotoxin 1 (ShET1) and *Shigella* enterotoxin 2 (ShET2) are produced by the *Shigella* strains which induce fluid secretion from the intestinal cells that produce the watery part of the diarrhoea (Fasano et al. 1997; Nataro et al. 1995).

Recent reports suggest that *Shigella flexneri* bacteria secrete some effector proteins and these effector proteins are responsible for the downregulation of the proinflammatory signals, maybe to balance the extremity of the inflammation to an extent that is beneficial for the bacteria. Now it is very much clear that *Shigella flexneri* skilfully avoids and utilizes the harmful responses of the human immune system.



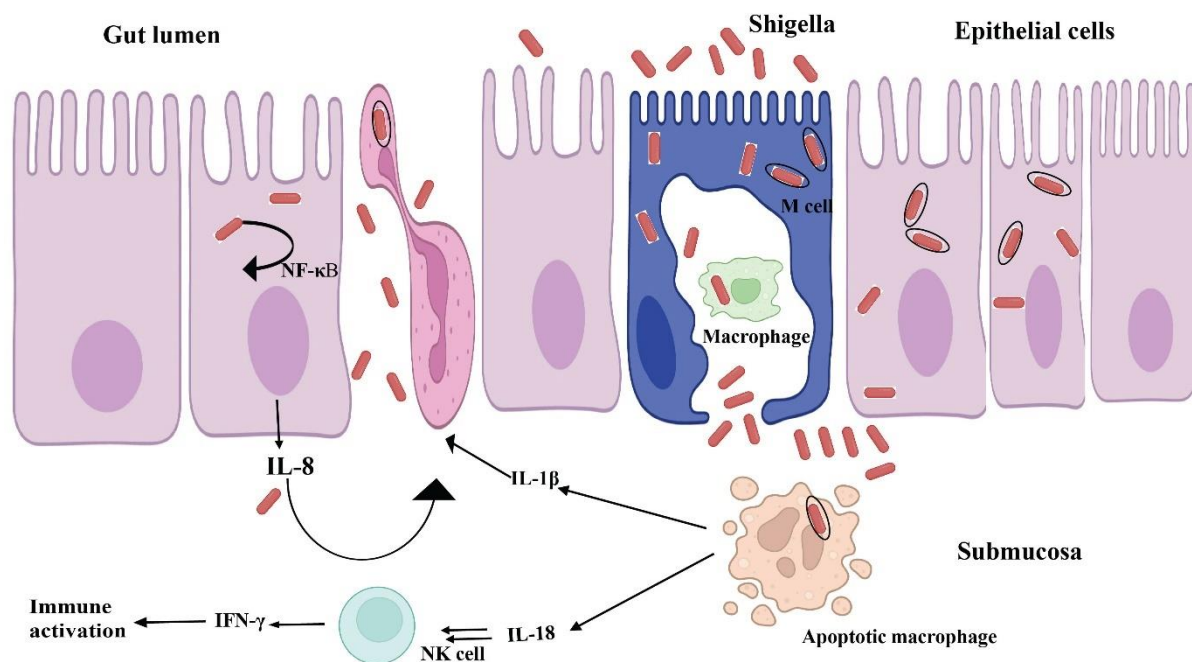


**Figure 2.2:** Mechanism of cellular pathogenesis of *Shigella* spp. This figure is adapted from Schroeder and Hilbi 2008.

## 2.4 Shigellosis and epidemiology:

Shigellosis is a major source of morbidity and mortality in all age groups throughout developing and developed countries, and it is a global public health issue. The human body is the only natural host for *Shigella* spp. Children aged below five years have the highest incidence of shigellosis which is most frequently contracted in childcare facilities in the United States and Europe. During the epidemics caused by *Shigella dysenteriae* 1, more or less all age groups suffered. Currently, *Shigella flexneri* is the major responsible strain for bacillary dysentery in many low-income and middle-income countries (**Figure 2.3**). On the other hand, *Shigella sonnei* is the second most common *Shigella* species for shigellosis to occur in high-income countries, especially in North America and Europe and 80% of all *Shigella* infections occur in this zone (Gu et al. 2012). Various surveys were executed in different treatment centres. The research revealed that between 30- 50% of instances of dysentery and between 5- 15% of cases of diarrhoea were linked to *Shigella*. The major cases of *Shigella* infections are found in endemic shigellosis. Endemic *Shigella* is responsible for 10% of diarrhoeal diseases cases in developing countries among children younger than five years old (Ferreccio et al.

1991) and 70% of diarrhoeal deaths (Bennish et al., 1990; Kotloff et al., 1999). *Shigella flexneri* is one of the hyperendemic species in developing countries and is responsible for approximately 10% of all diarrhoeal cases among children below five years. A multi-centre study on shigellosis was conducted in six Asian countries (Pakistan, China, Bangladesh, Vietnam, Thailand, and Indonesia) which reported that *Shigella flexneri* is the most reported *Shigella* spp. (68%) except in Thailand (Von Seidlein et al. 2006). In developed countries, *Shigella sonnei* is involved in common outbreaks and transmission occurs through uncooked food or contaminated water. In general, the disease caused by *Shigella sonnei* is less severe. In recent years globally 5% of cases of shigellosis caused by *Shigella boydii* and *Shigella dysenteriae* have been reported. *Shigella dysenteriae* was the main reason of diarrhoeal disease more than 100 years ago but the epidemic and endemic due to this pathogen is now quite rare (Bardhan et al. 2010; Gu et al. 2012). There were many epidemics of *Shigella dysenteriae* in the late 19th and early 20th centuries. Then this pathogen disappeared and it reappeared as an epidemic in 1968 in Central America, Asia, and Africa (Weill et al. 2016). Later the frequency of *Shigella dysenteriae* was replaced by *Shigella flexneri* and it is also gradually replaced by *Shigella sonnei* (Blaser, Pollard, and Feldman 1983; Kostrzewski and Stypulkowska-Misiurewicz 1968). The fourth species, *Shigella boydii* was first found in the Indian subcontinent and Latin America and uncommonly encountered all over the world (Fernandez-Prada et al. 2004; Rolfo et al. 2012). *Shigella* outbreaks are very common and have been reported widely. In California a serious outbreak of shigellosis occurred between 2014 and 2015 and *Shigella sonnei* was the responsible strain for this outbreak (Kozyreva et al. 2016). There were approximately 1,200 cases of shigellosis caused by *Shigella flexneri 2a* in Morobe Province on the northern coast of Papua New Guinea, and five people died as a result (Benny et al. 2014). Meanwhile, in Taiwan, there were fifty-five cases of shigellosis caused by *Shigella flexneri 2a*, *Shigella sonnei*, and *Shigella flexneri 3b* (Ko et al. 2013). A total of 10,827 *Shigella* isolates were identified between 2001 - 2011 in Bangladesh with the predominant species detected being *Shigella flexneri*, followed by *Shigella sonnei*, *Shigella boydii*, and *Shigella dysenteriae*, respectively (Ud-Din et al. 2013). In a previous study, it was reported that 96 students in a rural elementary school in Sichuan province (China) suffered from shigellosis after drinking untreated well water and the causative agent was *Shigella flexneri 2b* (He et al., 2012). Two outbreaks occurred in 2009 in Sweden and the causative agent was *Shigella dysenteriae* (Löfdahl et al. 2009) and *Shigella sonnei* that affected air travelers departing from Hawaii (Gaynor et al. 2009). In Parison City (Iran) severe diarrhoea was experienced by 701 inmates and *Shigella flexneri 3a* was the causative agent (Ranjbar et al. 2010). In Austria, a

foodborne outbreak of shigellosis occurred and it was caused by *Shigella sonnei* (Kuo et al. 2009) and other *Shigella* spp. (Muller et al. 2009). The growth of shigellosis and the HIV epidemic coexist in many developing nations. *Shigella* infection worsens in patients with HIV-associated immunodeficiency, which can result in bacteremia and chronic or recurring intestinal illness (Batchelor, Kimari, and Brindle 1996).

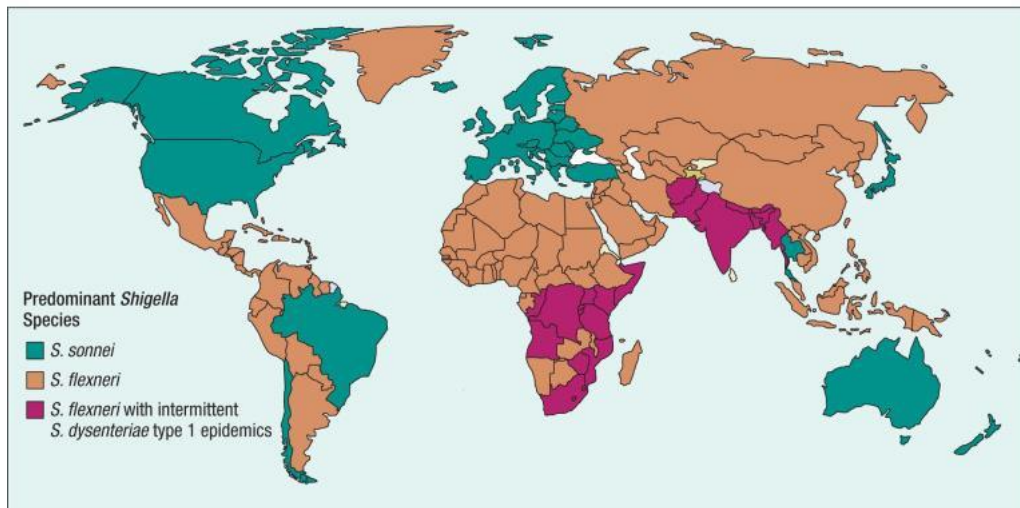


**Figure 2.3.** Worldwide distribution of Shigellosis. This figure is extracted from **Bennish and Ahmed 2020**.

### 2.5 Immunity development of *Shigella* infection:

In several studies, it was shown that *Shigella* infection provides protective immunity. In endemic areas, the effect of shigellosis reached its peak within the first five years of life and the immunity develops after several exposures during childhood (Taylor et al. 1986). The incidence of shigellosis declines with time. During the development of vaccines, it is found that the immunity was serotype-specific (e.g., directed to the LPS O antigen of the organism). In the early phase of *Shigella* infection, the antibody response to somatic antigens is seen and anti-LPS antibodies are produced. Mainly the IgM response is seen and it reaches the peak within a few weeks and it disappears after 1-2 years.

It was reported in one study that primary *Shigella* infection provides 76% protectivity against reinfection by the same serotype in children (Ferrecchio et al. 1991). Moreover, it was also seen that significant protectivity against the homologous strain is increased also for the adult volunteers (64-74% protective efficacy) (Kotloff et al. 1995). Therefore, it may be claimed that

a person who recovers from a *Shigella flexneri* 2a infection is only protected against reinfection with homologous serotypes.

### **2.6 Treatments for shigellosis:**

#### **2.6.1 Regular treatment of shigellosis:**

A commonly used treatment for shigellosis is the maintenance of the balance of electrolytes in the body. According to the World Health Organization (WHO), the use of oral rehydration therapy (ORS) together with zinc supplements is one of the most effective therapies for bacillary dysentery. Zinc mainly helps to reduce the duration and the frequency of expelling loose stools (Nichter, Acuin, and Vargas 2008). In case of severe dehydration intravenous fluids are also given. Long-term breastfeeding has been demonstrated to be an effective method of lowering the incidence of shigellosis in early children (CLEMENS et al. 1986). Specific antibodies are present in the milk of the woman those who live in the endemic areas and it helps to reduce the severity of the disease in infants (Hayani et al. 1991). Therefore, the WHO advises a few clinically proven antibiotics to treat shigellosis (Christopher et al., 2010). Antibiotics mainly reduce the duration of the fever and severe diarrhoea and also reduce the risk of transmission of the disease from person to person. In practice, quinolones (nalidixic acid, ofloxacin, norfloxacin, and ciprofloxacin) beta-lactams (ampicillin, ceftriaxone, pivmecillinam, cefixime, and amoxicillin), macrolides (azithromycin and erythromycin) and other antibiotics (tetracycline, furazolidone, sulfonamides, and cotrimoxazole) are commonly used for the treatment of bacillary dysentery caused by *Shigella*. Ciprofloxacin and azithromycin are given orally to children and adults and it is considered as first-line of treatment for shigellosis. In 2017, according to the suggestion of WHO, ciprofloxacin was considered the first choice for shigellosis treatment of children and adults whereas azithromycin, ceftriaxone, and cefixime were considered as second choice (WHO Technical Report Series 2011). According to WHO, trimethoprim-sulfamethoxazole is also the popular choice for the treatment of shigellosis and nowadays antibiotics are mostly used to treat bacillary dysentery in children. Antibiotics should follow some of the basic principles during treatment: first, the drug that is used for the treatment should be present in serum with therapeutic concentration but the drug should not be present in a considerable concentration in the stool (Haltalin et al. 1968; Nelson, Kusmlesz, and Shelton 1982). Second, some antibiotics are able to exceed serum minimal inhibitory concentration but these are not always effective for the treatment of shigellosis. For example, amoxicillin is absorbed better than ampicillin but

least effective (Nelson and Haltalin 1974). The severity of the disease and the threat of increasing multidrug-resistant strains provide strong support for vaccine development.

Shigellosis can be prevented with active vaccines, as has been demonstrated for other infectious diseases, and it is a crucial step in reducing mortality and morbidity rates from the disease globally. Since *Shigella* spp. naturally infect mainly humans, an effective vaccine can significantly reduce the disease globally. To develop a safe and effective *Shigella* vaccine different vaccine strategies have been used over several decades. Although a licensed vaccine is not available yet.

### **2.6.2 Current scenario of antimicrobial resistance among *Shigella* spp.:**

*Shigella* spp. can develop resistance activity against different antibiotics available on the market. Over the last few decades, the *Shigella* species have progressively become antibiotic resistant and it is a critical challenge in pharmaceutical and clinical research due to their serious impact on health. The IDSA (Infectious Disease Society of America) is worried about the growing antibiotic-resistant species in the USA and also other places in the world (Spellberg et al. 2008). Different bacterial factors, as well as various social factors such as high mutation rate, misuse of antibiotics by humans, increasing population rate, and the migration of people, are mostly involved in the increase of multi-drug resistant species (Liu et al., 2016). The exchange of segments of genetic material between bacterial cells is also a major reason for the development of antimicrobial resistance activity. There are three processes in prokaryotes for the intracellular movement of DNA: transformation, conjugation, and transduction. Transformation involves the transfer of small segments of genetic material between closely related bacterial cells by contrast in transduction the transfer of genetic material occurs through bacteriophages while in conjugation genetic elements pass through the sexual pilus, The newly acquired susceptible bacteria show resistance activity (Frost et al. 2005).

Previously different first-line antibiotics such as nalidixic acid, ampicillin, chloramphenicol, tetracycline, and trimethoprim-sulfamethoxazole were used for the treatment of shigellosis. As the resistance activity of the *Shigella* is increased day by day newer drugs such as ceftriaxone, azithromycin, and ciprofloxacin are the choice for the treatment of shigellosis (WHO Technical Report Series 2011). But the resistance activity of the *Shigella* spp. against these antibiotics has also increased. *Shigella* spp. has been linked to several reports of drug resistance, cross-resistance, and multidrug resistance, and this resistance activity is continuously increasing

(Klontz and Singh 2015). In 2000-2010, a total of 1376 *Shigella* isolates were gathered from Foodborne Diseases Active Surveillance Network sites (FoodNet sites) and evaluated in the US National Antimicrobial Resistance Monitoring System (NARMS) (Shiferaw et al. 2012). In the result, it was observed that among them 826 isolates (74%) were resistant to ampicillin, 649 (58%) to streptomycin, 402 isolates (36%) to trimethoprim-sulfamethoxazole (TMP-SMX), 355 isolates (32%) to sulfamethoxazole-sulfisoxazole, 312 isolates (28%) to tetracycline, 19 (2%) to nalidixic acid, and 6 (0.5%) to ciprofloxacin (Shiferaw et al. 2012). It was also seen that *Shigella* isolates resistant to trimethoprim-sulfamethoxazole (TMP-SMX) was 75% among the person with a history of international travel, 58% Hispanic persons, 40% among the white person whereas 25% of isolates were resistant to trimethoprim-sulfamethoxazole (TMP-SMX) and ampicillin, 5% isolates were resistant to ampicillin, TMP-SMX, and chloramphenicol. Moreover, 5% of isolates (49 *Shigella flexneri* isolates, 33%, and 3 *Shigella sonnei*, 0.3%) were resistant to chloramphenicol, sulfamethoxazole-sulfisoxazole, streptomycin, tetracycline, and chloramphenicol. Male individuals were infected more likely (7% versus 3%) than female individuals (Klontz and Singh 2015).

In the 1940 s the sulfonamide drugs were found highly effective against *Shigella dysenteriae* 1. Later in the 1960s ampicillin, tetracycline, and co-trimoxazole were found to be highly beneficial but from the 1960s to 1980s the resistance activity to these drugs increased (Nelson, Kusmiesz, and Jackson 1976). In the early 1980s, it was seen that nalidixic acid is more beneficial for the treatment of shigellosis in Children and adults (Bhattacharya et al. 1987) but within a short period of time, nalidixic acid-resistant *Shigella dysenteriae* type 1 was found at several parts of the world (Munshi et al. 1987; Sen et al. 1988). Later, it was reported that different fluoroquinolones such as ciprofloxacin and norfloxacin are more effective than nalidixic acid in the treatment of shigellosis (Bennish et al. 1990; Bhattacharya et al. 1991). In 2002 in eastern India norfloxacin and ciprofloxacin-resistant *Shigella dysenteriae* type 1 strain were found but these strains were ofloxacin sensitive (Sur et al. 2003). In 2003, similar isolates were found in Bangladesh that are resistant to all common antibiotics including ofloxacin (Naheed et al. 2004). In addition, 200 *Shigella sonnei* strains were isolated from Bangladesh and it was found that all these strains were resistant to some common frequently used antibiotics such as trimethoprim-sulfamethoxazole, nalidixic acid, ciprofloxacin, mecillinam and ampicillin at a ratio of 89.5, 86.5, 17, 10.5, 9.5% respectively (Ud-Din et al. 2013). Some ciprofloxacin-resistant *Shigella sonnei* strains were found in South Asia and these strains established transmission in the low endemicity locations such as Australia, USA, and Europe

(Bowen et al. 2015). The annual report of the National Salmonella, Shigella & Listeria Reference Laboratory (NSSLRL) showed that among the 45 *Shigella* isolates, 93% are multidrug resistant. Different azithromycin-resistant *Shigella* strains were also identified a decade ago within the HIV-positive populations. It was mentioned in a study that high levels of nalidixic acid and ciprofloxacin-resistant *Shigella* strains were found in Asia and Africa than in Europe and America. Increasing the resistant activity of various *Shigella* strains to third-generation cephalosporin leaves a small option for treatment.

### 2.6.3 Development of vaccines:

The Global Enteric Multi-centre Study (GEMS) recognized the *Shigella* bacteria as one of the top two agents responsible for diarrhoeal disease in seven developing countries in sub-Saharan Africa and South Asia (Kotloff et al., 2013). Similarly, another multisite birth cohort study (MAL-ED) was organized by eight different countries in Africa, Asia, and South America, and the *Shigella* spp. was identified as the major cause of diarrhoeal disease in the community during the second year of life. When military personnel and travelers travel from different parts of the world to diarrhoeal-prone areas, the risk of infection due to *Shigella* spp. is increased. As the number of multi-drug-resistant bacteria is increasing day by day, the treatment of the disease with antibiotics is not so effective at present. Therefore, the development of a vaccine is considered one of the top priorities for public health.

In his autobiography, Kiyoshi Shiga mentioned that initially, he focused on the development of the *Shigella* vaccine. At first, he developed a heat-killed whole-cell vaccine and injected it into himself being the primary subject and the response was harsh. Later he developed an oral and a serum-based passive immunization vaccine. Thousands of Japanese citizens received this oral vaccine, and his work was published.

The protective performance of the anti-*Shigella* vaccine is dependent on the serotype present because the immunity in *Shigella* is species-specific. Thus, knowing the serotype distribution among clinical isolates is one of the crucial steps for vaccine development. Initially, heat or acetone-killed whole-cell vaccine was developed but it was not very effective. Therefore, live attenuated vaccines were developed. Different *Shigella* vaccine candidates such as attenuated *Shigella flexneri* and *Shigella sonnei* strains, killed *Shigella flexneri* strains, or specific polysaccharides have been tested in animal models. A vaccine made up of polysaccharide conjugate of *Shigella sonnei* and *Shigella flexneri* has indicated safety and immunogenicity in

children. Nowadays various types of vaccines such as live oral *Shigella* vaccines, killed whole-cell oral *Shigella* vaccines, candidate vaccines, several glycoconjugates, and subunit vaccines have been developed by researchers but all these are under phase trials. At present no licensed vaccine is commercially available. Thus, priority is given to alternative development of treatment against *Shigella* spp. specifically *Shigella flexneri* 2a and *Shigella dysenteriae* 1.

### **2.6.4 Importance of searching for an alternative treatment:**

Infectious disease mostly affects developing countries and malnutrition, poor hygiene, unhealthy lifestyle, and unsafe drinking water causes a higher rate of morbidity and mortality and socio-economic injury. The limited healthcare system is one of the major drawbacks of developing countries. Nowadays the global expansion of antimicrobial resistance causes an increased rate of morbidity and mortality in developing countries due to endemic infections. A recent study suggested that if effective measures have not been taken today, 10 million death cases and a GDP loss of \$100 trillion will occur by 2050 (O'Neill 2016). The global surveillance report of the World Health Organization in 2014 showed that >50% of clinically important bacteria in five to six WHO-marked regions develop resistance activity against third-generation antibiotics and 45% of deaths in South East Asia and Africa occur due to the infection by multi-drug resistant bacteria (WHO 2014). Therefore, there is an urgent need to develop some novel and alternative therapeutic strategies for treatment.

Therefore, for the treatment of shigellosis phage therapy could be the most promising option. Before the discovery and widespread use of antibiotics, bacteriophages are used for treatment purposes. After the discovery of antibiotics, phage therapy was completely neglected (Summers 2001). The host specificity feature of bacteriophages makes them a potential therapeutic agent and can be applied to human tissue without causing any harm (Weber-Dąbrowska, Dąbrowski, and Šlopek 1987) is they are easily available and their processing cost is also lower (Nagel et al., 2016). Furthermore, for many years, Eastern Europe has successfully carried out experimental anti-dysentery experiments employing phages (Hoyle and Kutter 2021).



### 2.7 General introduction of bacteriophages:

#### 2.7.1 Biology of bacteriophages:

Bacteriophages are viruses that infect and replicate only within the host bacterial cells. They are innumerable in nature and considered as the most common biological entities on the earth. There are at least  $10^{30}$  -  $10^{31}$  phage particles within the biosphere. Extreme habitats, oceanic and terrestrial surfaces, dirt, and seas are all places where they can be found. In addition, phages are also found in hospitals, waste-water and where host bacteria can live, and also in animal and human tissue samples. Every day 4-50% of bacteria are killed by phages and phages are the driver of global geochemical cycles and a pool of the greatest genetic diversity on Earth (Suttle 2005). The number of phages needed to infect a host cannot be determined by a single method, but molecular and conventional methodologies can be combined to create a more complete picture of the viral population (Clokier et al., 2011). All the bacteriophages consist of a nucleic acid encapsidated inside the protein-encoded capsid. The capsid specifically protects the genetic material and mediates the delivery of the genome into the host cell (**Figure 2.4**). Detail structure of the bacteriophages can be visualized by electron microscopy.

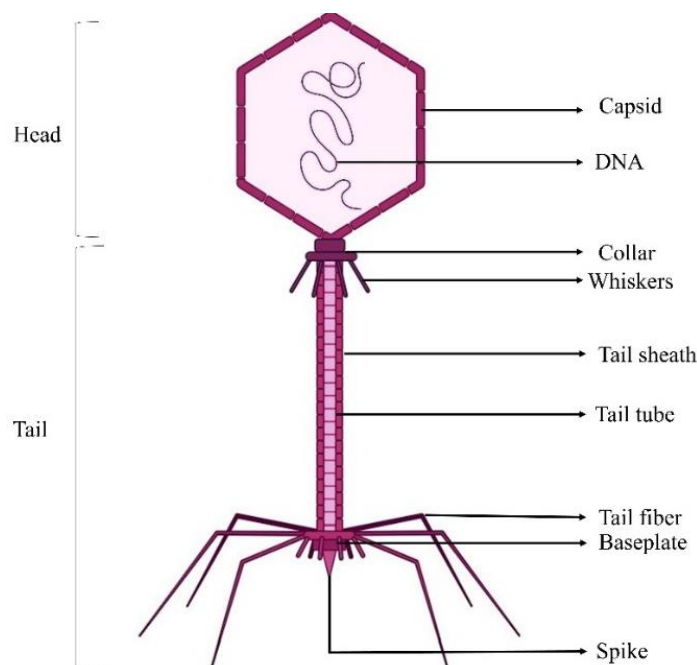


**Figure 2.4:** Structure of a T4-like bacteriophage.

### 2.7.2 History of bacteriophage:

Bacteriophages (BPs) are viruses and they can infect and kill their host bacteria without affecting human or animal cells or other beneficial microflora. Bacteriophages were first discovered in 1915 by William Twort, and in 1917 by Felix d'Herelle. The word "bacteriophages," which is derived from the Greek word "phagein," which means "to eat," was proposed by d'Herelle. He also introduced the term plaque, 'the circular clear zone of lysis' where a single phage infects and kills its host bacteria. Following their discovery, d'Herelle noticed that the phage titers in the stool samples of dysentery patients steadily increased. This observation sparked scientists' curiosity about the possibility that these bacteriophages might have therapeutic value. When Staphylococcal phage was injected locally into the area of cutaneous boils, Bruynoghe and Maisin (1921) from Louvain saw a decrease in swelling and pain. This was the first report of phage therapy (Düzgüneş, Sessevmez, and Yildirim 2021).

Phage therapy was widely applied to patients of any age suffering from a wide range of ailments in the Soviet Union as a result of Felix d'Herelle's work with his Georgian colleagues. The results of the phage therapy were considered very satisfactory and several reports were published (d'Herelle 1931; Summers 2001). Since the majority of these publications were written in Russian, they did not make it to the West. As a result of this fact, the majority of clinical trials did not adhere to international standards. Some results were interpreted and disseminated among English-speaking scientists, but they were met with skepticism (Chanishvili 2012). Many successful early phage therapy trial report was there but several reasons were also there for the failure of the phage therapy. The failure of early phage therapy in the West is due to a number of factors, including a lack of understanding of phage biology, the availability of safe and effective antimicrobial drugs following World War II, and flaws in the diagnostic bacteriology techniques available at that time. However, the use of bacteriophages continued in Russia and in Eastern Europe as most of the antibiotics were not available in these countries (Abedon et al. 2011). The situation has completely changed in the last 30 years. In the last few decades, the multi-drug resistant species are increased but the discovery and development of new antibiotics are minimal therefore phage therapy regain its importance (Perros 2015). The study of bacteriophages contributes to numerous important biological science discoveries, including the recognition of DNA as the genetic material, the deciphering of the genetic code, the phenomenon of restriction and modification, and the creation of molecular recombinant technology. Different phage-derived proteins are currently

being used as diagnostic agents (Smith et al., 2001), therapeutic agents (Loeffler et al., 2001), and for drug discovery (Liu et al., 2004).

### **2.7.3 Origin of bacteriophage:**

It is an important subject of discussion among evolutionary biologists whether bacteriophages are living entities. The discovery of the Mimivirus, a double-stranded DNA virus particle growing in amoebae that contains a 1,181,404–base pair genome fueled the debate (Raoult et al. 2004; la Scola et al. 2003). Influenced by the genome size of the viruses, overlapping particles, cellular organisms (Koonin 2005), and the observation that the capsid protein of the viruses is the only major component that is unique to the viral world (Krupovič and Bamford 2008), All the organisms are divided into capsid encoding organism and ribosome encoding organism by Raoult and Forterre (2008). According to these authors, the last universal common ancestor and the viral particles it contained were contemporaneous with a previous form of capsid from which all viruses today descended. The similarities drawn between the architecture of the capsid proteins of the human adenovirus, algal phycodnavirus PBCV-1, and tectivirus PRD1 corroborate this viewpoint. If we examine the other instances, similar connections between the herpesvirus and tailed dsRNA bacteriophages were discovered (Baker et al., 2005). All these observations suggested that all the viruses have a common origin that shares the same capsid architecture but infects different hosts (Krupovič and Bamford 2008). Recent research has cast doubt on the notion that viruses are living things that symbolize the long history of the Tree of Life. Because they cannot evolve from themselves and lack a self-maintenance system, viruses were eliminated by Moreira and Lopez-Garcia (2009) from the Tree of Life. Based on the observation that viruses do not share any genetic material with each other, they oppose the single common origin of cellular life (Ranea et al. 2006) to a polyphyletic origin of viruses. Moreira and Lopez-Garcia compared the viral capsid to the icosahedral shell of a bacterial protein-based organelle and concluded that this form of molecular design would potentially be susceptible to convergence. The evolutionary biologists, who emphasize the significance of viruses in the precellular period of evolution (Koonin, Senkevich, and Dolja 2009) and restrict horizontal gene transfer (Ludmir and Enquist 2009), rejected this viewpoint once more.

### 2.7.4 Life cycle of bacteriophages:

The first stage of the infection starts with the attachment of the phage to the bacterial cell surface receptor such as lipopolysaccharide, outer membrane protein (OMP), flagella, and fimbriae. This process was facilitated by tail fibers or the tail spikes of phages. Some of the tail fibers of bacteriophages have a depolymerase enzyme that helps to depolymerize the bacterial cell wall (Prokhorov et al. 2017). The binding of the tail part to the receptor is followed by a structural rearrangement of the baseplate that triggers the contraction of the tail fiber. When the phage tail fiber contracts, the phage injects its genetic material inside the bacterial cytoplasm. During the ejection of the phage genome, the phage tail tube penetrates into the host cell periplasm, and during this penetration, the virus uses a variety of depolymerase and lysins (Figure 2.5). When the tail tube fiber attaches to the cell wall, a transmembrane phage DNA delivery channel is formed and the ejection of the DNA occurs through this channel.

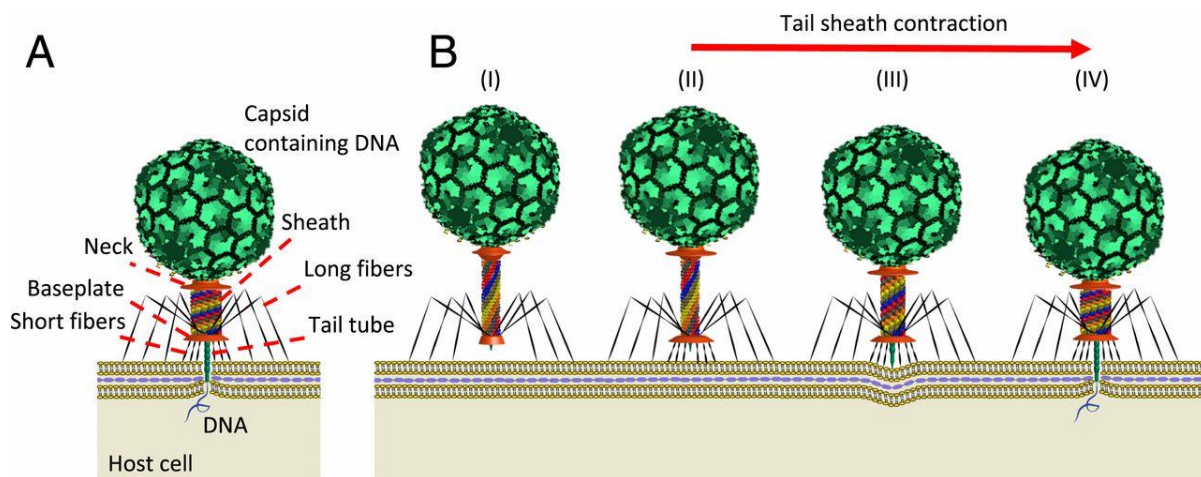


**Figure 2.5:** Schematic diagram of the DNA injection mechanism of T4 bacteriophage. This figure is extracted from **Maghsoodi et al. 2019**.

Like all other viruses, phages are very much species-specific (Young 2013). A single bacteriophage infects a limited number of bacterial strains or even a specific strain within a species. When a bacteriophage infects its host, it follows one of two types of replication strategies- lytic cycle and lysogenic cycle. Bacteriophages adhere to bacteria and introduce their genomes to their cytoplasm during the lytic replication cycle. It utilizes host cell machinery for the production of the viral genome and capsid proteins which assemble and

produce multiple copies of original phages. Bacterial cells are then lysed and new virions are released into the environment to infect other bacterial cells (Young 2013). Additionally, during the lysogenic replication cycle, the phage attaches to the susceptible host cell and injects its genetic material into the cytoplasm of the host cell. In this case, the phage genome is integrated into the host cell genome and maintained as an episomal element. Then it is replicated and passes through the daughter cell killing the previous host cell. Integrated phage genomes are termed prophages and the infected bacteria is known as lysogen (**Figure 2.6**). In some cases, due to some environmental conditions phage genome detaches from the bacterial DNA and enters the lytic stage (Salmond and Fineran 2015).

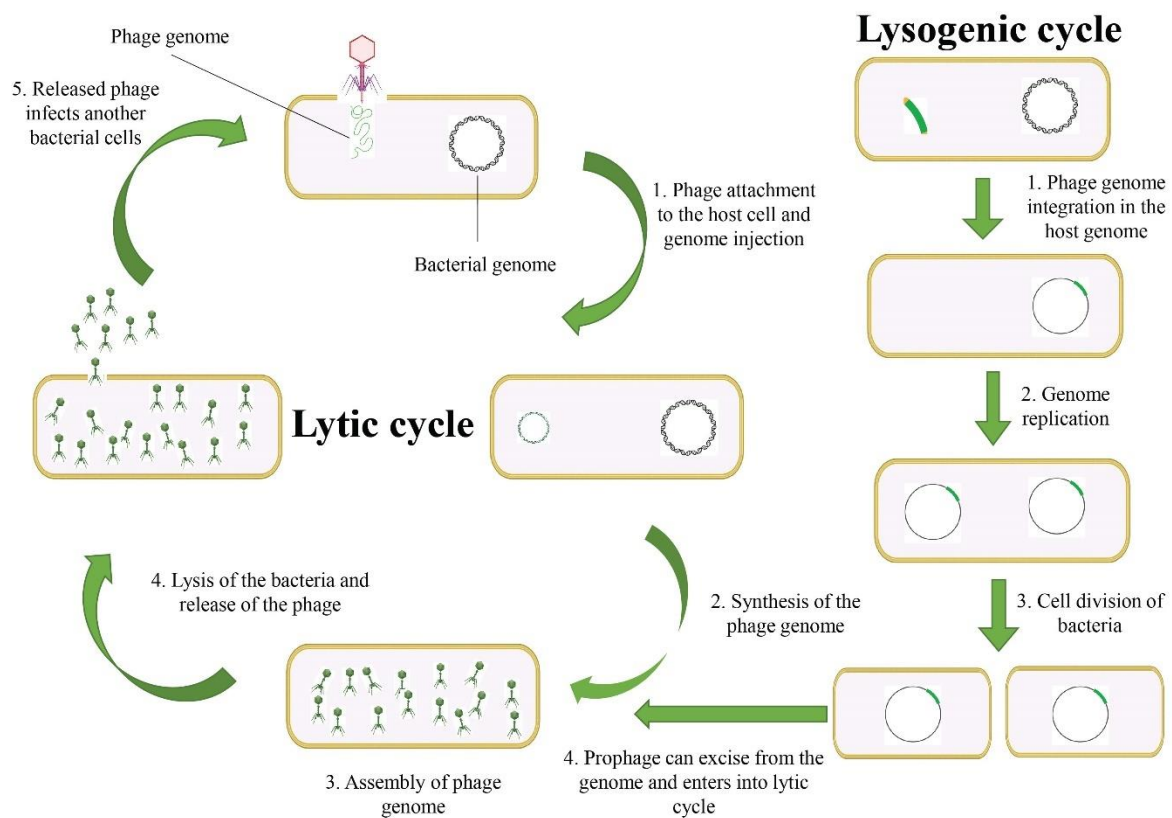


**Figure 2.6:** Lytic and lysogenic life cycle of bacteriophage. The figure is adapted from Stone et al. 2019.

### 2.8 The classification of bacteriophages:

#### 2.8.1 Morphological and structural diversity:

Bacteriophages are bacterial viruses that infect and replicate within their host bacteria and they constitute one of the major groups of viruses (Ackermann, 2011). They are present everywhere in the biosphere where their host bacteria are present. The classification of bacteriophages nowadays remains challenging because the number of bacteriophages reached millions. Whereas molecular biology has allowed living organisms a progressive shift from character-based classifications to genetic markers-based classification (Sunagawa et al. 2013) but till date, no satisfying methods for phage classification exists. Bacteriophages were initially classified based on the nature of their nucleic acid and phage virion morphology. A bacteriophage virion is made up of single- or double-stranded DNA or RNA that is enclosed in a protein-based capsid. This genetic material can be polyhedral (*Corticoviridae*, *Leviviridae*, *Tectiviridae*, *Microviridae*, and *Cystoviridae*), pleomorphic (*Plasmaviridae*), filamentous (*Inoviridae*) or connected to the tail (*Caudovirales*). International Committee on the Taxonomy of Viruses (ICTV) used virion morphology, nucleic acid composition (ssDNA, ssRNA, dsDNA, or dsRNA) and host range to classify bacteriophages. For example, in 1999 ICTV reported that the tailed bacteriophages were classified into 3 families, 16 genera, and 30 species whereas in 2018 ICTV reported that the phage was grouped into five families, 26 subfamilies, 363 genera, and 1,320 species ([https://talk.ictvonline.org/taxonomy/p/taxonomy\\_releases](https://talk.ictvonline.org/taxonomy/p/taxonomy_releases)).

#### 2.8.2 Tailed phages:

In the literature study, it was described that 95% of bacteriophages belong to the order of *Caudovirales* or tailed double-stranded phages and *Caudovirales* are divided into three major families based on their different tail morphology: *Siphoviridae*, *Myoviridae* and *Podoviridae*, *Herelleviridae* and *Ackermannviridae*. 60% of phages belong to *Siphoviridae* family with long, double-layered non-contractile tails; 25% phages are from *Myoviridae* family with long, double-layered contractile tails; and 15% of phages belong to the family of *Podoviridae* with short, stubby tails. Lastly, *Herelleviridae* and *Ackermannviridae* were created recently because the meta-analysis and network-based approach revealed that these two classifications represent a distinct group within the *Myoviridae* phage (Adriaenssens et al. 2012; Barylski et al. 2020).

Tailed phages are composed of protein and DNA in a 1:1 ratio. In double-stranded DNA phages, the DNA winds tightly into the viral capsid in such a way that it tends to form a condensed

layer with a rigid protein shell and it constitutes 20-50% of its mass (Earnshaw and Harrison, 1977). All *Caudovirales* bacteriophages have icosahedral symmetry (20 sides/12 vertices) or elongated derivatives (with known triangulation numbers of T=4, 7, 13, 16, and 52). The size of the phage head depends on the genome size packaged inside the capsid. The diameter of the phage heads varies between 45-185 nm.

All the members of *Caudovirales* shared the same major capsid protein fold (MCP fold) or HK97 fold. This fold was identified by X-ray crystallographic study of the capsid structure of phage HK97 (Duda and Teschke 2019).

In tailed bacteriophages, there is a knob-like structure in the capsid portal vertex that connects the head and tail structure known as portal protein or connector (Orlova et al. 2003). This portal complex also plays a vital role in the phage infection cycle. This connector part controls the entry of the genetic material and assembly of the tail part of the phage to the immature head during morphogenesis. In tailed bacteriophages, DNA transport can be achieved by the conformational change in the portal protein structure (Donate et al., 1988; Valpuesta et al., 1992) or by binding of head completion proteins that close the portal channel forming the connector (Jiang et al. 2006).

The major reason for the high infection efficiency of the tailed bacteriophage is a specially designed part known as the tail. The tail is present in 96% of all bacteriophages and it mainly attaches to the bacterial cell wall and injects its genetic material. Tail shafts have six-folded or three-fold symmetry and it is composed of helical subunits varying from 3 to 825 nm in length. Based on the tail morphology there are three groups of phages: *Myoviridae* (long, contractile tail), *Siphoviridae* (long, non-contractile tail), and *Podoviridae* (short, non-contractile tails) (**Figure 2.7**). All the long-tailed phages contain a large gene (usually > 2 kbp) encoding a tape measure protein and this protein is responsible for determining the phage tail length. *Myoviridae* bacteriophages have a very complex tail structure and it consists of a baseplate with tail fibers and a long, non-contractile tube surrounded by a contractile sheath. For instance, bacteriophage T4 has a tail sheath consisting of 22 different proteins (Leiman et al., 2004; Mesyanzhinov, 2004). The non-contractile tail is composed of multiple copies of one protein, known as the major tail protein. The capsid and tail joining protein gpFII of the *Siphoviridae* phage lambda have a similarity in their tertiary fold with its tail tube protein gpV and it takes the same quaternary structure when assembled in the phage (Cardarelli et al. 2010). This gpV protein has a structural similarity with the tail tube protein of *Myoviridae* phage as

## CHAPTER 2

well as some of the components of the type VI secretion system such as the Hcp1 protein (Pell et al. 2009). When the signal is initiated for the genome ejection, the DNA is passed through the tail and the conformational changes occur. In the case of *Myoviridae* phages signal is transmitted through the tail sheath whereas in case of *Siphoviridae* changes occur in the tail tube (Plisson et al. 2007). Lastly in the case of *Podoviridae* phages the inner protein might be ejected from the head to generate a delivery channel (Kemp, Garcia, and Molineux 2005). The family of *Podoviridae* bacteriophages has a very short and non-contractile tail. A tube-like extension of the tail part of the *Podoviridae* phage penetrates into the cell membrane and transfers the genetic material (Pell et al. 2009).

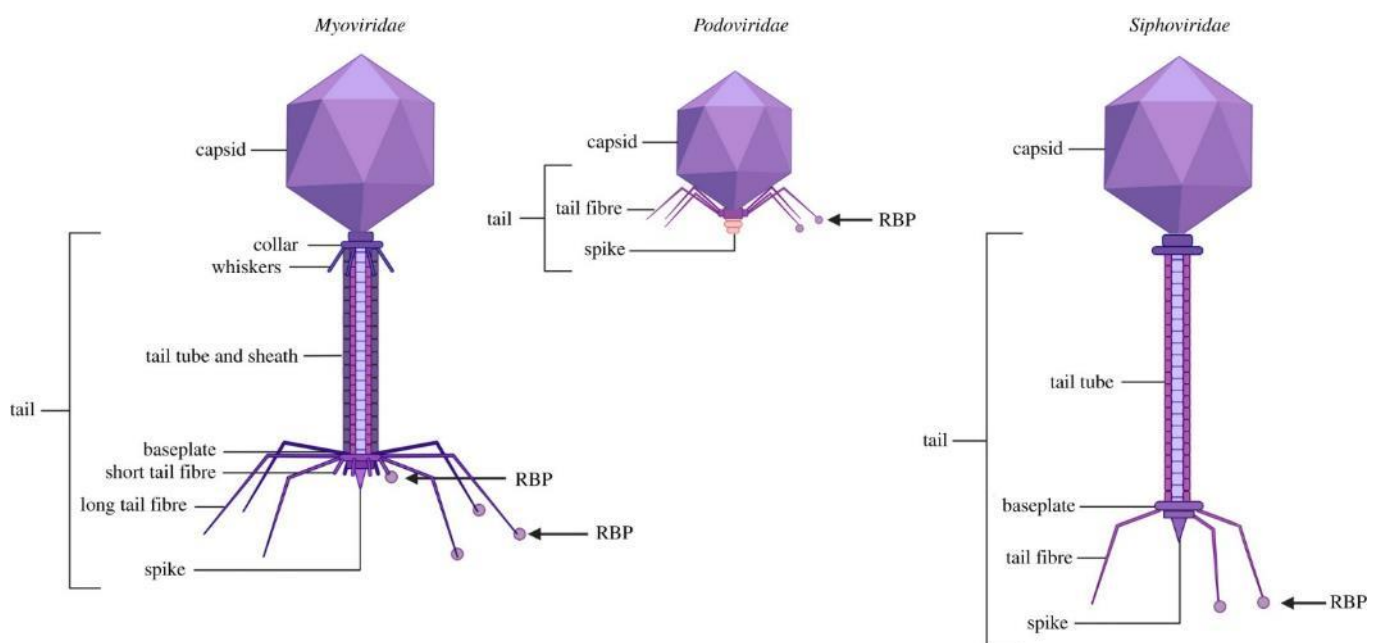


**Figure 2.7:** The basic morphology of tailed bacteriophages belongs to the *Caudovirale* family. From left to right *Myoviridae* bacteriophage (long contractile tail), *Podoviridae* bacteriophage (short stubby tail), *Siphoviridae* bacteriophage (long non-contractile tail). This figure is extracted from **Ongena, Briegel, and Claessen 2021**.



### 2.8.3 Membrane containing phages:

Bacteriophages belong to the family of *Tectiviridae* and *Corticoviridae* composed of non-tailed icosahedral virions that contain an internal lipid membrane and linear or circular double-stranded genome. The specialty of these two families of phages is the presence of the trimeric major capsid proteins composed of a double  $\beta$ -barrel structure (Benson et al. 1999). The structural analysis study of the major capsid protein structure revealed that it contains an N-terminal  $\alpha$ -helix which interacts with the lipid of the membrane and it shares structural homology with the major capsid protein of adenovirus. The phages belonging to these two families don't have any tail to deliver their genome to Gram-negative host bacteria. The membrane of this phage transforms into a proteolipid tube and pierces the host cell membrane to insert its genome (Peralta et al. 2013). Phages belonging to the member of *Cystoviridae* contain a lipid membrane that surrounds the icosahedral capsid of the phage (Vidaver, Koski, and Van Etten 1973). *Plasmaviridae* is another category of membrane-containing viruses. The phages that belong to this category do not have any capsid structure. The genome of these phages is enclosed in a proteinaceous lipid-containing vesicle (Greenberg and Rottem 1979). For example, the *Archoleplasma* virus belongs to this *Plasmaviridae* category that infects the wallless *Archoleplasma* bacteria genus and after the infection, new virions are released by membrane budding without cell lysis (Krupovic 2018).

### 2.8.4 Bacteriophages with small icosahedral capsids:

Microviridae bacteriophages contain a ssDNA genome surrounded by a small icosahedral capsid structure. The capsid structure is built on a protein fold (containing a  $\beta$ -barrel structure) and has a similarity with the eukaryotic ssDNA virus. The proteins are involved in the genome delivery of phage to the host cell. *Microviridae* phage is further divided into two subfamilies *Bullavirinae* and *Gokushovirinae*. *Bullavirinae* has pentameric major spike protein at the end of the capsid vertex whereas *Gokushovirinae* contains a 'mushroom-like' protrusion that extends along the three-fold icosahedral axes of phage capsid (Chipman et al. 1998).

The family of *Leviviridae* phages has an icosahedral head and ssRNA genome. This kind of phage consists of two kinds of proteins: Major capsid proteins and a single copy of maturation protein. This maturation protein interacts with the host receptor during phage adsorption and also interacts with genomic RNA during genome packaging (Valegård et al. 1990). The MCP protein interacts with the initiation codon of the replicase encoding gene and controls the

replication cycle (Peabody 1993). Recently the cryo-electron microscopic study of viral capsid was performed and this study revealed that the ssRNA genome of the phage is involved in the assembly of virion by forming a secondary scaffold structure (Koning et al. 2016). The genome packaging mechanism of the family of *Leviviridae* phages is completely different from the *Caudovirales*. In the case of the *Caudovirale* family, the phage capsids are first assembled and then filled with the genome (Casjens 2011).

### **2.8.5 Phages with filamentous morphology:**

*Inoviridae* phages belong to this group. The morphology of *Inoviridae* family phages is quite different. Phage particles of this group contain an ssDNA genome surrounded by thousands of copies of major capsid proteins that assembled and extrude from the host bacterial cell in a continuous manner (Rakonjac et al. 2017). The major capsid protein (MCP) of this family of phages is composed of a long  $\alpha$ -helix with an N-terminal signal peptide (Xu et al. 2019). The signal peptide is cleaved before the proteins of the phages are assembled into a long cylindrical spiral shell with a C-terminus attached directly to the ssDNA genome (Russel and Model 1981).

## **2.9 Basic characterization of bacteriophages:**

### **2.9.1 Host specificity:**

Host specificity is one of the major advantages of bacteriophage. This trait has the effect of making them harmless to all prokaryotic cells outside of their host range in addition to eukaryotic cells. In fact, there is mounting evidence that the microorganisms that live inside our bodies have a significant impact on our general health. By contrast, antibiotic therapy can have a significant adverse effect on our normal microbiota due to its more widespread, broad-range impact leading to major side effects. The ability of the bacteriophage to infect a variety of hosts would seem to be a sign of the success of phage therapy as it would enhance the possibility of phages to come into contact with a susceptible bacterial cell. It is essential for the survival of the phage population (Koskella and Meaden 2013). Bacteriophages used for therapeutic purposes are not always able to infect a variety of bacterial strains therefore use of a phage cocktail is another better option for the treatment.

### 2.9.2 Determination of lytic and virulent nature:

Phages that can only undergo the lytic cycle or virulent phages are ideal for therapeutic purposes as their multiplication is almost always followed by lysis of the infected cell. These phages are also sometimes called “professionally lytic” (Hobbs and Abedon 2016). During the phage selection process, virulent and temperate phages can tentatively be differentiated as they respectively produce clear and turbid plaques on a bacterial lawn. The next step is to establish whether a potential phage can propagate effectively both *in vitro* and *in vivo* after it has been established that it is strictly virulent and not a superspreader. For the *in vitro* study a one-step growth curve is usually performed to find out if the phage qualifies with a large burst size and short latent phase. Once the ability of bacteriophage to proliferate *in vitro* has been confirmed, *in vivo*, tests should be carried out to demonstrate that the virus can also replicate effectively at the infection site if the target host is present.

### 2.9.3 Safety and toxicity:

After the isolation, it is necessary to perform genome sequencing and analysis of a bacteriophage. The absence of lysogeny-related genes such as the lytic cycle repressor, integrases, or site-specific recombinases can be determined by analysis of the phage genome sequences. Additionally, genome analysis is the most reliable technique to confirm if the phage genome encodes any toxin or antimicrobial resistance determinants. In fact, the phage should never be considered for therapeutic uses if there are any such genes. Additionally, it is preferable to pick a propagation host that does not have prophages or virulence/antibiotic resistance markers (Gill and Hyman 2010). Besides not being carriers of “bad genes”, bacteriophages must be harmless when administered to patients. As mentioned in the previous point it should not infect non-target bacteria and leave the normal microbiota undisturbed. However, it is important to remember that before treatment, phages need to be well purified to remove any harmful stuff.

### 2.9.4 Antibiofilm activity:

Biofilm formation is one of the common defense mechanisms of bacteria in both natural and artificial environments, including inside the human body. Thus, biofilms support bacterial pathogenicity particularly in the event of persistent infections (Costerton, Stewart, and Greenberg 1999). The ability of these multicellular structures to withstand attacks from the

immune system or antimicrobial substances enables the bacterial cells to survive in situations that would ordinarily be adverse (De la Fuente-Núñez et al. 2013). Due to their difficult-to-remove nature, biofilms are a significant issue that must be resolved in order to effectively battle diseases. In this regard, bacteriophages may be a fascinating alternative to traditional antibiotics or disinfectants due to their unique properties (Geredew Kifelew, Mitchell, and Speck 2019). However, it is necessary to demonstrate that a given phage is a useful antibiofilm agent. One intriguing characteristic of some phages is the presence of genes encoding for exopolysaccharide depolymerases, which can destroy the polysaccharide component of the extracellular matrix of biofilms and enable the phage to enter the deeper levels of this complex structure and disperse the biofilm (Latka et al., 2017; Pires et al., 2016). The domain of a depolymerase is often displayed at the tip of the phage as tail fibers. On the other hand, lysin is another enzyme encoded by lytic bacteriophages that is capable to cleave the bacterial peptidoglycan cell wall from the inside and outside respectively (Schmelcher et al., 2012; Yan et al., 2014).

### **2.9.5 External factors affecting bacteriophages:**

#### **2.9.5.1 Temperature:**

Temperature is a crucial factor for bacteriophage survivability (Olson et al., 2004). It is important to the processes of attachment, penetration, multiplication, and duration of the latent phase. Fewer phage genetic components enter bacterial host cells at temperatures below optimum levels, which limits the number of them that can participate in the multiplication phase. The latent stage may last longer at higher temperatures (Tey et al. 2009). Furthermore, the prevalence, viability, and storage of bacteriophages are all influenced by temperature. Good phage stability was observed for over 6 months when stored at 4°C. It was previously reported that tailed phages were the most resistant to storage and showed the longest survivability; some of them retained viability even after 10–12 years at 4°C (Łobocka, Głowacka, and Golec 2018).

#### **2.9.5.2 pH factor:**

Another important factor influencing phage stability is the acidity of the environment. Some phages can be kept in solution or dry form for a long time at neutral pH (6 to 8) (Jończyk et al. 2011). Phage titers generally decrease slowly with pH. In addition to limiting the growth of

some phages below pH 4.5, pathogenic bacterial food contamination risk is typically decreased as well (Watanabe et al. 2007). For example, the phage T4 (*Myoviridae* family) is unstable at pH < 5. Moreover, stomach acid can negatively affect the survival of phage in the event of phage oral injection, which could result in therapy failure. Therefore, additional protection is desirable to enhance phage survival in the gastrointestinal tract. Phage encapsulation in natural biopolymer-derived matrices has been used as a strategy to improve phage stability (Dini et al. 2012; Metters and Hubbell 2005). However, for this type of method, the choice of biopolymer is crucial, and various requirements must be met, including the capacity to be modified quickly, to not be harmful, and to be environmentally benign. Therefore, new strategies are constantly developing. Lytic phage genetic engineering has historically been challenging, but with the development of new techniques like Bacteriophage Recombineering of Electroporated DNA (BRED), it is now turning into a straightforward procedure that is less expensive than encapsulation and doesn't need specialized tools or reagents (Marinelli et al., 2012).

### **2.9.5.3 Salinity:**

Bacteriophages need salts at low concentrations for a successful infection process and their growth. At low concentrations, the salt ions at low concentrations start interacting with proteins and then stabilize the protein structure by neutralizing protein charges. But, at high concentrations, the salt increases the thermal denaturation process of the proteins and can also unfavorably affect the stability of the phage nucleic acid structure (Fennema 1996; Silva et al. 2014).

## **2.10 Bacteriophage genomics:**

### **2.10.1 Background study:**

The genome of the bacteriophages is short in length and easy to isolate so phages were the first whose full-length genome were sequenced. Phage  $\phi$ X174 genome was sequenced at the beginning. The length of the genome was 5386bp and it was a single-stranded DNA (Sanger et al. 1977). The first complete sequence of double-stranded DNA was determined for lambda phage and the genome length was 48,502bp (Sanger et al. 1977). After a short period, a T7 phage genome with 39,936bp length was reported (Dunn, Studier, and Gottesman 1983). Ten

years later the first double-stranded genome of the tailed phage mycobacteriophage L5 was sequenced (Hatfull and Sarkis 1993).

It was reported in previous studies that the diversity of the bacteriophage is quite high. The total population of bacteriophage in the biosphere is about  $10^{31}$  particles and viral ecologists also calculated that there are  $10^{23}$  phage infections per second occur (Hatfull and Hendrix 2011). Little to no nucleotide sequence similarity exists across bacteriophages recovered from various bacterial sources. This further indicates that the phage population is not only large but also very diverse (Kwan et al. 2006).

There are two primary goals of the advancement of phage genomics. First, a question is arisen after seeing the phage population is how phage genomics related to hosts and each other. Second is phage genomics largely used for the development of biotechnological, genetic, and clinical tools.

### **2.10.2 Genomic diversity of bacteriophages:**

According to the NCBI report (National Institute of Biotechnology Information) till 2019, a total of 8437 complete phage genomes were divided into 12 families (based on ICTV classification) with one unclassified group. Among them, more than half of the genome is from the member of the *Siphoviridae* family with a long flexible non-contractile tail. In a SEA-PHAGES (Science Education Alliance–Phage Hunters Advancing Genomics and Evolutionary Science) program 1,537 *Siphoviridae* bacteriophages infecting *Mycobacterium smegmatis* was isolated and their genome sequencing was performed (Jordan et al. 2014). SEA-PHAGES program is jointly administered by Graham Hatfull's group at the University of Pittsburgh and the Howard Hughes Medical Institute's Science Education division. Among the remaining 17% phages belong to the *Myoviridae* family with long contractile tails and 12% belong to the *Podoviridae* family with short stubby tails. According to this study, double-stranded tailed phages (family of *Caudovirales*) are the most abundant group (>85%) in the public genomic database. In the near future, the proportion of the tailed bacteriophages will be reduced as new phages are continuously discovered. For example, 258 new single-stranded DNA phages were identified in the gut of the marine invertebrate *Ciona robusta* (Creasy et al. 2018). Before this identification, the diversity in the family of *Microviridae* phages was underestimated. In addition, unclassified bacteriophages have been identified within the NCBI databases discovered through metagenomic studies that are yet to be isolated. For example, 283 non-

tailed dsDNA phages infecting *Vibrionaceae* bacterial family have been identified (Kauffman et al. 2018). Recently 10,295 *Inovirus*-like sequences are found and among them, 5,964 distinct species have been identified (Roux et al. 2019). This study further increases the 100-fold genomic diversity within the *Inoviridae* family. The number of complete phage genome sequences is continuously increasing today but this still represents a small fraction of the actual phage genomic diversity (**Figure 2.8**).

The range of the genome is also very diverse. The smallest dsDNA phage genome to date is reported that of *Leuconostoc* phage L5 and the genome size is 2,435 bp. The smallest double-stranded DNA phage genomes for *Podoviridae*, *Siphoviridae*, and *Myoviridae* are 11.5 kb (eg. *Mycoplasma* phage P1) (Tu et al. 2001), 21 kb (eg. *Lactococcus* phage c2) (Lubbers et al. 1995), 30 kb (*Pasteurella* phage F108) (Campoy et al. 2006) in sizes. These genomes are packaged inside the capsid of the bacteriophages and the size of the capsids varies according to the function of the genome size. Nowadays some of the jumbo phages whose genome size is >200 kb have been isolated and characterized and these phages show a unique genomic feature (Yuan and Gao 2017). The genome of these jumbo-size phages carries the replication and DNA metabolism genes. A new type of phage, known as mega phage with a genome size larger than 540 kb has recently been found from the human and animal gut metagenomes analysis and this phage is predicted to infect *Prevotella* species (Devoto et al. 2019). These phages are seen widely in the human, baboon, and pig gut microbiomes.

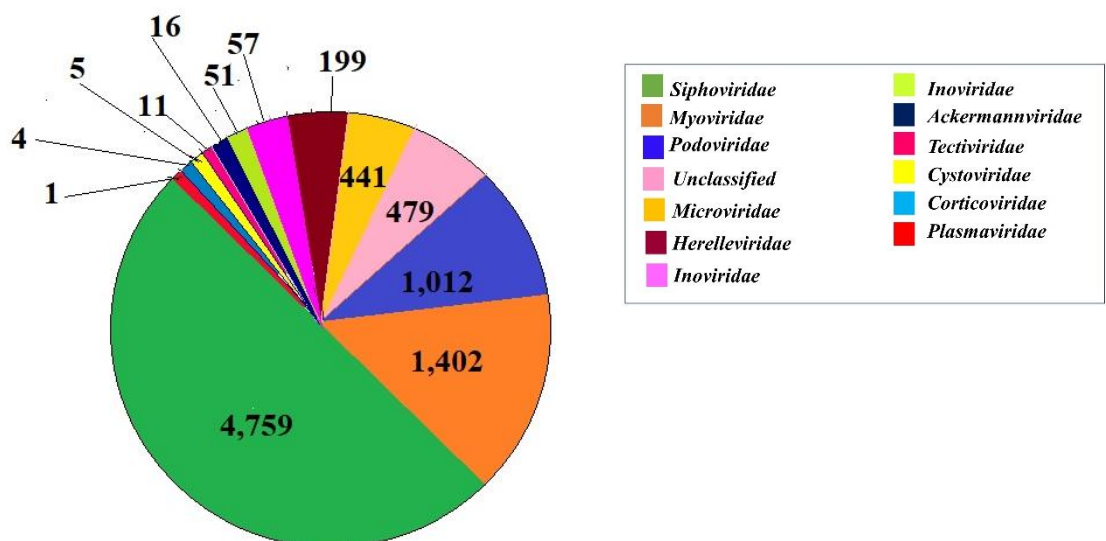


**Figure 2.8:** Number of complete genomes and genome size distribution in phage families. This figure is adapted from **Dion, Oechslin, and Moineau 2020**.

### **2.10.3 Metagenomics of bacteriophage:**

There are a large number of phages in the biosphere but the genome diversity of phages is difficult to comprehend (Bergh et al., 1989). Bacteriophages can infect different host bacteria that may have little or no sequence similarity. Phages can also infect a single host and may also display sequence differences (Grose and Casjens 2014). When the nucleotide distance and gene content was measured by pair-wise comparison of 2,333 phages, the data showed that there is no detectable homology in 97% of cases (Mavrich and Hatfull 2017). New techniques such as viral metagenomics help to understand the size of phage global diversity.

Metagenomics of the bacteriophage provides an alternative structure of the phage genome that is complementary to whole genome sequencing. The presence of a large percentage of unknown sequences and their substantial genetic diversity are two of the most prominent characteristics of phage metagenomics. The first metagenomic study was published in 2002 from seawater samples (Breitbart et al. 2002). To construct the virome (the viral sequence acquired from viral metagenomics) a good quality nucleic acid (Brum and Sullivan 2015), reduced cost of sequencing, and, a set of analytical tools (Breitbart et al. 2018) are required. In recent years there are at least 90 studies of virome from aquatic environments (Williamson et al. 2017), 38 studies of virome from the human gut, and 8 studies from the soil (Williamson et al. 2017). Viral metagenomic studies of marine samples have been performed in three research consortia: the Pacific Ocean virome (Brum et al. 2015), the Tara Ocean (Hurwitz and Sullivan 2013), and the Malaspina Oceanic research expeditions (Duarte 2015). These studies help to characterize the ocean double-stranded DNA viruses in detail (Coutinho et al. 2017; Roux et al. 2016). Additionally, in 2003 the first human gut virome was published (Breitbart et al. 2003). In 2014, a phage abundantly present in the gut of humans called crAssphage was discovered by a metagenomic study (Dutilh et al. 2014). All these studies suggested that the phage genetic diversity still remain uncharacterized but in the case of marine and human sample, the result is different.

### **2.10.4 Evolution of bacteriophage:**

It was reported that the bacteriophage genome showed greater novelty in the biological world. The proteins encoded by the genome of the bacteriophage are unrelated to most of the known proteins. The question is what is the function of these phage proteins? The microbial ecology suggested that when bacteriophages infect the host bacteria, the host restriction system against



bacteriophage may be activated. There are several host-mediated protection systems such as CRISPER's (Deveau, Garneau, and Moineau 2010), restriction-modification (King and Murray 1994), Toxin-antitoxin system (Fineran et al. 2009), and tRNA cleavage (Amitsur, Levitz, and Kaufmann 1987) as well as some phage-encoded mechanism to generate genome diversity in high frequency (Medhekar and Miller 2007). Phages also carry some genes that counteract host protection systems such as RNA repairing (Zhu, Yin, and Shuman 2004), and anti-restriction systems (McMahon et al. 2009) and also provide some genes that protect the phages from other viruses. Therefore, it can be said that phages are able to encode their own restriction enzyme, immunity system, and toxin-antitoxin systems.

### **2.11 Contribution of electron microscopy in the study of bacteriophages:**

#### **2.11.1 Importance of electron microscopy:**

For a long time, light microscopy was used to visualize various biological objects that are not visible to the naked eye (Ram, Ward, and Ober 2006). Ernst Ruska and Max Knoll built the first transmission electron microscope in the early 1930s (Knoll and Ruska 1932). The development of the transmission electron microscope has widened the structural biology field. Keith Porter took the first electron micrograph of eukaryotic cells ten years after the development of the transmission electron microscope (Porter, Claude, and Fullam 1945). The electron microscope uses a beam of electrons to create an image of a sample at a higher magnification and greater resolution than the image created by light microscopy. The wavelength of electrons (less than 0.1 nm) is shorter than the wavelength of visible light (wavelength 400-700 nm). The charge of the electron beam creates an electromagnetic field to focus the electrons (Orlova and Saibil 2011) and the shorter wavelength of the electron beam allows one to visualize the detail of small objects. However, biological samples are sensitive to electron irradiation and they are also not stable under a vacuum which is necessary for the electron to produce an image. These factors contribute to reducing the image resolution.

At the very beginning, shadow casting on the samples with heavy metal vapor was used to increase the contrast before examining them under the transmission electron microscope (HALL 1966). This process gave information regarding the size and shape of the sample but could not produce any internal structural detail. Metal shadowing also increased the roughness of the sample film which made detailed observation of the samples difficult.

### 2.11.2 Use of negative staining to study bacteriophages:

In 1959 Brenner and Horne introduced a method called negative staining of the sample (Brenner and Horne 1959). Negative staining is a simple and rapid method to visualize and examine the morphology of various organelles, macromolecules, and viruses (e.g. bacteriophages). Negative staining is used to visualize different biological samples under a transmission electron microscope. In this method, a drop of the biological sample is placed on a support matrix and stained with heavy metal salt e.g., uranyl acetate (Harris and De Carlo 2014), uranyl formate, phosphotungstic acid, or ammonium molybdate. Thereafter the sample is air-dried and later checked under the transmission electron microscope (**Figure 2.9**). In negative staining, however, the samples are unstained but are made visible against a dark background. This method generally involves staining a liquid sample in order to study the morphological shape and size. But at times arrangement of cells may be difficult or too delicate to stain. But this technique does not produce any fine details of the sample and the actual shape or structure sometimes gets distorted due to the stain deposition. The technique was applied at first to visualize tobacco mosaic virus and turnip yellow mosaic virus.

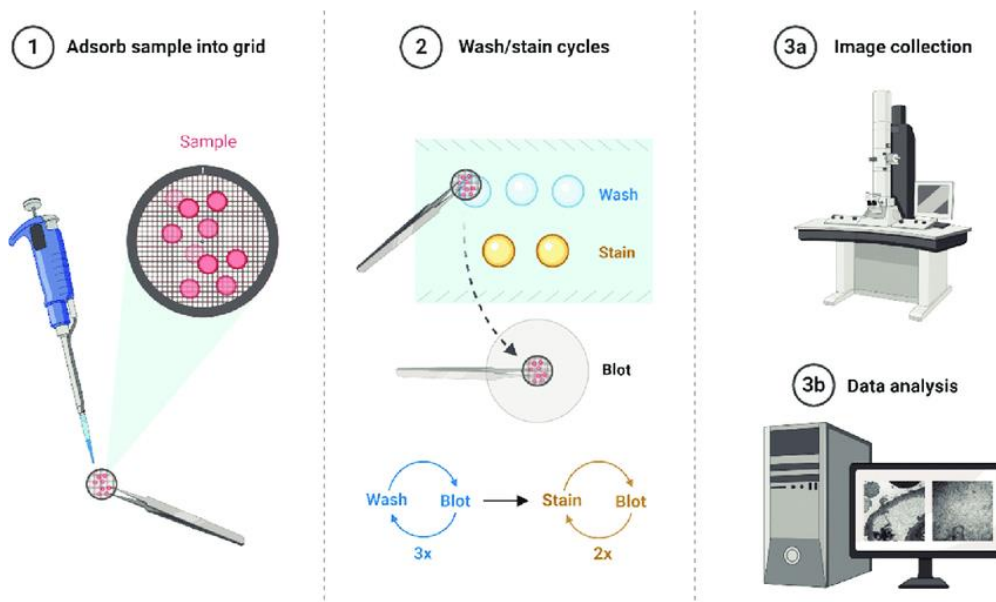


**Figure 2.9:** Schematic diagram of the negative staining and visualization using transmission electron microscopy. This figure is extracted from **Hacking and Bijol 2021**.

### 2.11.3 Use of cryo-electron microscopy to study the structure of bacteriophages:

Before the development of electron microscopy, X-ray crystallography was the only choice to determine the structure of the virus (eg. bacteriophages) and other biological molecules (Harrison et al. 1978). Cryo-electron microscopy is a technique that has the ability to provide three-dimensional structural information of different biological molecules and bacteriophages without crystallizing them. Modern cryo-electron microscopy began with the establishment of the unique specimen preparation technique by Dubochet and coworkers (Adrian et al. 1984). In this technique, the specimen is prepared to keep the biological sample in its native condition (Adrian et al. 1984). The main advantage of cryo-electron microscopy over negative staining is getting a high-resolution near-native structure. In the cryo-EM technique, the direct observation of the biological specimen is possible without any chemical fixation. By using cryo-EM, a high-resolution structure can be obtained, but it also depends on how the specimen is prepared and the technical specification of the cryo-electron microscope.

The method of sample preparation is based on the fast freezing (at a speed of  $10^4$  °C/second) of the different biological samples using a cryogenic agent such as liquid ethane. High-speed freezing helps the sample to be fixed in a vitreous state. A vitrified form of ice helps to preserve the specimen in a hydrated near-native state. If the freezing process occurs too slowly, crystalline ice is produced that further disturbs the structural integrity of the specimen. Crystalline ice formation also degrades the quality of the image as the electrons are diffracted. The sample is kept in liquid nitrogen after freezing to maintain the temperature until the sample is introduced into a sample holder. The low temperature of the sample is also maintained inside the sample holder when images are captured. No contrasting agents are used during the imaging and images are taken at a very low electron dose to prevent radiation damage of the sample (**Figure 2.10**). The signal-to-noise ratio of the cryo-EM sample is usually very low. Another inherent problem is the occurrence of beam-induced sample motion when the specimen is exposed to an electron beam that blurs the captured images.

With the technical advancement in various fields of electron microscopy, high-quality images are now easily produced. Previously tungsten filament or LaB6 filament was used as an electron source. Nowadays field emission guns (FEG) (Williams and Carter 2009), improved optics, better microscope design, and automated data collection software have revolutionized the imaging and reconstruction process.

Previously photographic film was used as a recording device in cryo-EM imaging. The images of the cryo-EM are intrinsically noisy due to the use of a low electron dose. The perfect image detector will add no noise. The use of photographic film was very inconvenient and time-consuming. Moreover, a limited number of images were possible to collect each day and the films were further needed to develop. Thus, an expensive densitometer was needed to digitize the images. Therefore, CCD cameras were developed to reduce this inconvenience. Automated microscope alignment and image acquisition were possible with this CCD camera (Cheng et al. 2010). The scintillator layer inside the CCD camera results in the conversion of incidence electrons into visible light photons and this conversion causes the loss of resolution and sensitivity. In the last few years the commercial availability of direct electron detector (DED) after its development initiated the revolution in biological transmission electron microscopy (Brilot et al. 2012). The signal-to-noise ratio of the DED is much higher than the photographic film or scintillator-based CCD cameras. The fast readout of the direct electron detector camera split the dose into short frames followed by the alignment of frames which is carried out computationally after data collection. As a result, beam-induced motion has also been minimized.

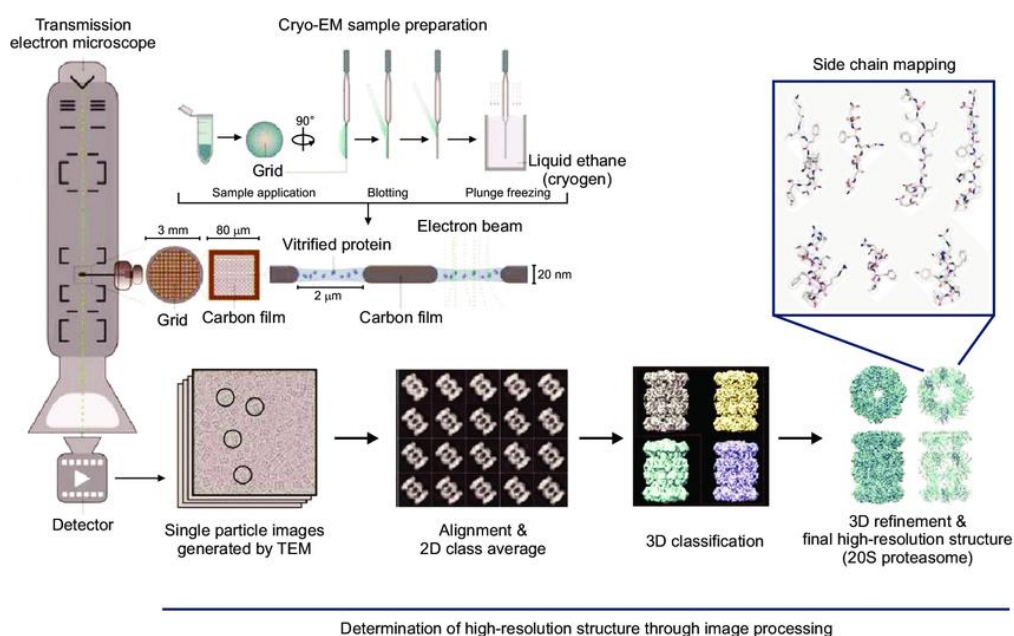


**Figure 2.10:** A step-by-step workflow of single particle cryo-electron microscopy imaging and data processing. The figure is extracted from **Chung and Kim 2017**.

### **2.11.4 Use of scanning electron microscopy to study bacteriophages**

Scanning electron microscope (SEM) is also a useful tool for the visualization of the morphology of various biological samples. The images are obtained with an SEM by scanning the sample surface with a high-energy electron beam. When the electrons interact with samples, secondary electrons, and backscattered electrons are produced that provide information on the cells or tissue surfaces.

For SEM imaging the electrically conductive sample surface is needed. To create a conductive sample surface, the SEM samples are often sputter-coated with electrically-conducting metal commonly gold or gold-palladium alloy. The initial dehydration of samples is required for the sputter coating. To visualize the wet sample another approach of imaging can be used using an environmental SEM(ESEM). In ESEM the differential pumping technique allows increasing the pressure to about 10-20 torr around the sample. Bacteria can be visualized by this ESEM but the flagella and fine details can't be visualized clearly. Sample drying is also needed for this technique. ESEM is useful for larger specimens that can be visualized below 1000X magnification (Bergmans et al. 2005).

## **2.12 Structural studies of bacteriophages:**

### **2.12.1 Overview of bacteriophage structure:**

Bacteriophages are obligatory parasites, requiring the host cell machinery to reproduce. These parasites consist of a genome packed inside a proteinaceous structure and sometimes lipids are also present there. To start the infection process phage particles are attached to the host cell surface by recognizing the receptor on the host cell surface. After the attachment, the phage particles inject their genome inside the host cell. Once entered into the host cell cytoplasm, phages hijack the cellular components of bacteria and shut down the defense mechanism. The protein biosynthesis machinery of bacteria gets stopped and phage genes are expressed. Phages use the host replication machinery to replicate their genome, which is then packed into self-assembling bacteriophage particles. At the end of the lytic cycle of phages, newly formed progeny phage particles are released and eventually, the host cell lysis takes place (Abedon 2006).

Bacteriophages are non-enveloped viruses composed of a stable outer capsid structure. The packed genome remains inside the capsid. To date, most of the isolated bacteriophages

discovered have linear, double-stranded DNA genomes. The head part of the bacteriophage is connected to the tail through the connector protein complex. At the end of the tail, an adsorption device remains present, known as a baseplate. There are different types of capsids reported for bacteriophages. Most of them have an icosahedral capsid whereas some of the bacteriophages have helical capsids. The majority of icosahedral capsids feature 532-point group symmetry and contain 60 identical and non-identical protein subunits. The tail structure of the phages is very fascinating as tails evolved with receptor binding, penetration, and delivery of the genome. The tailed phages belong to the *caudovirale* order. According to the metagenomic study, 96% of phages belong to this category. This order is further divided into three families according to their tail morphology- *Myoviridae* phages have a long contractile tail with a sheath around the central tube, *Siphoviridae* phages have a long non-contractile tail, and *Podoviridae* phages have a short non-contractile tail (Ackermann, 2007). Bacteriophages have tail fibers attached to the bottom of the tail. Other tailless phages include polyhedral, filamentous, and pleomorphic phages that have ssDNA or RNA genomes.

### **2.12.2 Importance of bacteriophage structure determination:**

Nowadays a problem has arisen that many disease-causing bacterial strains continuously modify themselves and become resistant to the potent drugs used for treatments. This sometimes results in ineffective treatment and makes the condition worse. The use of bacteriophages in the management of bacterial infections is an alternative strategy to prevent this resistance. Phage therapy initially focuses on the treatment of various bacterial infections in animals (Malik et al., 2017). Understanding the mechanism of phage infection requires knowledge of their structures, host range, and stability of the phages in response to external stimuli (pH, temperature, salt, etc). Moreover, how a phage interacts with its host and how the cell replication machinery aids in bacteriophage reproduction inside the cell are also important to understand. For example, *Myoviridae*, *Siphoviridae*, and *Podoviridae* phages change their tail morphology differently during infection. The structural studies of bacteriophages help us to understand the mechanistic detail to further expand our knowledge of phage biology.

### **2.12.3 Three-dimensional structure determination by Single particle analysis:**

The principle of single particle analysis is described as the averaging of many copies of the multiple views of two-dimensional images of a three-dimensional object. After the averaging of those images, a three-dimensional reconstruction of that object is calculated. For this reason,

single-particle analysis (SPA) is sometimes known as single-particle averaging. In SPA multiple views of the same objects in various orientations are needed to sort out identical views of the particle in different groups to increase the signal-to-noise ratio (SNR). To date, various three-dimensional structures of different biological molecules such as viruses, bacteriophages, and different protein and protein complexes were determined. De Rosier and Klug used the Fourier transformation approach to determine the symmetry and construct the object's three-dimensional structure in 1968 (De Rosier & Klug, 1968). Later in 1971, the detailed process of three-dimensional structure reconstruction from negatively stained images of a virus particle was described by Crowther (Crowther 1971).

The two basic steps of the image reconstruction workflow are the search for the orientation of all projections of an object and 3D reconstruction. There are multiple steps between these two steps. The cryo-EM images are collected in defocused and low-dose conditions to get a high-resolution structure. Nowadays automated data collection software facilitates the collection of a large set of data in a comparatively short period for reconstruction. There are some data acquisition software: UCSFImage4 (Li et al. 2015), Leginon (Suloway et al. 2009), serialEM (Mastronarde 2005), etc and these systems are freely available. E pluribus unum or EPU (FEI, Eindhoven) is an example of a commercial system that is also used mainly for automated data collection. The estimation of accurate CTF is important for both the initial evaluations of the micrograph and structure determination. Thus, CTF estimation is an important step in image processing. To estimate the CTF various parameters like spherical aberration, acceleration voltage, defocus, amplitude contrast and astigmatism must be known. Among them, voltage and spherical aberration are instrumental parameters. During the image collection defocus needs to be set. Nowadays different software such as ctfind (Rohou and Grigorieff 2015), e2ctf.py (Bell et al. 2016), and gctf (Zhang 2016) are available for the estimation of the CTF. After the CTF estimation, the particles are picked from the CTF-corrected images. Particles can be picked in a manual or semi-automated or fully automated manner. Several software for the particle picking programs such as Relion-auto pick (Scheres 2012c), e2boxer.py (Tang et al. 2007), scipion (de la Rosa-Trevín et al. 2016), Signature (Chen & Grigorieff, 2007) and FindEM (Roseman 2004) are also nowadays available. After picking the particles the first step of the single particle structure determination is the grouping of the data into homogeneous subsets which is also known as 2D class averaging. There are several reasons to start the reconstruction process with 2D class averaging: 1) There are many bad particles present in the 2D dataset which can be removed by simply deleting those class averages. 2) The success rate

of 3D analysis is low if only a few restricted views are available since the angular distribution of the particle views is incomplete. 3) high-quality class averages contain high SNR input data which is important for computational ab initio 3D structure determination. The central section theorem serves as the foundation for the computational ab initio 3D structure determination (CROWTHER RA, DEROSIER DJ, and KLUG A 1970; Ter-Pogossian 1984) which states that Fourier transforms of the 2D projections of the same 3D structure lies on planes centered at the origin of 3D Fourier transform of the object. The Fourier transform of a pair of 2D projections of the same 3D structure intersects along a line, known as a common line. The common line approach was first implemented on icosahedral viruses (Crowther et al. 1970;). The common line approach of orientations is implemented in various software packages. This approach can be done in Real space (IMAGIC) and Fourier space (EMAN, SIMPLE), and class averages are used for this approach rather than the single image (Elmlund and Elmlund 2012; Van Heel et al. 2000; Tang et al. 2007). The stochastic hill climbing (SHC) algorithm is a recently used approach to determine the 3D structure and it also shows great promise in producing 3D initial model. This SHC approach was first implemented in the SIMPLE software package (Elmlund and Elmlund 2012). Once a 3D initial map is reconstructed, it undergoes several cycles of refinement to get the final map. Recently the refinement is based on maximum likelihood algorithms (Scheres, Valle, Nuñez, et al. 2005; Scheres, Valle, and Carazo 2005; Sigworth 1998) and Bayesian analysis (Scheres 2012c, 2012a). The maximum likelihood algorithm in Relion contains a model for the noise and automates judgments about filtering and weighting that were previously done by expert users (Scheres 2012b). The Bayesian analysis approach, combined with the use of a direct electron detector has been extremely successful to produce a high-resolution structure. Sometimes a starting model is required for a highly challenging structure.

### **2.13 Application of bacteriophages for therapeutic purpose**

#### **2.13.1 Early history of phage therapy:**

The discovery of the bacteriophage has many controversies. In 1896 a British bacteriologist Ernest Hankin reported the presence of an antibacterial agent (against *Vibrio cholerae*) in the water of the Ganges and Jamuna rivers in India and he also suggested that this unidentified antibacterial agent is responsible for limiting cholera epidemics. After two years the Russian bacteriologist Gamaleya discovered the same type of antibacterial agent against *Bacillus subtilis* (Samsygina and Boni 1984). However, none of their findings were further discussed



## CHAPTER 2

before 1915. A medically trained bacteriologist Frederick Twort from England reported about the existence of phage in 1915. But his finding was not pursued due to some financial difficulties (Summers 1999; Twort 1915). After two years in 1917, a French-Canadian microbiologist Felix d’Herelle officially discovered the bacteriophage at the Institute of Pasteur in Paris. Besides this d’Herelle and his coworkers isolated the lytic bacteriophages against pathogenic bacteria and also introduced the term “phage therapy” (Fruciano and Bourne 2007). From 1919 onwards phages were started to use for therapeutic purposes before the discovery of the first antibiotic penicillin.

After the major success of *Shigella* phages to treat bacillary dysentery, the expectations of the researcher increased to use phages as therapeutic agents (Krueger and Scribner 1941). However, at that time researchers exactly did not know about the mechanism of phages to infect bacteria and particularly how phages kill the bacteria. Moreover, the discovery of antibiotics in the 1940s declined the interest in phage research (Matsuzaki et al. 2005). Then phage therapy research became limited in Eastern European countries only. In Western Europe, phage therapy research was neglected due to a lack of regulatory framework, inconsistent results, and complications in the patenting procedure (Figure 2.11).

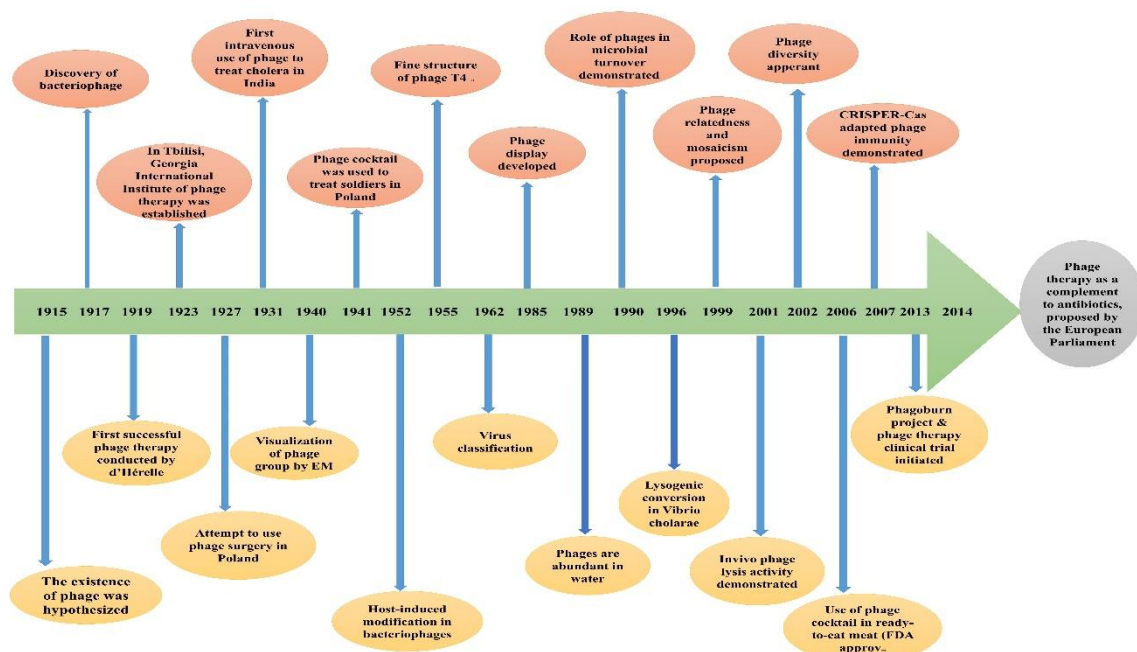


**Figure 2.11:** Milestones of bacteriophage research. This figure is adapted from Elbreki et al. 2014; Salmond and Fineran 2015.

### 2.13.2 Current status of phage treatment:

Nowadays the interest is continuously growing to use bacteriophage for the treatment of infectious bacterial disease and phage therapy regain its popularity (Fischetti 2001). Before the discovery of antibiotics, researchers were trying to use bacteriophages for the treatment of bacterial diseases. In recent times due to the availability of various molecular tools, the understanding of phage control techniques, and evaluation helped phage biologists to increase the application of phages for various purposes. In Eastern Europe, phage has been administered orally in the form of a tablet or liquid, intravenously, topically, and rectally for almost 90 years, and to date, there is no side effect (Sulakvelidze, Alavidze, and Morris 2001). These studies further increase the interest to use phage as a potential therapeutic and biocontrol agent (**Table 2.1**).

There are currently several academic researchers working in the subject of bacteriophage technology and products, along with 11 US and international biotechnology companies. The main aim of these companies and researchers is to use bacteriophages mainly in the food industry and for treatment purposes (**Figure 2.12**). Two US-based phage companies, Novolytics and Intralytics, are using bacteriophage as biotechnology tools. Three phage-based cocktail products have been approved by the FDA and the United States Department of Agriculture (USDA) which is marked as a milestone in the phage therapy research field. The first approved phage product was ListShield™ which can be used against *Listeria monocytogenes* in ready-to-eat meat and poultry products (Mead et al. 2006). The second product was EcoShield™ which can be sprayed on red meat to reduce the growth of *Escherichia coli*. The SalmoFresh™ is the third FDA-approved product and it is used against *Salmonella enterica* spp to treat fresh and processed vegetables, fruits, and different seafoods (Scallan et al. 2011). Nowadays another phage cocktail product ShigaShield™ is currently undergoing FDA and USDA review to know whether it is a safe product (Soffer et al. 2017). According to the report, this product is able to reduce the load of *Shigella* bacteria in various food products infected with *Shigella sonnei*. Currently, a phage cocktail product NOVO12 is released by Novolytix Company, and this product is administered in gel form against Methicillin-resistant *Staphylococcus aureus* bacterial infections. The European Union also supports phage therapy research. In 2013 a project Phagoburn was funded by the European Commission and the aim of this project is to use the phage to protect the burn wound patient from bacterial infections. In April 2014 European parliament passed a report in which phage

## CHAPTER 2

therapy was prioritized to combat antibiotic resistance. All these studies actually help to increase interest in phage therapy research and hopefully, in the near future, the scope of phage-based product development will increase.



**Figure 2.12:** List of some FDA-approved phage-based products.

**Table 2.1:** Activity and the center of phage therapy, adapted from S. S. Tang et al., 2019.

Name of the Phage therapy center	Country	Activities
Center for phage therapy	Poland	Bacteriophages have been used to treat the bacterial infection since 1980s ( <a href="http://www.iitd.pan.wroc.pl">http://www.iitd.pan.wroc.pl</a> ).
Eliava Phage Therapy Center	Georgia	A network of eight laboratories where phage research and application occurred since 1923s ( <a href="http://www.mrsaphages.com">http://www.mrsaphages.com</a> ).
Novomed	Georgia	Deliver effective treatment through phage therapy in many areas of medicine. Treatments are available for local Georgians and foreign patients, especially those with chronic wounds, osteomyelitis, or other types of acute and chronic infections ( <a href="http://www.phagetherapy.com">http://www.phagetherapy.com</a> ).
Phage Therapy Center	Georgia	Established in 2004 and provides excellent treatment for patients who have bacterial infections that are difficult/non-healing, chronic, drug-resistant or have not responded to conventional antibiotic therapies ( <a href="http://www.phagetherapycenter.com">http://www.phagetherapycenter.com</a> ).
Phage International Inc.	The United States	Treats patients with chronic, drug-resistant or difficult-to-treat infections ( <a href="http://www.phageinternational.com">http://www.phageinternational.com</a> ).

### 2.13.3 Advantages and limitations of phage therapy:

Theoretically, there are no bacteria that cannot be lysed by a single bacteriophage. Therefore, phage therapy has several advantages compared to antibiotic treatment. Bacteriophages are highly specific to the host bacterial strain. Therefore, during infection, it would not disturb the beneficial microflora (Loc-Carrillo and Abedon 2011). In contrast, antimicrobial drugs have a broad-spectrum activity which leads to the non-specific killing of both pathogens and members of the normal flora.

Since there have been no major negative effects associated with phage therapy in humans during or after treatments, it is thought to be safer than using antibiotics (Sulakvelidze et al. 2001). However, some mild side effects (e.g., fever) have occasionally been reported due to the release of endotoxins from bacteria when they are lysed by phages inside the human body. Therefore, bacteriophages are significantly safer and better tolerated. But in the case of antibiotics treatment, several side effects including allergies, intestinal disorders, and secondary infections are reported (Sulakvelidze et al. 2001).

Bacteriophages are self-replicating and self-limiting. They multiply exponentially as the number of host bacteria rises, may reduce as the number of host bacteria falls, and lastly may remain present in undetectable low concentrations after the host bacteria are eliminated (Almeida et al. 2009). Therefore, very few doses of bacteriophage can effectively kill the bacteria in the infection site and will not continue to persist after treatment. In contrast, antibiotics can be metabolized and removed but there is still a chance that the leftover substance could accumulate in tissues. Additionally, antibiotics spread throughout the body and are unable to concentrate at the site of the infection. Antibiotics must be administered in large quantities and often to compensate for the loss in other body parts (Sulakvelidze et al. 2001).

During the course of phage therapy, bacteria can evolve resistance to phages, but it is typically easy to choose and purify a new phage with lytic activity against the phage-resistant bacterial mutants in a matter of days or weeks. In this scenario, phage cocktail in place of a single bacteriophage is also another way to overcome the problem of phage-resistant mutants. In contrast, the development of a new antibiotic is usually very time-consuming and expensive. Bacteriophages can be engineered to be able to overcome the limits of antibiotic treatment using the current large-scale, inexpensive, DNA sequencing and DNA synthesis technology (Viertel, Ritter, and Horz 2014).

Apart from the advantages, there are also some limitations of phage therapy that should be considered before using phages as a therapeutic candidate.

It is challenging to use phages against the wide variety of bacterial variations due to the specificity and narrow host ranges of phages. In this situation, before carrying out phage therapy, the nature of the pathogen and confirmation of phage susceptibility are required. The use of a phage cocktail can overcome this situation (Sulakvelidze et al. 2001).

Phage particles may be quickly eliminated from the body by the defense mechanisms of the host, such as antibody neutralization, which reduces the number of phages present at the infection sites (Almeida et al. 2009). These issues may be handled by choosing phage mutants that can persist in the circulatory system or by administering the same phage to the organism repeatedly (Barrow and Soothill 1997).

Some lytic and temperate phages have the potential to transmit genes to bacteria that can confer antibiotic resistance and encode pathogenicity (Almeida et al. 2009). This could increase virulence and cause non-pathogenic strains to become pathogenic. This problem could be solved by carefully selecting appropriate phages, sequencing phage genomes to prevent the transfer of virulence genes, and creating genetically altered mutant phages.

### **2.14 Bacteriophages against *Shigella* bacteria:**

#### **2.14.1 *Shigella* bacteriophages:**

In 1917 Felix d'Herelle isolated a bacteriophage for therapy and it was a *Shigella* bacteriophage (D'herelle and Roux n.d.). Before the year 2000, most of the research work on *Shigella* phages was used to identify the *Shigella* strains or to know the capability of lysogenic phages to alter the serotype of the host (Financsek et al. 1976) from the host range, and there was very little information about the phage. Earlier the *Shigella* phages were collected from the clinical samples of shigellosis patients and their maintenance was not so easy. The first modern *Shigella* bacteriophages (for example, SfI, SfII, SfIV, SfV, Sf6, SfX, Sf101, and SfMu) were isolated from the lysogenic clinical strain of virulent *Shigella flexneri* and all these phages were capable to alter the surface properties of the bacterial strain by integrating its genome inside the host genome. Nowadays modern techniques are used to determine the serotype of the strain. The

surface antigen of the bacteria is known as the serotype and this surface antigen is responsible for the classification of the bacterial strains within the species.

Gram-negative bacteria contain lipopolysaccharide on their surface and it acts as a surface antigen. The study of the above-mentioned phages revealed that the phage encodes O-antigen modifying enzymes that are responsible for the modification of the LPS structure of the host cells. When multiple phages coinfect the same host cell there is a possibility of the production of a new serotype.

Previously the *Shigella* phages were isolated from the clinical strains and most of them were lysogenic. In recent years the lytic *Shigella* phages are now been isolated from environmental samples such as wastewater, river, or streams. Most of these isolates are used for the clinical control of shigellosis but these strains also described the prevalence and the diversity of *Shigella* phages. To date, many lytic *Shigella* phages were isolated from different areas and they are divided into a few main groups. The largest family belongs to the T4-like *Myovirus* subfamily (*Tevenvirinae*) with a genome size of 164.0-176.0 Kbp. Next, a large group of phage belongs to the T-1-like *Siphoviridae* sub-family (*Tunavirinae*) with a genome size of 47.7-51.9 Kbp and FelixO1- like *Myoviridae* subfamily (*Ounavirinae*) with a genome size 85.9-90.4 Kbp. Some of the *Shigella* phages also belong to the *Podoviridae* subfamily (Subramanian, Parent, and Doore 2020).

In our study, a *Myoviridae Shigella* bacteriophage was isolated from the environmental sample and characterized.

### **2.14.2 Phage-based control of *Shigella* infection:**

The birth of phage therapy is historically related to the *Shigella* spp. In 1915 an outbreak of severe hemorrhagic dysentery occurs among the French troops stationed at Maisons-Laffitte. Felix d'Herelle is the person who is responsible for the determination of the cause of this disease. d'Herelle prepared bacteria-free filtrate from the stool sample of the hospitalized soldiers and mixed it with the *Shigella* strains culture collected from the patients. The mixed sample was then plated on the agar and the bacterial growth was observed. During this experiment, d'Herelle first observed the small size clear zone of lysis in the plate, later known as “plaque” (Summers 1999). In 1919 Felix d'Herelle first applied phage to treat the symptoms of dysentery. Interestingly the phage was an anti-dysentery *Shigella* phage and it was injected into a patient with severe dysentery. After receiving the phage, the patient recovered very

quickly and the symptoms of dysentery also disappeared after receiving the phage therapy (Summers 1999). After the success of this therapy, the phage was applied successfully in various dysentery cases and all these studies were reported in various scientific articles over 20 years. In another report, *Shigella flexneri* was identified in *Shigella*-affected children in the US state of Maryland and 5 to 1300 ml of phage was given orally and rectally to the children (DAVISON 1922). In another study, it was reported that shigellosis was treated with the use of 10 ml of phage which was administered orally. The interesting part of this study was that the mortality rate and the longevity stay in the hospital were reduced compared to the control study. In another report of bacillary dysentery patients in France in 1933 were treated with oral administration of 5-10 ml of polyvalent Shiga-Flexner phage with alkaline water during an outbreak that occurred in the ships at the port of Brest. The blood and the mucous were stopped and within 4 days the stool of the patient reverted to normal. The same physician also applied phage to the newborn in a camp to stop an outbreak (Goodridge 2013).

On the other hand, there were some cases of failure of phage therapy. In one study it was reported that 70 infants (aged below 2 years old) were treated with one ounce of bacteriophage per hour and among them, there were 22 successful cases. The reason behind the lower success rate may be due to the phage used in this study being strain-specific and the phage effective against 17 bacterial strains out of 94 bacterial strains. In another phage therapy research was conducted by the British army and in this study, the work was divided into four scales. Among them, two scales gave an unsatisfactory result whereas the result of the third case was also unimpressive and the third one was published in British Medical Journal. In the last experiment there were 32 enrolled cases among them 18 were control cases and the remaining 14 were phage-treated cases (Boyd and Portnoy 1944; Goodridge 2013).

Though there were some unsuccessful cases of phage therapy still it got success in many of the cases. For example, daily three times phage was given to patients with dysentery outbreaks (caused by *Shigella sonnei*). Interestingly after two days, the epidemic had been stopped and no further case was found for the next one year (Haler 1938). In another study in Poland (1941) it was found that 10 ml of phage mixture containing sodium bicarbonate was given with tea or coffee to infected patients and it was effective against *Shigella* infection. The Hirszfild Institute of Immunology and Experimental Therapy (HIIET) in Poland (in 1957) used bacteriophage to treat shigellosis and other infectious diseases caused by antibiotic-resistant bacterial strains (Sulakvelidze, Alavidze, and Morris 2001). A clinical trial to evaluate the efficacy of the phage

against shigellosis was conducted in 1960 in Tbilisi, Georgia. In this study, 6-7 years old 30,769 children were involved. These kids were split into two groups, one group received dried *Shigella* phage tablets, while the other received an oral placebo once a week for each kid. The children were monitored on a regular basis for 109 days. The dysentery infection was four-fold higher for the placebo-treated children than those treated with bacteriophage (Babalova et al. 1968). Research published in 1984 indicated that patients treated for shigellosis using phage-mediated therapy experienced a ten-fold decrease in diarrhoea. (Anpilov and Prokudin 1984). An experiment was conducted in 1993, in which the phage was used to treat shigellosis and salmonellosis with a combination of antibiotics (Milyutina and Vorotyntseva 1993). The result showed that the combination therapy was more effective than the antibiotic alone. During the 21<sup>st</sup> century, many articles reported the success rate of phage therapy. The phage efficiency was checked against some antibiotic-resistant *Pseudomonas* and *Streptococci* as well as some multidrug-resistant *Enterobacteriaceae* family members such as *Shigella*, *Escherichia*, *Salmonella*, *Klebsiella*, *Serratia*, and *Proteus* (Kumari, Harjai, and Chhibber 2011). This study further confirmed that the efficacy rate of phage to treat shigellosis was higher. Another study was performed to check the efficacy of *Shigella*-specific phages and phage cocktails to inhibit the *Shigella* bacteria in chicken products. The result of this study showed that the high concentration of *Shigella* phage ( $3 \times 10^8$  PFU/g) can reduce the load of bacteria more effectively than the low concentration of bacteriophage ( $1 \times 10^8$  PFU/g) (Zhang, Wang, and Bao 2013). All the above-mentioned studies suggested that the phages were able to reduce the load of *Shigella* bacteria effectively. In the near future phage therapy can be used as an effective alternative against multi-drug resistant *Shigella* spp. and hence the pressure to produce new antibiotics is reduced.





# CHAPTER 3

## Objectives



### 3.1 OBJECTIVES

Bacteriophages (phages), are among the most prevalent and diverse organisms found in any environment and also in the mammalian GI tract. They have been increasingly recognized as potential tools to control pathogens. Phages are capable to inhibit the growth of specific food-borne and water-borne pathogens without disturbing the beneficial microflora. Moreover, phages have demonstrated enough promise in treating bacterial infections. starting from the initial therapeutic usage to the recent treatment of *Shigella* infections with the resurgence of phage therapy due to the increase in antibiotic resistance. Aiming to explore an alternative treatment strategy for shigellosis caused by *Shigella* spp. there is a continuously growing interest recently observed within the phage research community to isolate and characterize novel *Shigella* phages from the environment or patients. Here, we aim to study the morphological, biological, genomic, and proteomic characterization of a newly isolated lytic *Shigella* bacteriophage. The structural characterization as well as the phage host infection study is also an important part of this work. The efficacy of bacteriophages both alone and in combination with antibiotics or other phages has also been studied to remove or control bacterial biofilm formation. The overall aim of this thesis work is to understand the ability of this phage as a potential biocontrol and therapeutic candidate in the future.

The specific objective of my work is as follows:

**Objective 1** Isolation and characterization of a lytic bacteriophage.

**Objective 2** Structural characterization of bacteriophage Sfk20 by single particle cryo-electron microscopy and image processing and prediction of phage structural proteins by deep learning and homology modeling.

**Objective 3** To study the *in vitro* phage-host interaction by electron microscopy.

**Objective 4** Antibiofilm activity of the isolated bacteriophage against host bacteria.



# CHAPTER 4

## **Materials & Methods**



## CHAPTER 4

### 4.1 List of chemicals:

Serial No.	Reagents	Company	Country
1.	Acrylamide	HiMedia	India
2.	Acetone	Merck	India
3.	Agar 100 resin kit	Agar Scientific	UK
4.	Agarose	HiMedia	India
5.	Ammonium acetate	HiMedia	India
6.	Ammonium sulfite	Qualigens	India
7.	Amyl acetate	Qualigens	India
8.	Ammonium persulfate	HiMedia	India
9.	Ampicillin sodium salt	HiMedia	India
10.	BamHI	HiMedia	India
11.	Beta mercaptoethanol	Sigma-Aldrich	USA
12.	BglII	HiMedia	India
13.	Bromophenol blue	HiMedia	India
14.	Cacodylic acid, Sodium salt	Ted Pella	USA
15.	Coomassie brilliant blue	Sigma-Aldrich	USA
16.	Chloroform	Qualigens	India
17.	Dimethyl sulfoxide (DMSO)	Merck	India
18.	Dithiothreitol (DTT)	SRL	India
19.	DNase I	HiMedia	India
20.	EcoRI	Sigma-Aldrich	USA
21.	EcoRV	HiMedia	India
22.	EDTA	Qualigens	India
23.	Ethanol	HiMedia	India
24.	Glacial acetic acid	Qualigens	India
25.	Glutaraldehyde	Sigma-Aldrich	USA
26.	Glycerol	Merck	India
27.	Glycine	Merck	India
28.	Gram crystal violet	HiMedia	India
29.	Hexamethyldisilazane	Sigma-Aldrich	USA
30.	HindIII	Sigma-Aldrich	USA
31.	Hydrochloric acid	Merck	India
32.	Lauryl sulfate sodium salt (SDS)	HiMedia	India

## CHAPTER 4

33.	Lead citrate	Polaron	India
34.	Magnesium chloride hexahydrate	HiMedia	India
35.	Methanol	Merck	India
36.	MluI	HiMedia	India
37.	N, N' bisacrylamide	HiMedia	India
38.	Osmium tetroxide	Agar Scientific	UK
39.	Phosphate buffered saline	HiMedia	India
40.	Proteinase K	HiMedia	India
41.	PstI	Sigma-Aldrich	USA
42.	RNase I	HiMedia	India
43.	Sodium acetate	HiMedia	India
44.	Sodium carbonate	Merck	India
45.	Sodium chloride	HiMedia	India
46.	Sodium hydroxide	HiMedia	India
47.	Sodium periodate	HiMedia	India
48.	Sucrose	HiMedia	India
49.	Tris-Base	HiMedia	India
50.	Tris HCl	HiMedia	India
51.	TEMED	HiMedia	India
52.	Uranyl acetate	BDH Chemicals	England

### 4.2 List of equipment:

Serial No.	Equipment	Model	Manufacturer	Country
1.	Agarose gel electrophoresis apparatus	AE-6111	ATTO	Japan
2.	Agarose gel electrophoresis powerpack	minipack-250	GENEI	India
3.	Autoclave	LabTech	DAIHAN LABTECH CO., LTD.	Korea
4.	Biological Safety cabinet	NK system	NIPPON MEDICAL & CHEMICAL INSTRUMENTS CO., LTD	Japan
5.	Centrifuge	SORVALL LEGEND X1R	Thermo SCIENTIFIC	USA
6.	Drying oven	MOV-112	SANYO Electric Co., LTD.,	Japan
7.	Embedding oven	MK111	Agar SCIENTIFIC	UK

## CHAPTER 4

8.	EM TRIM	LEICA EM TRIM	LEICA	Germany
9.	Gel doc	GelDoc Go Imaging System	BIORAD	USA
10.	GPU enabled workstation for image processing	Vantageo-2000 Series	Teqsys Global Solutions Pvt. Ltd	India
11.	Hydrophilic Treatment device	HDT-400	JEOL DATUM	Japan
12.	Knife maker	LEICA EM KMR 2	LEICA	Germany
13.	Light microscope	Primo Star	ZEISS	Germany
14.	Microcentrifuge	MC-01	TARSONS	India
15.	Micropipette		TARSONS	India
16.	Nanodrop	μCuvette G1.0	Eppendorf	Germany
17.	pH meter		EUTECH INSTRUMENT (Thermo Fisher Scientific)	USA
18.	Refrigerator	SANYO LABCOOL	Sanyo Trading Co., Ltd.	Japan
19.	Scanning electron microscope	FEI Quanta 200	FEI	Netherlands
20.	SDS- PAGE gel electrophoresis gel apparatus	Mini-PROTEAN® 3	BIORAD	USA
21.	SDS-PAGE gel electrophoresis powerpack	POWER PAC Basic	BIORAD	USA
22.	Shaking water bath	BS-11	JEIO TECH	Korea
23.	Sputter coater	SC7640	Polaron	UK
24.	Transmission Electron microscope	FEI Tecnai 12 BioTwin	FEI	Netherlands
25.	Vacuum evaporator	JEE-400	JEOL	Japan
26.	Vortex	G-560E	SCIENTIFIC INDUSTRIES INC.	Japan
27.	Weighing machine	ZSP250	SCIEN TECH	USA
28.	Ultracentrifuge	Sorvall WX100	Thermo Fisher Scientific	Japan
29.	Ultramicrotome	LEICA ULTRA CUT	LEICA	Germany
30.	UV/VIS Spectrophotometer	Optizen 2120UV PLUS	Mecasys Co., Ltd	Korea

## CHAPTER 4

---

### 4.3 Preparation of the media:

#### 4.3.1 Preparation of LB broth:

Luria Bertani broth	25 gms
Double distilled water	1000 ml

25 gms Luria broth was added to 1L of double distilled water and mixed thoroughly. It was then autoclaved (15 lbs/atm pressure) and stored at 4°C.

#### 4.3.2 Preparation of Nutrient broth:

Luria Bertani broth	13.5 gms
Double distilled water	1000 ml

13.5 gms Luria broth was added to 1 L of double distilled water and mixed thoroughly. It was then autoclaved (15 lbs/atm pressure) and stored at 4°C.

#### 4.3.3 Preparation of Tryptone Soya broth:

Tryptone Soya broth	30 gms
Double distilled water	1000 ml

30 gms of Tryptone Soya broth was suspended in 1000 ml of double distilled water. It was then autoclaved (15 lbs/atm pressure) and stored at 4°C.

#### 4.3.4 Preparation of Luria Bertani agar:

Luria Bertani Agar	40 gms
Water	1000 ml

In a conical flask, 40 gms of nutrient agar was added to 1 L of double distilled water. The conical flask was then plugged with non-absorbent cotton and put into an autoclave for sterilization at 15 lbs/atm pressure. After sterilization, the conical flask containing molten agar was equally divided into several Petri plates. After solidification, the plates were stored in a 4°C refrigerator in an inverted condition.

## CHAPTER 4

---

### 4.3.5 Preparation of Nutrient agar:

Nutrient Agar	28 gms
Water	1000 ml

In a conical flask, 28 gms of nutrient agar was added to 1 L of double distilled water. The conical flask was then plugged with non-absorbent cotton and put into the autoclave for sterilization at 15 lbs/atm pressure. After sterilization, the conical flask containing molten agar was equally divided into several Petri plates. After solidification, the plates were stored in a 4°C refrigerator in an inverted condition.

### 4.3.6 Preparation of Soft agar:

Luria Bertani broth	25 gms
Agar (bacteriological grade)	1 %
Double distilled water	1 L

25 gms Luria Bertani Broth and 1% agar (bacteriological grade) were mixed in 1 L double distilled water. The mixture was heated until the agar melted. 3 ml of the molten soft agar was poured into small test tubes in each. Then each tube was plugged with non-absorbent cotton and put into an autoclave for sterilization at 15 lbs/atm pressure. After sterilization, it was stored at 4°C.

## 4.4 Preparation of buffers:

### 4.4.1 Preparation of Tris-MgCl<sub>2</sub> buffer (0.1-0.01M, pH- 7.4):

Tris HCl	13.22 gms
Tris base	1.94 gms
MgCl <sub>2</sub> , 7H <sub>2</sub> O	2.033 gms
Double distilled water	1 L

In a 1 L lab bottle, 13.22 gms of Tris-HCl, 1.94 gms of Tris base, and 2.033 gms of MgCl<sub>2</sub> were added. The volume was made up to 1 L with water; the pH of the solution was 7.4 at room temperature.



## CHAPTER 4

---

### 4.4.2 Preparation of SM buffer:

Sodium chloride (NaCl)	5.8 gms
MgSO <sub>4</sub> , 7H <sub>2</sub> O	2 gms
Tris-Cl (1M, pH-7.5)	50 ml
Double distilled water	1 L

To prepare 1 L of SM buffer, 5.8 gms NaCl, and 2 gms MgSO<sub>4</sub>, 7H<sub>2</sub>O was dissolved in 800 ml of double distilled water. Thereafter Tris-Cl was added and the volume was adjusted up to 1 L. It was sterilized by autoclaving at 15 lbs/atm pressure. It was stored at room temperature.

### 4.4.3 Preparation of 0.4 M Sodium Cacodylate:

Sodium Cacodylate	42.8 gms
Double distilled water	500 ml

In a 1 L of lab bottle, 42.8 gms of sodium cacodylate was added to 200 ml of distilled water and mixed thoroughly. Then the volume was adjusted up to 500 ml and it was then stored at 4°C.

### 4.4.4 Preparation of 3% buffered glutaraldehyde:

0.4 M Sodium Cacodylate	25 ml
25% Glutaraldehyde	12 ml
Double distilled water	63 ml

In a 100 ml lab bottle, 25 ml of 0.4M sodium cacodylate and 12 ml of 25% glutaraldehyde were added. The volume was adjusted up to 100 ml.

## CHAPTER 4

---

### 4.4.5 Preparation of 0.2 M Sodium Cacodylate:

Sodium Cacodylate	21.4 gms
Double distilled water	500 ml

In 1 L of the bottle, 42.8 gms of sodium cacodylate was added to 200 ml of distilled water and mixed thoroughly. Then the volume was adjusted up to 500 ml. It was then stored at 4°C.

### 4.4.6 Preparation of 0.1 M Sodium Cacodylate:

0.4 M Sodium Cacodylate	312.5 ml
0.2 M HCl	50 ml
Double distilled water	887.5 ml

In a 1 L lab bottle, 887.5 ml double distilled water and 312.5 ml sodium cacodylate was added and the pH was adjusted using 0.2 M HCl.

### 4.4.7 Preparation of Electrophoresis buffer for SDS-PAGE gel:

Glycine	14.3 gms
Tris	3.0 gms
SDS	1.0 gms

In a 1000 ml bottle, 500 ml of double distilled water was taken. 14.3 gm of glycine, 3.0 gms tris, and 1 gm of SDS were added. Finally, the water was added up to 1000 ml.

### 4.4.8 Preparation of Sample loading buffer:

Solution C	0.5 ml
25 mM DTT	48 mg
50% glycerol	1.25 ml
10% SDS	240 mg
Double Distilled water	0.75 ml
Bromophenol blue	0.025%
β- mercaptoethanol	0.75 ml

## CHAPTER 4

---

In a 15 ml centrifuge tube 0.5 ml solution C, 48 mg of 25 mM DTT, 1.25 ml of 50% glycerol, 240 mg 10% SDS, and 0.75 ml double distilled water were added and mixed properly. Thereafter 0.025% bromophenol blue and 0.75 ml of  $\beta$ - mercaptoethanol was added.

### 4.4.9 Preparation of 10 X TAE (Tris-acetate EDTA) buffer:

Tris	48.5 gms
Glacial acetic acid	11.4 ml
0.5 M EDTA	20 ml
Double distilled water	1 L

In 500 ml double distilled water 48.5 gms of Tris was added. Next 11.4 ml glacial acetic and 20 ml of 0.5 M EDTA mixed with the solution. The volume was made up to 1 L. The buffer solution was stored at room temperature.

### 4.4.10 Preparation of 1X TAE buffer:

10 X TAE	100 ml
Double distilled water	900 ml

In a 1000 ml Lab bottle, 100 ml of 10X TAE buffer was taken. Next 900 ml of double distilled water was added. The buffer solution was stored at room temperature.

### 4.4.11 Preparation of 50 mM Sodium acetate buffer:

Sodium acetate	0.82 gms
Double distilled water	200 ml

In a 500 ml beaker, 150 ml of double distilled water was added and 0.82 gms of sodium acetate was added to it. The pH was adjusted up to 5.2. the water was adjusted up to 200 ml. It was then stored at room temperature.

## CHAPTER 4

---

### 4.5 Preparation of various reagents:

#### 4.5.1 Preparation of 2% Uranyl acetate:

Uranyl acetate	2 gms
Double distilled water	100 ml

2 gms of uranyl acetate was added to 100 ml of double distilled water and mixed properly. The solution was stored at room temperature.

#### 4.5.2 Preparation of Lead citrate:

Lead citrate	0.2 gms
Double distilled water	100 ml

To 100 ml of double distilled water, 0.2 gms of lead citrate was added. It was mixed properly. Then 1N NaOH solution was added dropwise until the pH rises to 12.

#### 4.5.3 Preparation of 2% Osmium Tetraoxide:

Osmium Tetraoxide	250 mg
Double distilled water	12.5 ml

250 mg of osmium tetraoxide was dissolved into 12.5 ml double distilled water and stored in a black bottle (to avoid light) at room temperature.

#### 4.5.4 Preparation of 1% working osmium tetraoxide [1% OsO<sub>4</sub>]:

2% osmium tetraoxide	2 ml
0.2M Sodium Cacodylate	2 ml

2% osmium tetraoxide was dissolved into 2 ml of sodium cacodylate and mixed properly.

## CHAPTER 4

---

### 4.5.5 Preparation of hardening reagent:

Agar 100 Resin	6 gms
Dodecenyl Succinic Anhydride (DDSA)	2.25 gms
Methyl Nadic Anhydride (NMA)	3.75 gms
N-Benzyl dimethylamine (BDMA)	0.35 gms

6 gms of Agar 100 Resin was mixed with 2.25 gms dodecenyl succinic anhydride and methyl nadic anhydride. Next benzyl di-methyl amine (BDMA) was added. All the above-mentioned components were mixed well in a magnetic stirrer and kept overnight at 60°C.

### 4.5.6 Preparation of Solution A for SDS-PAGE:

Acrylamide	29.2 gms
N, N' bisacrylamide	0.8 gms

0.8 gms of N, N' bisacrylamide was dissolved in 30 ml water. Acrylamide was added in N, N' bisacrylamide solution gradually and stirred. When acrylamide was dissolved completely in N, N' bisacrylamide solution. Double distilled water was added to this solution up to 100 ml.

### 4.5.7 Preparation of Solution B for SDS-PAGE:

Tris HCl	18.13 gms
Sodium do-decyl sulfate	400 mg

18.13 gms Tris-base was dissolved in 90 ml distilled water. 400 mg SDS was added to the Tris-base solution. pH of the solution was adjusted using 3M HCl to pH 8.8. Finally, water was added up to 100 ml.

### 4.5.8 Preparation of Solution C for SDS-PAGE:

Tris-HCl	6 gms
Sodium do-decyl sulfate	400 mg

Tris base was dissolved in 80 ml distilled water and 400 mg SDS was added to the solution. pH of the solution was adjusted to 6.8 using the 3M HCl solution.

## CHAPTER 4

---

### 4.5.9 Staining solution for SDS-PAGE:

Ethanol	50 ml
Double distilled water	40 ml
Acetic acid	10 ml
Coomassie brilliant Blue	5 gms

In a 100 ml lab bottle 50 ml of ethanol, 40 ml of double distilled water, and 10 ml of acetic acid were added. 5 gms of Coomassie brilliant blue was dissolved in the solution. The solution was stored at room temperature.

### 4.5.10 Preparation of destaining solution:

Ethanol	50 ml
Double distilled water	40 ml
Acetic acid	10 ml

In a 100 ml lab bottle 50 ml of ethanol, 40 ml of double distilled water, and 10 ml of acetic acid were added. The solution was stored at room temperature.

### 4.5.11 Preparation of fixing solution:

Methanol	100 ml
Acetic acid	10 ml
Double distilled water	90 ml

In a 250 ml lab bottle, 100 ml of methanol was taken and 10 ml of acetic acid and 90 ml of double distilled water were added. The solution was stored at room temperature.

### 4.5.12 Preparation of 10% APS solution:

APS (Ammonium per sulfate)	20 mg
Double distilled water	200 $\mu$ l

## CHAPTER 4

---

20 mg Ammonium persulfate was added to the 200  $\mu$ l double distilled water and mixed properly and stored at room temperature.

### 4.5.13 Preparation of 10mM periodate solution:

50 mM sodium acetate solution	100 ml
Sodium periodate	0.21 gms

To 100 ml 50mM acetate solution(pH-5.2) 0.21 gms of sodium periodate was added. The solution was mixed properly and stored at room temperature.

### 4.5.14 Preparation of 1 % agarose gel:

1 X TAE buffer	30 ml
Agarose (medium EEO)	0.3 gms

In a conical flask 0.3 gms of agarose then the powder was mixed with 30 ml of 1X TAE buffer and it was then boiled until the agarose is completely dissolved. Then the solution was cool down in running tap water to about 50°C. The agarose solution was then poured into the gel tray. The gel tray was kept at 4°C to solidify properly.

### 4.5.15 Preparation of 12.5 % resolving gel:

Solutions	Amount
Solution A	4.2 ml
Solution B	2.5 ml
Double distilled water	3.3 ml
APS	23 $\mu$ l
TEMED	5.5 $\mu$ l

In a 15 ml centrifuge tube 1.5 ml of Solution A, 1.125 ml of Solution B, 0.62 ml of double distilled water were taken. 5  $\mu$ l of TEMED was added to the solution. Finally, the APS was added and mixed gently and poured immediately into the glass sandwich plates.

## CHAPTER 4

---

### 4.5.16 Preparation of stacking gel:

Solutions	Amount
Solution A	1.5 ml
Solution C	0.75 ml
Double distilled water	1.8 ml
APS	10 ml
TEMED	7 ml

After the solidification of the resolving gel, the stacking gel was prepared. In a 15ml centrifuge tube 1.5 ml of Solution A, 1.125 ml of Solution B, and 0.62 ml of double distilled water were taken. 5  $\mu$ l of TEMED was added to the solution. Finally, the APS was added and mixed gently and the mixture was poured immediately on top of the resolving gel.

### 4.5.17 Preparation of 40% Sucrose solutions:

Sucrose	8 gms
Double distilled water	20 ml

In a 50 ml lab bottle, 10 ml water was taken. 8 gms of sucrose was added and mixed properly. Gently the water was added up to 20 ml. Thereafter the solution was autoclaved (15lbs/atm pressure) and stored at 4°C.

### 4.5.18 Preparation of 30% Sucrose solutions:

Sucrose	6 gms
Double distilled water	20 ml

In a 50 ml lab bottle, 10 ml water was taken. 6 gms of sucrose was added and mixed properly. Gently the water was added up to 20 ml. Thereafter the solution was autoclaved (15 lbs/atm pressure) and stored at 4°C.

### 4.5.19 Preparation of 20% Sucrose solutions:

Sucrose	4 gms
Double distilled water	20 ml



## CHAPTER 4

---

In a 50 ml lab bottle, 10 ml water was taken. 4 gms of sucrose was added and mixed properly. Gently the water was added up to 20 ml. Thereafter the solution was autoclaved (15 lbs/atm pressure) and stored at 4°C.

### 4.5.20 Preparation of 10% Sucrose solutions:

Sucrose	4 gms
Double distilled water	20 ml

In a 50 ml lab bottle, 10 ml water was taken. 4 gms of sucrose was added and mixed properly. Gently the water was added up to 20 ml. Thereafter the solution was autoclaved (15 lbs/atm pressure) and stored at 4°C.

### 4.5.21 Preparation of 20% Sodium chloride solutions:

Sodium chloride	20 gms
Double distilled water	100 ml

In a 100 ml lab bottle, 50 ml water was taken. 20 gms of sodium chloride was added and mixed properly. Gently the water was added up to 100 ml. Thereafter the solution was autoclaved (15 lbs/atm pressure) and stored at 4°C.

### 4.5.22 Preparation of 15% Sodium chloride solutions:

Sodium chloride	15 gms
Double distilled water	100 ml

In a 100 ml lab bottle, 50 ml water was taken. 15 gms of sodium chloride was added and mixed properly. Gently the water was added up to 100 ml. Thereafter the solution was autoclaved (15 lbs/atm pressure) and stored at 4°C.

### 4.5.23 Preparation of 10% Sodium chloride solutions:

Sodium chloride	10 gms
Double distilled water	100 ml

## CHAPTER 4

---

In a 100 ml lab bottle, 50 ml water was taken. 10 gms of sodium chloride was added and mixed properly. Gently the water was added up to 100 ml. Thereafter the solution was autoclaved (15 lbs/atm pressure) and stored at 4°C.

### 4.5.24 Preparation of 5% Sodium chloride solutions:

Sodium chloride	5 gms
Double distilled water	100 ml

In a 100 ml lab bottle, 50 ml water was taken. 5 gms of sodium chloride was added and mixed properly. Gently the water was added up to 100 ml. Thereafter the solution was autoclaved (15lbs/atm pressure) and stored at 4°C.

### 4.6 Bacterial strains:

*Shigella flexneri 2a* was used in this study as host bacteria. Other bacterial strains such as *Shigella flexneri 3a*, *Shigella flexneri 6*, *Shigella flexneri 4*, *Shigella flexneri 1b*, *Shigella sonnei*, *Shigella dysenteriae 1*, *Shigella boydii*, *Salmonella typhi*, *Salmonella typhimurium*, *Salmonella enteritidis*, *ETEC*, *Vibrio cholerae O1* was also used in this study. All these strains were collected from the Division of Bacteriology of ICMR- National Institute of Cholera and Enteric Diseases.

### 4.7 Colony forming unit (CFU) calculation:

A colony-forming unit calculation was performed to know the concentration of the bacteria in the culture condition. and it was determined by serial dilution. Briefly, the bacterial culture was serially diluted into the broth. The 100 µl of serially diluted bacterial culture was added to the agar plates and spread properly with an L-shaped spreader. The plates were incubated at 37 °C incubator overnight. The next day the number of colonies was counted and CFU was calculated according to the formula given below:

$$\text{CFU/ml} = \frac{\text{Number of colonies} * \text{dilution factor}}{\text{Volume of the culture plate}}$$

### 4.8 Growth curve of bacteria:

One single colony of *Shigella flexneri 2a* bacteria was added to the 5 ml of LB broth and kept in a 37°C shaker incubator overnight, the next day the OD of the culture was measured. According to the calculation the overnight culture was added to the 40 ml of the LB broth and kept under shaking conditions. The OD was taken in a UV/VIS spectrophotometer (Optizen 2120UV PLUS) 30 minutes time intervals up to 9 hours.

### 4.9 Isolation, propagation enrichment, and purification of phage sample:

The *Shigella flexneri 2a* strain was used as a host bacterium for isolation and the propagation of the bacteriophage in this study. For this purpose, lake water sample was collected from the diarrheal outbreak area of Kolkata. 25 ml of water sample was taken in a conical flask. 25 ml of 10X phage broth media and 5 ml of early log phase culture of *Shigella flexneri 2a* were mixed with the 25 ml water sample. This suspension was then incubated for 24 hours at 37°C with constant shaking at 101 rpm. The next day the culture was centrifuged at 10000 rpm for 10 minutes at 4°C to remove the bacterial cells. The supernatant was collected and filtered through the 0.22 µm syringe-driven membrane filter (HiMedia, India). Thereafter the 10µl of the filtered sample was spotted on the surface of the *Shigella flexneri 2a* 2457T bacterial lawn that was prepared in a Petri plate. After getting the clear zone of lysis appeared in the plate the filtered supernatant was diluted serially ( $10^{-1}$  to  $10^{-8}$ ) in sterilized Tris-MgCl<sub>2</sub> buffer (0.1-0.01M, pH- 7.4), 100µl of each serial dilution mixed with 250 µl of early log phase culture of *Shigella flexneri 2a* and this suspension was added to 3 ml of molten soft agar at 50°C. Thereafter it was decanted onto the solid agar plate to make a double agar layer plate. The plates were then incubated at 37 °C overnight. Next day a single plaque was scrapped from the plate and mixed with Tris-MgCl<sub>2</sub> buffer (0.1-0.01M, pH- 7.4) properly. This mixture was then centrifuged at 10000 rpm for 10 minutes at 4°C and plaque assay of the collected supernatant was performed. The single plaque collection procedure was performed three times to ensure the phage suspension contain a single phage. The isolated bacteriophage was then propagated in the *Shigella flexneri 2a* (2457T) strain following the soft agar overlay method (Yuan et al. 2015). For this purpose, an early log phase culture of *Shigella flexneri 2a* (2457T) was infected with the bacteriophage. The infected bacterial cell suspension was added to 3 ml molten soft agar and thereafter it was poured into the plate and the plate was incubated at 37°C till confluent lysis occur. The Tris-MgCl<sub>2</sub> buffer (0.1-0.01M, pH- 7.4) was added to the plate. The top agar

layer was then scrapped from the plate and collected in then centrifuged tube. It was then centrifuged at 10000 rpm for 10 minutes at 4°C in a 2-16 K Sigma tabletop centrifuge and the supernatant was collected and chloroform was added to it. The supernatant was then stored at 4°C.

To concentrate the phage samples, the next day the supernatant was centrifuged in a Sorvall RC100 ultracentrifuge using fixed-angle rotor T-865 at 25000 rpm for 1:30 hours at 4°C. The supernatant was discarded and the pellet was resuspended in Tris-MgCl<sub>2</sub> buffer (0.1-0.01M, pH- 7.4). The sample was then centrifuged at 10000 rpm for 10 minutes at 4°C to remove the agar and bacterial debris. The supernatant containing phage was then purified by the sucrose step gradient method. For the purification of the bacteriophage by the sucrose step gradient method, the phage sample was added to the top layer of preformed sucrose gradient 10%, 20%, 30%, and 40%. It was then centrifuged using TH-660 swing-out rotor at 30000 rpm for 2 hours at 4°C at sorvall RC100 ultracentrifuge (Dutta and Ghosh 2007). During centrifugation, the phage sample was passed through the gradient. After centrifugation, the pellet was resuspended in Tris-MgCl<sub>2</sub> buffer (0.1-0.01M, pH- 7,4) and purified by dialysis against Tris-MgCl<sub>2</sub> buffer (0.1-0.01M, pH- 7.4) for overnight with three successive changes of the buffer at 4°C. The phage stock was then stored at 4°C.

### **4.10 Plaque assay:**

A plaque assay was performed to know the concentration of the purified phage sample and it was determined by serial dilution. Briefly, the purified phage sample was diluted serially and it was mixed with the log phase culture of bacterial cells. The phage-infected bacteria were then mixed with the molten soft agar and decanted in the agar plate. Plates were dried at room temperature and incubated at 37°C overnight. The next day plaques were counted and the concentration of the phage was determined by PFU counts.

### **4.11 Methods involved to determine morphology using transmission electron microscopy:**

#### **4.11.1 Carbon coating of the grid:**

A mica sheet was cut freshly and the surface of the mica sheet was attached with the tape to the filter paper in a Petri dish. It was placed within the vacuum evacuator chamber JEOL 400

where two small graphite rods were connected to a high-voltage circuit. The Chamber of vacuum evacuator of JEOL 400 with mica sheet was evacuated to a sufficiently high vacuum; the current was applied across the graphite rod in 5-10 seconds until the required amount of carbon was deposited on the mica sheet and the light brown color of the filter paper in the Petri dish indicated it.

10 X 1 cm of adhesive tape was dissolved in 50 ml amyl acetate reagent and the solution was stored in a bottle. Then the grids were kept on filter paper in a glass Petri dish. The mat surface was kept upward. The glue was added in a drop-by-drop manner onto the grids with a Pasteur pipette in such a way that the grids were wet uniformly. The sticky grids were kept under infrared light to become dry and stored in a clean Petri dish.

The carbon-coated mica sheet was kept in the moist chamber (at 4°C) for a few hours in such a way that the carbon coating position does not touch any substance and it helps the detachment of carbon film from the mica. The sticky grids were placed on a wire mesh under the surface of distilled water in a petri dish. The coated mica piece was taken out from the moist chamber and it was then slowly and carefully dipped into the water at an angle of 40°- 45°, in such a manner that the carbon film glided off and floated in the water. The wire mesh carrying the grids was raised upwards and grids became covered by a coat of carbon producing a solid transparent support film. The carbon-coated grids were dried under infrared light, taken away from wire mesh, and stored in a Petri dish for further use.

### **4.11.2 Glow-discharge of the carbon-coated grids:**

Carbon grids were glow discharged immediately before use. Carbon-coated grids are hydrophobic in nature. They can be made hydrophilic by subjecting them to glow discharge. Glow discharge is an important method that is utilized for cleaning and modifying surfaces. Carbo-coated grids were placed on a glass slide and were kept in a JEOL HDT 400 hydrophilic treatment device. The chamber was evacuated and glow discharge was carried out for a minute. The grids were ready and used within 30 minutes.

### **4.11.3 Negative staining of the samples:**

Negative staining relies on the principle of staining the background rather than the sample which gives better visual information about the sample. 5 µl sample was put on hydrophilic

300 mesh carbon-coated copper grids (Ted Pella, USA) and allowed to adsorb for 1 minute. Then the excess fluid was blotted off with a piece of filter paper and the sample was stained with 2% uranyl acetate solution by applying drop by drop. The excess liquid was blotted with filter paper. The grids were air-dried and observed under a transmission electron microscope (FEI Tecnai 12 BioTwin TEM).

#### **4.11.4 Transmission electron microscopy of the samples:**

The negatively stained grids were examined in an FEI Tecnai 12 BioTwin transmission electron microscope (FEI, Netherlands) operating at 100 kV using 100 µm C2 aperture and 50 µm objective aperture. Images were taken on an SIS MegaViewIII CCD camera (SIS, Herzogenrath, Germany). Magnification of the microscope was calibrated with negatively stained beef catalase crystal (Ted Pella, USA).

#### **4.12 Host range analysis and efficiency of plating calculation of phage Sfk20:**

A host range assay was performed to know the infectivity of the bacteriophage Sfk20 against many other enteric bacterial strains present in the laboratory (**Table 4.1**). It was determined by the spot assay method (Kutter 2009) on the basis of the phage's ability to form clear plaque in the bacterial lawn culture in an agar plate. Briefly, 10 µl of purified phage sample was spotted in the middle of the lawn culture of different enteric bacteria in agar plates. Plates were incubated overnight at 37°C; the visible clear zone of lysis was checked the next day.

The purified phage sample was serially diluted and the plaque assay was performed with all bacterial strains (giving a visible clear spot) including the host strain. The EOP of the primary host strain was considered as 1. The EOP values were calculated as the ratio of the PFU value of phage with a susceptible bacterial strain and the phage with an indicator (*Shigella flexneri* 2a, 2457 T) bacterial strain.

Table 4.1: Bacterial strains used for the host range analysis

Bacterial species	Strain no.
<i>Shigella flexneri 2a</i>	2457T
<i>Shigella flexneri 3a</i>	UB811
<i>Shigella flexneri 1b</i>	03075/19
<i>Shigella flexneri 4</i>	C2529
<i>Shigella flexneri 6</i>	UB812
<i>Shigella sonnei</i>	IDH00968
<i>Shigella boydii 1</i>	NK02379
<i>Salmonella enteritidis</i>	520833
<i>Salmonella typhimurium</i>	PH-94
<i>Salmonella typhi</i>	KOL 551
<i>ETEC</i>	IDH07942
<i>Vibrio cholerae O1</i>	MAK757

#### 4.13 One-step growth curve and adsorption kinetics:

The one-step growth curve of bacteriophage was carried out by a method described elsewhere with some modifications (Ahamed et al. 2019). Briefly, the *Shigella flexneri 2a* (2457T) strain was grown in LB medium at 37 °C. then 20 ml of early log phase culture (OD600 = 0.5) of the bacteria was harvested by centrifugation at 5000 X g at 4°C for 10 minutes. The supernatant was discarded and the pellet was resuspended in 1ml of LB medium. Thereafter the bacteriophage was added at an MOI of 0.1. The mixture was incubated for adsorption at 37°C for 5 minutes and diluted in Luria broth with a maximum volume of 10 ml and reintubated at 37°C. During incubation at 37°C aliquots were taken out at different time intervals up to 80 minutes and phage titer was calculated by soft agar overlay method. Burst size was calculated as a ratio of the average phage particles produced after the burst and the average number of phage particles adsorbed.

The adsorption assay was performed by a method described elsewhere with some modifications (Adams 1959). Briefly, 1 ml of early log phase culture (OD600 = 0.5) of *Shigella flexneri 2a* was mixed with phage at an MOI of 0.1 and incubated aerobically at 37°C. Samples were taken at 4 minutes intervals (up to 20 minutes) and immediately diluted into Tris-MgCl<sub>2</sub> buffer (0.1-

0.01M, pH- 7.4). The diluted sample was centrifuged at 8000 rpm for 5 minutes. The titer of the unadsorbed phage was assessed using the soft agar overlay method.

### **4.14 Phage stability assay under various physiological conditions:**

#### **4.14.1 Stability of phage Sfk20 under various temperatures:**

To evaluate the heat-resistant capacity of bacteriophage thermal stability experiment was performed as mentioned earlier with some modifications (Shahin, Bouzari, and Wang 2018). Phage suspension was taken in various microcentrifuge tubes and incubated at different temperatures (4°C, 25°C, 37°C, 50°C, 60°C, and 70°C) for one hour. After one hour of incubation, the phage suspensions were serially diluted and the number of active phages was determined by the soft agar overlay method.

#### **4.14.2 Phage sensitivity at various pH:**

To evaluate the phage stability at various pH conditions (Jamal et al. 2015), the aliquots of the LB broth were taken into various tubes. The pH of the medium was adjusted to a range of 3-13. Phage suspension was added to the LB broths and incubated at 37°C for 1 hour. Thereafter the phage viability was examined by the soft agar overlay method.

#### **4.14.3 Phage stability under ultraviolet irradiation:**

Phage stability under UV light irradiation was evaluated. For this purpose, purified and phage suspensions were kept under UV light at different time intervals of 5, 10, 15, and 20 seconds (Dutta and Ghosh 2007). After that phage viability was tested by the soft agar overlay method.

#### **4.14.4 Stability of phage virion at different saline conditions:**

To test the phage viability at the hypersaline condition an experiment was conducted. Briefly, 10µl of purified phage Sfk20 sample was added to 15 ml of sterile double distilled water containing 0%, 5%, 10%, 15% 20% NaCl and stored at 4°C for 28 days. Periodically the phage titer was assessed by plaque assay (Seaman and Day 2007).



### 4.15 Phage Sfk20 receptor identification:

#### 4.15.1 Proteinase K treatment:

This assay was performed as described earlier with some modifications (Hao et al. 2021; Kiljunen et al. 2011). Briefly, to examine the effect of proteinase K on phage adsorption, the log phase culture of *Shigella flexneri 2a* was treated with Proteinase K (0.8mg/ml) at 55°C for 2 hours, washed with Luria broth (LB), and phage adsorption assay was performed at an MOI of 0.1 as described above (Kiljunen et al. 2011). A control experiment without proteinase K was also conducted to confirm the possible effect was not due to the incubation of host bacteria at 55°C.

#### 4.15.2 Periodate treatment:

Another experiment was performed to study whether the periodate is responsible for destroying phage-host interaction (Hao et al. 2021; Kiljunen et al. 2011). Log phase culture of *Shigella flexneri 2a* was centrifuged at 5000 rpm for 5 minutes and the bacterial pellet was suspended in sodium acetate (50mM, pH 5.2) and Sodium acetate containing 10mM periodate. The cells were allowed to incubate at room temperature (protected from light) for 2 hours. After incubation cells were washed and treated with phage and an adsorption assay was done.

### 4.16 The bacteriolytic activity of phage Sfk20:

The overnight culture of *Shigella flexneri 2a* culture was diluted up to a 1:100 ratio and incubated at 37°C under shaking conditions until the early exponential phase was reached. Next, the phage Sfk20 was added at a MOI of 0.1, 1, and 100 and a control culture without adding phage was used. The samples were then incubated at 37°C temperature under shaking conditions. The CFU of the samples was calculated every 2 hours intervals up to 12 hours.

### 4.17 Genomic characterization of the phage Sfk20:

#### 4.17.1 Isolation of the genomic DNA of phage Sfk20:

Phage DNA was isolated from the purified phage sample using the DNA isolation kit (Norgen, Canada) using according to the protocol provided by the manufacturer. Briefly, 1 ml of purified phage sample ( $1 \times 10^{11}$  PFU/ml) was taken in a 15 ml tube and 500 µl of lysis buffer (provided by the manufacturer) was added to the phage lysate. The tube was then vortexed for 10 seconds.

In the next step, 650 µl of phage lysate was added to each of the spin columns containing the collection tube. Then the spin columns were centrifuged at 8000 rpm for 1 minute. The flowthrough was discarded. This previous step was repeated twice until the entire lysate pass through the spin column. Next 400 µl of Wash solution A (provided by the manufacturer) was added to the spin column and it was centrifuged at 8,000 rpm for 1 minute. The flowthrough in the collection tube was discarded. The column was washed for a second time with wash solution A and centrifuged at 8,000 rpm for 1 minute. The flowthrough was discarded. This step was further repeated. Next, the column was centrifuged at 14000 rpm for 2 minutes in order to thoroughly dry the resin of the column. Next, the spin column was transferred to the 1.7 ml elution tube provided with the kit. 75 µl of Elution Buffer B (provided by the manufacturer) was added to the column and centrifuged for 1 minute at 8000 rpm. The flowthrough from the elution tube was collected and stored at -20°C. Next, the concentration of the DNA was measured in a nanodrop (Eppendorf, Germany).

### **4.17.2 Restriction digestion of the DNA and separation using DNA gel electrophoresis:**

The isolated DNA sample was digested with seven different restriction enzymes: EcoRI, BamHI, HindIII, PstI, EcoRV, BglII, and MluI (Shahin et al. 2021). Briefly, in a 500 µl centrifuged tube double distilled water and buffer (provided with the restriction enzyme) were added. Next, the DNA sample was added and at last, the restriction enzyme was added to it. All the materials were added according to the manufacturer's protocol. The solutions were kept in an incubator at 37°C for 2 hours (**Figure 4.1**). After 2 hours of loading dye was mixed with the solution and a short spin was given. Next, the agarose gel was prepared to run the digested DNA. To prepare 1% agarose gel, in a conical flask 30 ml of 1X TAE buffer was added and 0.3 gm of agarose powder was added to it. The solution was then heated for 1-3 minutes until the agarose was dissolved completely. The agarose solution was cool down in a 65°C water bath. The solution was then poured into a previously prepared gel tray with the well comb. The gel was left for a few minutes until it became solidified. After the solidification, the comb was removed. The gel tray was then placed into a gel box filled with 1X TAE buffer. The digested DNA solutions were then loaded in 1% agarose gel and 250 bp to 25 kbp DNA molecular marker (high range DNA ladder, HiMedia) was also loaded. DNA fragments were separated by agarose gel electrophoresis at 100 V for 1 hour and the gel was placed in a container containing the ethidium bromide (EtBr) solution for staining. It was incubated into the staining solution for 10-15 minutes and then it was destained for 5 minutes. After the staining, the DNA gel was

checked under Gel doc (BIO-RAD, USA) The fragments of DNA were separated in the gel depending on their length.

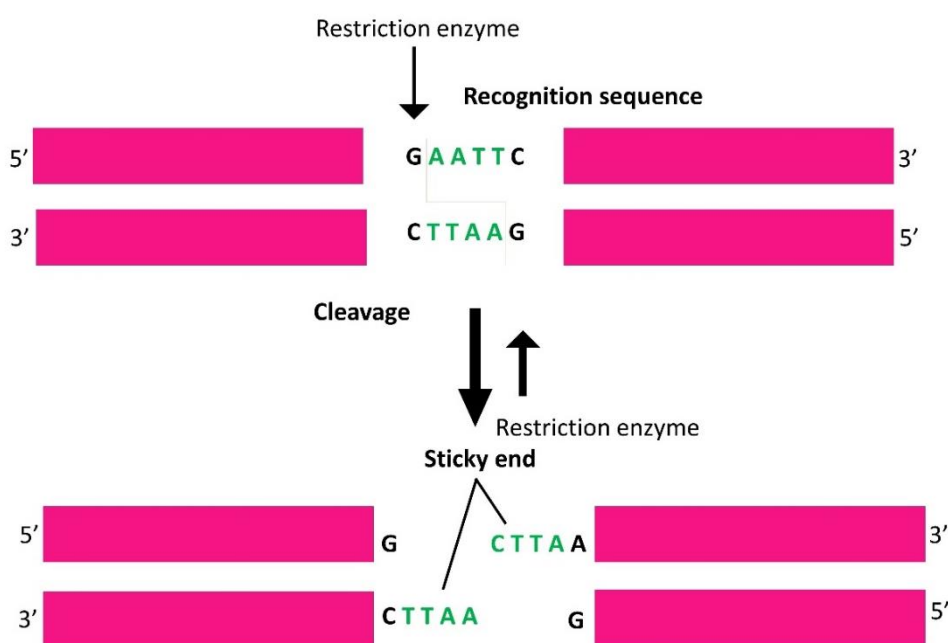


**Figure 4.1** Restriction digestion of genomic DNA.

### 4.17.3 Genome sequencing and analysis:

Phage Sfk20 whole genome sequencing was performed by Xcelris (Ahmedabad, India) using Next Generation Sequencing on an Illumina Platform and the sequencing end data was assembled with CLC Genomics Workbench v.6.0.5 with reads map back option. The obtained sequence was analyzed for similarity search against nucleotide by BLASTN, NCBI program. Potential open reading frames were predicted and annotated using Genemark and Prokaryotic GeneMark.hmm version 3.25 respectively. The putative functions of those ORFs were analyzed by BLASTP, NCBI program. Using the BLASTP and PSI-BLAST programs against the non-redundant databases; the predicted ORFs were queried from translated sequences. The genome map of phage Sfk20 was drawn using the CG viewer server (<http://view. ca/>) (Stothard and Wishart 2005). The genomic comparison of phage Sfk20 with closely related *Myoviridae* *Shigella* phages was illustrated in the form of a linear figure using the Easyfig application (<http:// mjsull. github. io/ Easyfig/ files. html>) (Sullivan, Petty, and Beatson 2011). In addition, tRNAs were predicted using ARAGORN (<http:// 130. 235. 244. 92/ ARAGORN/>) and tRNAscan-SE (<http:// lowelab. ucsc. edu/ tRNAscan- SE/>) (Laslett and Canback 2004;

Schattner, Brooks, and Lowe 2005). The nucleotide sequence of the genome of Sfk20 was submitted at GenBank under accession number MW341595.

#### **4.17.4. Phylogenetic analysis:**

For phylogenetic analysis two predicted ORFs were selected based on their amino acid sequences. The amino acid sequence of baseplate wedge protein (ORF189, protein\_id: QPP47184) and terminate large subunits (ORF163, protein\_id: QPP47158) was chosen. The amino acid sequences of Sfk20 were aligned with those of other reference *Myoviridae* bacteriophages using MUSCLE and then the phylogenetic tree was constructed using “ONE CLICK” at Phylogeny.fr.

### **4.18 Proteomic characterization of phage Sfk20:**

#### **4.18.1 Isolation of phage Sfk20 proteins:**

1 ml of highly concentrated and purified bacteriophage was taken in a microcentrifuge tube. It was then kept in a boiling water bath for 5-10 minutes. Thereafter the boiled sample was cooled down.

#### **4.18.2 Protein profile analysis by running SDS-PAGE:**

To check the protein profile of bacteriophage denaturing SDS-PAGE was performed as described by Laemmli (Laemmli 1970). At first, the gel plates were cleaned properly. Next, the gel plates were joined to form a cassette and it was clamped in a vertical position. Thereafter the 12.5% resolving gel was prepared as mentioned in the reagent preparation section and using a Pasteur pipette the gel solution was added to the gel cassette gently until it reached 1cm away from the bottom of the comb. To create a smooth surface upper edge of the resolving gel, double distilled water was added. The stacking gel was then prepared in a 50 ml centrifuge tube as mentioned in the chemical reagent preparation section. When the resolving gel was set properly inside the gel cassette the excess water was discarded and stacking gel was added onto the surface of the polymerized resolving gel. Immediately after the pouring the Teflon comb was inserted into the stacking gel solution. In this condition, the gel was kept at room temperature for 20 minutes to set properly. Next, the sample was prepared. For this purpose, 20 µl of phage protein sample was mixed with the loading dye and boiled under the boiling water bath for five minutes. After the rapid boiling, the sample was cooled down. 10 µl of the sample was then

loaded in the pre-determined lane of the stacking gel. The 5 µl of pertained protein ladder was loaded in the lane. Next, the electrophoresis apparatus was connected to the power pack and the Sodium do decyl sulfate-poly acryl amide gel electrophoresis was performed at room temperature in 80KV in 1X SDS gel running buffer until the sample was entered from stacking gel to resolving gel After entering into the resolving gel the electrophoresis was performed at 120KV for 1 hour. After the run the chamber of the gel apparatus was dismantled and gel plate was opened to remove the gel. The stacking gel was discarded and kept it in the fixative solution for 15 minutes in the rocking platform. After the fixation of the protein the gel was stained with a previously prepared staining solution for 15-20 minutes and during the staining the gel was kept under the rocking platform. Lastly, the destaining solution was added to the gel after discarding the staining solution and kept under rocking conditions overnight. In the very next day, the destaining solution was changed twice and the visible bands had appeared after the removal of the excess stain.

### **4.18.3 Phage proteomic analysis using LC-MS/MS:**

#### **4.18.3.1 In-solution tryptic digestion:**

Purified phage Sfk20 was extracted as mentioned earlier. The extracted protein was dried under a vacuum in a speed vac and resuspended for denaturation in 6M urea in ammonium bicarbonate. Next to reduce the di sulfide bond 100 mM of DTT was added to make the final concentration 10 mM in the protein solution and it was then incubated at 56°C for 1 hour in the dark. In the solution free thiol (-SH) was present and it was then alkylated with iodoacetamide to make the final concentration 55mM. The solution was then incubated at room temperature for 30 minutes. The reduced and alkylated protein solution was mixed with ammonium bicarbonate to reduce the urea and finally digested with trypsin.

#### **4.18.3.2 LC-MS/MS analysis:**

The digested peptide sample was then mixed with formic acid and analyzed by LC-MS/MS on 1200, 1D nano-LC (Agilent Technologies, San Diego) that was coupled to Nanomate Triversa (Advion) and LTQ – Orbitrap Discovery (Thermo Fisher Scientific, USA). LC-MS/MS spectra were searched using a PEAKS engine against the phage genome. For protein identification the following options were used peptide mass error tolerance: 10.0 ppm, Fragment mass error

tolerance: 0.6 Da, enzyme: trypsin, Max Missed Cleavages: 2, fixed modification: carbamidomethyl (C), variable modifications: oxidation (M), deamidation (NQ).

The in-solution tryptic digestion and LC-MS/MS analysis process were at C-CAMP (NCBS, India) according to the previously mentioned protocol (Abril et al. 2020; Junqueira et al. 2008; Olsen et al. 2005; Wiese et al. 2007).

### **4.19 Structural characterization of phage Sfk20:**

#### **4.19.1 Sample preparation of cryo-electron microscopy:**

For cryo-electron microscopy sample preparation, holey carbon grids, as well as R1.2/1.3 300 mesh gold grids (Quantifoil), were used for the study. The grids were glow discharged for 130 seconds at 20 mA to make the grid surface hydrophilic just before the sample preparation. In a FEI Vitrobot IV automated plunger around 3  $\mu$ l of freshly prepared highly concentrated and purified phage Sfk20 sample was applied to the glow discharged grid and waited for 10 seconds. After the adsorption, the excess sample was blotted for 5 seconds from both sides. The condition of the plunger was kept at 4°C and 100% humidity. Then the grid containing the sample was quickly plunged into liquid ethane to form glasslike ice with the same near-native intact state inside. The cryo-fixed grids were transferred into cryo-grid boxes and preserved under liquid nitrogen until further use.

#### **4.19.2 Cryo-EM data collection:**

Cryo-EM data was acquired using Thermo Scientific™ Talos Arctica transmission electron microscope at 200 kV equipped with K2 Summit Direct Electron Detector. Images were collected automatically using Latitude S automatic data collection software (Gatan Inc) at nominal magnification 33,500x at the pixel size 1.49Å at specimen level. The images were collected at low dose conditions of about 80 e-/Å<sup>2</sup> with a defocus range of -0.75  $\mu$ m and -2.25  $\mu$ m and the calibrated dose was 4 e-/Å<sup>2</sup> per frame was subjected to the sample. Data were recorded for 8 sec for a total of 20 frames. Around 829 movies were collected for phage Sfk20 for further processing.

### 4.19.3 Cryo-EM data processing:

#### 4.19.3.1 Computational processing of Sfk20 capsid structure:

For the analysis of the capsid part, EMAN 2.9 software was used in a Linux platform Ubuntu 18.04 LTS version. Initially, the micrographs were imported and motion correction was performed (**Figure 4.2**). After that .hdf files were generated and the particles were picked from those files. Next, the capsid part of the Sfk20 phage particles was picked using the graphical interface “e2boxer.py” in EMAN 2.9 (Ludtke, Baldwin, and Chiu 1999) with 1296 box size and 1.49Å/pixel (**Figure 4.4**). A total of 425 particles were selected from 759 micrographs. After picking the particles the CTF correction was performed. For the CTF correction in EMAN 2.9 software the graphical interface “e2ctf\_auto.py” program was used with 200V, 1.49Å/pix, Cs 2.7 parameters and the hires option was also checked. The hires option of the automated CTF processing gave a hint that data may extend to near-atomic resolution. After the CTF correction, the boxed-out raw particles were taken and class averaged using the program e2refine2d.py. This step had two purposes: First some of the good class averages were prepared which were required to make an initial 3-D map for refinement. Second, it was possible to identify some fractions of bad particles and those were removed from the dataset. After several rounds of 2D classifications, some of the good class averages (which look similar) were selected for further processing. From the class averages the initial model was prepared and the refinement cycles were performed with imposing C5 symmetry. The refinement cycle(e2refine\_easy) was repeated until the model converged. In every case, 2D projection images of just the previous 3D models (for eg. threed.1.mrc) and CTF-corrected raw particles (excluding bad particles) were classified into different class averages with respect to the 2D projection images. The previous 3D model was further refined using the newly formed 2D class averages and previously formed refined 3D model. This process was repeated several times until a converged 3D model was generated. The final 3D structure was generated after a few refinements and considered as a final 3D structure. Visualization of all the models was done by UCSF Chimera software.

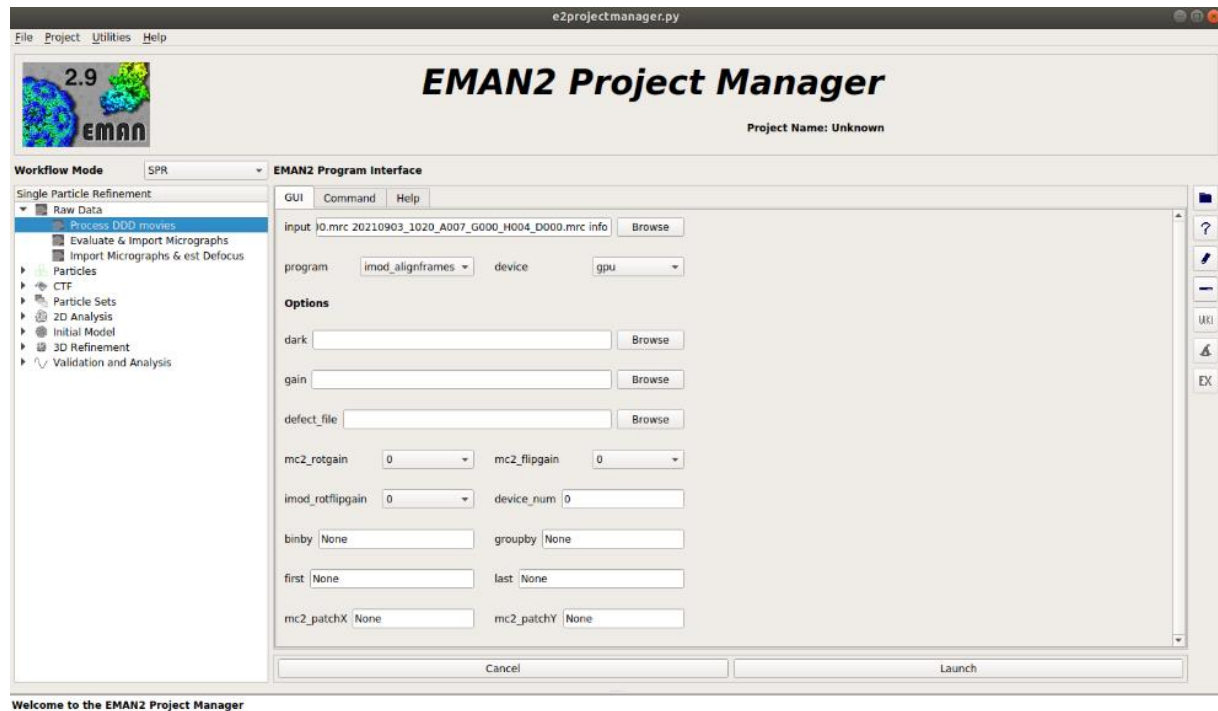


Figure 4.2: Processing of the DDD movie files into micrograph using EMAN 2.9.

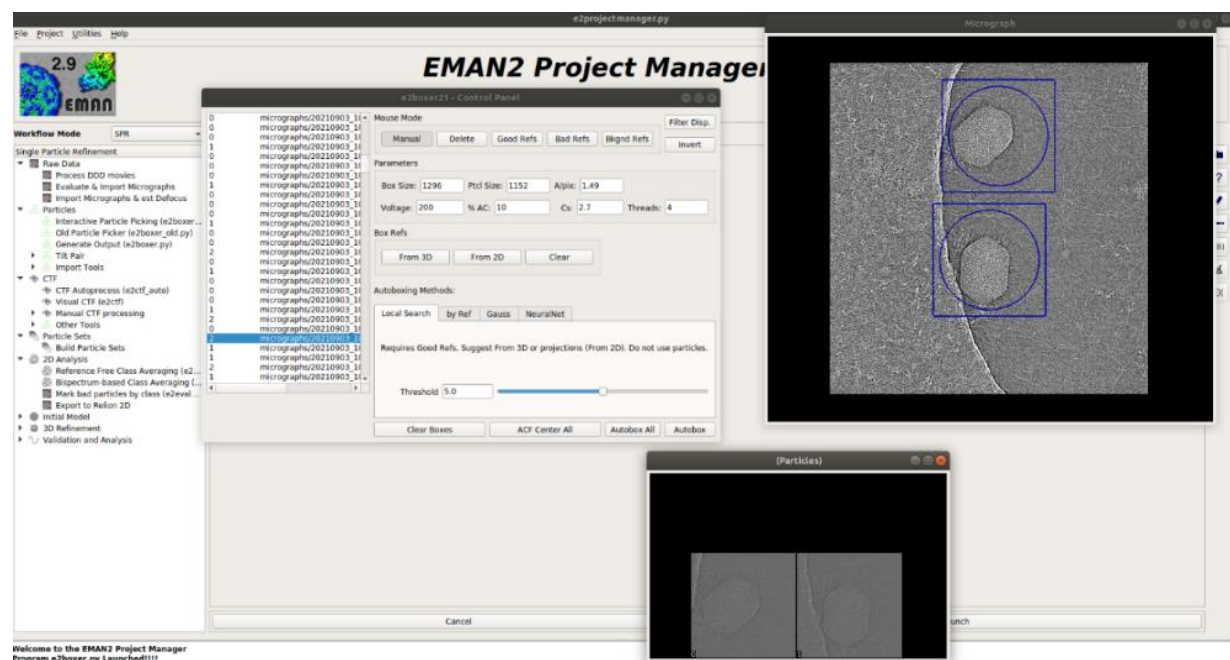


Figure 4.3: Particle picking of the bacteriophage capsid.



### 4.19.3.2 Processing of phage Sfk20 head-to-tail connector structure:

The head-to-tail connector part of the phage Sfk20 act as a portal gatekeeper. The phage genome has passed from this portal gatekeeper. For the analysis of the capsid part of the phage Sfk20, the neck part of the Sfk20 phage was picked from intact phage particles using the graphical interface program “e2boxer.py” in EMAN 2.9 (Ludtke et al. 1999) with box size 512, ptcl size 480 and 1.49A/pixel. A total of 375 particles were selected from 759 micrographs. The boxed-out particles were then undergone CTF correction. For the CTF correction in EMAN 2.9 software, the graphical interface “e2ctf\_auto.py” program was used using 200V, 1.49A/pix, Cs 2.7 parameters, and the hires box was also checked. The class averaging of the CTF-corrected particles was performed using the program e2refine2d.py. Some of the good class averages were further chosen from the class averages. The good class averages were further generated by applying C12 symmetry. The reconstructed model was further refined using e2refine\_easy. A few cycles of refinement were performed to get a final reconstructed structure. Visualization of all the models done by UCSF Chimera software.

### 4.19.3.3 Processing of the tail part of phage Sfk20:

The long contractile tail of the Sfk20 phage has a helical symmetry. For the analysis of the tail part, Relion 3.1 software was used. At first, the movie files were imported using the parameters 1.49A/pixel, voltage 200, and spherical aberration 2.7 mm (**Figure 4.4**). The beam-induced motion correction was performed using “MotionCor2”. The CTF correction was performed using the graphical interface “CTF estimation”. Next, the particles were picked manually using the “Manual picking” program, and for picking the helical tail part “pick star-end coordinate helices (He and Scheres 2017)” option was selected. A total of 1000 particles were picked and extracted for further processing of the tail. The extracted particles were sorted using “Subset selection” where the bad particles were rejected from the dataset. The good particles were used to prepare a new set for the 2D class averaging. After several rounds of class averaging the good class averages were selected for 3D classifications and further processing was done.

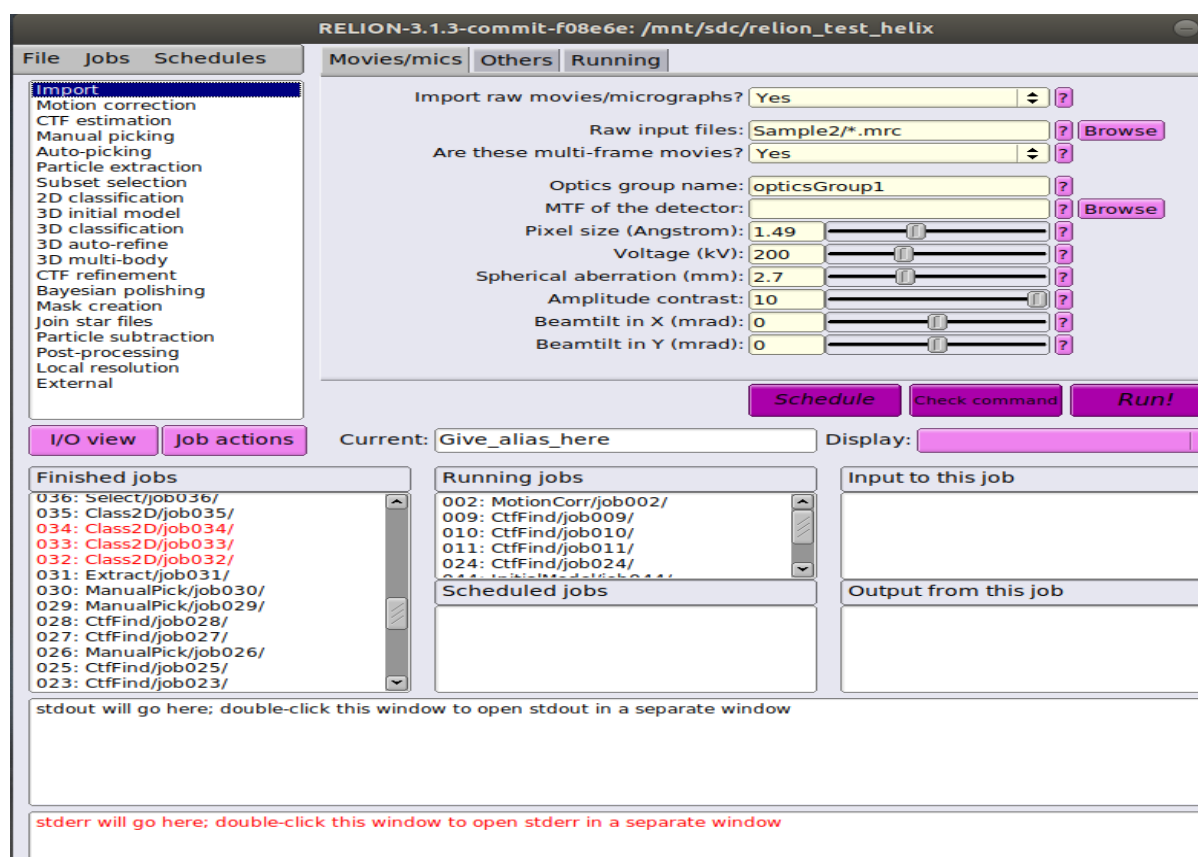


**Figure 4.4:** Helical reconstruction of the phage Sfk20 tail part.

#### 4.19.3.4 Processing of the baseplate part of phage Sfk20:

At the periphery of the Sfk20 phage particles, the baseplate part was present. This is the multiprotein complex of phage Sfk20 that controls the recognition of the host cell, attachment to the host cell, contraction of the viral tail sheath, and genome ejection. The baseplate part of the phage Sfk20 was also reconstructed using EMAN 2.9 (Ludtke et al. 1999) software. For this purpose, the baseplate part of the intact phage particle was boxed out using the graphical interface “e2boxer.py” in EMAN 2.9 using box size 360, ptcl size 352, and 1.49Å/pixel size. A total of 271 baseplate particles were selected from 759 micrographs. The CTF correction of the boxed-out particles was performed using the program “e2ctf\_auto.py” in EMAN 2.9. The parameters used for the CTF corrections were voltage 200, 1.49Å/pix, and Cs 2.7 respectively and the hires option was also included. The class averaging of the CTF-corrected particles was performed using the program e2refine2d.py. Some of the good class averages were chosen from all class averages. The good class averages were further reconstructed by applying C6 symmetry. The reconstructed model was further refined using e2refine\_easy. A few cycles of

refinements were performed to get a final reconstructed structure. Visualization of all the models done by UCSF Chimera software.

#### **4.19.4. UCSF- Chimera:**

The UCSF chimera software packages were used for the visualization of the 3D models of the different parts of the phage particle (Pettersen et al. 2004). Chimera is developed by the Resource for Biocomputing, Visualization, and Informatics. It is one of the most well-known and user-friendly software packages for visualization and model building. UCSF Chimera expandable program for the interactive visualization and studies of molecular structure and associated data including macromolecular assemblies, density maps, etc. The sequence alignment, docking, and conformational changes of X-ray crystallographic structure can be studied by Chimera software. High-quality image animation can be created. Chimera is freely downloadable for academic, government, non-profit and personal use.

#### **4.20 Structure prediction of phage Sfk20 proteins using neural network-based and homology modeling-based methods:**

A user-friendly interface for accessing AlphaFold2 and ESMFold has recently been made available through Jupyter Notebooks in Google Colaboratory. The ColabFold-AlphaFold2 and ColabFold-ESMFold notebooks were used to predict the structure of a few important phage structural proteins detected using LC-MS/MS. Also, the Phyre2 server was used for the prediction of the selected structural proteins. The result obtained from the three approaches were compared.

From the list of the proteins identified by LC-MS/MS six important structural proteins were selected for this study. The amino acid sequences of those selected proteins were collected from the NCBI database (MW341595). Their structures using ColabFold-AlphaFold2 (**Figure 4.5**) (Mirdita et al., 2022), ColabFold-ESMFold (**Figure 4.6**) (Mirdita et al. 2022), and Phyre2 (**Figure 4.7**) (Kelley et al. 2015). The predicted final structure was submitted to the DALI server to identify the structural homolog (**Figure 4.8**) (Holm 2022). The structural homolog or the experimental structures were collected from the PDB and the predicted structures were aligned with the PDB homologs using the UCSF Chimera matchmaker tool (Pettersen et al. 2004). Their template modeling scores or TM scores were determined using the TM-align program (Zhang and Skolnick 2004). The protein structures predicted using AlphaFold2 and

## CHAPTER 4

ESMFold were color-coded using UCSF ChimeraX based on per residue estimate of confidence (pLDDT) of both the neural-network-based models (Pettersen et al. 2021).

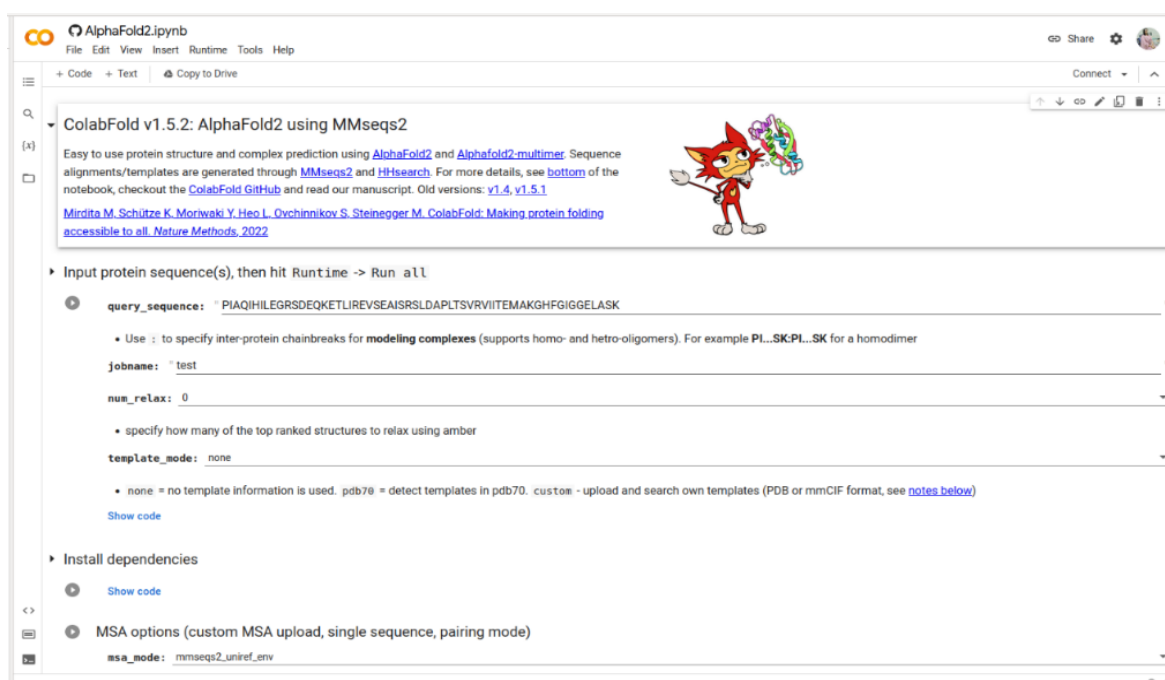


**Figure 4.5** User-friendly interface for AlphaFold2 available through Jupyter Notebooks in Google Colaboratory.

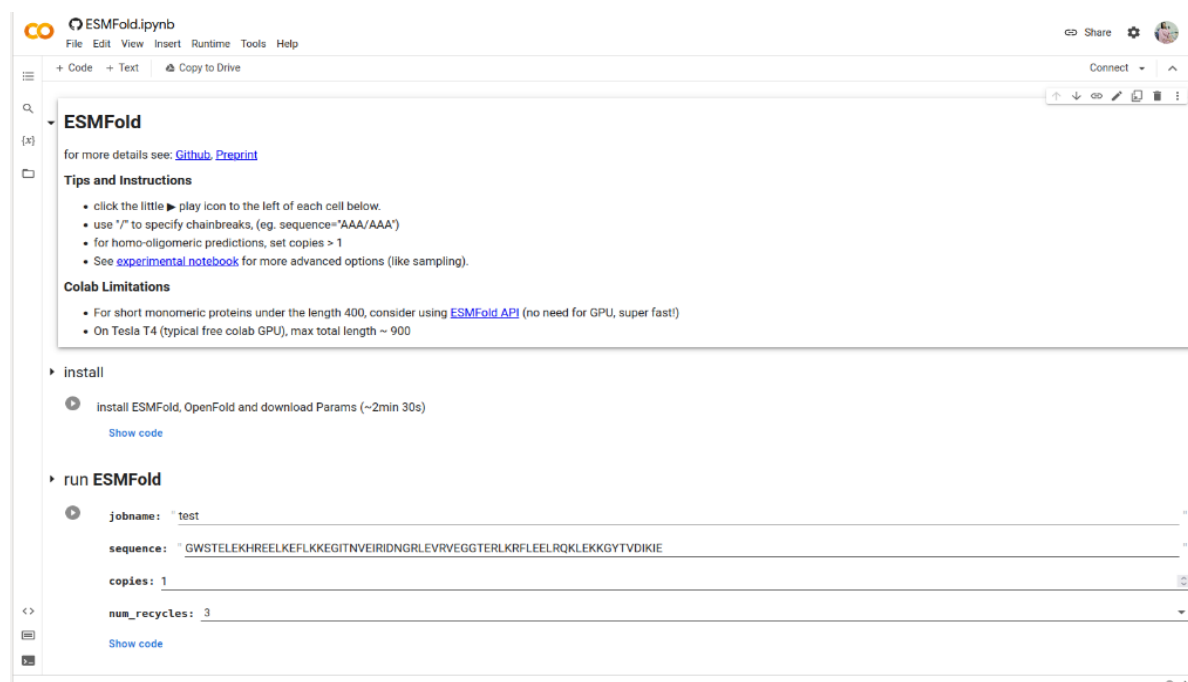


**Figure 4.6** User-friendly interface for ESMFold available through Jupyter Notebooks in Google Colaboratory.

Standard Mode | [Login](#) for job manager, batch processing, Phyre alarm and other advanced options

Retrieve Phyre Job Id [Fetch](#)

# Phyre<sup>2</sup>

Protein Homology/analogy Recognition Engine V 2.0

Subscribe to Phyre at Google Groups  
 Email:   
[Subscribe](#)  
[Visit Phyre at Google Groups](#)  
[Follow @Phyre2server](#)

Log in (top left-hand corner of this web page) to use our Expert Mode features, including batch job submission and One-to-One threading. Registering for this is quick and easy on our [Login page](#).

You can use "One-to-One Threading" to model your sequence against your own in-house structures and those from the [Protein Data Bank](#), as well as models downloaded from the [AlphaFold Protein Structure Database](#).

If you have more than 5 or 6 sequences to model, it is easier for you (and better for everyone!) if you use "batch" processing (under Expert Mode).

**Please do not use "Intensive mode" unless your search using "normal mode" indicates that a single model does not cover most of your sequence.** For most users, most of the time, 'normal mode' will give you the answer you require in a fraction of the time.

Current Phyre2 server load = 4% (normal running)

E-mail Address

Optional Job description

Amino Acid Sequence

Modeling Mode ☒ Normal ☐ Intensive ☐ Test

Please tick as appropriate: ☒ NOT for Profit ☐ FOR Profit (Commercial) ☐ Other

[Phyre Search](#) [Reset](#)

**Figure 4.7:** Homology modeling software Phyre 2.

# DALI

## PROTEIN STRUCTURE COMPARISON SERVER

[About](#) [PDB search](#) [PDB25](#) [AF-DB search](#) [Pairwise](#) [All against all](#) [Tutorials](#) [References](#) [Statistics](#) [Download](#)

The Dali server is a network service for comparing protein structures in 3D. You submit the coordinates of a query protein structure and Dali compares them against those in the Protein Data Bank (PDB). In favourable cases, comparing 3D structures may reveal biologically interesting similarities that are not detectable by comparing sequences.

Check queue status [here](#). Megausers please consider downloading the standalone program.

You can perform three types of database searches:

- **Heuristic PDB search** - compares one query structure against those in the Protein Data Bank
- **Exhaustive PDB25 search** - compares one query structure against a representative subset of the Protein Data Bank
- **Hierarchical AF-DB search** - compares one query structure against a species subset of the AlphaFold Database

and two types of structure comparisons of user selected structures:

- **Pairwise** structure comparison - compares one query structure against those specified by the user
- **All against all** structure comparison - returns a structural similarity dendrogram for a set of structures specified by the user

Citation:

1. Holm L, Laiho A, Toronen P, Salgado M (2023) DALI shines a light on remote homologs: one hundred discoveries. *Protein Science* 23, e4519

**Figure 4.8:** Structural homolog was identified using DALI server.

### 4.21 Study of bacteriophage Sfk20 life cycle by electron microscopy

#### 4.21.1 Phage-host interaction study by TEM:

To study the life cycle of bacteriophage Sfk20 the log phase culture of *Shigella flexneri* 2a was infected with phage Sfk20 and incubated at 37°C. Samples were taken out at around 15, 30, and 60 minutes respectively, and immediately centrifuged at 7,000 rpm for 5 minutes. The supernatant was discarded. In the next step, the cell pellet was resuspended in 3% glutaraldehyde in 0.1 ml cacodylate buffer and stored at 4°C overnight (Majumdar et al. 1988). In this experiment, glutaraldehyde was used as the primary fixative. The next day the fixed cells were centrifuged at 3000 rpm for 5 minutes. The supernatant was discarded and the pellet was washed with phosphate buffer by centrifugation. The secondary fixation was done in 1% Osmium tetroxide (OsO<sub>4</sub>) in 0.2 M cacodylate followed by incubation for 1 h at room temperature. After pelleting down, the sample was dehydrated with a series of ascending concentrations of ethanol (30%, 50%, 70%, 90%, and 100%). The samples were then embedded in resin Agar 100 and polymerization was done at 60°C overnight. The ultrathin sections (40–50 nm) of the control and infected cells are cut with a Leica Ultracut UCT ultramicrotome (Leica Microsystems, Germany). The sections were picked up in 300 mesh thin bar nickel or copper grids (Agar Scientific, United Kingdom), and dual-stained with 2% aqueous uranyl acetate and 0.2% lead citrate. The grids were airdried and immediately checked and examined under an FEI Tecnai 12 BioTwin Transmission Electron Microscope (FEI, Netherlands) at an accelerating voltage of 100 kV.

#### 4.21.2 Phage-host interaction study by SEM:

To visualize the phage Sfk20 lytic cycle by scanning electron microscopy samples were taken out in microcentrifuge tubes from the mixture of the bacteria-bacteriophage at early, mid, and late phase. The mixture was then immediately centrifuged at 7,000 rpm for 5 minutes. The supernatant was discarded and the sample was fixed with 3% glutaraldehyde in 0.1 ml cacodylate buffer and stored at 4°C overnight. Next day the fixed sample was centrifuged at 7,000 rpm for 5 minutes and the pellet was dehydrated in 30% ethanol for 10 minutes, 50% ethanol for 10 minutes, 70 % ethanol for 10 minutes, 90% ethanol for 10 minutes, and finally with 100% absolute ethanol for 15 minutes. All dehydrated sample was treated with a 1:1 ratio of absolute ethanol and hexamethyldisilazane (HMDS) for 10 minutes and 100% HMDS for 1 hour. The tubes were left in the fume hood to evaporate the HMDS completely. The next day

the samples were mounted on specimen stubs and sputter coated with gold (sputter coater gold, Polaron, 240V) and immediately examined under FEI Quanta 200 scanning electron microscope (FEI, Netherlands).

### **4.22 *Shigella* biofilm formation and degradation study by phage Sfk20:**

#### **4.22.1 Biofilm degradation assay using phage Sfk20 and ampicillin:**

##### **4.22.1.1 Biofilm degradation assay study by scanning electron microscopy:**

A qualitative biofilm degradation assay of phage Sfk20 on *Shigella flexneri* 2a was performed following a previous method with some modifications (Nickerson et al., 2017). Glass coverslips were used for this assay. 10 µl of an overnight culture of *Shigella flexneri* 2a was added on coverslips submerged in LB media in 6-well plates and incubated at 37°C for 24 hours and 48 hours respectively. After 24 hours and 48 hours, the biofilm was treated with phage Sfk20 ( $10^{10}$ PFU/ml), ampicillin (256 µg/ml) alone, and a combination of both of them. The treated samples were incubated overnight at 37°C. The next day the planktonic cells were removed and the coverslips were fixed with 3% glutaraldehyde in 0.1 ml cacodylate buffer and stored at 4°C overnight. Next day the fixative was removed and the samples were dehydrated in 30% ethanol for 10 minutes, 50% ethanol for 10 minutes, 70 % ethanol for 10 minutes, 90% ethanol for 10 minutes, and finally 100% absolute ethanol. All dehydrated sample was treated with 1: 1 ratio of absolute ethanol and hexamethyldisilazane (HMDS) for 10 minutes and 100% HMDS for 1 hour. These well plates were left in the fume hood to evaporate the HMDS completely. The next day the coverslips were mounted on specimen stubs and sputter coated (sputter coater gold, Polaron, 240V) with gold and immediately examined under FEI Quanta 200 scanning electron microscope (FEI, Netherlands).

##### **4.22.1.2. Quantitative assay of biofilm degradation:**

The quantitative experiment on the ability of Sfk20 to degrade the biofilm alone or in combination with an antibiotic was also performed. Briefly, 10 µl of an overnight culture of *Shigella flexneri* 2a was added to the wells of a 96-well flat-bottom polystyrene microtiter plate (Nickerson et al., 2017) containing 200 µl fresh broth. Then the bacterial cells were grown at 37°C for 48 hours under a static condition (Yazdi, Bouzari, and Ghaemi 2018). On the following day, the planktonic cells were removed and the biofilm was treated with Sfk20 ( $10^{10}$ PFU/ml),

ampicillin (256 µg/ml), and their combination. The plates were then incubated overnight at 37°C. The next day the phage and antibiotics were removed and the wells were gently washed twice with 1X phosphate-buffered saline (PBS). Then the wells were stained with 1 % crystal violet. Afterward, the wells were washed with distilled water and set to air dry. The crystal violet stain was then dissolved in Dimethylsulfoxide (DMSO). The total biomass of the biofilm was measured by a plate reader at the absorbance of 595 nm (iMark Microplate Reader S/N 21673) followed by a statistical analysis of the data.

### **4.22.2. Biofilm degradation assay using phage cocktail**

#### **4.22.2.1. Preliminary characterization of the other cocktail member phage Sfk23:**

For the preparation of the phage cocktail, another phage was selected from the laboratory and its morphology was examined under a transmission electron microscope as mentioned previously in this chapter.

A host range and efficiency of plating assay were performed to know the infectivity of the bacteriophage Sfk23 against many other enteric bacterial strains present in the laboratory as mentioned previously.

#### **4.22.2.2. Preparation of phage cocktail of phage Sfk20 and Sfk23:**

For the preparation of the phage cocktail, both purified Sfk20 and Sfk23 phages were used. Phage cocktail was prepared based on the criteria that the phages were isolated from the samples with different locations, and to the most degree, this warrants that the isolated phages are different without the knowledge of the genome sequences. The phage cocktail was prepared using the protocol mentioned earlier (Chen et al. 2019) with some modifications. A  $10^{11}$  PFU/ml concentration of each purified phage solution was combined in an equal proportion to create the phage cocktail. The concentration of the phage cocktail was measured using plaque assay as mentioned earlier in this chapter.

#### **4.22.2.3 Biofilm formation and degradation in microtiter plate:**

Mature biofilm was formed according to the standardized protocol (Mallick, Mondal, and Dutta 2021). Briefly, 48 hours of matured biofilm was grown on the 96-well flat-bottom polystyrene microtiter plate. On the following day, the planktonic cells were removed and the biofilm was treated with Sfk20 ( $10^{11}$  PFU/ml), Sfk23 ( $10^{11}$  PFU/ml), and their combination ( $2.2 \times 10^{11}$ ). The



plates were then incubated overnight at 37°C. The next day the phages and the cocktail were removed and the wells were gently washed twice with 1X phosphate-buffered saline (PBS). Then the wells were stained with 1 % crystal violet. Afterward, the wells were washed with distilled water and set to air dry. The crystal violet stain was then dissolved in Dimethylsulfoxide (DMSO). The total biomass of the biofilm was measured by a plate reader at the absorbance of 595 nm (iMark Microplate Reader S/N 21673) followed by a statistical analysis of the data.

### **4.22.3. Statistical analysis:**

Statistical analysis of the data was performed by two-way ANOVA with Graph-Pad Prism 5.00



# CHAPTER 5

## Objective 1 (Part I)

Morphological and biological  
characterization of a lytic *Shigella*  
phage Sfk20



### 5.1 INTRODUCTION

Diarrhoea is one of the major causes of morbidity and mortality in the world particularly in developing and under-developed countries. It contributes to about 4% of all deaths and 5% of the loss of health to disability worldwide (Caramia et al. 2015). Diarrhoea is the fifth major cause of death among all populations and also the reason for the death of one in nine children below five years old (Anteneh, Andargie, and Tarekegn 2017). The rate of diarrheal disease is different on various continents of the world. The incidence of diarrheal disease is quite high in South Asia and sub-Saharan Africa.

Gram-negative bacterial pathogens are the major cause of diarrheal diseases. Various genera such as *Shigella*, *Salmonella*, *Escherichia*, *Campylobacter*, *Enterobacter*, *Klebsiella*, *Proteus*, *Yersinia*, and *Serratia* are included in this group. Among these genera, *Shigella* spp. is one of the most common significant pathogens for diarrheal disease. *Shigella*-infected bacillary dysentery is commonly known as Shigellosis. There are four different types of *Shigella* spp.: subgroup A (*Shigella dysenteriae*); subgroup B (*Shigella flexneri*); subgroup C (*Shigella boydii*) and subgroup D (*Shigella sonnei*). Each subgroup is divided into different serogroups. *Shigella flexneri* is the leading cause of shigellosis in low-income and middle-income countries.

Different antimicrobial agents such as ampicillin, azithromycin, erythromycin amoxicillin, norfloxacin, ofloxacin, nalidixic acid, ciprofloxacin, etc are commonly used for the treatment of shigellosis (Christopher et al., 2010). Due to the rapid and indiscriminate use of antibiotics, several resistant strains are increasing and spreading globally. *Shigella* spp. became resistant to various antibiotics and the treatment of shigellosis with antibiotics is expensive and time-consuming (Taneja and Mewara 2016). Half of the *Shigella* strains in different parts of the world are resistant to multiple antibiotics (Qiu et al. 2013). Moreover, no effective commercially available vaccines are there. Hence, finding an alternative way of treatment is necessary. Lytic bacteriophages have the potential to be used as an alternative to antibiotics because phages are host specific and they do not disturb other bacteria present in the same environment.

The majority of the bacteriophages belong to the order *Caudovirale* and they are also known as tailed bacteriophages. The order *Caudovirales* are further subdivided into three families: *Myoviridae* (long contractile tail), *Siphoviridae* (long non-contractile tail) *Podoviridae* (Short, contractile tail). Different phage characteristics such as morphology, nucleic acid content,

## CHAPTER 5

---

physicochemical properties of the phage virion, and genomic data are used for the classification of the phage by the International Committee of the Taxonomy of Viruses (ICTV) (Ackermann, 2007a). Among all the characteristics, the morphology and the nucleic acid contents are the major determinants for the classification.

In this section of the work, we have discussed the morphology of the newly isolated bacteriophage Sfk20 and its host *Shigella flexneri 2a* bacteria. The biological characterization has also been discussed in this section.

## 5.2 RESULTS

### 5.2.1 Morphology and growth curve of the *Shigella flexneri* 2a bacteria:

#### 5.2.1.1 Morphology determination of *Shigella flexneri* 2a bacteria using scanning electron microscopy and transmission electron microscopy:

*Shigella flexneri* 2a is a gram-negative, rod-shaped, facultative anaerobic bacteria. In this study exponentially grown *Shigella flexneri* 2a strain (2457T) was examined under a scanning electron microscope (FEI Quanta 200). The scanning electron micrograph of *Shigella flexneri* 2a in **Figure 5.1 (A)** showed the rod-shaped, non-flagellated morphology of the bacteria. Exponential culture of the glutaraldehyde fixed *Shigella flexneri* 2a bacterial cells were sectioned, stained, and checked under a transmission electron microscope (FEI Tecnai 12 BioTwin). The transmission electron micrograph of the ultrathin section of the host bacteria was shown in **Figure 5.1 (B)** The intact double-layer membrane around the periphery of the bacterial cell and the internal cellular materials were visible in the micrograph.

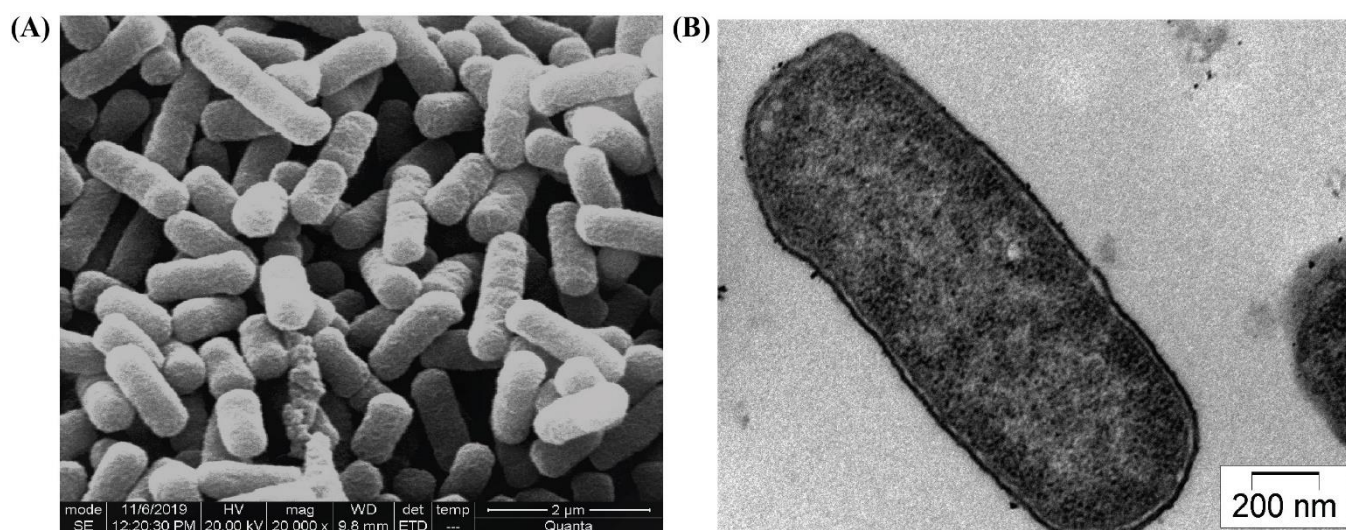


**Figure 5.1:** Electron micrograph of *Shigella flexneri* 2a bacteria: (A) scanning electron micrograph and (B) ultrathin section of *Shigella flexneri* 2a bacteria.

### 5.2.1.2 *Shigella flexneri* 2a growth curve:

The growth curve of the *Shigella flexneri* 2a 2457T strain was constructed using the values of optical density (OD) at 600 nm as shown in **Figure 5.2**. The bacterial sample was collected every 30 minutes up to 10 hours. The OD<sub>600nm</sub> values at each time point were measured.

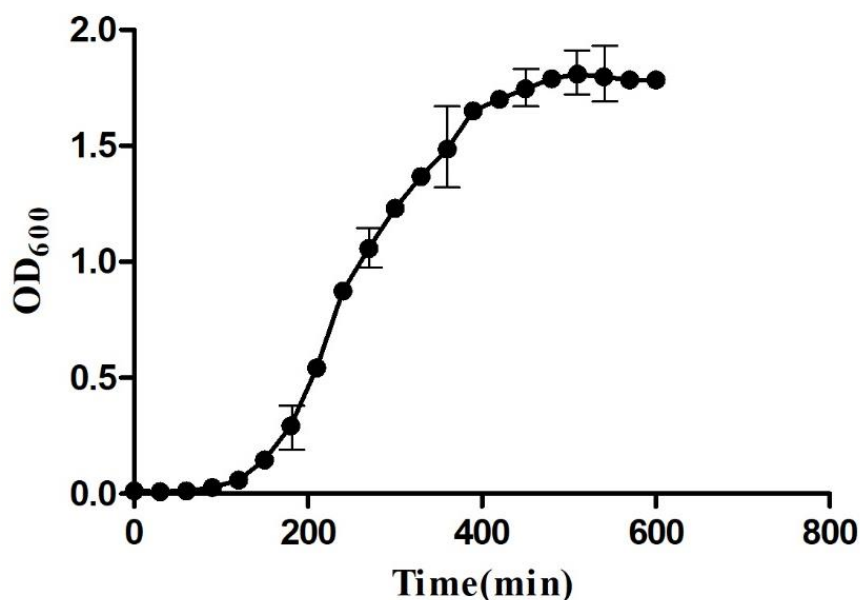


**Figure 5.2:** The growth curve of *Shigella flexneri* 2a, 2457T bacteria.

### 5.2.2 Isolation and purification of bacteriophage:

#### 5.2.2.1 Spot assay:

Bacteriophage was isolated from the environmental water sample of a diarrhoeal outbreak area, Kolkata. The newly isolated bacteriophage was named Sfk20 following the rules of the new phage nomenclature (Adriaenssens and Rodney Brister 2017). After isolation, the phage sample was concentrated and purified using ultracentrifugation and sucrose step gradient centrifugation. After purification, the phage sample was spotted on the lawn culture of *Shigella flexneri* 2a in an agar plate. The clear zone of lysis was visible after overnight incubation as shown in **Figure 5.3**. It further confirmed that the isolated bacteriophage is capable of infecting and lyse the *Shigella flexneri* 2a strain.



**Figure 5.3:** A visible clear zone of lysis in the middle of the plate.

### 5.2.2.2 Morphology of the bacteriophage plaque:

The concentration of the purified bacteriophage was estimated by the plaque assay method. Phage Sfk20 infected and lysed the bacterial cell within a very short period and produced a small visible zone of lysis or plaque as shown in **Figure 5.4**. The diameter of the plaque was 0.1 mm approximately. The plaque morphology indicated that Sfk20 was a lytic bacteriophage.

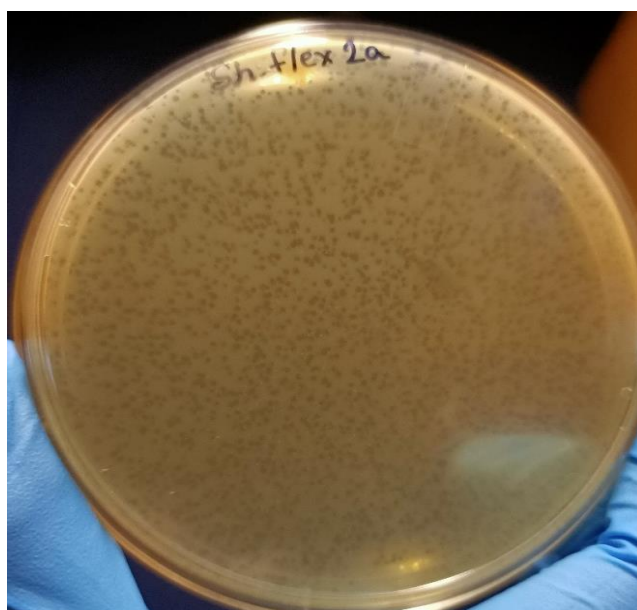


**Figure 5.4:** Phage Sfk20 plaques are formed in the double-layered agar plate.

### 5.2.3 Morphology of the bacteriophage Sfk20:

#### 5.2.3.1 Transmission electron micrograph of Phage Sfk20:

The purified bacteriophage sample was negatively stained and checked under a transmission electron microscope. Transmission electron micrograph revealed that the phage Sfk20 has a prolate head of  $91.08 \pm 4.92$  nm length and  $62.34 \pm 4.82$  nm width ( $n=20$ ), and a long contractile tail with  $99.59 \pm 4.92$  nm length and  $18.66 \pm 2.52$  nm width ( $n=20$ ). Based on the morphology, bacteriophage Sfk20 was classified as a member of the *Myoviridae* family, *Caudovirale* order (Ackermann 2007). The transmission electron micrograph of the intact phage Sfk20 was shown in **Figure 5.5 (A)**. Gram-negative bacteria constitutively release spherical, membrane-enclosed outer membrane vesicles (OMVs) filled with periplasmic contents that are thought to have originated from endocytic cells. The release of OMVs allows bacteria to interact with the surroundings, especially in hostile environments to act as a defense mechanism of bacterial cells. During the phage infection, outer membrane vesicles also engage themselves to block the bacteriophages as a first line of defense as shown in **Figure 5.5 (B)**. Here, the contracted tail of the *Myoviridae* phage Sfk20 particles around the OMV confirms the interaction between them.

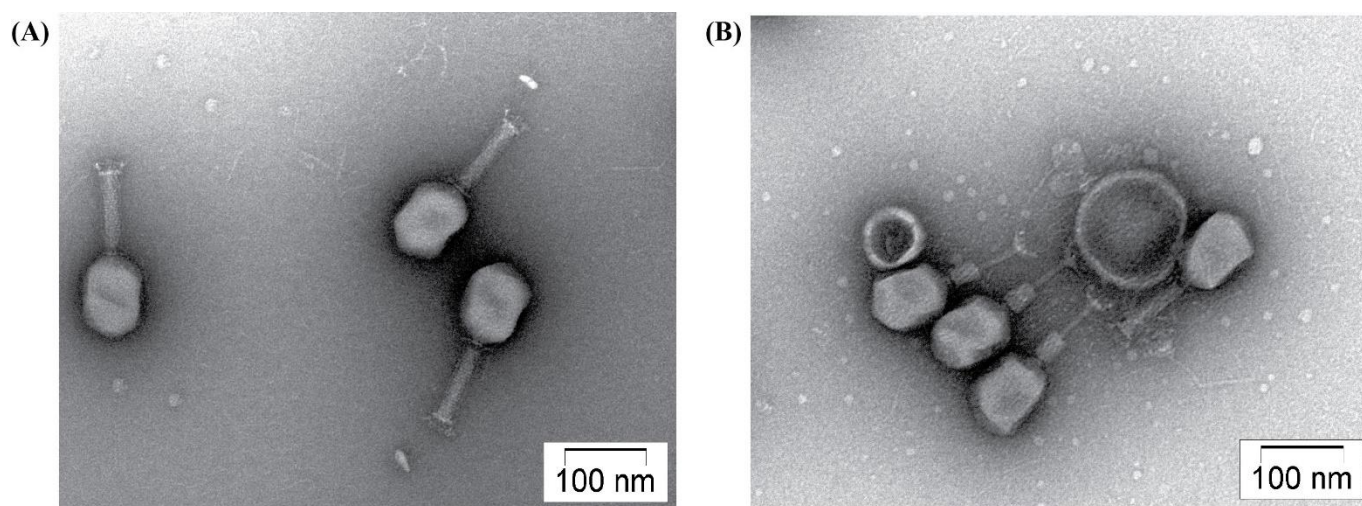


**Figure 5.5:** Transmission electron micrograph of phage Sfk20: (A) negatively stained image of phage Sfk20 has a prolate-shaped head and a long contractile tail and (B) phage Sfk20 interacting with an OMV particle. The contractile tails are visible.



### 5.2.3.2 Scanning electron micrograph of Phage Sfk20:

One drop of glutaraldehyde fixed phage sample was taken on a specimen stub holder of SEM, dried and later the sample was checked under a scanning electron microscope. The scanning electron micrograph (**Figure 5.6**) of phage particles was taken at a low magnification which revealed the prolate-shaped phage head with the tail attached.

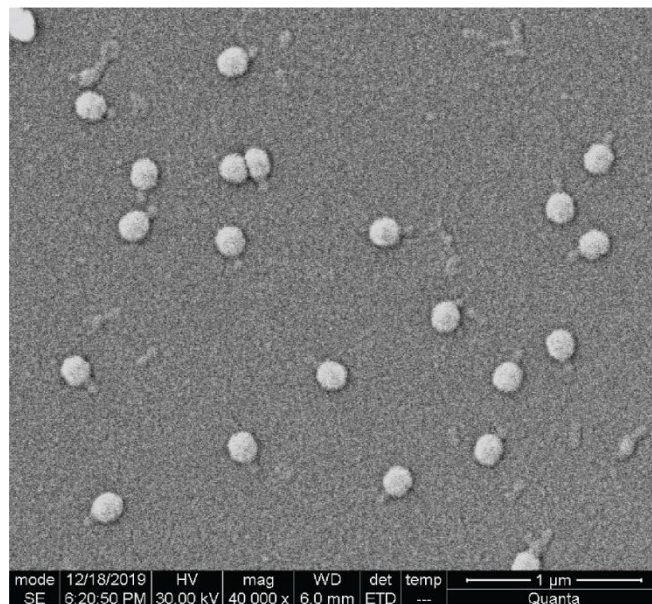


**Figure 5.6** Scanning electron micrograph of phage Sfk20. The prolate-shaped head with an attached tail is visible in the image.

## 5.2.4 Host range analysis of bacteriophage and Efficiency of plate calculation:

### 5.2.4.1 Host range analysis:

A collection of eight strains: *Shigella flexneri* 2a, *Shigella flexneri* 3a, *Shigella flexneri* 1b, *Shigella flexneri* 4, *Shigella flexneri* 6, *Shigella sonnei*, *Shigella dysenteriae* 1, *Shigella boydii*, two typhoidal *Salmonella* strains: *Salmonella typhi*, two non-typhoidal *Salmonella* strains: *Salmonella typhimurium*, *Salmonella enteritidis*, and one *Vibrio cholerae* O1, one *E. coli* strain *ETEC* were used to study the host range. This study revealed that Sfk20 can infect and lyse different *Shigella flexneri* serotypes: 1b, 2a, 3a, *Shigella dysenteriae* 1, and *Shigella sonnei* but could not infect *Shigella flexneri* serotype: 4, 6 and *Shigella boydii*, Phage Sfk20 could also infect and lyse *Salmonella typhimurium*, *Salmonella enteritidis* but could not infect *Salmonella typhi*, *ETEC*, and *Vibrio cholerae* O1 (Table 5.1).

**Table 5.1:** Host range analysis of phage Sfk20

Bacterial species	Strain no.	Infectivity
<i>Shigella flexneri</i> 2a	2457T	+
<i>Shigella flexneri</i> 3a	UB811	+
<i>Shigella flexneri</i> 1b	03075/19	+
<i>Shigella flexneri</i> 4	C2529	-
<i>Shigella flexneri</i> 6	UB812	-
<i>Shigella sonnei</i>	IDH00968	+
<i>Shigella dysenteriae</i> 1	NT4907	+
<i>Shigella boydii</i> 1	NK02379	-
<i>Salmonella enteritidis</i>	520833	+
<i>Salmonella typhimurium</i>	PH-94	+
<i>Salmonella typhi</i>	KOL 551	-
<i>ETEC</i>	IDH07942	-
<i>Vibrio cholerae</i> O1	MAK757	-

### 5.2.4.2 Efficiency of plating:

The efficiency of the plating (EOP) assay was performed to know the efficiency of phage to infect various bacterial cells (**Table 5.2**). The study revealed that the *Shigella flexneri 2a* produced the highest EOP value. The value of EOP was also on the higher side for other *Shigella* strains such as *Shigella flexneri 1b*, *Shigella flexneri 3a*, *Shigella sonnei*, and *Shigella dysenteriae 1* compared to the *Salmonella typhimurium* and *Salmonella enteritidis* strains. This study further indicated that *Shigella flexneri 2a* was the most suitable host strain of phage Sfk20 and it is a *Shigella* phage.

**Table 5.2:** Efficiency of plating of phage Sfk20

Bacterial species	Strain no.	EOP value
<i>Shigella flexneri 2a</i>	2457T	1
<i>Shigella flexneri 3a</i>	UB811	0.80
<i>Shigella flexneri 1b</i>	03075/19	0.79
<i>Shigella sonnei</i>	IDH00968	0.62
<i>Shigella dysenteriae 1</i>	NT4907	0.61
<i>Salmonella enteritidis</i>	520833	0.000192
<i>Salmonella typhimurium</i>	PH-94	0.000296

## 5.2.5 Biological characterization of the bacteriophage Sfk20:

### 5.2.5.1 One-step growth curve of Sfk20:

The one-step growth curve of phage Sfk20 was performed at an MOI of 0.1. From this study, the latent phase and the burst size were calculated. In the result, a tri-phasic curve was obtained with a typical lag phase, burst phase, and stationary phase. A latent period of 20 minutes and an average burst size were calculated as 123 PFU per infected cell (**Figure 5.7**).

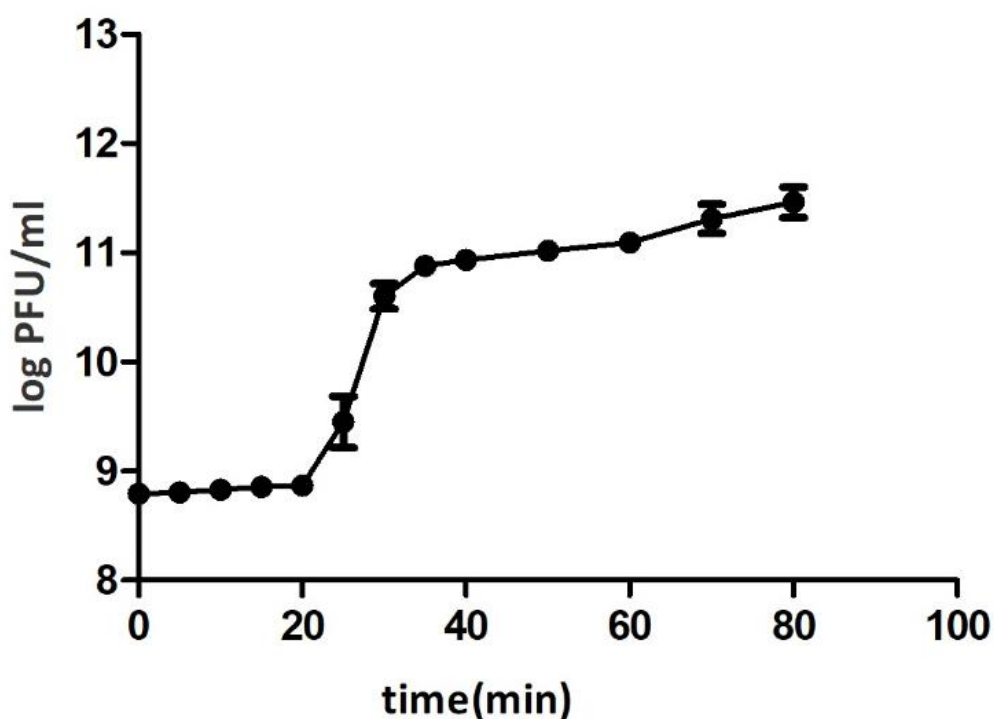


**Figure 5.7:** Growth characteristics of *Shigella* phage Sfk20. The values are shown as the mean of three determinations.

### 5.2.5.2 Phage Adsorption Kinetics:

A phage adsorption assay was performed to assess how rapidly the phage particle was adsorbed. Around 94% of bacteriophage was adsorbed within the first 8 minutes as shown in **Figure 5.8**. After that, the phage adsorption rate slowed down.

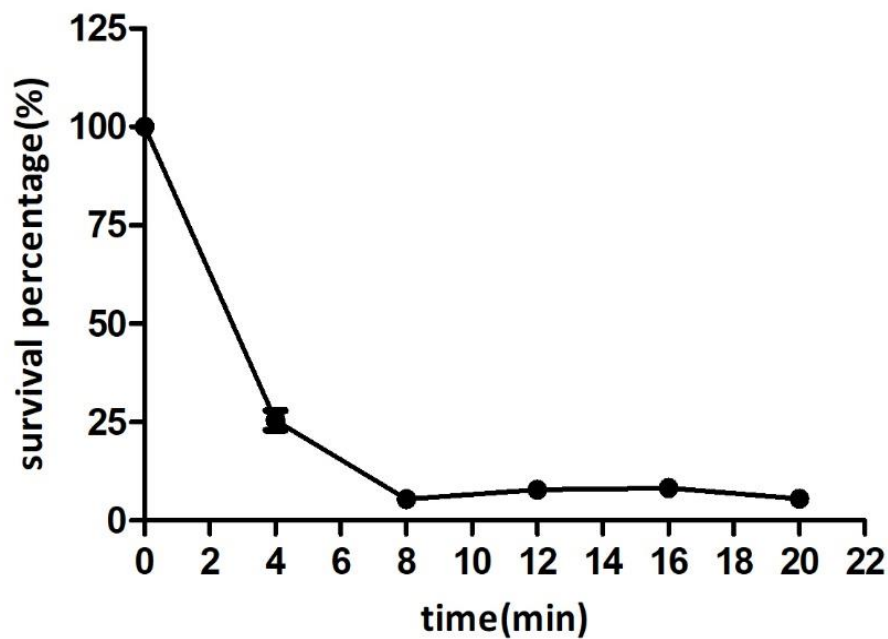


**Figure 5.8:** Adsorption kinetics of *Shigella* phage Sfk20. The values are shown as the mean of three determinations.

## 5.2.6 Physicochemical characterization of the bacteriophage Sfk20:

### 5.2.6.1 Stability of phage Sfk20 at various temperatures:

The ability of the phages to tolerate various temperatures is one of the key features that make them effective biocontrol agents. Therefore, the stability of phage Sfk20 was assessed at various temperature conditions. Phage Sfk20 was highly stable at 4°C to 37°C temperature as shown in **Figure 5.9**. The phage activity was reduced above 37°C temperature and significantly reduced at 50°C. At 50°C approximately only about 25% of phages remained active. But they were completely inactivated at 70°C or above.

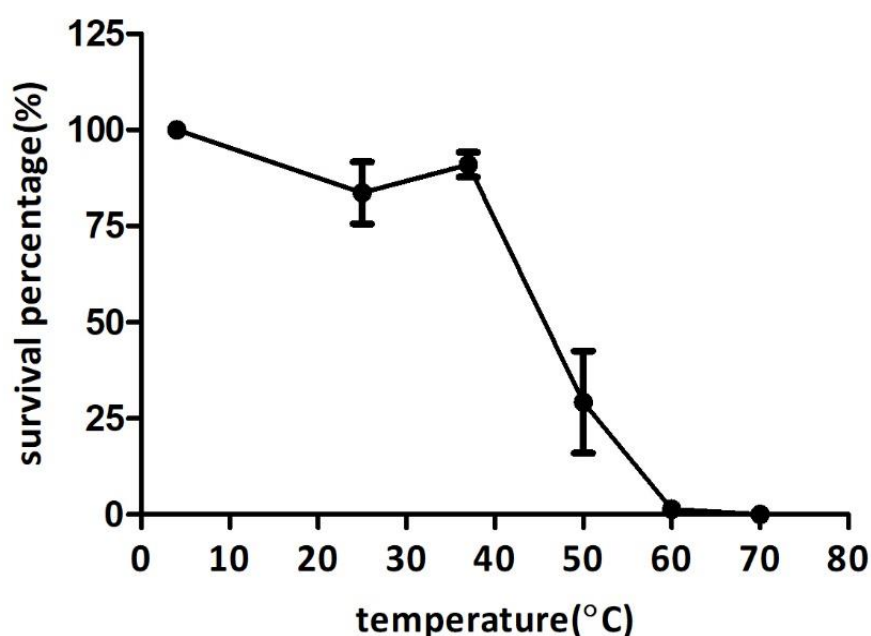


**Figure 5.9:** Stability of phage Sfk20 was tested at various temperature conditions (4°C to 70°C). The values are shown as the mean of three determinations.

### 5.2.6.2 Stability of phage Sfk20 at various pH:

Stability of phage Sfk20 was tested at various pH ranging from 3 to 13. Phage Sfk20 remained highly stable at pH 7- 9 range as shown in **Figure 5.10**. The phage viability started decreasing below pH 7 and above pH 9. Phage Sfk20 was completely inactivated below pH 5 and above pH 11.

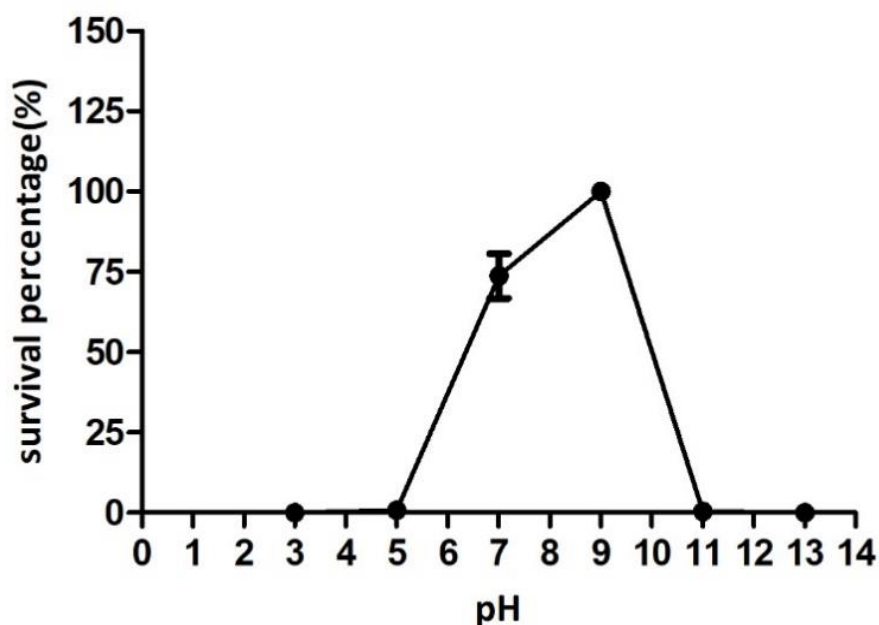


**Figure 5.10:** Sfk20 stability at pH ranging from 3-13. The values are shown as the mean of three determinations.

### 5.2.6.3 Stability under ultra-violet radiation:

Ultra-violet radiation is a mutagenic substance. In the presence of ultraviolet rays, phages can be damaged as the lytic activity of phage is destroyed. Phage Sfk20 was tested under ultra-violet light at various time points. It was shown in **Figure 5.11** that phage Sfk20 is highly sensitive to ultraviolet radiation and remains moderately stable only up to 5 seconds but completely inactivated after 15 seconds.

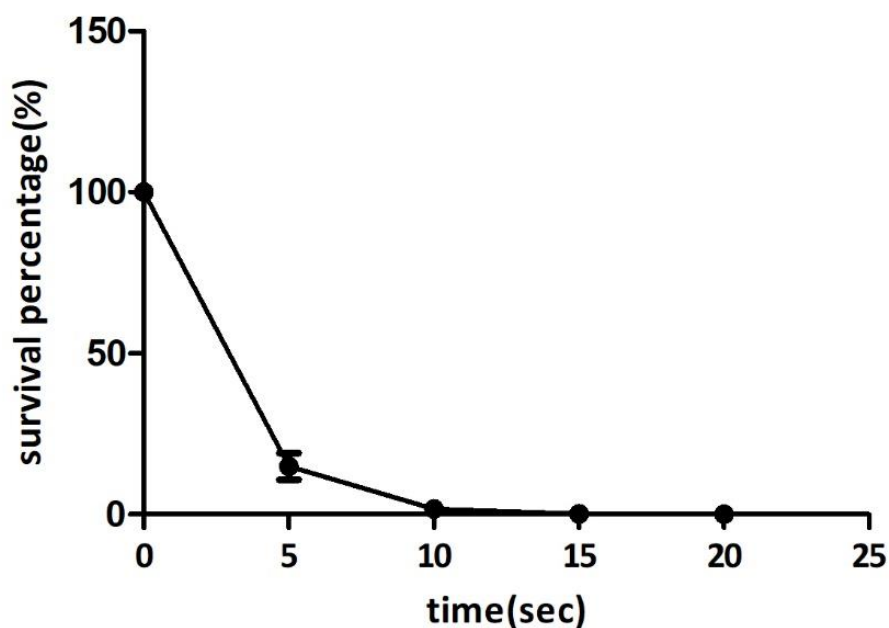


**Figure 5.11:** Sfk20 stability under ultra-violet light for 20 seconds. The values are shown as the mean of three determinations.



#### 5.2.6.4 Stability of phage Sfk20 at various saline conditions:

Phage Sfk20 was isolated from the lake water with low salt concentrations. Therefore, the stability of the phage Sfk20 was tested at various saline conditions for up to 28 days to understand if the phage was able to survive in high salt concentrations. Phage Sfk20 was found to be quite stable at 0-5% salt concentration. The number of active phages was significantly decreased at 10% and further destroyed at 20% salt concentration as shown in **Figure 5.12**.

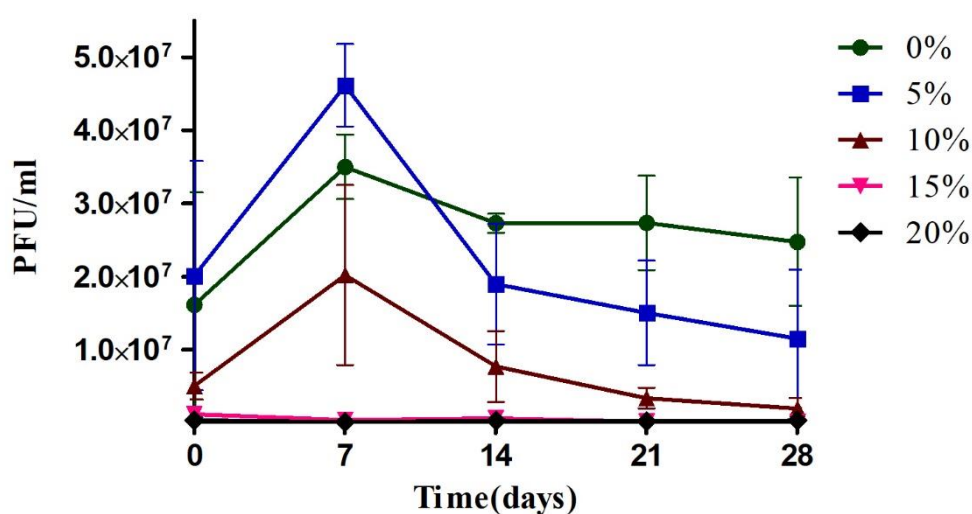


**Figure 5.12:** Survival of the phage Sfk20 virions suspended in the double distilled water adjusted with 0-20% NaCl concentration. The reduction in phage number up to 28 days is shown. The values are shown as the mean of three determinations.

### 5.2.7 Receptor identification of Phage Sfk20:

Phage adsorption to the surface of the host bacteria through a receptor is a crucial step for phage infection. Phages can utilize both LPS and OMPs as their receptors (Koebnik, Locher, and Van Gelder 2000; Wright, McConnell, and Kanegasaki 1980). Therefore, it is necessary to know if membrane LPS or protein acts as a receptor for the bacteriophage Sfk20 during infection. To determine the nature of the receptor, *Shigella flexneri 2a* was treated with proteinase K and periodate separately before infecting with phage in both cases. No change was observed in attachment efficiency on the bacterial surface after treatment with proteinase K. But in case of the periodate-treated sample, a significant number of phages were found in the supernatant that indicates the receptor of the periodate-treated bacteria was unable to bind to phage Sfk20 as shown in **Figure 5.13**. Therefore, we conclude that periodate is responsible to destroy the cognate receptor of Sfk20 on *Shigella flexneri 2a*, not proteinase K. This experiment showed the carbohydrate nature of the receptor most likely a lipopolysaccharide (LPS).

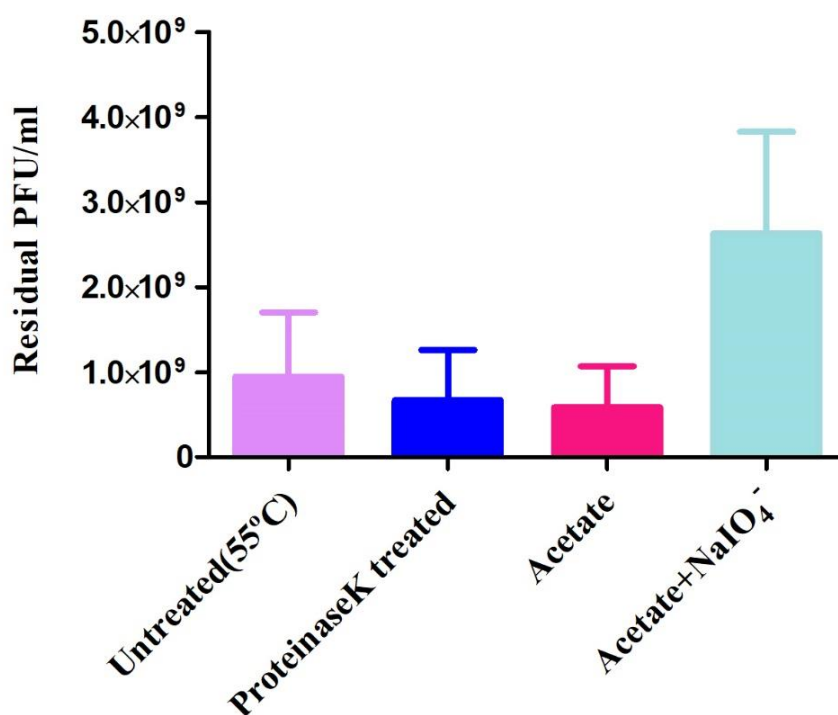


**Figure 5.13:** Effects of Proteinase K and periodate treatment in adsorption of Sfk20 bacteriophage to *Shigella flexneri 2a* strain. The values are shown as the mean of three determinations.

### 5.2.8 In-vitro bacteriolytic activity:

Bacteriolytic effect of phage Sfk20 was examined by adding them to the early exponential phase culture of *Shigella flexneri* 2a at an MOI of 0.1, 1, and 100 respectively. The result showed that at low phage concentration (0.1 MOI) bacterial growth remains undisturbed possibly due to less numbers of infected bacterial cells. But the reduction of bacterial cells is quite prominent when phage Sfk20 is added at MOI 1 and 100 as shown in **Figure 5.14**. Therefore, *in vitro*, bacterial reduction assay confirmed that phage Sfk20 can destroy the pathogenic *Shigella* strain to act as a potential biocontrol agent.

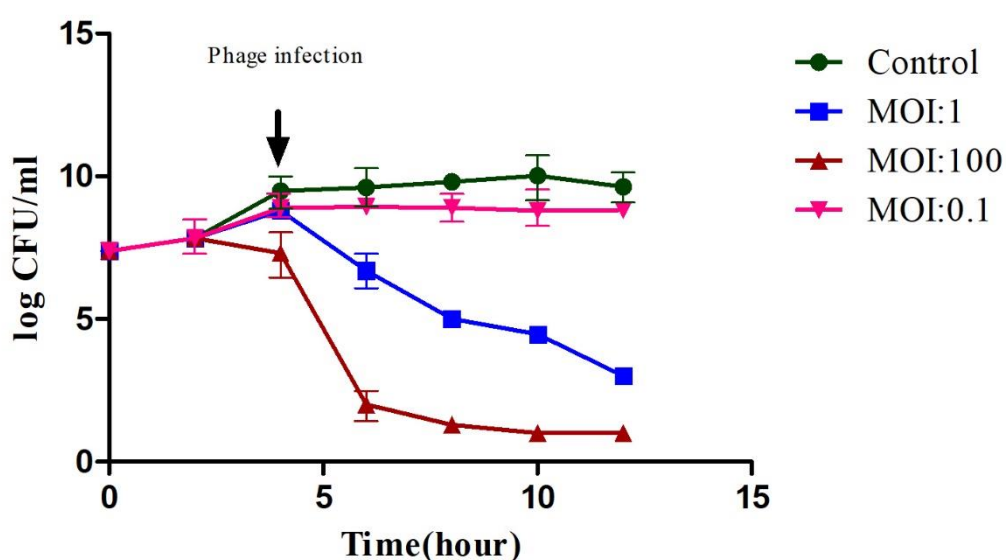


**Figure 5.14:** The bacteriolytic activity of phage Sfk20 against *Shigella flexneri* 2a. Early exponential cultures of *Shigella flexneri* 2a co-cultured with Sfk20 phage at MOIs 0.1, 1 and 100, respectively. The growth curve of *Shigella flexneri* 2a was used as a control. The values are shown as the mean of three determinations.

### 5.3 DISCUSSION

*Shigella* is one of the major responsible strains for diarrheal outbreak to occur in various developing and underdeveloped countries. A repeated episode of diarrheal disease causes severe damage to the gastrointestinal tract. As a result, an inadequate number of healthy microbiomes are established and their growth and development were also delayed (Lee et al. 2014). Unfortunately, the development of the vaccine against this pathogen has not been highly effective. The rapid increase of multidrug-resistant *Shigella* causes serious treatment challenges (Bhattacharya et al. 2015; Puzari, Sharma, and Chetia 2018). Therefore, some novel solutions are urgently needed to treat antibiotic-resistant bacterial infections. Virulent lytic phages can selectively infect and destroy the bacterial population including drug-resistant strains, using a mechanism distinct from antibiotics. Therefore, interest to control the MDR *Shigella* strains using phages as an alternative to antibiotic treatment is continuously growing. The *Myoviridae* bacteriophage Sfk20 used in this study appeared as a promising biocontrol agent against shigellosis.

To date, several studies have been reported to show the *in vitro* antimicrobial activity of many isolated phages and their successful application in phage therapy since the early nineteenth century in a regular manner. Many promising studies have failed to show positive outcomes in recent controlled human trials (Wittebole and Opal 2020). Early phage therapy mostly failed due to inadequate knowledge of the fundamental phage biology, lack of a specific regulatory framework, complicated procedures for phage patenting, and unsophisticated purification and storage procedure. Phages have beneficial characteristics but with some restrictions. Unknown gene function of phages, host immune responses, phage stability, CRISPR-Cas, and scarcity of pharmacokinetic and pharmacodynamics models for dose optimization are some genuine concerns to implementing phage therapy as an approved alternative. Also, low pH sensitivity, phage-neutralizing antibodies, phage loss, and enzymatic degradation are some of the big concerns in human phage therapy. Meanwhile, compassionate phage therapy is in limited use in cases when all available therapeutic options are exhausted.

In this study, a lytic virulent phage Sfk20 was isolated from the water sample from a diarrheal outbreak area of Kolkata, India, and *Shigella flexneri* 2a was used as a host bacterium for phage propagation. Host range analysis and high EOP value showed sensitivity of Sfk20 towards *Shigella flexneri* serotypes 1b, 2a, and 3a whereas Sfk20 could not infect *Shigella flexneri* serotypes 4 and 6. In developing countries, the predominant serotypes of *Shigella flexneri* are

1b, 2a, 3a, 4a, and 6 though serotype 2a is predominant in industrialized countries including India (Kotloff et al., 1999). In this work, we have chosen *Shigella flexneri* as the host strain as nowadays it has been reported to progressively develop antibiotic resistance (Ashkenazi et al. 2003). Compared to other *Shigella* spp.: *Shigella flexneri*, *Shigella sonnei*, and *Shigella dysenteriae*, the frequency of infection through *Shigella boydii* has been rarely reported (Bratoeva, John, and Barg 1992; Ranjbar et al. 2008) and there are limited studies published on *Shigella boydii* (Kania et al. 2016). It was also reported that *Shigella boydii* outbreaks are rare in developed countries. Another study from India reported *Shigella flexneri* (60%) as the prevalent serogroup followed by *Shigella sonnei* (23.8%), *Shigella dysenteriae* (9.8%), and *Shigella boydii* (5.7%) (Pazhani et al. 2005). The Global Enteric Multicenter Study (GEMS) reported that only 5.4% of 1130 *Shigella* isolates were identified as *Shigella boydii* (Livio et al. 2014). It has been reported as one of the most prevalent serotypes only in Bangladesh (Akter et al. 2019). Other than *Shigella* strains, two non-typhoidal *Salmonella* strains: *Salmonella enteritidis* and *Salmonella typhimurium* are found to be sensitive to phage Sfk20.

The stability of phages at various temperatures and pH ranges makes them highly suitable agents for phage therapy. In this work, phage Sfk20 was found quite stable in the range of 4–37°C and remained stable for at least up to six months without losing viability in the usual storage temperature of 4°C. It also showed high stability in the range of pH 7–9 which is neutral to slightly alkaline. The phage stability in various pH provides valuable information to consider the oral administration of this phage during therapy. The acidic environment of the gastrointestinal tract is one of the major challenges for phage therapy during phage administration (Ly-Chatain 2014). Most of the bacteriophages are found sensitive toward low pH. Phage Sfk20 also showed complete inactivity at pH < 5. Therefore, nowadays new methods and technologies have been developed to protect the phage during therapy. Oral applications of phages predated by gastric neutralization are a practice in a few European countries where phage therapy has always received substantial consideration (Slopek et al. 1983). Also, encapsulation of phages in liposomes or biopolymeric microparticles is another highly accepted technology to enhance phage survival while passing through the gut. The release of phages in a slow and controlled manner from their encapsulated form help in ensuring that the phage concentration remains at a therapeutically effective level and this strategy also allows phage to amplify when the concentration of the bacteria (Malik et al. 2017). However, the selection of a biopolymer is not so easy and the synthesis process has to satisfy certain features. Therefore, to overcome this limitation an alternative approach to encapsulation such as “natural coating”

have been developed based on genetic engineering by displaying phospholipids on the surface of the phages. This natural coating process not only protects from the acidic pH of the GI tract but also maintains the infection ability of phages (Nobrega et al. 2016). Previously the genetic engineering of the lytic phages was quite difficult but with the development of the new technique of Bacteriophage Recombineering of Electroporated DNA (BRED) the natural coating become easy and cheaper (Marinelli et al. 2008, 2012). Therefore, the sensitivity of Sfk20 at low pH could be controlled during its trial in future phage therapy.

The phage sensitivity in various saline conditions was also tested. Salinity is the measure of the number of dissolved salts in water. It is expressed in percentage (%) or parts per thousand (ppt). Freshwater from rivers generally has a salinity value of 0.5ppt (0.05%) or less. Our study showed that the phage Sfk20 remains highly stable at 0%-5% salt concentration and remains moderately stable up to 10% salt concentration. It was found that in high salt concentrations, phage Sfk20 viability is reduced. In contrast, a temperate phage  $\phi$ gspC isolated in 2007 from Great Salt Plains National Wildlife Refuge was reported to remain stable at high saline conditions (Seaman and Day 2007).

The one-step growth curve of phage Sfk20 suggests a latent period (20 min) and a large burst size of 123 pfu per cell. A large burst size favours its application in phage therapy. Earlier reports on T4 revealed that if tRNA genes were deleted the burst size and protein synthesis rate eventually lowered down (Wilson 1973). But some reports revealed that bacterial physiological states could affect the burst size of phages (Bolger-Munro et al. 2013).

Bacteriophages can bind to specific host receptors on bacterial cells, allowing them to identify their host from a diverse bacterial community during infection (Holst Sørensen et al., 2012). The cell envelope of gram-positive and gram-negative bacteria has been studied intensively during the last decade and reported that lipopolysaccharide (LPS) serves as a significant outer membrane element of Gram-negative bacteria. Different parts of LPS are known to serve as a receptor for many phages of various genera. For example, lipopolysaccharide (LPS) serves as a receptor for phage Sf6 in *Shigella flexneri*, and for T2-like and T4-like phage in *Shigella dysenteriae*, for T3, T4, and T7 phages in *E. coli*, for P22 phage in *S. enterica* Typhimurium serovar, for K139 phage in *V. cholerae*, and for phage  $\phi$ YeO3-12 and  $\phi$ R1-37 in *Y. enterocolitica* (Al-Hendy, Toivanen, and Skurnik 1991; Baxa et al. 1996; Chua, Manning, and Morona 1999; Kiljunen et al. 2005; Krüger and Schroeder 1981; Lindberg 2003; Nesper et al. 2000; Pajunen, Kiljunen, and Skurnik 2000; Phalipon and Sansonetti 2007; Pinta et al. 2010;

Prehm et al. 1976; PRICE 2003; Skurnik et al. 1995). In this study, the receptor of phage Sfk20 was examined and the experiment suggests that the functional receptor of phage Sfk20 on the host *Shigella* bacteria contains a carbohydrate moiety.

*In vitro* bacteriolytic activity of phage Sfk20 was tested at different MOI. At lower MOI the concentration of viable bacteria remained normal but when the phage was added at higher MOI, the viable bacterial count started decreasing. This assay is an essential step for phage titer optimization, which is one of the crucial stages of phage therapy. It might be possible that high MOI may weaken phage proliferation in the natural environment because a large number of phage adsorption events leads to outer membrane destabilization and subsequent lysis of the bacteria which prevents phage replication and release (lysis from without) (Brown and Bidle 2014). Another possibility is that high phage titer may induce the host immune system, thus limiting phage therapy (Kocharunchitt, Ross, and McNeil 2009). Therefore the *in vitro* bacterial reduction assay showed that phage Sfk20 can destroy the pathogenic *Shigella* strain and act as a potential biocontrol agent.



# CHAPTER 6

## Objective 1 (Part II)

Genomic and proteomic  
characterization of *Shigella* phage  
Sfk20





### 6.1 INTRODUCTION

During the development of modern molecular biology and genetics, three T- even phages (T2, T4, and T6) were the major model system and also had a profound effect on biological research. Indeed, research on these bacterial viruses between 1920 and 1960 laid the groundwork for the emergence of molecular biology as a subject of study that was freely incorporated into every branch of the life sciences. The first isolated T-even phage was T2 and thereafter closely related T4 and T6 phages were isolated and all three phages were treated as the same biological entity. Bacteriophages T2 and T4 were used as a model of many fundamental biological concepts such as the recognition of different genetic material as nucleic acid, the confirmation that the genetic code is triplet, mRNA discovery, the significance of recombination in DNA replication, DNA repair mechanism, DNA restriction and modification, the gene definition study by recombinational, functional and mutational analysis; translational bypassing and others. Soon the attention was switched from T2 to T4 and it was chosen as the experimental model. A benefit of using T4 as a model system is that the virus completely inhibits host gene expression, allowing researchers to distinguish between macromolecular synthesis in the host and phage. Important insights into macromolecular interactions, substrate channeling, and cooperation between phage and host proteins within such complexes have been gained through examination of the complex T4 capsid's assembly as well as the operation of its nucleotide-synthesizing complex, replisome, and recombination complexes (Miller et al. 2003).

The T-even phages and their relatives were assigned as the T4-like virus genus by the International Committee for the Taxonomy of Viruses (ICTV) and the T4-like virus genus belongs to one of the six genera of the *Myoviridae* family. *Myoviridae* phages are tailed phages that contain an icosahedral head, and long contractile tails and belong to the Caudovirales order. The phages belonging to the T4 virus genus show similarity in morphological features with well-characterized T4 bacteriophages when visualized under the transmission electron microscope (Karam and Miller 2010).

Bacteriophages that share an evolutionary relationship with the T4 phages are very common in nature and they have been detected by simple plating techniques using various genera or species as their host. In the last few years, several hundreds of T4-related phages have been isolated from nature. They have been isolated from various environmental locations and for a different number of bacterial species. All of these phage samples were isolated from raw sewage and mammalian stool samples using the same *E. coli* sample that is commonly used

in the laboratory to enumerate the T4 phages (Ackermann 2007; Ackermann and Krisch 1997). Among them, some of the T-even related phages use other bacterial genera such as *Shigella*, *Salmonella*, *Vibrio*, *Pseudomonas*, *Klebsiella*, *Aeromonas*, marine cyanobacteria as their host instead of *E. coli* (Ackermann 2007; Ackermann and Krisch 1997). The advanced genome sequencing technology developed over the last few years has made it possible to sequence and analyze these phage genomes including both close and distant phylogenetic relatives of T4 bacteriophage. Genome sequencing has shown that there is a high degree of diversity among T4 relatives.

Bacterial and phage peptides detection is valuable in the case of pathogen identification. Mass spectrometry has been used in several studies to characterize the proteome of a variety of phage species. In this chapter, the genomic and proteomic characterization of phage Sfk20 was described. Nanoscale liquid chromatography integrated into tandem mass spectrometry (LC-MS/MS) had been used in this study for the analysis and detection of the phage proteins based on specific diagnostic peptides.

## 6.2 RESULT

### 6.2.1 Genomic characterization of phage Sfk20:

#### 6.2.1.1 Restriction digestion of phage genomic DNA:

Phage genomic DNA was isolated using a phage DNA isolation kit. Then the concentration of the isolated DNA was measured and the concentration was noted as 86.2 ng/μl. Seven restriction endonucleases: EcoRI, BamHI, HindIII, PstI, EcoRV, BglII, and MluI were used to digest the isolated phage DNA. However, the phage genome appeared to be resistant to digestion by all six restriction enzymes except EcoRV. The digestion pattern of the phage genomic DNA has been shown in **Figure 6.1**. Based on this result it was suggested that the genome of the phage Sfk20 is a double-stranded genome.

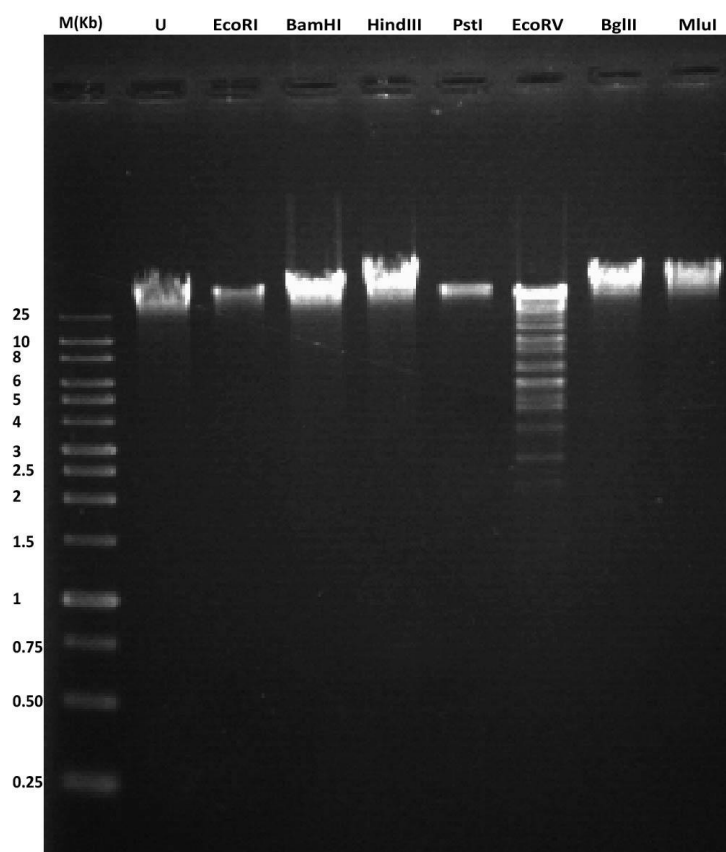


**Figure 6.1:** Phage genomic DNA was digested with different restriction enzymes. After overnight digestion, the restriction fragments were separated by electrophoresis on 1% agarose gel stained with ethidium bromide. High-range ladder ranging from 250bp-25kb (Lane 1). uncut DNA (Lane 2), EcoRI (Lane 3), BamHI (Lane 4), HindIII (Lane 5), PstI (Lane 6), EcoRV (Lane 7), BglII (Lane 8), and MluI (Lane 9).

### 6.2.1.2 Whole genome sequencing of phage Sfk20 using Next generation genome sequencing (NGS):

After isolation of the phage Sfk20 genome, it has been sequenced and deposited in GenBank as shown in **Figure 6.2** The NCBI accession number of the genome is MW341595. The genome analysis study showed that the complete genome length of phage Sfk20 was 164878 bp and G+C content was 35.62%. The genome length and the G+C content of phage Sfk20 placed it close to the T4 bacteriophage family. The detailed genome analysis study suggested that there were 241 (among them 205 complement strands and 36 direct strands) open reading frames (ORF) and ATG was the predominant start codon (97%). GTG was the uncommon codon for the six ORFs: ORF19, ORF68, ORF76, ORF89, ORF104, and ORF118. There was also some variability in stop codons: Ochre (TAA), Amber (TAG), and Opal (TGA). The predominant stop codon was TAA (63.90%). Some TGA stop codons were also there and the least frequent stop codon was TAG. The longest ORF of phage Sfk20 was ORF36 (protein-id: QPP47031) which was placed in the morphogenesis cluster. ORF36 encoded a gene that was very similar to the large distal long-tail fiber subunit of *Myoviridae Shigella* phage SH7. After genome analysis, a total of 10 tRNA was identified in the Sfk20 phage genome. The functions of tRNA in the phage genome are still not clear though a widely accepted fact is phage tRNA gives considerable independence from host translational machinery (Albers and Czech 2016).

**National Library of Medicine**  
National Center for Biotechnology Information

Nucleotide

GenBank

### Shigella phage Sfk20, complete genome

GenBank: MW341595.1  
[FASTA](#) [Graphics](#)

LOCUS MW341595 164878 bp DNA linear PHG 16-DEC-2020

DEFINITION Shigella phage Sfk20, complete genome.

ACCESSION MW341595

VERSION MW341595.1

DBLINK BioProject: [PRJNA678164](#)  
BioSample: [SAMN16789369](#)

KEYWORDS .

SOURCE Shigella phage Sfk20

ORGANISM [Shigella phage Sfk20](#)  
Viruses; Duplodnaviria; Heunggongvirae; Uroviricota;  
Caudoviricetes; Straboviridae; Tevenvirinae; Tequatrovirus.

REFERENCE 1 (bases 1 to 164878)

AUTHORS Mallick,B., Mondal,P. and Dutta,M.

TITLE Direct Submission

JOURNAL Submitted (07-DEC-2020) Division of Electron Microscopy, ICNR-  
National Institute of Cholera and Enteric Diseases, P-33 C.I.T.  
Road Scheme-XM, Beliaghata, Kolkata, West Bengal 700010, India

COMMENT ##Assembly-Data-START##  
Assembly Method :: CLC genomic workbench v. 6  
Coverage :: 2x  
Sequencing Technology :: Illumina  
##Assembly-Data-END##

**Analyze this sequence**  
[Run BLAST](#)  
[Pick Primers](#)  
[Highlight Sequence Features](#)  
[Find in this Sequence](#)

**Related information**  
[Assembly](#)  
[BioProject](#)  
[BioSample](#)  
[Protein](#)  
[Taxonomy](#)  
[Genome](#)  
[PubMed \(Weighted\)](#)

**Figure 6.2** The genome sequence data was deposited in GenBank and the NCBI accession number is MW341595.

### 6.2.1.3 Comparative genomic analysis of phage Sfk20:

The whole genome sequence of phage Sfk20 was compared to the nucleotide sequence database using BLASTn. All of the ORF of phage Sfk20 showed close homology with the other T4-like phages such as pSs-1, SH7, Sfphi01, Sf21, and Sf23 as reported in the GenBank database. T4-like phages are one of the best-characterized groups and all the T4-like phages have some common characteristics: i) large genome size which is ranged from 164.0–176.0 kb (Subramanian, Parent, and Doore 2020) ii) the G+C content ranging from 35% to 43%, iii) phage morphology similar to the myoviridae family, iv) similarity in the host range. The phage Sfk20 showed 95-97% sequence similarity with other five T4-like *Shigella* bacteriophages: pSs-1 (NC\_025829), SH7 (KX828711), SfPhi01 (LC465543), Sf21 (NC\_042077) and Sf23 (MF158046). Phage Sfk20 showed the highest similarity with the phage pSs-1. A detailed study of all the above-mentioned phages were given in **Table 6.1**. According to the mega blast search result, it was suggested that the phage Sfk20 belongs to the member of the T4-like virus genus

and *Myoviridae* family. Based on the biological and genomic properties some of the recently identified *Shigella* species were discussed in **Table 6.2**.

Easyfig genome comparison tool was used in this study to compare the sequence homology of phage Sfk20 with the other related T4 like *Myoviridae Shigella* phages: pSs-1, SH7, SfPhi01, Sf21, Sf23. The alignment of phage Sfk20 with the other five T4-like *Shigella* phages showed that the degree of homology was quite higher and the genes of all the six phage genomes are quite similar. The phage genome contains a block of a clustered gene that encodes the predicted structural and functional genes. Here in this **Figure 6.3** the green arrows indicated the coding sequence locations and blue-shaded regions exhibited the degree of homology between Sfk20 and other phages. In some cases, the genes were arranged in opposite directions.

**Table 6.1:** Comparison of genomic properties of phage Sfk20 with closely related *Myoviridae* phages

Phage name	Genome length (bp)	GC content (%)	Host species	Identity (%)	Accession Number
<b>Sfk20 (Present study)</b>	164878	35.6	<i>S. flexneri 2a</i>	-	MW341595
<b>pSs-1</b>	164999	35.5	<i>S. sonnei</i>	97.91	NC_025829
<b>SH7</b>	164870	35.4	<i>S. flexneri</i>	96.03	KX828711
<b>SfPhi01</b>	168000	35.4	<i>S. flexneri</i>	95.34	LC465543
<b>Sf21</b>	166002	35.5	<i>S. flexneri</i>	95.40	NC_042077
<b>Sf23</b>	167678	35.4	<i>S. flexneri</i>	95.46	MF158046

**Table 6.2:** Comparison of some recently published *Shigella* phages based on biological properties

Phage name	Genome length (bp)	GC content (%)	Total/identified ORF	t-RNA	Latent period (min)	Burst size (PFU/cell)	Host sensitivity toward <i>Shigella</i> strains
<b>Sfk20 (Present study)</b>	164878	35.6	241/92	10	20	123	<i>S. flexneri</i> , <i>S. sonnei</i> , <i>S. dysenteriae</i>
<b>pSs-1</b>	164999	35.5	266/121	10	25	97	<i>S. flexneri</i> , <i>S. sonnei</i>
<b>pSf-1</b>	51,821	44.0	94/26	-	10	86.86	<i>S. flexneri</i> , <i>S. sonnei</i> , <i>S. boydii</i>
<b>pSf-2</b>	50,109	45.4	83/22	-	30	16	<i>S. flexneri</i>
<b>Sfin-1</b>	50,403	45.2	82/23	-	5	27-28	<i>S. flexneri</i> , <i>S. sonnei</i> , <i>S. dysenteriae</i>
<b>vB_SflM_004</b>	85,887	38.6	135/48	-	30	139	<i>S. flexneri</i> , <i>S. sonnei</i>

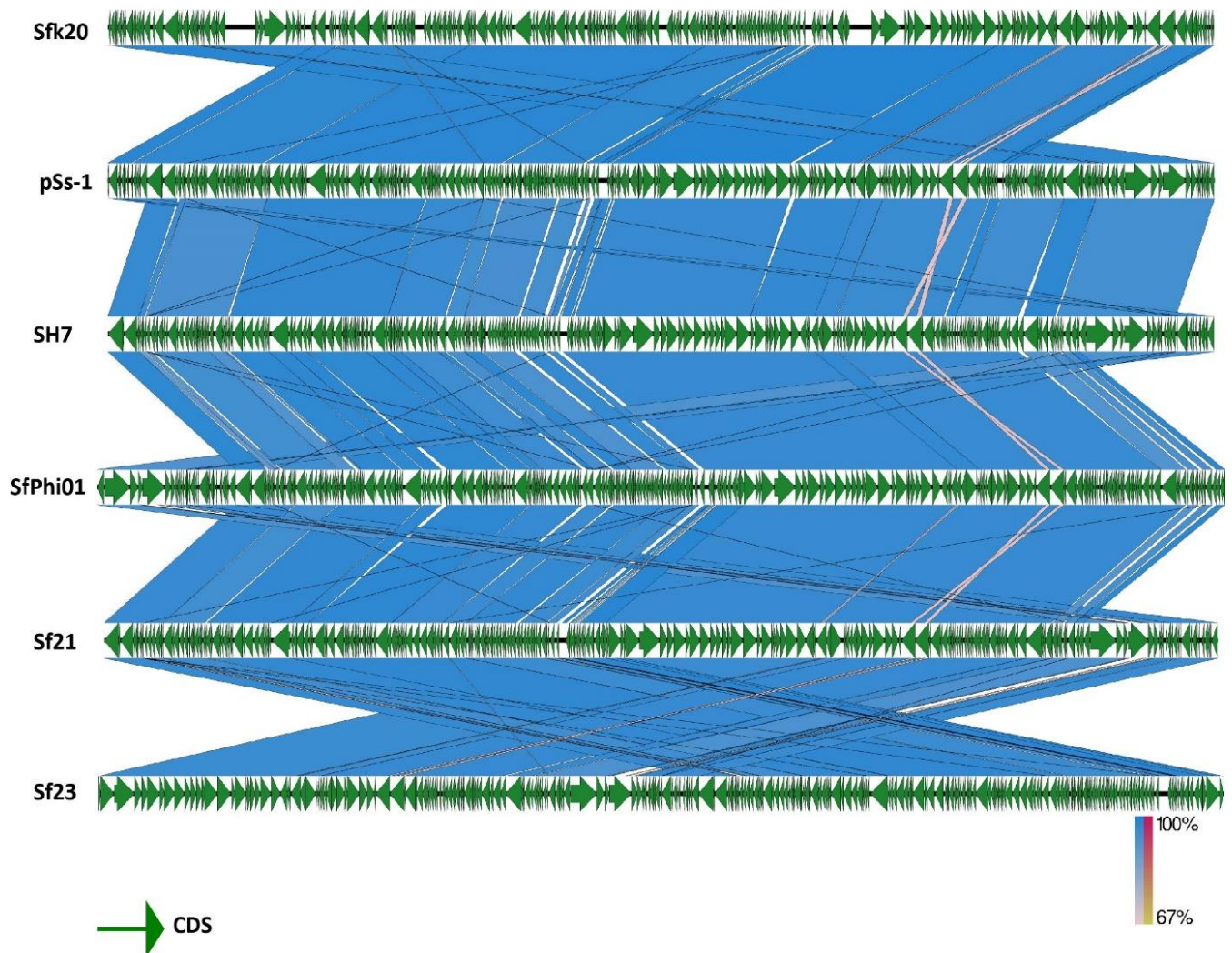


**Figure 6.3:** Easyfig schematic alignment of phage Sfk20 genome with five closely related phages using BLASTn program. Green arrows indicate the coding sequence location shaded blue lines indicate the degree of homology between pairs.



### 6.2.1.4 Functional group division of phage Sfk20 proteins:

The phage ORFs were divided into four different functional groups based on their functions: i) DNA replication/modification/transcriptional regulation/signal transduction proteins ii) phage morphogenesis proteins iii) phage genome packaging proteins iv) host lysis proteins. Using the CG view server, a schematic diagram of phage Sfk20 was drawn. The inner ring represents coding sequence locations (CDS) colored in blue; tRNA in this ring is marked in pink color as shown in **Figure 6.4**. The ORFs were mainly annotated as phage DNA replication and modification proteins, phage morphogenesis proteins, phage genome packaging proteins, and host lysis proteins (Topka-Bielecka et al. 2020). Factual gene information such as the positions, directions, amino acid range, putative function of each ORFs, and their function in the phage life cycle was mentioned in **Table 6.3**.

#### 6.2.1.4.1 Phage DNA metabolism/replication/modification/transcription and signal transduction and regulation protein:

There were several genes in the genomic cluster that codes for metabolism/replication/modification/transcription proteins such as thymidine kinase (ORF150), single-stranded DNA-binding protein (ORF29), gyrase (ORF46), DNA topoisomerase II (ORF59), 3'-5' exonuclease (ORF66), DNA primase (ORF84), DNA helicase (ORF89), dCMP hydroxy methylase (ORF93), DNA polymerase (ORF96), clamp loader small subunit (ORF98), sliding clamp DNA polymerase accessory protein (ORF100), replication factor C small subunit (ORF99), sliding clamp DNA polymerase accessory protein (ORF100), GIY-YIG nuclease family (ORF16), endonuclease (ORF122), ribonucleotide reductase of class III large subunit (ORF121), RNA polymerase binding protein (ORF101), site-specific RNase (ORF157), MotB (ORF64), sigma factor (ORF110), transcription modulator (ORF77), anti-sigma factor (ORF39) and several other genes responsible for the DNA replication, modification, transcriptional regulation, and signal transduction. The presence of a large number of DNA metabolism-related genomes reduces the dependence of phage to host bacteria.

#### 6.2.1.4.2 Phage morphogenesis proteins:

Phage morphogenesis proteins were present all over the genomic cluster but most predominantly present between ORF168 to ORF222. Different phage morphogenesis proteins: head completion protein (ORF186), baseplate wedge proteins (ORF187, ORF188, and ORF

189), baseplate wedge and completion tail fiber socket (ORF191), neck protein (ORF195), Tail sheath stabilizer and completion proteins (ORF197), tail sheath protein (ORF200), Tail tube protein (ORF201), prohead core protein (ORF203), capsid and scaffold protein (ORF204), prohead assembly protein and protease (ORF205), major capsid protein (ORF207), PKD domain protein (ORF212 ) baseplate hub protein (ORF 219), baseplate protein ( ORF220) and baseplate distal hub subunit(ORF222) protein were identified in this region. There were also some phage morphogenesis proteins such as head vertex assembly chaperone (ORF90), different tail fiber proteins (ORF34, ORF35, ORF36), head decoration proteins (ORF81) and baseplate wedge protein (ORF41) were also identified outside this cluster.

### **6.2.1.4.3 Phage genome packaging proteins:**

The genome packaging is initiated from the double-strand ends. The terminase genes are responsible for the initiation of the genome packaging. This complex contains a large terminase subunit (ORF163), a small terminase subunit (ORF198), and a putative terminase subunit (ORF199) present in the phage Sfk20 genome. The complex of DNA and terminase subunit proteins translocated during the packaging from the cytosol to portal protein which is present in the capsid vertex to form a “packasome” which utilizes the energy of the ATP hydrolysis to translocate DNA into the phage head (Rao, Thaker, and Black 1992).

### **6.2.1.4.4 Host lysis proteins:**

In the genome cluster, there were two main lysis genes: ORF38 codes the protein holin and ORF166 codes the protein endolysin. Both of these proteins were lysis proteins and helped to release the progeny bacteriophage by lysing the host cell membrane. Holin mainly made the pores in the host cell membrane and made the path for the endolysin which degrade the peptidoglycan layer of the bacterial cell and newly formed phage was released in the environment. In the genomic cluster, some of the other lysis genes that code some of the lysis proteins such as spackle periplasmic protein (ORF86), rI lysis inhibition (ORF148), transglycosylase SLT domain-containing protein (ORF156) and all these genes played regulatory roles during the lysis pathway. The lysis of the host cell is extensively delayed when more phage attacks the infected cells at any time after the 5 minutes of infection. This signal was mediated by the rI protein, which regulates the assembly of the holin.

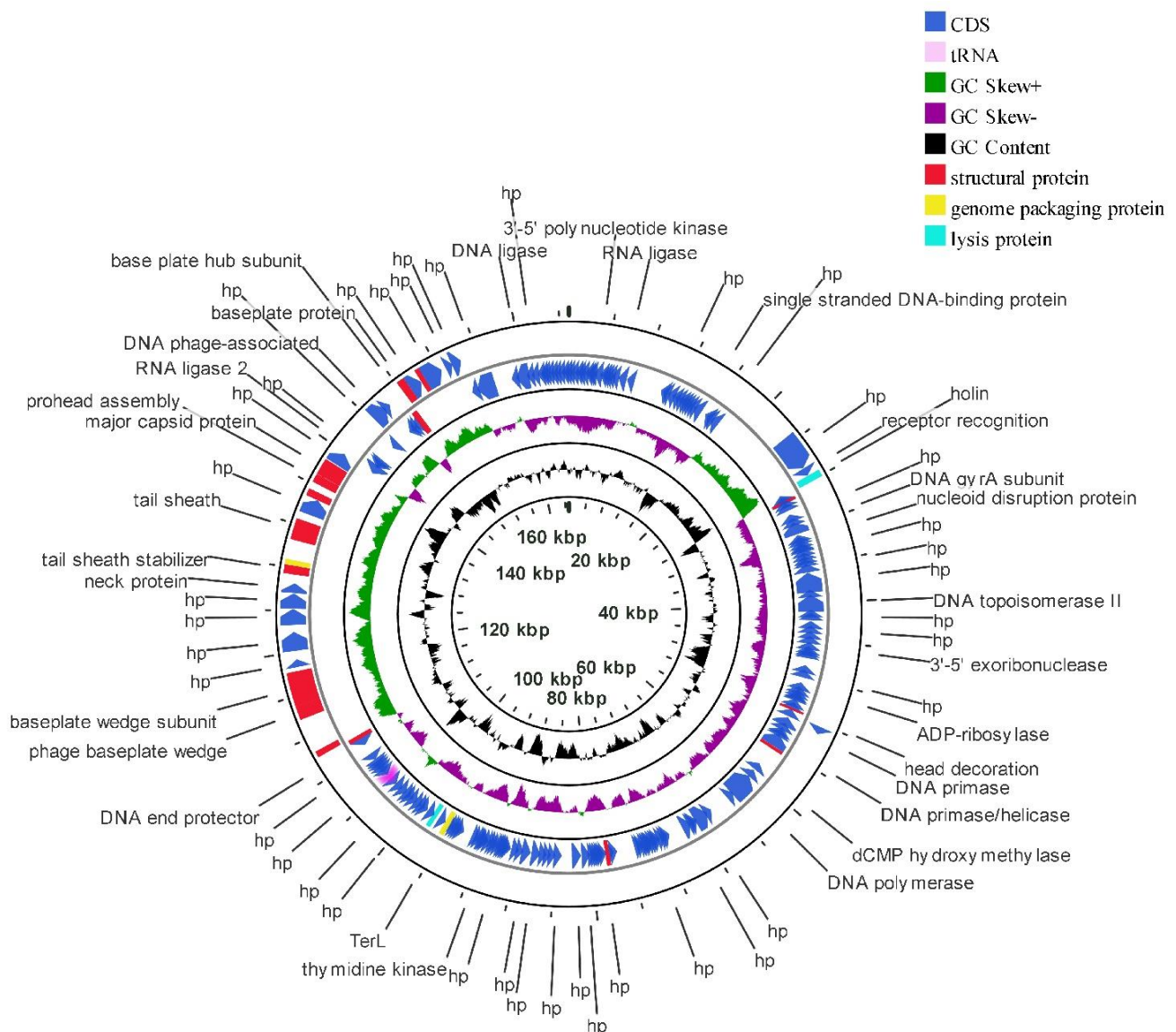
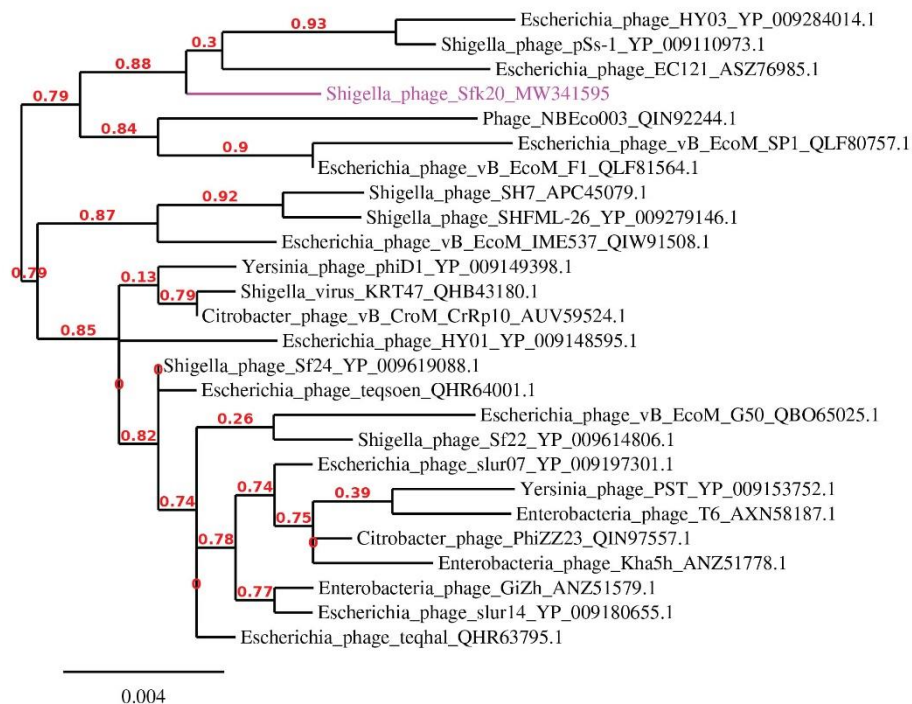


**Figure 6.4:** Schematic map of phage Sfk20 genome prepared using CGView. The outer ring represents coding sequence locations (CDS) in blue color; tRNA was marked in pink color. Hypothetical proteins were denoted as hp. The different functional ORFs were indicated in different colors. Red ORFs represent the structural proteins, yellow ORFs represent the genome packaging proteins and the cyan ORFs represent lysis proteins.

### 6.2.1.5. Phylogenetic analysis:

Structural proteins of phages are commonly used for phage taxonomy therefore baseplate wedge protein is one of the important structural proteins. The packaging reaction of phages can be selectively catalyzed by the terminase enzyme, and the bigger subunit of the terminase holoenzyme is responsible for translocating the cleaved DNA into the empty prohead (Ding et al. 2020). Therefore, in order to decipher the evolutionary relationships of Sfk20 with the other closely related homologous phages, sequences of the baseplate wedge protein (ORF189) and the terminase large subunit (ORF163) of Sfk20 were aligned with that of the other closely related phages. The reference sequences were collected from the NCBI database. As shown in **Figure 6.5 (A) & (B)** the phage Sfk20 showed the highest relationship with all the T4-like *Myoviridae* bacteriophages. The phylogenetic analysis allowed the revision of classification based on the morphology of investigated phages. Therefore, this study suggested that the phage Sfk20 belongs to the T4-like virus genus, *Myoviridae* family, and *Caudovirales* order.

(A)



(B)

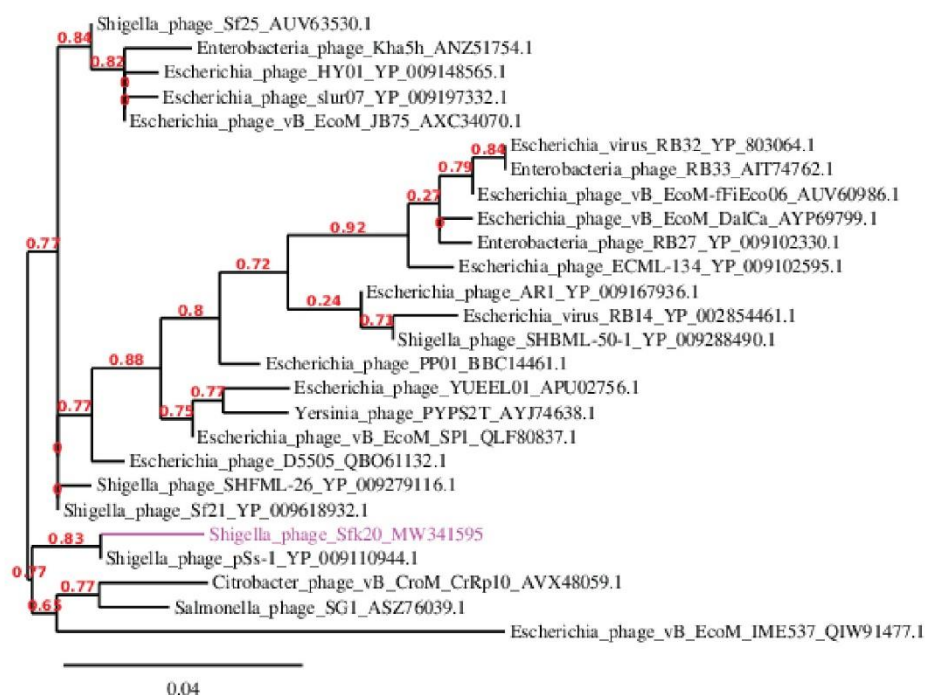


**Figure 6.5:** Phylogenetic trees of Sfk20 were constructed based on: (A) the baseplate wedge subunit and (B) the terminase large subunit (TerL) using “ONE CLICK” at Phylogeny.fr (<https://www.phylogeny.fr>)

## CHAPTER 6

**Table 6.3:** All predicted ORFs, Their positions in the Sfk20 phage genome, strand, their function and their role in the phage life cycle.

ORFs	Start	Stop	Strand	Protein name	Function in phage life cycle
ORF1	106	342	-	Hypothetical protein	
ORF2	342	923	-	dCMP deaminase	Nucleotide metabolism
ORF3	920	1255	-	Hypothetical protein	
ORF4	1255	1491	-	Hypothetical protein	
ORF5	1485	2012	-	Hypothetical protein	
ORF6	2075	2350	-	Hypothetical protein	
ORF7	2353	2553	-	Hypothetical protein	
ORF8	2546	2743	-	Hypothetical protein	
ORF9	2743	3648	-	3'-5' polynucleotide kinase	DNA damage repair
ORF10	3648	3968	-	Hypothetical protein	
ORF11	3972	4196	-	Hypothetical protein	
ORF12	4193	4492	-	Hypothetical protein	
ORF13	4489	4842	-	Hypothetical protein	
ORF14	4833	5336	-	Hypothetical protein	
ORF15	5401	6309	-	RNA ligase	RNA repair
ORF16	6578	6988	-	GIY-YIG nuclease family	Genome repair and recombination
ORF17	7016	8194	-	Aerobic NDP reductase small subunit	Genome replication and repair
ORF18	8246	10510	-	Ribonucleoside-diphosphate reductase subunit alpha	Genome replication
ORF19	10501	10788	-	Hypothetical protein	
ORF20	10781	11044	-	Hypothetical protein	
ORF21	11068	11928	-	Hypothetical protein	
ORF22	11928	12134	-	Hypothetical protein	
ORF23	12131	12712	-	Dihydrofolate reductase	Genome synthesis
ORF24	12712	12957	-	Hypothetical protein	

## CHAPTER 6

ORF25	12966	13301	-	Hypothetical protein	
ORF26	13312	13554	-	Hypothetical protein	
ORF27	13609	13974	-	Hypothetical protein	
ORF28	14018	14269	-	Hypothetical protein	
ORF29	14262	15197	-	Single stranded DNA-binding protein	Genome replication and recombination
ORF30	15297	15950	-	Hypothetical protein	
ORF31	15947	16285	-	Late promoter transcription accessory protein	Signal transduction and regulation
ORF32	16263	16532	-	Double-stranded DNA binding protein	Genome replication and recombination
ORF33	16541	17446	-	Hypothetical protein	
ORF34	22041	22559	+	Putative hinge connector of long tail fiber	Phage morphogenesis
ORF35	22622	23278	+	Hinge connector of long tail fiber distal connector	Phage morphogenesis
ORF36	23287	26598	+	Large distal long-tail fiber subunit	Host infection
ORF37	26630	27409	+	Receptor recognition	Phage morphogenesis
ORF38	27440	28096	+	Holin	Host lysis
ORF39	28097	28369	-	Anti-sigma factor	Host transcription inhibition
ORF40	28382	28534	-	Hypothetical protein	
ORF41	28531	28809	-	Baseplate wedge tail fiber connector	Phage morphogenesis
ORF42	28799	28918	-	Hypothetical protein	
ORF43	29095	29391	-	Hypothetical protein	
ORF44	30189	30824	-	Hypothetical protein	
ORF45	30910	31059	-	Hypothetical protein	
ORF46	31056	32384	-	DNA gyrase subunit	Genome replication
ORF47	32854	32934	-	Activator of host PrrClysyl-tRNA endonuclease	RNA repair

## CHAPTER 6

ORF48	32934	33389	-	Nucleoid disruption protein	Host nucleoid destruction
ORF49	33449	33664	-	Hypothetical protein	
ORF50	33780	33977	-	Hypothetical protein	
ORF51	33985	34098	-	Hypothetical protein	
ORF52	34374	34580	-	Hypothetical protein	
ORF53	34663	35139	-	DNA endonuclease IV	Genome replication
ORF54	35153	35482	-	Hypothetical protein	
ORF55	35521	35715	-	Hypothetical protein	
ORF56	35744	36682	-	rIIB protector from prophage-induced early lysis	Genome replication
ORF57	36694	38871	-	hypothetical protein	
ORF58	38882	39085	-	Hypothetical protein	
ORF59	39140	40957	-	DNA topoisomerase II	DNA replication
ORF60	41027	41287	-	Hypothetical protein	
ORF61	41292	41663	-	Hypothetical protein	
ORF62	42264	42479	-	Hypothetical protein	
ORF63	42652	43140	-	Hypothetical protein	
ORF64	43217	43756	-	MotB	Transcription regulation
ORF65	43759	44259	-	Hypothetical protein	
ORF66	44323	45006	-	3'-5' exoribonuclease	Genome replication
ORF67	45006	45248	-	Hypothetical protein	
ORF68	45241	45486	-	Dextranase	Degradation of polysaccharide compounds
ORF69	45473	45733	-	Hypothetical protein	
ORF70	47056	47367	-	Hypothetical protein	
ORF71	47369	48115	-	Hypothetical protein	
ORF72	48233	48835	-	Putative adenylylating enzyme	Signal transduction and regulation



## CHAPTER 6

ORF73	48832	49455	-	ADP-ribosylase	Inhibit host transcription mechanism
ORF74	49523	49705	-	Hypothetical protein	
ORF75	49714	50184	-	molybdenum ABC transporter	Genome injection
ORF76	50177	50341	-	Hypothetical protein	
ORF77	50338	50493	-	Transcription modulator	Signal transduction and regulation
ORF78	50516	51001	-	Transcription modulator under heat shock	Signal transduction and regulation
ORF79	50982	51191	-	Hypothetical protein	
ORF80	51348	51560	-	Hypothetical protein	
ORF81	51659	51904	-	Head decoration	Phage morphogenesis
ORF82	51977	52495	-	Hypothetical protein	
ORF83	52567	52767	+	Hypothetical protein	
ORF84	52764	53792	-	DNA primase	Genome replication
ORF85	53795	53959	-	Hypothetical protein	
ORF86	53972	54265	-	Spackle periplasmic protein	Host lysis
ORF87	54324	54581	-	Hypothetical protein	
ORF88	54583	54765	-	hypothetical protein	
ORF89	54824	56251	-	DNA primase/helicase	Genome replication
ORF90	56261	56605	-	Head vertex assembly chaperone	Phage morphogenesis
ORF91	56598	57779	-	Putative RecA-like recombination protein	Genome repair
ORF92	57857	58699	-	Beta -glucosyl-HMC-alpha-glucosyl-transferase	Genome modification
ORF93	58696	59436	-	dCMP hydroxymethylase	Genome replication
ORF94	59590	59841	-	superinfection immunity protein	Superinfection exclusion
ORF95	59849	60229	-	hypothetical protein	
ORF96	60412	63108	-	DNA polymerase	Genome replication

## CHAPTER 6

ORF97	63187	63555	-	Translational repressor	Genome replication
ORF98	63557	64120	-	Clamp loader small subunit	Genome replication
ORF99	64122	65081	-	Replication factor C small subunit	Genome replication
ORF100	65131	65817	-	Sliding clamp DNA polymerase accessory protein	Genome replication
ORF101	65873	66262	-	RNA polymerase binding protein	Genome replication
ORF102	66272	66460	-	Hypothetical protein	
ORF103	66516	68066	-	Hypothetical protein	
ORF104	68195	68401	-	Hypothetical protein	
ORF105	68382	68645	-	Hypothetical protein	
ORF106	68642	69661	-	Hypothetical protein	
ORF107	69838	71040	-	alpha glucosyl transferase	Genome modification
ORF108	71456	71773	-	Hypothetical protein	
ORF109	71775	71993	-	Hypothetical protein	
ORF110	71977	72534	-	Sigma factor	Signal transduction and regulation
ORF111	72613	72882	-	Hypothetical protein	
ORF112	72879	73094	-	Hypothetical protein	
ORF113	73097	73423	-	Hypothetical protein	
ORF114	73476	73676	-	Hypothetical protein	
ORF115	73677	73808	-	Hypothetical protein	
ORF116	73816	74109	-	Hypothetical protein	
ORF117	74102	74278	-	Hypothetical protein	
ORF118	74436	74744	-	Glutaredoxin	Reducing agent for phage-induced ribonucleotide reductase
ORF119	74747	74959	-	Hypothetical protein	

## CHAPTER 6

ORF120	75075	75545	-	Anaerobic nucleotide reductase subunit	Genome replication
ORF121	75542	77359	-	Ribonucleotide reductase of class III large subunit	Genome replication
ORF122	77356	77829	-	Endonuclease	Genome replication
ORF123	77872	78048	-	Hypothetical protein	
ORF124	78048	78494	-	Protease inhibitor	Inhibit host protease
ORF125	78618	78938	-	Hypothetical protein	
ORF126	78949	79119	-	Hypothetical protein	
ORF127	79122	79337	-	Hypothetical protein	
ORF128	79334	79597	-	Thioredoxin	Signal transduction and modification
ORF129	79599	79841	-	Hypothetical protein	
ORF130	79828	80145	-	Hypothetical protein	
ORF131	80142	81071	-	Hypothetical protein	
ORF132	81124	82125	-	Hypothetical protein	
ORF133	83214	84104	-	Hypothetical I protein	
ORF134	84112	84513	-	Thioredoxin	Signal transduction and modification
ORF135	84569	85096	-	Hypothetical protein	
ORF136	85157	85459	-	Hypothetical protein	
ORF137	85561	86529	-	Hypothetical protein	
ORF138	86595	87605	-	Hypothetical protein	
ORF139	87605	88066	-	Hypothetical protein	
ORF140	88069	88590	-	Hypothetical protein	
ORF141	88597	89130	-	Hypothetical protein	
ORF142	89157	89261	-	Molybdopterin -guanine dinucleotide biosynthesis	Nucleotide metabolism
ORF143	89322	89495	-	Hypothetical protein	
ORF144	89485	89679	-	Hypothetical protein	
ORF145	89682	89885	-	Hypothetical protein	
ORF146	89885	90073	-	Hypothetical protein	
ORF147	90169	90555	-	Hypothetical protein	

## CHAPTER 6

ORF148	90552	90845	-	rI lysis inhibition	Host lysis
ORF149	90858	91070	-	Hypothetical protein	
ORF150	91113	91694	-	Thymidine kinase	Genome replication
ORF151	91696	91884	-	Hypothetical protein	
ORF152	91881	92066	-	Hypothetical protein	
ORF153	92063	92236	-	Hypothetical protein	
ORF154	92436	92648	-	Hypothetical protein	
ORF155	92620	93099	-	Hypothetical I protein	
ORF156	93436	93981	-	transglycosylase SLT domain-containing protein	Host cell lysis
ORF157	93989	94450	-	Site-specific Rnase	Host mRNA degradation
ORF158	94510	94788	-	Hypothetical protein	
ORF159	94788	95054	-	Hypothetical protein	
ORF160	95047	95268	-	Hypothetical protein	
ORF161	95268	95630	-	Hypothetical protein	
ORF162	95637	95966	-	Hypothetical protein	
ORF163	95963	96532	-	large terminase subunit	Genome packaging
ORF164	96656	97129	-	Hypothetical protein	
ORF165	97139	97555	-	Pyrimidine dimer DNA glycosylase endonuclease V	Nucleotide metabolism
ORF166	97615	98109	-	Endolysin/lysozyme	Host lysis
ORF167	98146	98586	-	nudix hydrolase	Hydrolase activity
ORF168	98583	99071	-	Putative transmembrane region domain containing protein	Phage morphogenesis
ORF169	99068	99430	-	Hypothetical protein	
ORF170	99412	99804	-	Hypothetical protein	
ORF171	99773	100393	-	Hypothetical protein	
ORF172	100435	101028	-	Hypothetical protein	
ORF173	101086	101421	-	Hypothetical protein	
ORF174	101477	101740	-	Hypothetical protein	
ORF175	101981	102544	-	Hypothetical protein	

## CHAPTER 6

ORF176	102671	103144	-	Hypothetical protein	
ORF177	103529	103879	-	Hypothetical protein	
ORF178	104810	105325	-	Hypothetical protein	
ORF179	105328	105618	-	Hypothetical protein	
ORF180	105621	106001	-	Hypothetical protein	
ORF181	106003	106188	-	Hypothetical protein	
ORF182	106259	106516	-	Hypothetical protein	
ORF183	107044	107286	-	Hypothetical protein	
ORF184	107286	108011	-	Deoxynucleoside monophosphate kinase	Genome replication
ORF185	108698	109522	-	DNA end protector	Genome replication and modification
ORF186	109522	109974	-	Head completion	Phage morphogenesis
ORF187	110022	110612	+	Baseplate wedge subunit	Phage morphogenesis
ORF188	113794	115137	+	Baseplate wedge	Phage morphogenesis
ORF189	115134	118232	+	Baseplate wedge subunit	Phage morphogenesis
ORF190	118723	119229	+	Hypothetical protein	
ORF191	119293	120159	+	Baseplate wedge completion tail fiber socket	Phage morphogenesis
ORF192	120159	121964	+	Hypothetical protein	
ORF193	122620	124170	+	Hypothetical protein	
ORF194	124180	125637	+	Hypothetical protein	
ORF195	125670	126599	+	Neck protein	Phage morphogenesis
ORF196	126601	127371	+	Hypothetical protein	
ORF197	127413	128231	+	Tail sheath stabilizer and completion protein	Phage morphogenesis
ORF198	128240	128734	+	Small terminase protein	Genome packaging
ORF199	128718	130550	+	Putative terminase subunit	Genome packaging
ORF200	130582	132561	+	Tail sheath	Phage morphogenesis
ORF201	132678	133169	+	Putative tail tube monomer	Phage morphogenesis
ORF202	133253	134827	+	Hypothetical protein	
ORF203	134827	135084	+	Prohead core	Phage morphogenesis

## CHAPTER 6

ORF204	135084	135509	+	Capsid and scaffold protein	Virion assembly
ORF205	135509	136147	+	Prohead core scaffolding protein and protease	Phage morphogenesis
ORF206	136178	136987	+	Prohead assembly	Phage morphogenesis
ORF207	137006	138571	+	Major capsid protein	Phage morphogenesis
ORF208	138655	139938	+	Hypothetical protein	
ORF209	139968	140972	-	RNA ligase 2	Genome replication
ORF210	140982	141260	-	Hypothetical protein	
ORF211	141247	141462	-	Hypothetical protein	
ORF212	141552	143546	-	PKD domain protein	Phage morphogenesis
ORF213	143556	144236	-	Hypothetical I protein	
ORF214	144287	145798	+	Hypothetical protein	
ORF215	145824	146054	+	ATP-dependent DNA helicase	Genome replication
ORF216	146306	146530	-	Hypothetical protein	
ORF217	146530	146943	-	Recombination mediator protein	Genome modification
ORF218	147010	147408	-	Hypothetical protein	
ORF219	147408	148034	-	Baseplate hub subunit	Phage morphogenesis
ORF220	148085	148834	+	Baseplate protein	Phage morphogenesis
ORF221	148834	150009	+	Hypothetical protein	
ORF222	150029	150487	+	Baseplate distal hub subunit	Phage morphogenesis
ORF223	150484	152256	+	Hypothetical protein	
ORF224	152757	153359	+	Hypothetical protein	
ORF225	153359	154324	+	Hypothetical protein	
ORF226	154353	154643	-	Hypothetical protein	
ORF227	154704	156761	-	Hypothetical protein	
ORF228	156765	158858	-	ADP-ribosyltransferase exoenzyme	Genome replication
ORF229	158911	159099	-	Hypothetical protein	
ORF230	159096	160556	-	DNA ligase	Genome replication
ORF231	160553	160822	-	Hypothetical protein	

## CHAPTER 6

---

ORF232	160822	161661	-	Hypothetical protein	
ORF233	161658	162116	-	Hypothetical protein	
ORF234	162109	162324	-	Hypothetical protein	
ORF235	162329	162616	-	Hypothetical protein	
ORF236	162658	163023	-	Hypothetical protein	
ORF237	163091	163423	-	Hypothetical protein	
ORF238	163534	163710	-	Hypothetical protein	
ORF239	163905	164153	-	Hypothetical protein	
ORF240	164301	164636	-	Co-chaperone GroES	Signal transduction and regulation
ORF241	164693	164863	-	Hypothetical protein	

## 6.2.2. Proteomic analysis of bacteriophage Sfk20:

### 6.2.2.1 Study of protein profile of the phage Sfk20:

Protein profile of bacteriophage Sfk20 was tested by running 12.5% SDS-PAGE gel. Two major bands with molecular weights at 53 kDa and 70 kDa and a few minor bands with molecular weights 13, 76, 100, and 155 kDa appeared as shown in **Figure 6.6**.

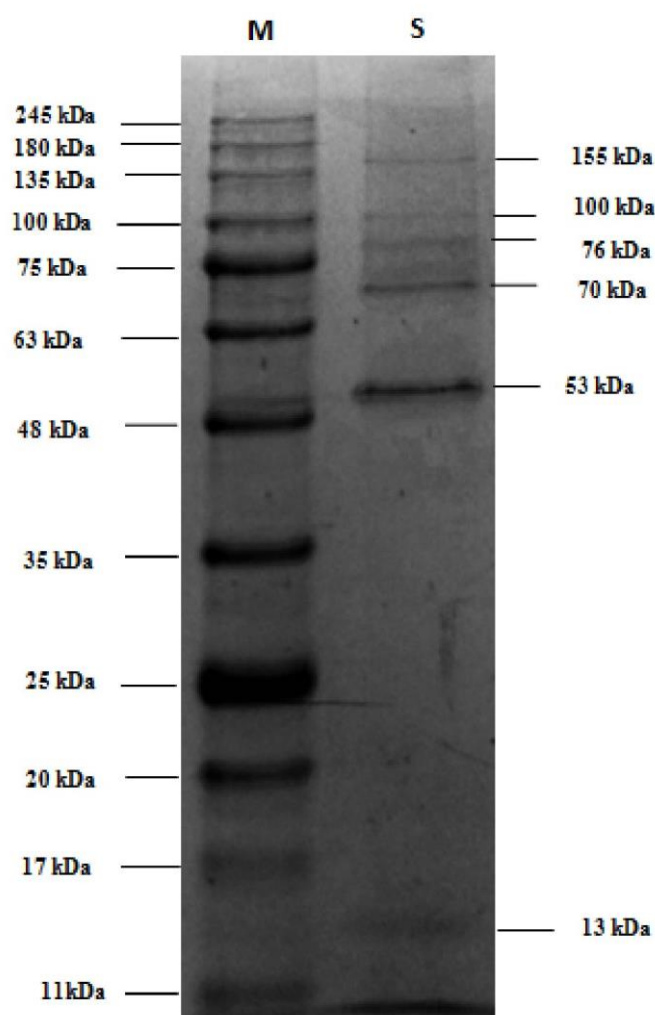


**Figure 6.6:** Protein profile of bacteriophage Sfk20. Lane M, prestained protein ladder (abcam Prism Ultra Protein Ladder, ab116028), Lane S bacteriophage proteins.



### 6.2.2.2 Proteomic analysis of bacteriophage Sfk20:

LC-MS/MS-based techniques are more reliable compared to other techniques because the phage peptides can easily be identified without the need for other approaches. In order to identify the total proteome detailed proteomic characterization using trypsin proteolysis followed by liquid chromatography-tandem mass spectrometry was performed. In this detailed proteomic characterization, a total of 40 virion proteins with sequence coverage of 12% to 86% were identified. In this proteomic analysis, the phage proteins with at least two unique peptides were considered. Although the major capsid protein (ORF207) was the most abundant protein with the highest numbers of identified peptides. A total of 107 peptides were identified for major capsid proteins and the molecular weight was identified as 56 kDa. Among the 40 identified proteins, there were 20 hypothetical proteins. From the remaining 20 proteins the 17 identified proteins belong to the phage morphogenesis modules which included one major capsid protein (ORF207), four baseplate wedge proteins (ORF187, ORF189, ORF190, ORF191), a PKD domain protein (ORF212), a putative tail tube monomer protein (ORF201), tail sheath stabilizer, and completion protein (ORF197), two putative hinge connector of long tail fiber protein (ORF34, ORF35), tail fiber protein (ORF36), one pro head core scaffolding protein and protease (ORF205), neck protein (ORF195), DNA end protector protein (ORF185), head decoration protein (ORF81), receptor recognition protein (ORF37), and tail sheath protein (ORF200). Among the remaining three functional proteins two proteins: helicase (ORF215), and ADP ribosyl transferase (ORF228) belongs to the phage DNA replication module, and phage endolysin (ORF166) belongs to the lysis module (**Table 6.4**).

**Table 6.4** Detection and identification of phage Sfk20 proteins by LC-MS/MS

ORF No.	Protein name	Molecular weight (Da)	No. of peptides	Coverage (%)
207	Major capsid protein	56099	107	68
200	Tail sheath protein	71352	47	68
212	PKD domain protein	70736	109	86
36	Long tail fiber protein	118710	31	47
228	ADP-ribosyl transferase exoenzyme	78016	40	64
194	hypothetical protein	52430	43	75
193	hypothetical protein	55420	26	72
227	hypothetical protein	75954	23	38
208	hypothetical protein	47019	24	62
189	baseplate wedge subunit	119054	24	29
202	hypothetical protein	61062	20	42
188	baseplate wedge	49921	16	49
192	hypothetical protein	66384	16	37
191	baseplate wedge completion tail fiber socket	31009	11	54
197	tail sheath stabilizer and completion protein	31556	10	54
164	hypothetical protein	17768	11	47
195	neck protein	34690	9	37
223	hypothetical protein	64400	10	30
196	hypothetical protein	29569	8	48
201	putative tail tube monomer	18434	8	50
221	hypothetical protein	44407	7	25
175	hypothetical protein	20868	6	36
35	hinge connector of long tail fiber distal connector	23296	5	48
182	hypothetical protein	9278	6	55

## CHAPTER 6

---

215	ATP-dependent DNA helicase	8804	7	72
176	hypothetical protein	17258	5	30
34	putative hinge connector of long tail fiber	18530	4	35
225	hypothetical protein	34877	3	15
187	baseplate wedge subunit	22952	7	34
190	hypothetical protein	19513	4	25
81	head decoration	9174	5	70
37	receptor recognition	26135	4	31
218	hypothetical protein	15096	3	26
185	DNA end protector	31654	4	18
205	Prohead core scaffolding protein and protease	23250	4	20
166	Endolysin	18606	5	35
147	hypothetical protein	14648	2	16
85	hypothetical protein	5885	2	61
224	hypothetical protein	22475	2	12
161	hypothetical protein	13863	2	20

### 6.3 DISCUSSION

Phages or bacteriophages, discovered in the early 20th century by Frederick Twort and Felix d'Herelle independently, are the most abundant and diverse biological organisms on the planet (Bergh et al., 1989). Phages are found in every ecosystem with different genome diversity from the gastrointestinal tract of humans to the global ocean (Nigro et al. 2017). In the aquatic environment, phages play a major role in the biogeochemical cycle, and in the human gut phages predominantly exist as lysogens which can influence their host (Kim & Bae, 2018). According to the public database as of 2019 most of the recognized bacteriophages are tailed phages with double-stranded genomes (dsDNA). Some less common phages can package their single-stranded DNA (ssDNA), single-stranded RNA (ssRNA), and double-stranded RNA (dsRNA) inside the capsid.

In this work, the phage Sfk20 genome was isolated and the digestion of the genome by restriction enzymes was performed. The digestion of the genome by restriction enzyme EcoRV suggested that the genome of Sfk20 is a double-stranded genome.

The Roche/454 sequencer launched the current wave of high throughput sequencing efforts in 2005. Other platforms, including SOLiD, Solexa (Illumina), Helicos, Ion Torrent, and PacBio, were then introduced (Eisenstein 2012). However, all these platforms produce very high sequence outputs compared with the throughput of conventional Sanger sequencing platforms. The genome sequencing of the phage Sfk20 genome was performed using next-generation sequencing on an Illumina-based platform. Comparative genome analysis of phage Sfk20 has helped to understand the genomic characteristics as well as the evolutionary relationship with the related phages. Sfk20 phage showed high nucleotide sequence similarity with T4-like phages: 97.91% with pSs-1, 96.03% with SH7, 95.34% with SfPhi01, 95.40% with Sf21 and 95.46% with Sf23.

Genome sequencing, analysis, and complete annotation provided sufficient information on the phage Sfk20 genome. The genes were distributed into the genome in various modules. The major modules contain various important genes that encode various proteins responsible for phage DNA replication and modification proteins, phage morphogenesis proteins, phage genome packaging proteins, and host lysis proteins (Topka-Bielecka et al. 2020). After the injection of the phage genetic material during infection, it started replicating inside the host cell. The genes of phage DNA replication modules encode various replication-related proteins such as DNA polymerase (ORF96), helicase (ORF215), primase (ORF84, ORF89),

endonuclease (ORF53, ORF122), DNA gyrase (ORF46), and DNA topoisomerase II (ORF59) helped to replicate the phage DNA. The phage tail is a crucial part, and the tail adsorption devices are experts in locating and interacting with receptors on the surface of bacteria (Ding et al. 2020). In the genome of phage Sfk20, the tail-associated ORFs that were assigned to tail structure protein were identified and categorized including tail fiber proteins (ORF34, ORF35, ORF36, ORF41), Tail sheath stabilizer and completion protein (ORF197), tail sheath protein (ORF200), tail tube protein (ORF201) and baseplate structural proteins (ORF187, ORF188, ORF189, ORF191) which were involved in tail assembly or in facilitating the penetration of the outer membrane of the host cell upon infection (Huang and Xiang 2020). Except for these tail structure proteins, the annotation results also identified other phage structure proteins, including the major capsid protein (ORF207), prohead core protein (ORF203), capsid and scaffold protein (ORF204), prohead assembly protein and protease (ORF205), PKD domain protein (ORF212) baseplate hub protein (ORF219), baseplate protein (ORF220) and baseplate distal hub subunit (ORF222). DNA packaging is often a crucial mechanism for the phage life cycle that involves several proteins interacting with the phage genome. Terminase enzymes that can specifically catalyze the packaging reaction of phages are composed of large and small subunits (Wang et al. 2019). The small subunit selectively binds to the genome and controls the packing process, whereas the large subunit is a multifunctional enzyme that plays a significant part in packaging. In gene annotating of phage Sfk20, the large terminase subunit and the small terminase subunit were found encoded by ORF163 and ORF198, respectively. The annotation results also identified another packaging protein: putative terminase subunit encoded by ORF199. Finally, after the formation of the new progeny phages, they must lyse the host cell in order to release into the surrounding environment. The genes of the lysis module encode lytic enzyme holin and endolysin that are responsible for the lysis of the bacterial cell and the release of the progeny. Phage-encoded muralytic enzyme endolysin hydrolyses the peptidoglycan layer present in the bacterial cell wall during the final stage of the phage reproduction event (O’Flaherty, Ross, and Coffey 2009). The presence of both holin and endolysin genes in the sequence of phage Sfk20 genome confirmed the lytic nature of this phage. Analysis of the phage Sfk20 genome confirmed the presence of lytic proteins and the absence of any lysogenic, toxin, or antibiotic resistance genes suggesting that the phage could be used as a safe biocontrol agent for host bacteria.

In the genome of phage Sfk20, around 10 tRNA including Arg, Asn, Tyr, Met, Thr, Ser, Pro, Gly, Leu, and Gln were identified. It was reported elsewhere that the phage tRNA is required in certain hosts that help to increase fitness in some environments.

Phylogenetic tree analysis of Sfk20 based on base plate wedge subunit and terminate large subunit with other related phages suggested that Sfk20 was closely related to other *Shigella* and *E. coli* phages and they probably evolved from a common ancestor.

According to the mega blast search result, Sfk20 belongs to the genus T4-like viruses; order *Caudovirales*; family *Myoviridae*; subfamily *Tevenvirinae*. Recently a total of 78 isolated *Shigella* phages were grouped according to family and genome size and phage Sfk20 falls in the largest T4-like Myoviridae family with a genome size of 164.0–176.0 kb (Subramanian et al. 2020). Comparative genome analysis and biological properties suggested that phage Sfk20 has the highest similarity with pSs-1 as shown in **Table 6.1**.

The proteomic analysis of phage Sfk20 was performed to identify the total proteome. In this study to identify the total proteins in-solution tryptic digestion of the isolated protein was performed and the digested proteins were analyzed by LC-MS/MS. The in-solution tryptic digestion takes less time and it is significantly the least labor intensive. Hence, in-solution tryptic digestion was chosen over in-gel tryptic digestion. When compared to other methods, LC-MS/MS-based techniques have significant advantages since they allow for the direct identification of phage peptides without the need for inference conclusions produced using different methodologies, such as genomic tools. LC-MS/MS analysis is a reliable method to rapidly identify and characterize phage proteins (Abril et al. 2020). In this study, 40 different proteins were identified by LC-MS/MS. Among them, 20 proteins were hypothetical. There were three functional proteins: (i) DNA helicase enzymes help in the unwinding of the DNA helix. Helicase mainly promotes the DNA replication cycle within the replisome (Lionnet et al. 2007). (ii) ADP ribosyl transferase mainly participates in the replication cycle by adding the ADP ribose moieties to a designated number of host proteins (Tiemann et al. 2004). (iii) Endolysins are phage-encoded peptidoglycan hydrolases that enzymatically degrade the host bacterium's peptidoglycan layer, leading to the programmed host cell lysis and the release of mature viral particles (Schmelcher et al. 2012). Seventeen phage structural proteins were also identified.



# CHAPTER 7

## Objective 2(Part I)

Structural characterization of  
*Shigella* phage Sfk20 using single  
particle cryo-electron microscopy  
and image processing



### 7.1 INTRODUCTION

Visualization of the virus morphology and structure is closely related to the development of electron microscopy. Tobacco mosaic virus was one of the first samples to be seen soon after the development and use of the first electron microscope (Kausche, Pfankuch, and Ruska 1939). Thereafter, electron microscopy became the main technique to detect, visualize, classify, and characterize different viruses as per their morphology (Goldsmith and Miller 2009). The structure determination of phages using transmission electron microscopy started in the '60s after the pioneer structure prediction work of Klug and Finch using negatively stained virus images (Klug and Finch 1965). Thereafter, the structure determination of other viruses using electron microscopy were started (De Rosier and Klug 1968). Cryoprotection was an essential part of sample preparation for TEM, enabling data acquisition at an appropriate resolution to create the first near-atomic model of a rotavirus-related particle. This study expanded the use of TEM towards high-resolution structure determination of viruses.

Bacteriophages after their discovery were studied extensively for their use in therapeutic purposes. The phage structural study is important to reveal their detailed organization that improves our understanding of the functions of every component which in turn proposes the usage of phages in medical treatments. The tailed bacteriophages are the most common among all phages which are divided into three groups: *Myoviridae* (long, contractile tail), *Siphoviridae* (long, non-contractile tail), and *Podoviridae* (short non-contractile tail). To date, the three-dimensional structure of a large number of *Siphoviridae* and *Podoviridae* bacteriophages have been reported compared to only a handful of *Myoviridae* bacteriophage studies. Complete three-dimensional structure determination of T4 bacteriophage was performed earlier and so far, it is perhaps the most extensively studied *Myoviridae* phage. T4 bacteriophage has a prolate-shaped head and long contractile tail.

To study the bacteriophage structures two very popular methods of choice are negative staining and cryo-electron microscopy. The phage samples are stained with heavy metal salts (uranyl acetate, uranyl formate, phosphotungstic acid, etc) in a negative staining technique. After air-drying, the stained samples are introduced into the vacuum chamber of the electron microscope to visualize. The metal salt reduces the chance of radiation damage thus the morphology and structure of the sample up to several nanometres resolution can be produced. This is a simple and rapid method to visualize the overall sample and to check the concentration, and homogeneity.



But a negatively stained sample can produce a three-dimensional structure only upto a limited low resolution. Cryo-electron microscopy makes it possible to visualize the virus in native conditions without using any chemical fixation and contrasting agents. In this method, the virus sample is frozen in liquid ethane. The rapid freezing help to produce vitreous ice that preserves the samples in near-native condition. After that, the samples were stored in liquid nitrogen to maintain the sample in a frozen state. While imaging, the samples were introduced into the microscope under a vacuum chamber using a specialized sample loading holder maintaining the temperature at -180°C, and images are obtained at low dose conditions to minimize sample damage.

In our present study, the three-dimensional structure of T4 like *Myoviridae Shigella* phage Sfk20 was determined using single-particle cryo-electron microscopy and image processing. It is clear from the morphological study that it has a prolate-shaped head, a head-tail connector, and a long contractile tail with tail spikes.

## 7.2 RESULT

### 7.2.1 Three-dimensional reconstruction of the various parts of bacteriophage Sfk20:

#### 7.2.1.1 Cryo-electron micrograph of phage Sfk20:

Bacteriophages in particular have varied symmetries in different components of their complete intact structure. Three-dimensional reconstructed image of bacteriophages is useful for understanding the organization of various components forming their full structure. These intricate biological systems were frequently researched using a "divide and conquer" (Baker and Johnson 1996) strategy. Following the approach, different components of phage Sfk20 were reconstructed separately and combined to form the whole intact structure of the phage.

Phage Sfk20 bacteriophage contains a prolate-shaped head, a long contractile tail and belongs to the family of *Myoviridae*, *Caudovirale* order. The long contractile tail of the phage Sfk20 was shown in **Figure 7.1(A)** and a representative image of the phage particle with the contracted tail was shown in **Figure 7.1(B)**.

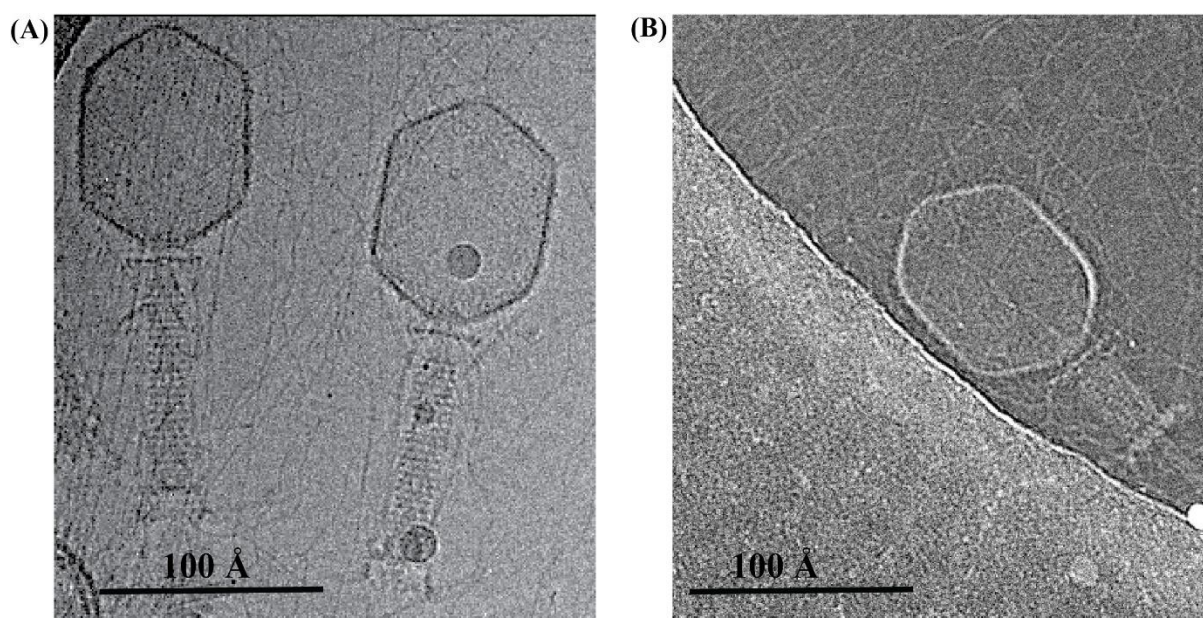


**Figure 7.1:** Cryo-electron micrograph of full Sfk20 bacteriophage particles: (A) native non-contracted tail conformation and (B) in the contracted tail state (magnification 45000X)

### 7.2.1.2 Three-dimensional reconstruction of the bacteriophage capsid head:

Phages have capsids that are highly organized proteinaceous structures to shield their genomes. An ATP-dependent packaging machine first assembles the head as an empty capsid, which is then filled with DNA. Tailed phages have either prolate or icosahedral capsids but all phage capsids possess a 5-fold rotational symmetry. Other elements, such as the packaged genome or the tail, are averaged out during the reconstruction of the capsid because they lack the required symmetry. Phage Sfk20 belongs to the family of *Myoviridae* and showed similarity with T4-like bacteriophages. Phage Sfk20 is composed of a large elongated (prolate) icosahedral capsid with a contractile tail. First, the Sfk20 capsid three-dimensional (3D) structure was reconstructed using EMAN 2.9 software. In the reconstruction process, initially, the capsid particles were picked from best-sorted 2D cryo images using a box size of 1296. Next, the reference free class averaging was run without imposing any symmetry using “e2refine2d.py” to generate class averages. After that, the good class averages were sorted from all the class averages that matched with 2D cryo-EM images of phage Sfk20 and revealed the presence of 5-fold symmetric capsid vertex. The images of some good class averages were shown in **Figure 7.2**. Finally, during the preparation of the 3D initial model of the phage capsid, the C5 symmetry was applied. The projection images of the initial model of phage Sfk20 capsid were shown in **Figure 7.3**. The reconstruction result after the final refinement was shown in **Figure 7.4**. The reconstructed 3D density map of the Sfk20 phage capsid showed a large, elongated icosahedral-shaped structure with an elevated, star knob-like 5-fold symmetry, a slightly elevated 3-fold, and a depressed 2-fold symmetry as appeared in **Figure 7.4 (A)**. The top view and bottom view showed the 5-fold symmetry as shown in **Figure 7.4 (B) and (C)**. One of the 5-fold vertex is replaced with the unique portal vertex through which the phage tail is attached to the capsid part.

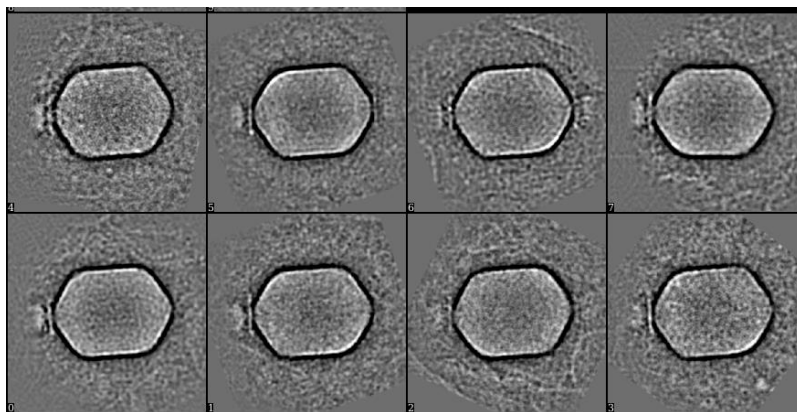


**Figure 7.2:** Set of good 2D class averages of the phage Sfk20 capsid.

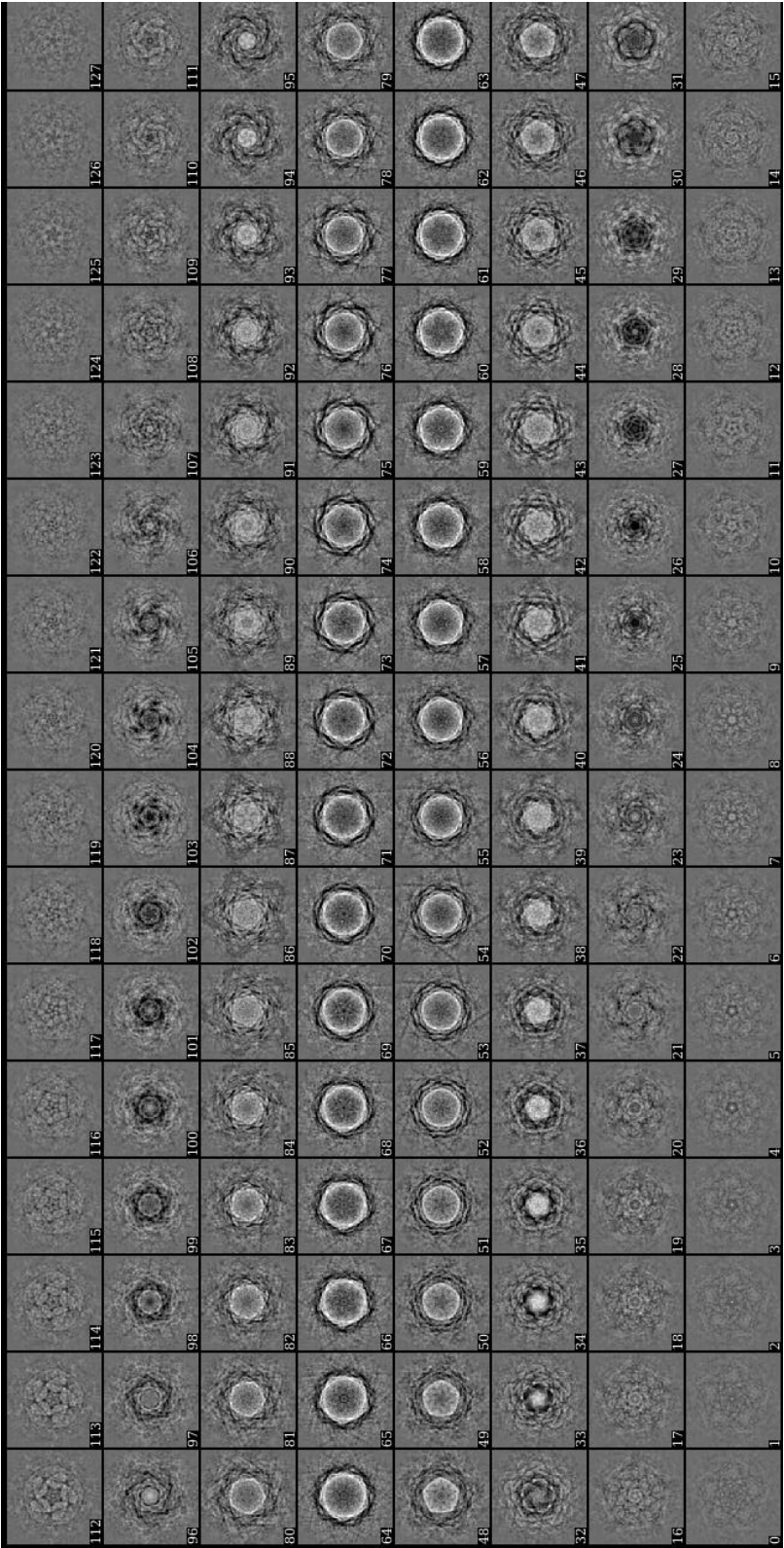


**Figure 7.3:** Projection images of the 3D initial model of phage Sfk20 capsid.

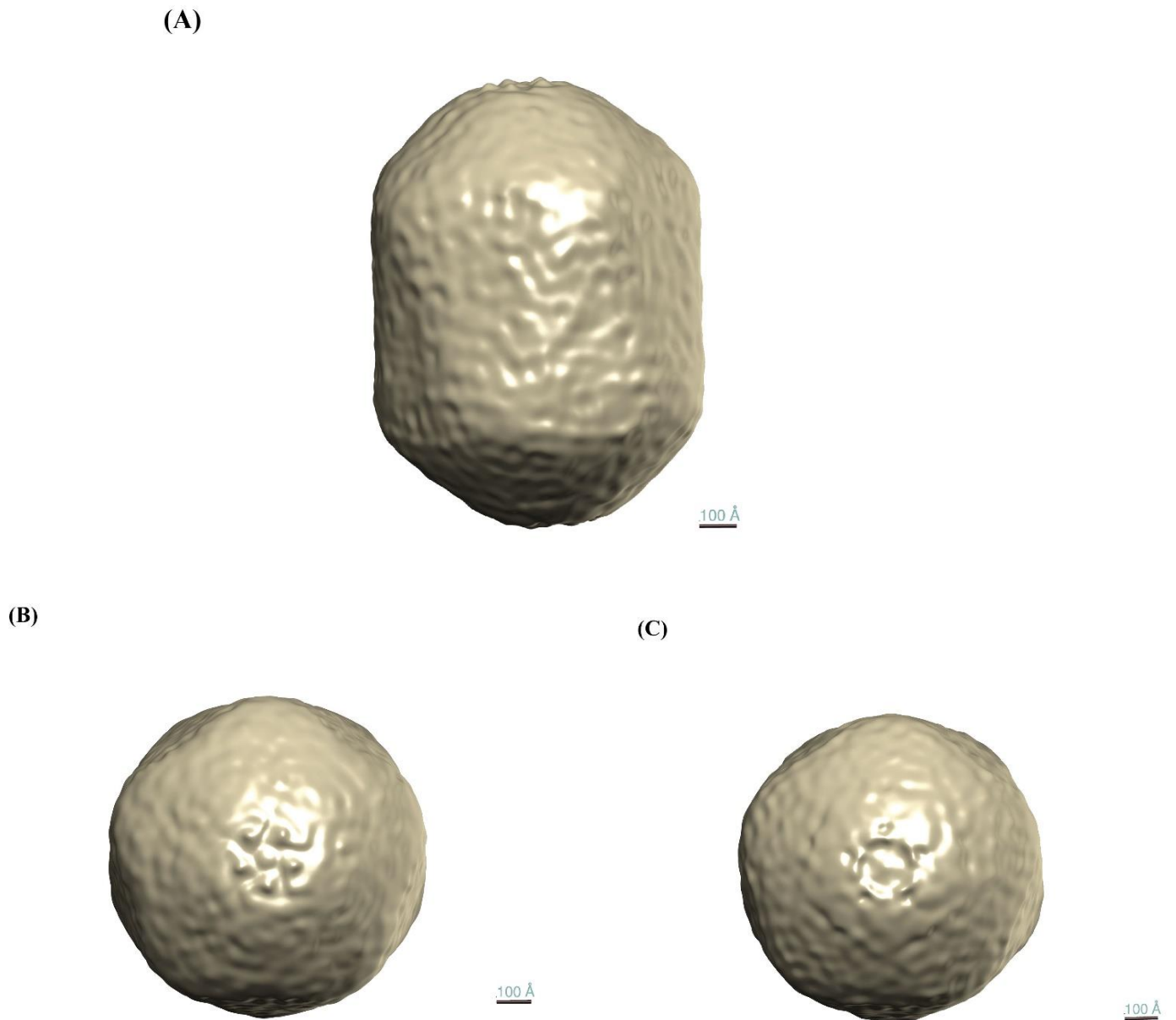


**Figure 7.4:** The density map of Sfk20 capsid: (A) the side view showed elevated 5-fold symmetry and a depressed 3-fold symmetry, (B) the top view of the capsid and (C) the bottom view of the capsid.

### 7.2.1.3 Three-dimensional reconstruction of the bacteriophage connector:

The capsid of the phage is connected with its unique tail through a multimeric protein complex which is known as a head-to-tail connector.

In this work, the 3D reconstruction of the phage head and tail connector part of the phage Sfk20 was performed using EMAN 2.9 software. At first, the connector parts of the phage Sfk20 were picked using “e2boxer.py”. Around 375 connector parts were picked. Next the reference free class averaging was performed without imposing any symmetry using “e2refine2d.py” to generate class averages. After that, from the class averages a subset of good class averages was prepared by visual checking. The images of the good class averages were shown in **Figure 7.5**. The class averages indicated a 12-fold symmetry. Therefore, the program “e2initialmodel.py” was run by applying 12-fold symmetry along the head-to-tail connector axis to build a set of 3-D models suitable for use as initial models. The best-looking initial model was chosen as the final model and the sections of projection images of the initial model of the phage head-tail connector were shown in **Figure 7.6**. The reconstructed 3D density map of the connector revealed that it is a funnel-shaped structure having two prominent rings. The bottom view of the connector revealed that it is a ring-shaped dodecameric structure. This connector acts as a channel to translocate the DNA from the capsid to the tail. A capsid vertex-to-connector junction was also shown in **Figure 7.7 (A)**. There is an opening on the top of the connector which is continuous till it reaches the tail as shown in **Figure 7.7 (B)**. The bottom view of the connector part also showed in **Figure 7.7 (C)**. A central section view of the connector part was shown in **Figure 7.7 (D)**

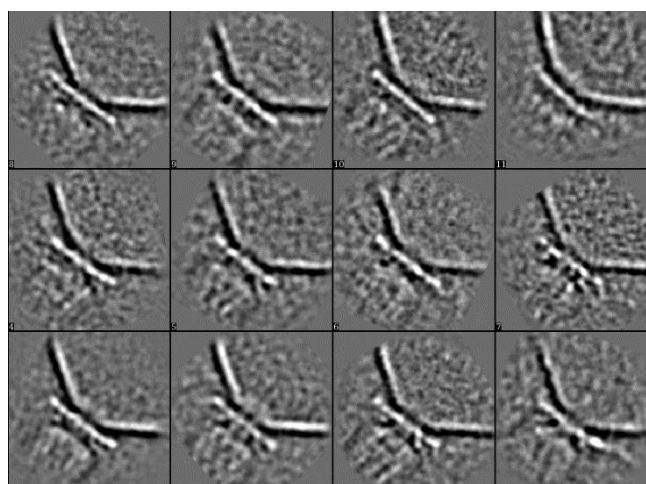


**Figure 7.5:** Good 2D class averages of the phage Sfk20 connector, used for further reconstruction purposes



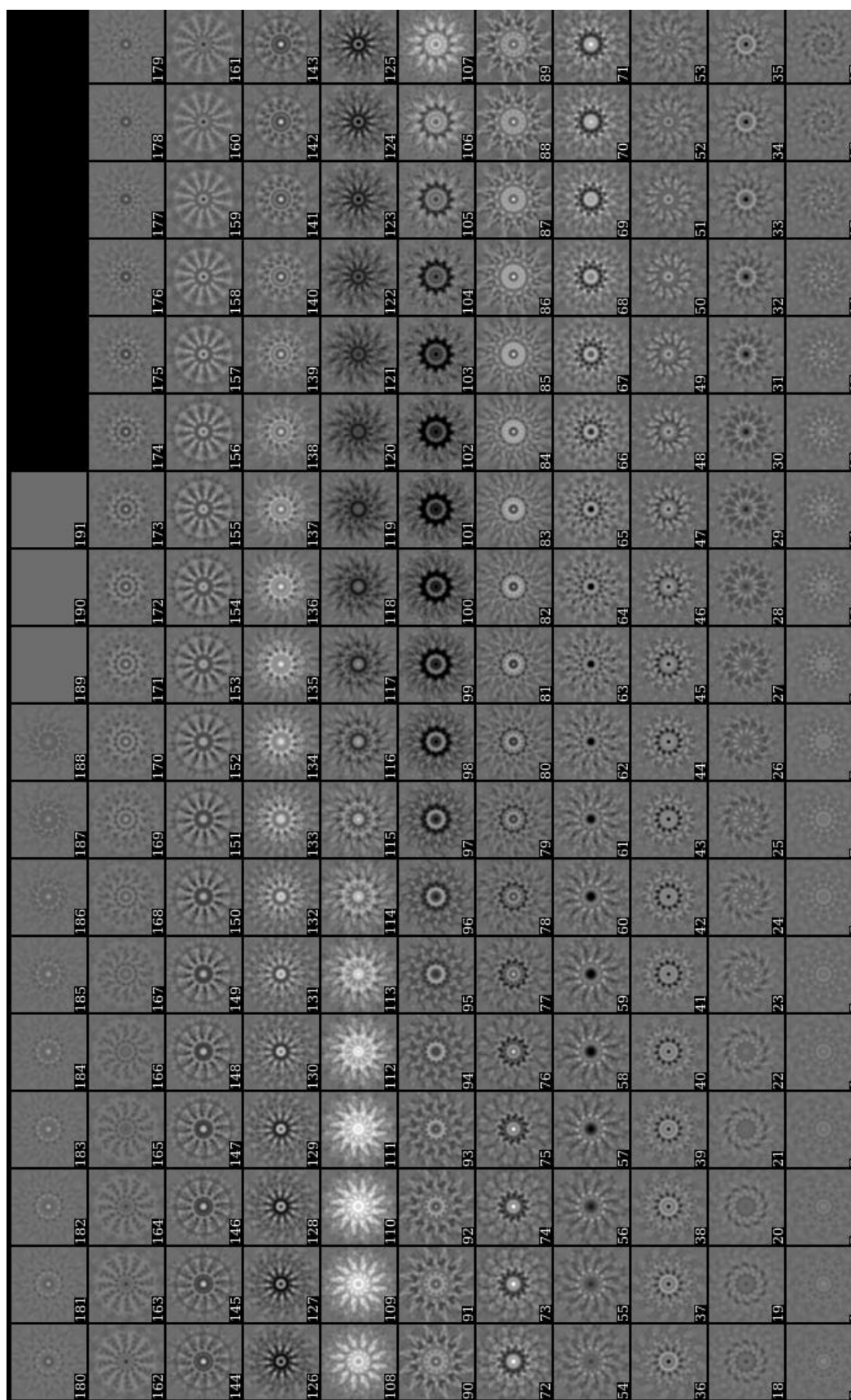


**Figure 7.6:** Projection images of the 3D initial model of the phage Sf1k20 connector.

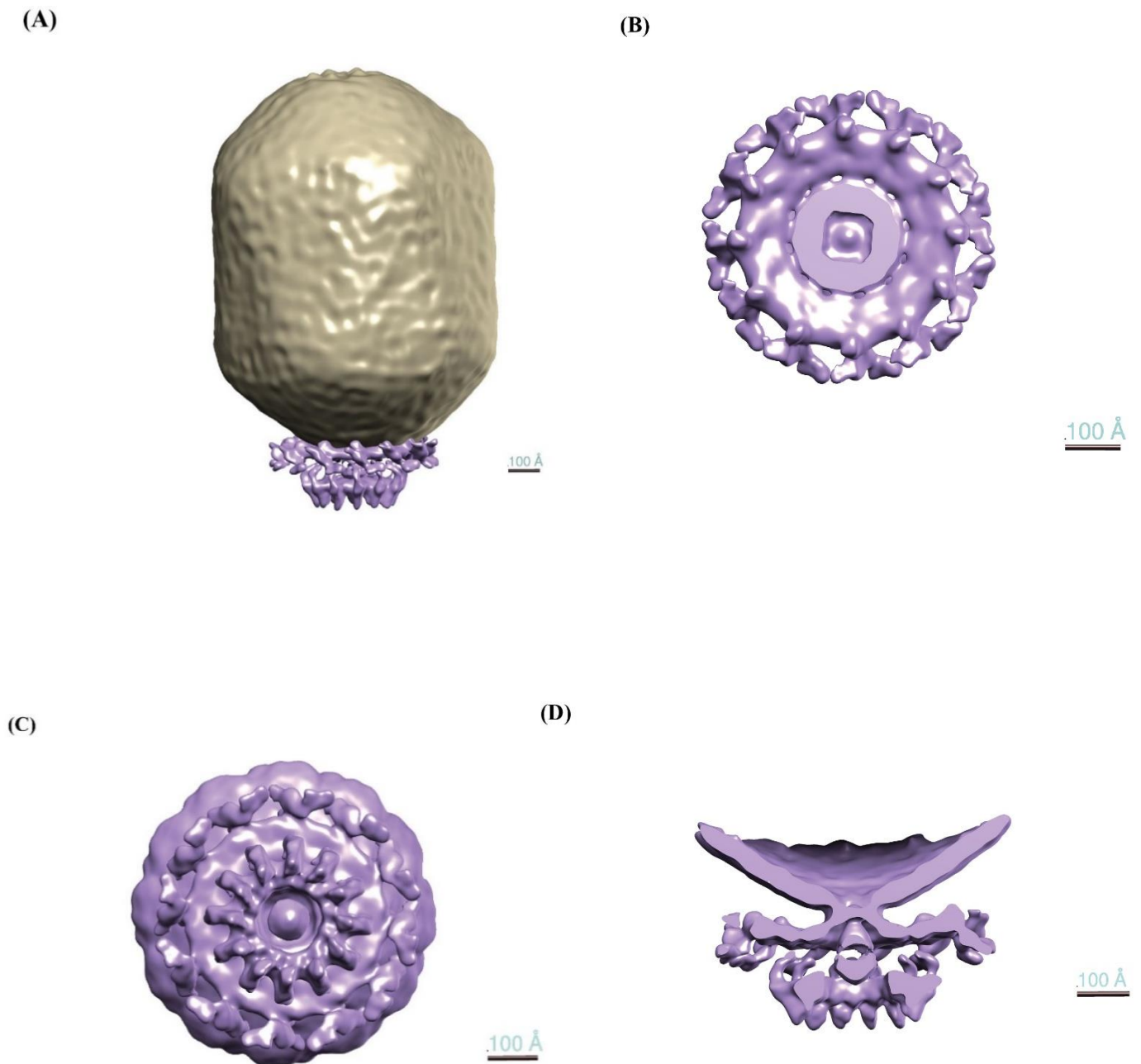


**Figure 7.7:** The density map of the phage Sfk20 head-to-tail connector: (A) capsid to connector junction, (B) top view of the connector, (C) bottom view of the connector and (D) The central section view of the connector part.



### 7.2.1.4 Three-dimensional structure of the bacteriophage tail:

For tailed bacteriophages, one particle is sufficient for infecting a single bacterial cell (E. 1994a). A specialized component of bacterial viruses known as a tail is a key factor in high infection efficiency. About 96% of all bacteriophages have a tail part, and it is made to adhere to bacteria, break through their cell membranes, and transfer the viral genome to the host. As discussed in the earlier chapters, bacteriophage Sfk20 belongs to the T4-like *Myoviridae* group. These phages have the most complex tail structures generally consisting of a long, non-contractile tube surrounded by a contractile sheath. Since the tail sheath of phage Sfk20 has a prominent helical structure, the 3D reconstruction of the tail part was done using Relion 3.1 helical reconstruction imposing helical symmetry as described in the materials and method section. The tail parts of the phage Sfk20 were picked manually using the “Manual picking” program from the micrograph. The images of the picked tail particles were shown in **Figure 7.8**. Next 2D class averaging was performed and some of the good class averages were selected for generating an initial model as shown in **Figure 7.9**. The reconstruction result of the final refinement was shown in **Figure 7.10**. The tail sheath proteins are organized as a helix around the central tube, as found in the 3D density map of the phage Sfk20 tail.

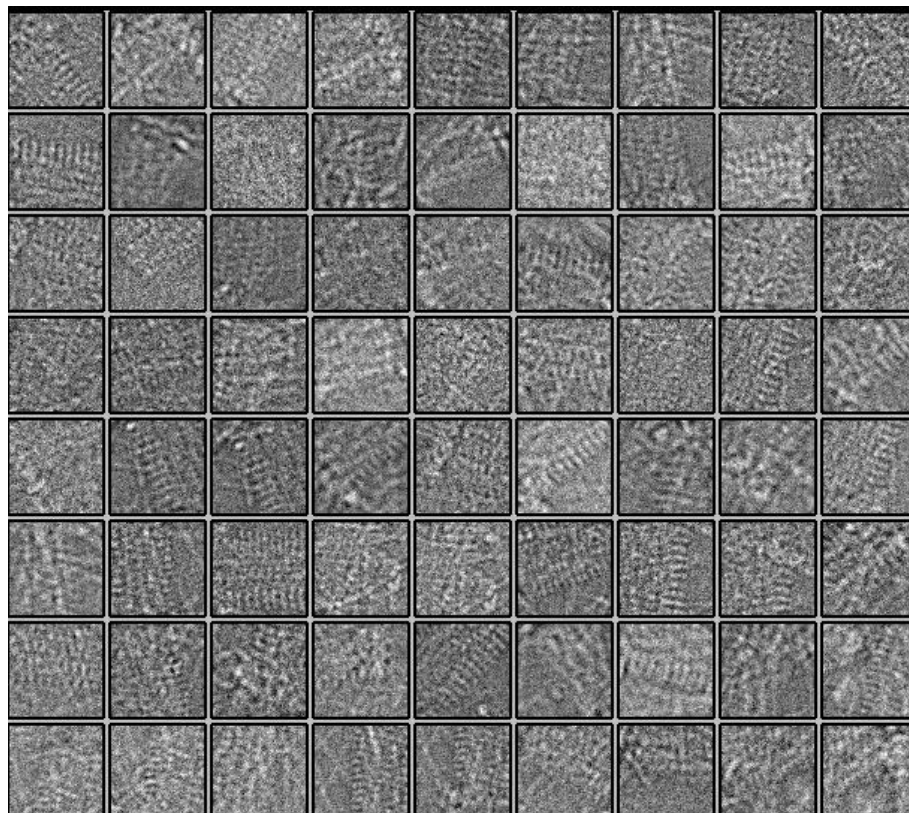


**Figure 7.8:** The tail particles of phage Sfk20.

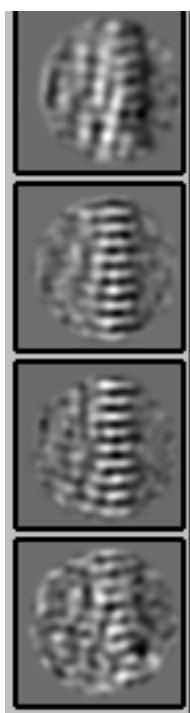


**Figure 7.9:** Few 2D class averages of the phage Sfk20 tail part, used for further reconstruction.

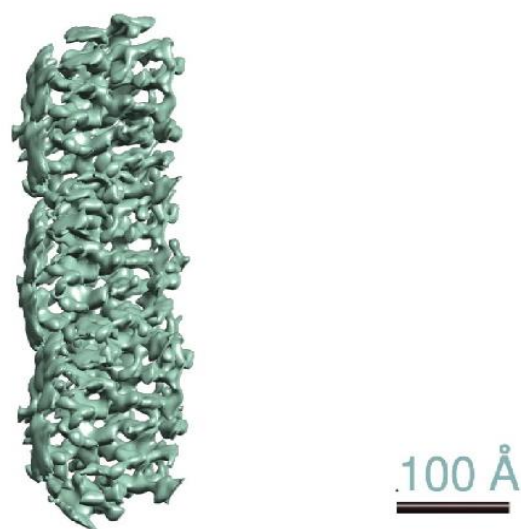


**Figure 7.10:** The density map of the phage Sfk20 tail. The helical tail sheath is quite prominent.

### 7.2.1.5 Three-dimensional reconstruction of the baseplate structure:

The *Myoviridae*-tailed bacteriophage Sfk20 belongs to the structurally complex virus groups. The baseplate, which is located at the end of the bacteriophage tail, is the component in charge of controlling the infectivity. Six similar wedges that encircle a central hub make up the baseplate. This small device of the phage is responsible for the recognition, adsorption, and infection in the host cell. The baseplate part of the phage Sfk20 was reconstructed using EMAN 2.9 software. The baseplate particles were picked from the micrograph containing intact phage particles. Next, the reference free class averaging was run without imposing any symmetry using “e2refine2d.py” to generate a set of class averages and the good class averages were sorted to make a subset with only good class averages. This particular process also helped to remove the bad particles from the data set. The images of the good class averages were shown in **Figure 7.11**. During the initial model reconstruction using “e2initialmodel.py” a 6-fold symmetry was applied. The projection images of the 3D initial model of the phage Sfk20 baseplate were shown in **Figure 7.12**. The final density map of the Sfk20 baseplate was shown in **Figure 7.13 (A)**. A needle-like structure was also found. It is mainly used by phage to puncture the host cell membrane during infection. The top view and the bottom views were shown in **Figure 7.13 (B)** and **(C)**. The largest part of this device was attached just behind the tail and became narrow at the end. The figure showed the attachment of the tail to the baseplate where the tail was marked in green colour and the baseplate was marked in blue colour as shown in **Figure 7.13 (D)**. Typically, the baseplate was depicted as a plate-like structure that organizes six protein subunits.

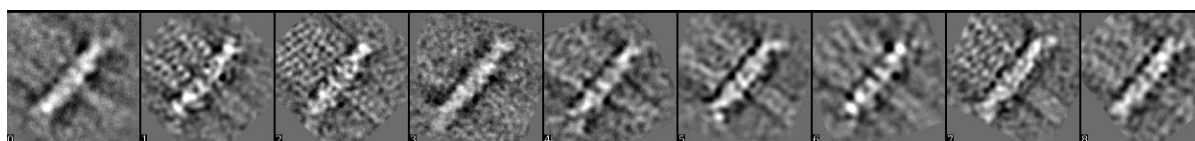


**Figure 7.11:** Good 2D class averages of the phage Sfk20 baseplate, used for further reconstruction purposes.

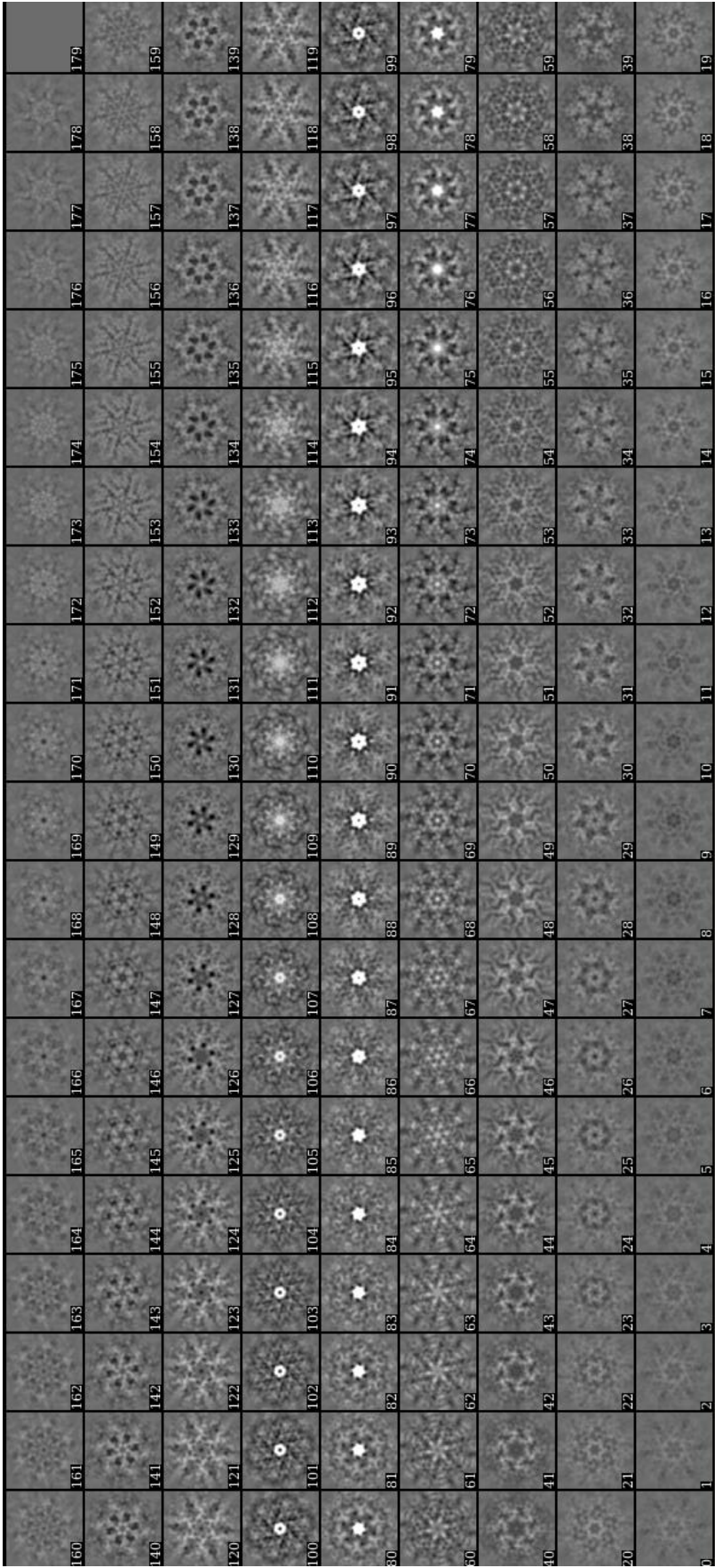


**Figure 7.12:** Projection images of the 3D initial model of the phage SfK20 baseplate.

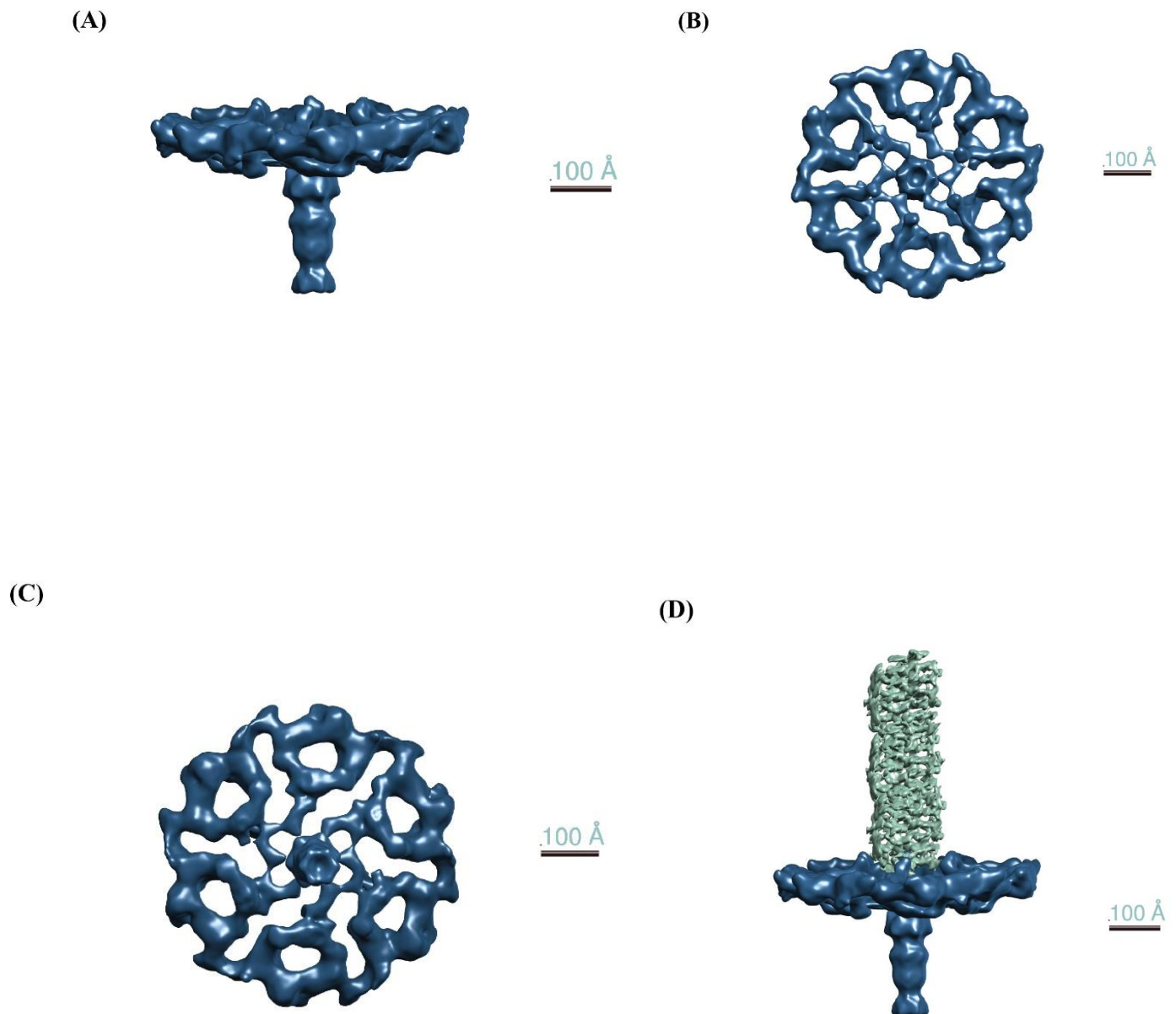


**Figure 7.13:** The density map of the baseplate of the Sfk20 bacteriophage: **(A)** the side view of the baseplate structure. The long piercing device was also visible, **(B)** the top view of the baseplate showed 6-fold symmetry, **(C)** The bottom view of the phage baseplate and **(D)** The baseplate (marked in blue) is attached to the tail part (in green).



### 7.2.2 Reconstruction of the intact phage Sfk20:

The different parts of the phage Sfk20 were reconstructed separately and later all four different parts were combined using UCSF Chimera. **Figure 7.14** showed an intact structure of *Myoviridae* phage Sfk20. The prolate-shaped head, a head-to-tail connector region, a long contractile tail, and a baseplate were quite clear from the 3D structure.

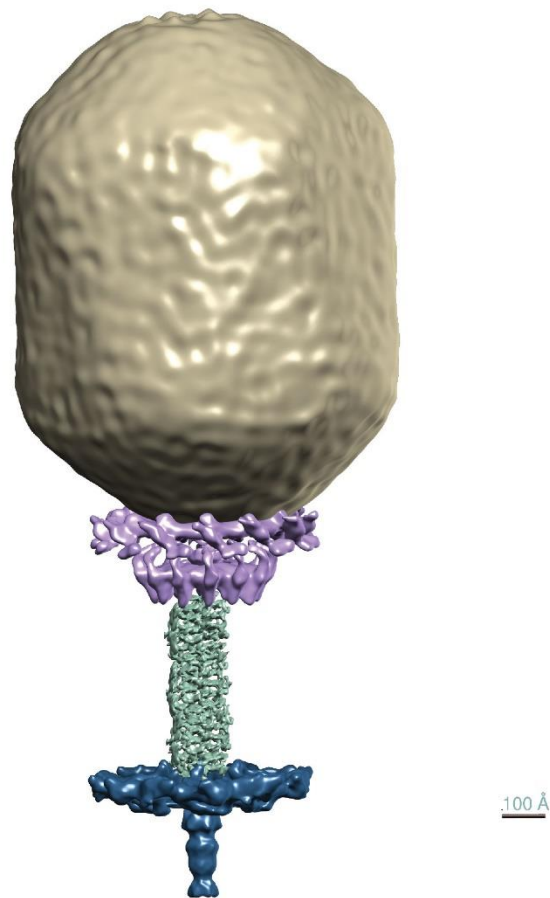


**Figure 7.14:** The three-dimensional reconstruction of intact phage Sfk20 structure with capsid, the portal vertex connector, tail, and baseplate complex.

### 7.3 DISCUSSION

The bacteriophages may have different shapes and sizes. But among all the phages, the tailed phages with double-stranded genomes are the most studied group of phages. The tailed phages have four major components: a capsid structure where the genome is densely packed, a head-to-tail connector or portal gatekeeper that helps to enter and exit of phage genome from the capsid, a tail part that acts as a channel during infection to eject the genome into the host cell and an adsorption apparatus at the periphery of the tail that helps to recognize the host cell and puncture it during the infection process.

The capsid of the tailed double-stranded DNA phages has a mismatch at one of its 5-fold vertex where the head-to-tail interface (HTI) is connected. One of the important components of the head-to-tail interface is the dodecameric portal protein. The portal protein represents the DNA packaging motor and acts as a nanomachine. The oligomeric head completion protein is also present in the HTI and also plays a dual role i) it makes an additional interface for ATP that produces energy during the packaging of the genome and ii) it also connects the portal proteins to the tail. Some HTIs also act as valves, closing the exit channel to stop the release of the DNA from the phage capsid and opening as soon as the phage attaches to the host cell. However, if the portal proteins are produced under naive conditions, without any other phage protein components, alternative symmetries other than dodecameric have been found for nearly all portal proteins *in vitro* (Cerritelli et al. 2003; Orlova et al. 1999).

The tail of the bacteriophage is one of the important parts of the infection. The tail of the *Myoviridae* and *Siphoviridae* phages is composed of a series of stacked rings. The adsorption apparatus is located on the distal end of the tail. It helps to recognize the receptor or the envelope chemistry of the host cell. Many tail fibers remain attached to the adhesion device or the baseplate helps to make a tight connection to the host cell. In *Podoviridae* phages, the baseplate part remains attached immediately to the HTI.

T4-like bacteriophage Sfk20 belongs to the family of *Myoviridae* as discussed in earlier chapters. The phages belonging to this group, inject their genome into the host cell using a highly efficient contractile injection machinery. The mechanism of DNA injection begins with the interaction of the host cell surface with the receptor-binding protein present at the tip of the long tail fiber (Prehm et al. 1976). The baseplate then goes through a significant conformational change, going from a high-energy dome structure to a low-energy star structure (Yap et al. 2016). The short tail fibers then rotate downward and irreversibly adhere to the cell surface.

The conformational change of the baseplate initiates the contraction of the tail sheath by releasing the tip of the tail tube. The sheath experiences a significant structural shift during contraction, going from a high-energy extended state to a low-energy contracted one (Kostyuchenko et al. 2005). During this time some changes occur in the tail sheaths. As a result, the tail tube and capsid both translate downward along the tail tube axis while concurrently rotating anticlockwise. When the sheath contracts, the tail assembly rotates and moves quickly, creating the motion necessary for the needle-like tip of the tail tube to enter the cell membrane.

In this work, the four major parts of phage Sfk20 such as head, portal protein, tail, and baseplate were reconstructed using single particle cryo-electron microscopy and image processing. The particles were picked from the intact images and processed using EMAN 2.9 and Relion 3.1 software. Phage Sfk20 is a T4-like *Myoviridae* phage that consists of a prolate-shaped head packaged with DNA by an ATP-dependent packaging machine. The head is prolate, meaning that it has two icosahedral ends and a cylindrical mid-section. Therefore, during reconstruction, C5 symmetry was applied. The phage neck is a knob-like structure that connects the head and tail. This protein is made up of various subunits, and controls the entry of genetic material by conformational changes which in turn contribute to phage tail assembly. During the reconstruction of the Sfk20 head-to-tail interface or the portal protein, the C12 symmetry was applied. From the reconstructed structure it was found that it is a ring-shaped dodecameric structure. The long contractile tail of the *Myoviridae* bacteriophage Sfk20 is responsible for the delivery of the genome to the host cell cytoplasm. The tail consists of the tail sheath that surrounds an inner tail tube. The tail sheath part is a helical object. Therefore, during the reconstruction of the tail part in Relion 3.1, helical symmetry was applied. The fact that a single projection image of a helical specimen will often contain all the data required to do a 3D reconstruction represents a significant advantage for helical objects versus asymmetrical particles in terms of structure determination. Additionally, helical reconstructions require significantly fewer parameters to be calculated than single-particle analyses, in theory. This is so that, unlike helical structures, where numerous copies of the repeating, asymmetrical unit have set relative orientations, single-particle analysis requires one to calculate the relative orientations for each individual particle projection image. Therefore, by averaging over a large number of asymmetrical units, one can effectively reduce the experimental noise once the parameters specifying helical symmetry and the orientation of the image of a helical object with respect to that symmetry have been established (He and Scheres 2017). The tail part remains attached to the baseplate. It is a dome-like structure assembled around a central hub.



The baseplate of the Sfk20 phage is a multi-protein molecular machine that controls host cell recognition, attachment, tail sheath contraction, and viral DNA injection. The Sfk20 baseplate was reconstructed using EMAN 2.9 software where C6 symmetry was applied. To our knowledge this is the first cryo-EM study of long tailed *Shigella* phage in India. Because of the frequently highly preserved structural and functional themes over extensive evolutionary time periods, the study of Sfk20 bacteriophage in general has provided essential biological and mechanistic insights.



# CHAPTER 8

## Objective 2(Part II)

**Prediction of phage Sfk20  
proteins using structure  
prediction-based approaches**



### 8.1 INTRODUCTION

Prediction of the structure of the protein or protein modeling is one of the most challenging topics of structural biology. To determine the structure of a protein, several laboratory-based methods such as X-ray crystallography, cryo-EM, spectroscopy, and NMR spectroscopy are available. The quality of the above-mentioned methods was continuously improved over the course of time. For example, the cryo-electron microscopy method is currently able to provide protein structure at atomic resolution (Callaway 2015). Although, a massive amount of experimental efforts has been given to solve structures of proteins still out of the billions of protein sequences only a limited number of protein structures have been solved to date. Hence, quick approaches and accurate computational machine learning-based methods of modeling are highly required to solve the structures of many unreported proteins. To establish such computational modeling methods, a set of sequences of unreported structures is released every two years interval in Critical Assessment of Structure Prediction or CASP competition and it allows the application of state-of-the-art algorithms to predict structures. This also helps to assess the advancement in modeling methods by comparing the predicted and reported structures.

At present there are two main approaches for the modeling of proteins: i) Homology modeling and ii) Neural network-based modeling (NNM) are prevailing. Homology modeling-based approaches use the homology detection algorithm to determine the three-dimensional structure of a protein. To generate a protein structure model, a homology modeling-based approach uses a known structure as a template. Different homology modeling software packages such as Modeller (Webb and Sali 2016), and Phyre2 (Kelley et al. 2015) are available to predict the structure of the protein when good templates are available. One of the major drawbacks of homology modeling is that the stability of the predicted models depends on the selected models. It fails to generate an accurate protein model when no known structure resembles a template. Web-based servers or homology modeling-based approaches were used routinely by computational biologists before the development of neural network-based approaches.

In 2021 DeepMind's machine learning-based structural algorithm was released and became a game changer in the field of structural biology. DeepMind-based machine learning was already used to generate protein models in the 13 CASP (CASP13 in 2018) (Jumper et al. 2021). But In CASP14 contest DeepMind structure prediction with AlphaFold2 produced a stunning result with astonishingly high prediction accuracy to evaluate the dataset and predict the protein

structure. It also indicates that the Deep learning-based techniques are now able to predict the structure accurately when compared to the experimental structure. This is one of the major achievements that opens a new path for structural biologists and non-structural biologists. In particular, AlphaFold2 uses Deep neural network modules designed for folding constraints, and the Neural network was instructed with self-supervised data from PDB. AlphaFold2 is able to predict three-dimensional structure from any of the given sequences of length not more than 1,400 amino acids. While neural network-based models are highly accurate to predict protein structure (Jumper et al. 2021), scientists are also trying to use large-scale language models for solving complex biological problems. Recently, Meta AI's researchers launched a line-up of advanced language models called Evolutionary Scale Modelling (ESM) for protein structure prediction. ESMFold is a protein structure prediction model which relies on these transformer models to understand and encode protein sequences (Lin et al. 2022).

We have discussed here the progress of different Deep learning-based algorithms and whether these algorithms are capable enough to predict the protein structure accurately. So here in our study, we tested the power of NN-based and homology modeling-based methods in predicting the high-confidence structure of phage structural proteins. As I have discussed earlier in CHAPTER 5 phage Sfk20 is a T4-like *Myoviridae* phage and its genome encoded various phage structural proteins. These structural proteins are important when phage morphogenesis takes place. There are several phage morphogenesis proteins involved in the formation of different parts of a bacteriophage when the progeny phage production takes place inside the host cell.

In this study, we tested the novel NN-based AlphaFold2 and ESMFold modeling methods to predict the phage structural proteins and thereafter the predicted structures were compared with the experimental structures collected from the PDB. We also used the TM-score and Root mean square deviation (RMSD) metric to estimate the accuracy of the prediction. We further compared the modeling with NN-based methods to the commonly used homology modeling-based method: Phyre2. We also examined this study on several structural proteins to determine which modeling method is capable of producing superior results.

### 8.2 RESULTS

#### 8.2.1 Comparison of the performance of the AlphaFold2, ESMFold, and Phyre2 for prediction of the phage protein structure:

In this work, the result of two NN-based methods: AlphaFold2 and ESMFold, and one widely used homology modeling-based method: phyre2 were used to predict the structure of different structural proteins of phage Sfk20 that were selected from the LC-MS/MS data. At first, the structures of proteins were predicted using AlphaFold2, ESMFold, and Phyre2. After the prediction of the structure top-scored RMSD (Root mean square deviation) value models were collected from PDB followed by the alignment of those experimental models with the predicted model using the UCSF Chimera Matchmaker tool (Pettersen et al. 2004). The TM-score of each of the predicted models was also calculated and plotted in the TM-score comparison graph for each of the predicted models. An average TM-score model was also plotted to determine the best method to predict Sfk20 phage proteins. Six structurally relevant proteins used in this study are described below.

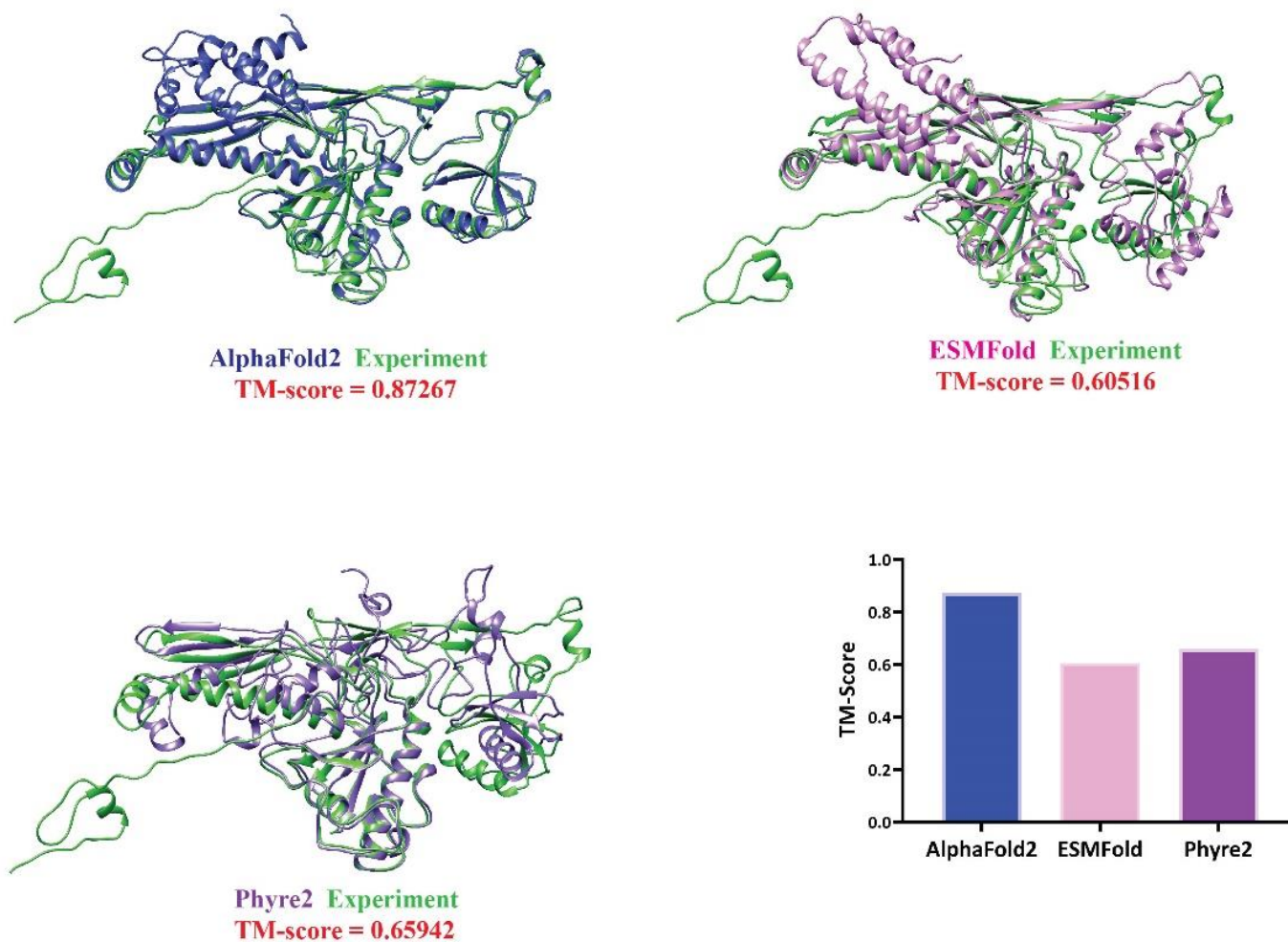
##### 8.2.1.1 Major capsid protein (ORF-207):

The capsid of the phage is a highly organized proteinaceous structure in which the genome remains packed (Carmody, Goddard, and Nugen 2021). The protein shell of the viral capsid is a stable and dynamic structure. The capsid structure withstands the high pressure of genomic material, protects the genomic material inside it during the transfer to the host and it also releases the genome once a susceptible host has been obtained (Conway et al. 2001). The phage Sfk20 is a T4-like *Myoviridae Shigella* bacteriophage composed of a large elongated (prolate) icosahedral head and a long contractile tail. The elongated icosahedron capsid is made up of three essential proteins: gp23 (it forms a hexagonal capsid lattice), minor capsid protein gp24 (forms 11 pentameric vertices), and gp20 (dodecameric portal vertex). The major capsid proteins played a vital role in genome packaging (Xue and Black 1990). In this study, a major capsid protein (ORF-207) was identified and its structure was predicted using AlphaFold2, ESMFold, and Phyre2. Top scored RMSD value experimental model 5VF3 was collected from the PDB. All predicted models were aligned with the experimental model: F-chain of 5VF3 (Chen et al., 2017). It was also observed that the AlphaFold2 model is nearly identical to the experimental model (**Figure 8.1**). The TM-score value of all the predicted models was also calculated and plotted. The TM-score plotted graph suggested that the AlphaFold2 predicted better than the ESMFold and Phyre2.

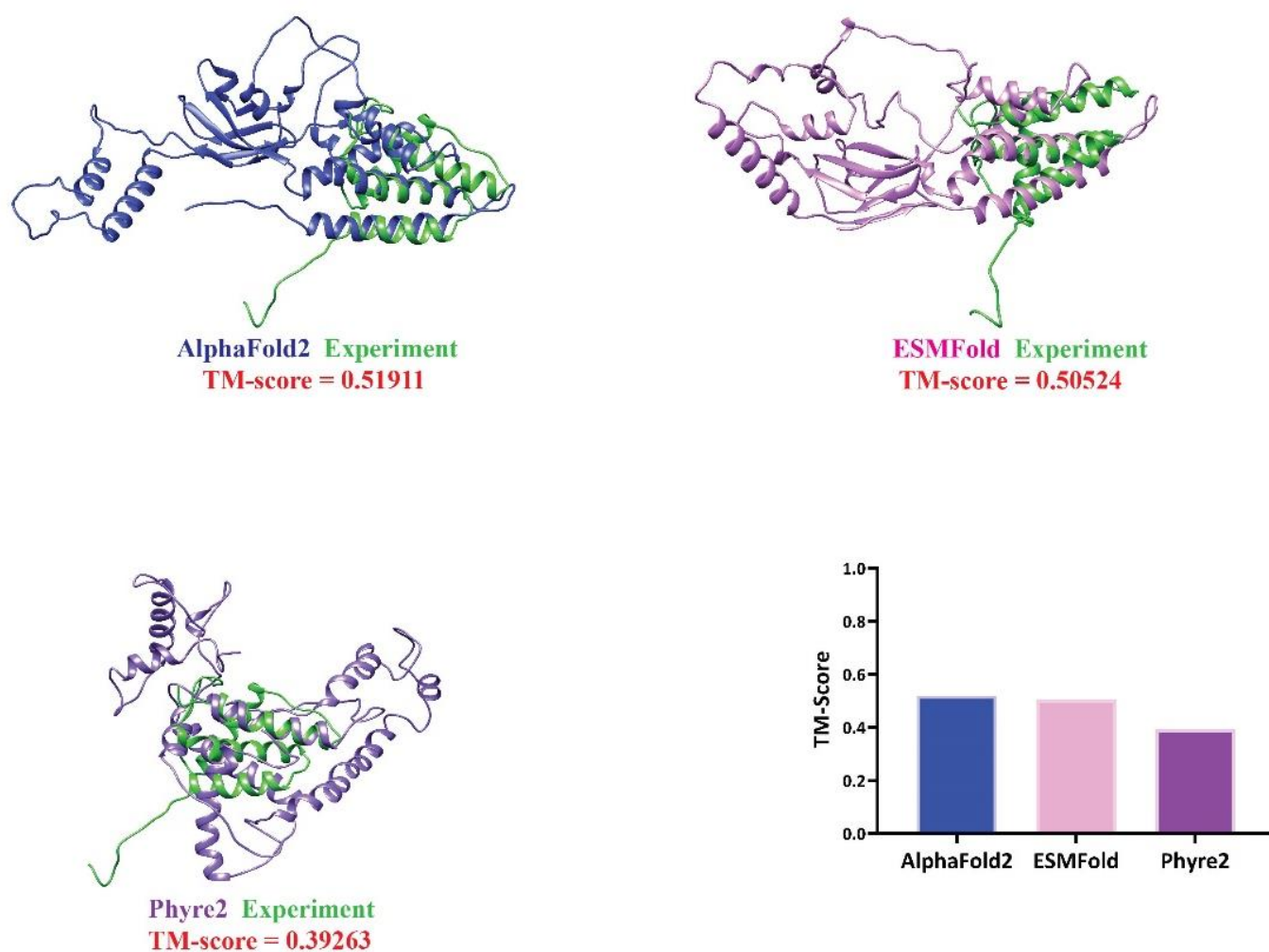
### 8.2.1.2. Neck protein (ORF-195):

In tailed bacteriophage near the head-to-tail interface, there is a knob-like structure assembled at the capsid portal vertex prior to attachment of the tail known as the neck or connector (Orlova et al. 2003). This protein is made up of different subunits and it controls the entry of genetic material by conformational changes which in turn contributes to phage tail assembly during morphogenesis. Double-stranded DNA is translocated through this portal protein channel (Newcomb et al. 2001; Valpuesta and Carrascosa 1994). After the translocation, DNA packaging is terminated. Upon termination, one end of the genome remains bound to the portal vertex (Tavares et al. 1996). DNA is packed inside the capsid in a dense arrangement that could exert pressure within the capsid shell (Earnshaw and Casjens 1980). This high internal pressure may cause the ejection of the DNA outside (Earnshaw and Casjens 1980; Tavares et al. 1996). After the encapsidation, the portal channel has to be closed to avoid the leakage of the genome. This thing can be achieved either by the conformational change of the portal protein (Hagen et al. 1976) or the binding of the head completion protein that plugs the portal pore to form a connector structure (Coombs and Eiserling 1977). In this study, a neck protein was identified in the proteomic analysis, and its structure was predicted using the above-mentioned programs. Thereafter the predicted models were aligned with the experimental model: A-chain of 5VGT (Liang et al. 2017) and the alignment result showed a structural similarity of 5VGT (tail adaptor protein, gp7 of a *Podoviridae* phage Sf6) and the predicted models (**Figure 8.2**). It was also observed that the calculated TM-score was lower for Phyre2 than the other two methods. This further concluded that AlphaFold2 and ESMFold have predicted better than Phyre2.

## Major capsid protein (ORF-207)



**Figure 8.1:** The structure of major capsid protein (ORF-207) was predicted using AlphaFold2, ESMFold, and Phyre2 and aligned with the experimental structure. Alignment result of AlphaFold2, ESMFold, Phyre2, and the experimental structure: 5VF3 was shown (Chen et al., 2017). A TM-score comparison graph of major capsid protein was shown. The experimentally solved models are shown in green; the modeling result of AlphaFold2, ESMFold, and Phyre2 are shown in blue pink, and purple respectively.

**Putative neck protein (ORF-195)**

**Figure 8.2:** The structure of putative neck protein (ORF-195) was predicted using AlphaFold2, ESMFold, and Phyre2 and aligned with the experimental structure. Alignment result of AlphaFold2, ESMFold, Phyre2, and the experimental structure: 5VGT (Liang et al. 2017) was shown. A TM-score comparison graph of neck protein was shown. The experimentally solved models are shown in green; the modeling result of AlphaFold2, ESMFold, and Phyre2 are shown in blue, pink, and purple respectively.

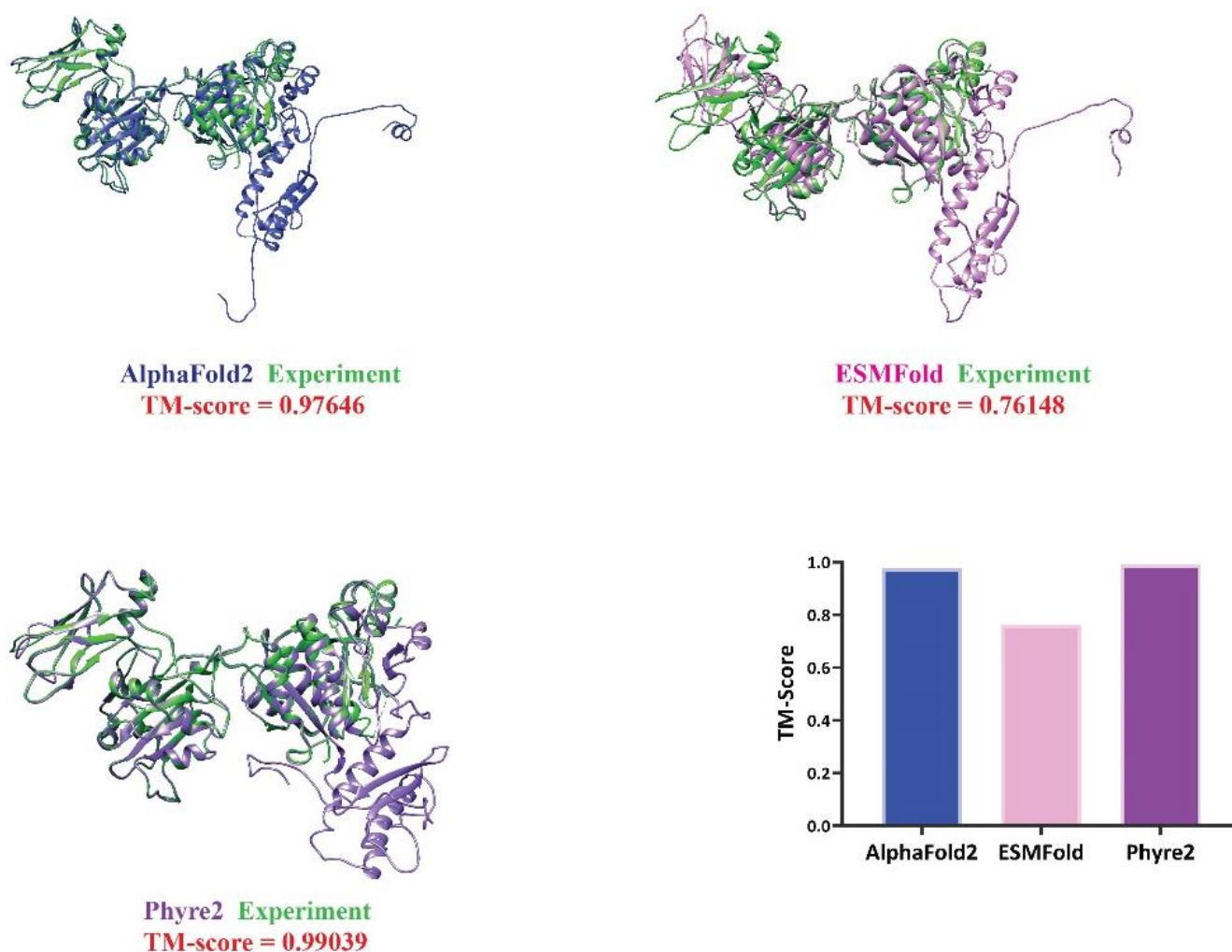


### 8.2.1.3 Tail proteins (ORF-200 and ORF-201):

For T4-like bacteriophages and others, one phage particle is enough to infect a single host bacterium (E. 1994b). The infection occurs through a specialized component known as the tail. The tail is present in 96% of bacteriophages. It is designed to attach to host bacteria, penetrate the cell wall of the bacteria, and transfer the phage genome inside the cell. There are three different groups of tailed bacteriophages- *Myoviridae* (long, contractile tail), *Siphoviridae* (long, noncontractile tail), and *Podoviridae* (short, non-contractile tail). Bacteriophage Sfk20 is a T4-like phage that belongs to the family of *Myoviridae*. The contractile tail of the T4 like *Myoviridae* bacteriophage acts as a sophisticated nanomachine that mediates a very high viral infection efficiency. *Myoviridae* phages have the most complex tail structure. The contractile tail of the *Myoviridae* phage consists of the contractile sheath (contracts during the infection) and non-contractile tube. The tail sheath consists of 138 copies of the tail sheath protein subunit(gp18) Leiman et al. 2004) surrounding the central tail tube which consists of the gp19 subunit (Moody and Makowski 1981). In our work, a tail sheath protein and a tail tube protein were selected and their structure was predicted using the three above-mentioned approaches.

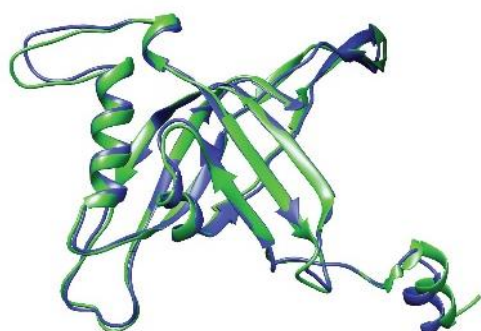
The predicted structure of tail sheath protein was aligned with the experimental structure: C-chain of 3FOA (Aksyuk, Leiman, Kurochkina, et al. 2009). A large structural similarity was found between the predicted structure and 3FOA-C as shown in **Figure 8.3**. The calculated TM-score also revealed that AlphaFold2 and Phyre2 predict more accurately than the ESMFold.

The predicted tail tube model was aligned with the experimental model: A chain of 5W5F (Zheng et al. 2017) (gp19 protein of phage T4) and a huge similarity between the predicted models and the experimental model was found in all three cases as shown in **Figure 8.4**. The calculated TM-scores also revealed that all three protein modeling approaches performed equally well to predict tail tube protein structure.

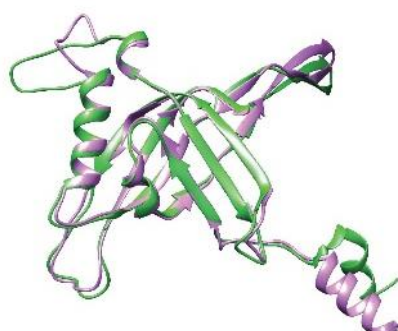
**Tail sheath protein (ORF-200)**

**Figure 8.3:** The structure of tail sheath protein (ORF-200) was predicted using AlphaFold2, ESMFold, and Phyre2 and aligned with the experimental structure. Alignment result of AlphaFold2, ESMFold, Phyre2, and the experimental structure: 3FOA (Aksyuk, Leiman, Kurochkina, et al. 2009) was shown. A TM-score comparison graph of tail sheath protein was shown. The experimentally solved models are shown in green; the modeling result of AlphaFold2, ESMFold, and Phyre2 are shown in blue pink, and purple respectively.

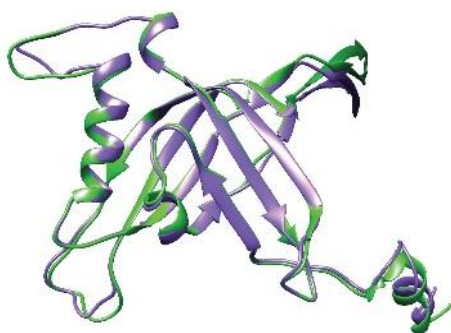
## Tail tube protein (ORF-201)



AlphaFold2 Experiment  
TM-score = 0.9473



ESMFold Experiment  
TM-score = 0.84965



Phyre2 Experiment  
TM-score = 0.95181

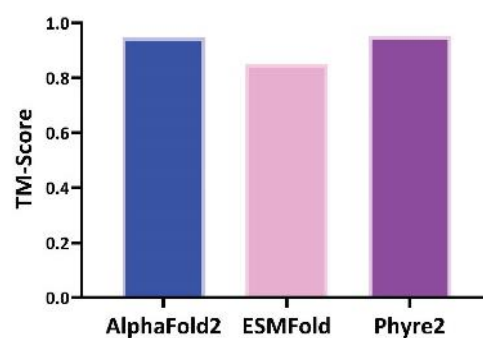


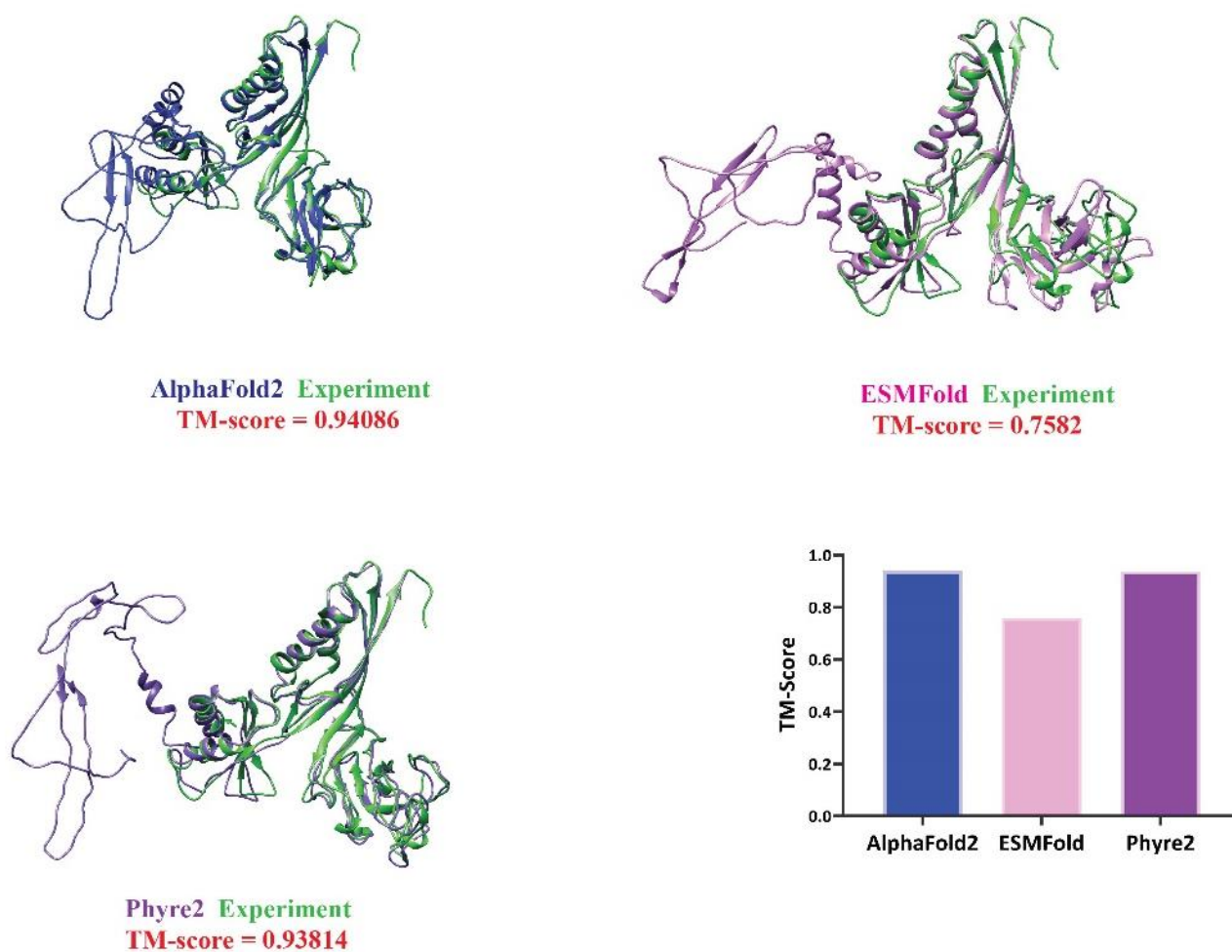
**Figure 8.4:** The structure of tail tube protein (ORF-201) was predicted using AlphaFold2, ESMFold, and Phyre2 and aligned with the experimental structure. Alignment result of AlphaFold2, ESMFold, Phyre2, and the experimental structure: 5W5F (Zheng et al. 2017) was shown. A TM-score comparison graph of tail tube protein was shown. The experimentally solved models are shown in green; the modeling result of AlphaFold2, ESMFold, and Phyre2 are shown in blue pink, and purple respectively.

### 8.2.1.4 Baseplate wedge proteins (ORF-188 and ORF-191):

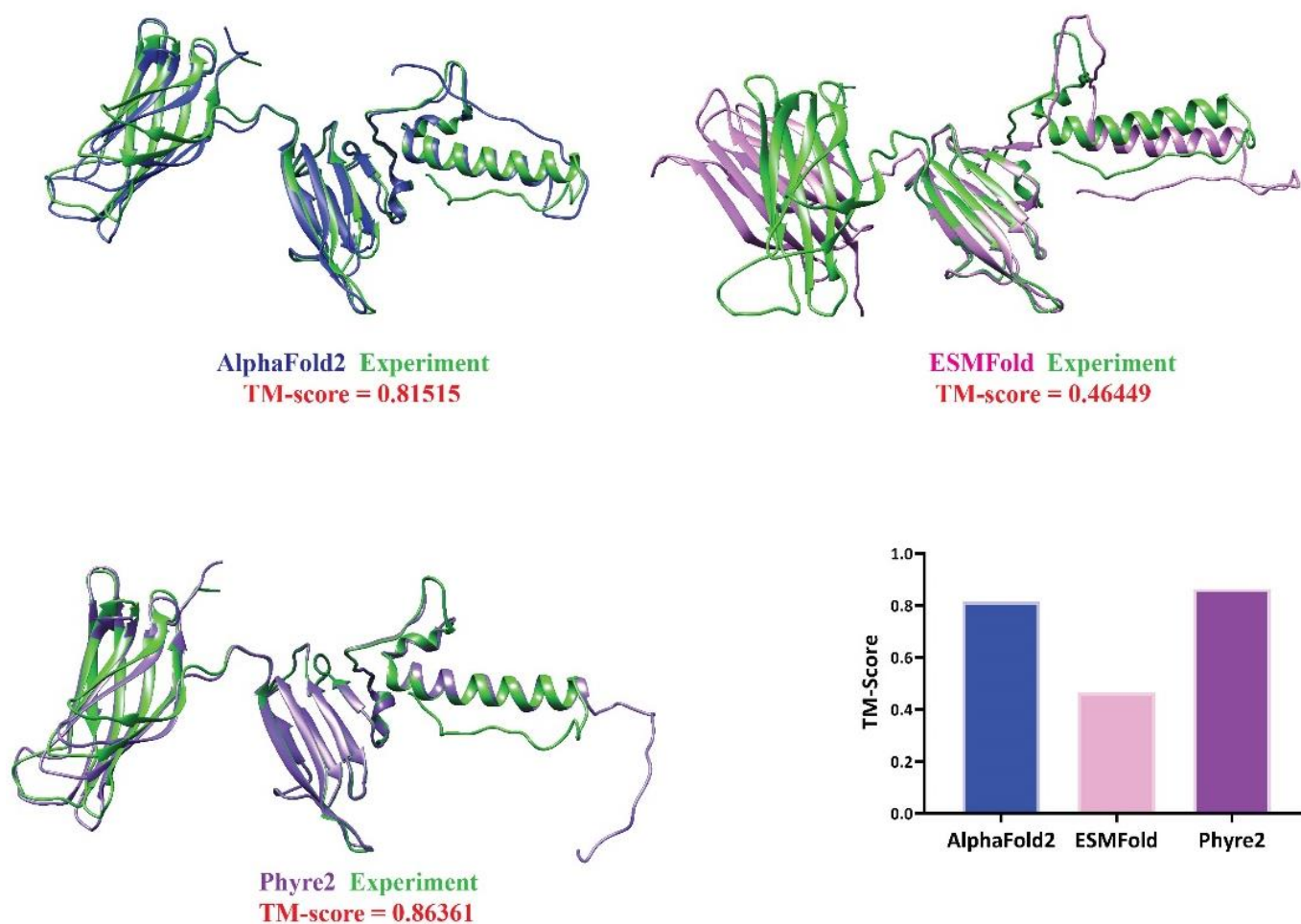
The baseplate of a T4-like bacteriophage is a multiprotein molecular complex that controls the attachment of phage to the host. It is the assembly of six wedges and a central hub. During infection, the long tail fiber attached to the cell surface and the baseplate change its conformation from a dome-shaped structure to a star-shaped structure leading to the contraction of the tail sheath which pushes the tail tube to create a passage for genome entry through the cell membrane (Aksyuk, Leiman, Shneider, et al. 2009). In this work, two baseplate protein: baseplate wedge protein and baseplate wedge completion tail fiber socket were identified and selected. Their structure was predicted using two neural network base software: AlphaFold2 and ESMFold and one homology modeling software: Phyre2.

The predicted model of baseplate wedge protein compared with the H chain of experimental model 3H3Y (Aksyuk, Leiman, Shneider, et al. 2009) (gp6 of phage T4) and TM-scores were calculated. The TM-score was very high for the model created by AlphaFold2 and Phyre2. The AlphaFold2 and Phyre2 predicted models were near to the experimental models whereas the ESMFold predicted model was slightly deviated as shown in **Figure 8.5**. Here, in this case, the AlphaFold2 and Phyre2 predicted better than ESMFold.

Next, the predicted structures of the baseplate wedge completion tail fiber socket were aligned with the R chain of experimental model 1ZKU (Kostyuchenko et al. 2005) (gp9 of phage T4), and the TM-score was calculated. It was found that the TM-scores of Phyre2 and AlphaFold2 predicted model was quite higher than the ESMFold as shown in **Figure 8.6**. The alignment results suggested that the AlphaFold2 and Phyre2 predicted better than ESMFold.

**Baseplate wedge protein (ORF-188)**

**Figure 8.5:** The structure of baseplate wedge protein (ORF-188) was predicted using AlphaFold2, ESMFold, and Phyre2 and aligned with the experimental structure. Alignment result of AlphaFold2, ESMFold, Phyre2, and the experimental structure: 3H3Y (Aksyuk, Leiman, Shneider, et al. 2009) was shown. A TM-score comparison graph of baseplate wedge protein was shown. The experimentally solved models are shown in green; the modeling result of AlphaFold2, ESMFold, and Phyre2 are shown in blue pink, and purple respectively.

**Baseplate wedge completion  
tail fiber socket (ORF-191)**

**Figure 8.6:** The structure of the baseplate wedge completion tail fiber socket (ORF-191) was predicted using AlphaFold2, ESMFold, and Phyre2 and aligned with the experimental structure. Alignment result of AlphaFold2, ESMFold, Phyre2, and the experimental structure: 1ZKU (Kostyuchenko et al. 2005) was shown. A TM-score comparison graph of baseplate wedge completion tail fiber socket was shown. The experimentally solved models are shown in green; the modeling result of AlphaFold2, ESMFold, and Phyre2 are shown in blue pink, and purple respectively.

**Table 8.1:** TM-score of all the predicted models

ORF No.	Protein name	Experimental model (PDB-ID)	AlphaFold2 TM-score	ESMFold TM-score	Phyre2 TM-score
207	Major capsid protein	5VF3-F	0.87267	0.60516	0.65942
195	Putative neck protein	5VGT-A	0.51911	0.50524	0.39263
200	Tail sheath protein	3FOA-C	0.97646	0.76148	0.99039
201	Tail tube protein	5W5F-A	0.9473	0.84965	0.95181
188	Baseplate wedge protein	3H3Y-H	0.94086	0.7582	0.93814
191	Baseplate wedge completion tail fiber socket	1ZKU-R	0.81515	0.46449	0.86361

## 8.2.2. TM-score and RMSD values:

The TM-score of each predicted model was calculated and plotted as mentioned earlier. An average TM-score graph was also plotted as shown in **Figure 8.7**. The TM-score of each predicted model is listed in **Table 8.1**. The root mean square deviation (RMSD) value of all the predicted models using AlphaFold2, Phyre2, and ESMFold was calculated. It was observed that the median RMSD values of AlphaFold2 and Phyre2 predicted models were lower than that of ESMFold models. The highest RMSD value (4.68 Å) observed in the case of ESMFold predicted major capsid protein (ORF-207) and the lowest (0.89 Å) in the case of Phyre2 predicted tail sheath protein (ORF-200). The distribution pattern of RMSD values showed that AlphaFold2 and Phyre2 predicted models have lower RMSD values than those of ESMFold models as shown in **Figure 8.8**. This suggested that AlphaFold2 and Phyre2 performed better than ESMFold for the structure prediction of phage Sfk20 proteins. This graph also suggested that AlphaFold2 and Phyre2 predicted structure showed greater similarity with experimental structure than ESMFold. The RMSD values of each predicted model were listed in **Table 8.2**.

The confidence with which AlphaFold2 and ESMFold predicted the individual amino acid residues (pLDDT-score) of the phage proteins were shown in **Table 8.3**.



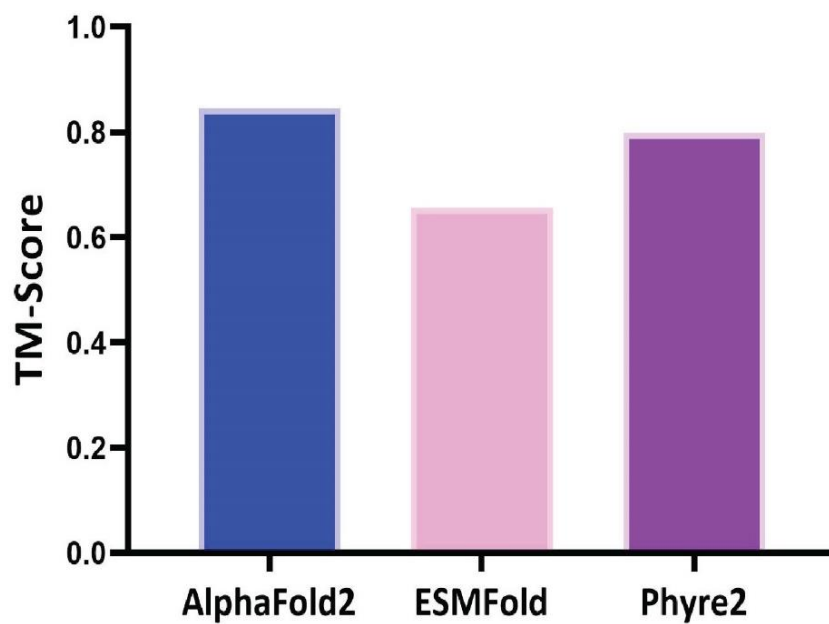


**Figure 8.7:** An average TM-score graph for all models predicted using AlphaFold2, ESMFold, and Phyre2.

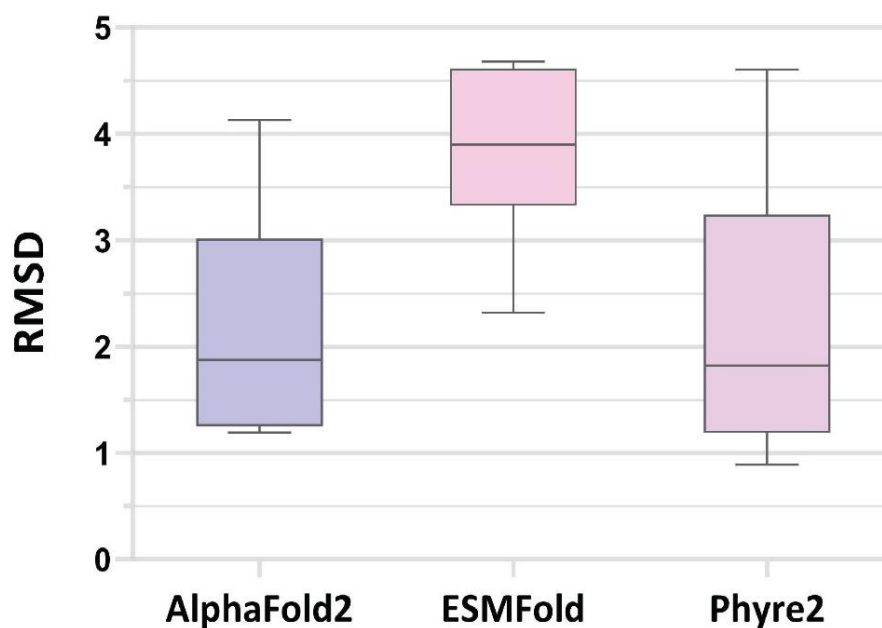


**Figure 8.8:** Box plots of RMSD values of AlphaFold2, ESMFold, and Phyre2 are shown from left to right, respectively.

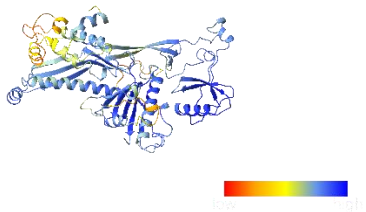
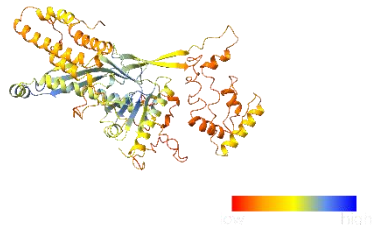
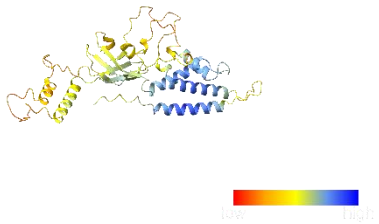
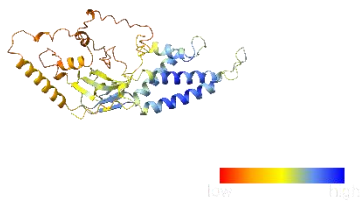


## CHAPTER 8

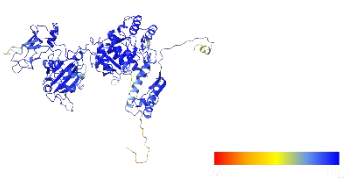
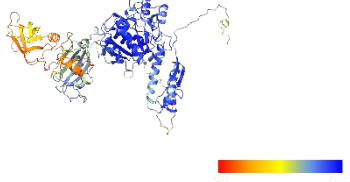
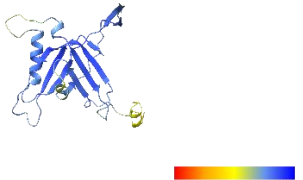
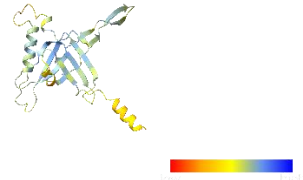
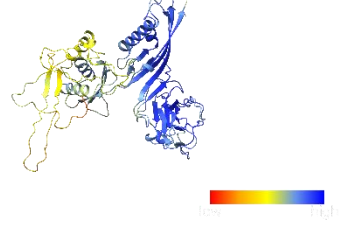
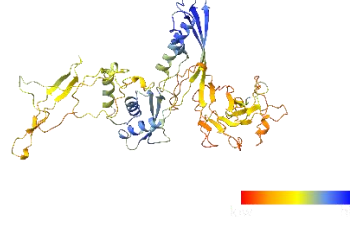
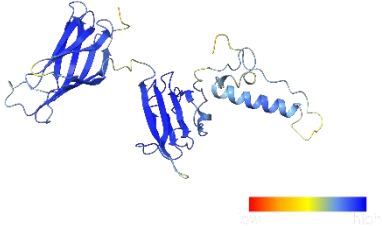
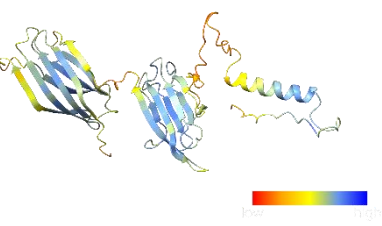
**Table 8.2:** RMSD values of all the predicted models.

ORF No.	Protein name	AlphaFold2 (RMSD value)	ESMFold (RMSD value)	Phyre2 (RMSD value)
207	Major capsid protein	2.13	4.68	4.6
195	Putative neck protein	4.13	4.59	2.79
200	Tail sheath protein	1.27	4.13	0.89
201	Tail tube protein	1.19	2.32	1.29
188	Baseplate wedge protein	1.62	3.66	1.58
191	Baseplate wedge completion tail fiber socket	2.64	3.67	2.06

**Table 8.3:** pLDDT score-based coloring of AlphaFold2 and ESMFold predicted models.

Protein Name	AlphaFold2	ESMFold
Major capsid protein (ORF-207)		
Putative neck protein (ORF-195)		

## CHAPTER 8

Tail sheath protein (ORF-200)		
Tail tube protein (ORF-201)		
Baseplate wedge protein (ORF-188)		
Baseplate wedge completion tail fiber socket (ORF191)		



AlphaFold pLDDT confidence measure



ESMFold pLDDT confidence measure

### 8.3 DISCUSSION

Over the past few decades, various techniques in the structural biology field (X-ray crystallography, nuclear magnetic resonance, and cryo-electron microscopy) were developed. Almost a decade ago the “resolution revolution” in cryo-EM has been started with the help of major technological advances that dramatically advanced the field of structural biology (Kühlbrandt 2014). Over time the improvement of these techniques helped us to understand the important biological processes in molecular level detail. The success rate of all these techniques depends on access to equipment/facility, the nature of the sample, and expertise. These techniques are also time-consuming and expensive. Therefore, nowadays the development of machine learning structure prediction algorithms such as AlphaFold and ESMFold are alternative and faster approaches that are now being used by the scientific community to get an initial idea about the structure of different proteins. Just from a single genome sequence, the structures can easily be predicted using these algorithms (Goulet and Cambillau 2022). AlphaFold and ESMFold notebooks are quite suitable and easy to use thereby accelerating the scope of the research. Not only experienced structural biologists but also non-experts can now be able to estimate the structure of their protein of interest within a few hours. In 2021, AlphaFold2, a deep learning-based protein structure prediction program was released by Google DeepMind and it can predict a protein structure with an accuracy comparable, in most cases, to that of experimental structures (Senior et al. 2020). AlphaFold2 produces a three-dimensional(3D) structure of a protein from the amino acid sequence by taking advantage of evolutionary information from a multiple-sequence alignment of homologs (Zhang and Skolnick 2004). Homology modeling-based software such as Phyre2 has also been used to predict the structures. Recently, Neural network-based and homology-based programs can accurately predict 3D protein structure from the amino acid sequences of novel phage proteins. The striking accuracy and high speed of these structure prediction programs have revolutionized the field of structure-based approaches to study newly isolated phages as exemplified by the human gut phageome (Shkoporov et al. 2019).

In this study six structurally relevant phage Sfk20 proteins such as major capsid protein (ORF-207), neck protein (ORF-195), two tail proteins (tail sheath protein, ORF-200, and tail tube proteins, ORF-201), two baseplate proteins (baseplate wedge protein ORF-188 and baseplate wedge completion tail fiber socket, ORF-191) were selected and their structures were predicted using two novel neural network-based methods: AlphFold2 and ESMFold and one homology

modeling based method: Phyre2. There are two major limitations of the phyre2 over the machine learning-based approaches. First, if homology cannot be detected between a user-provided sequence and a sequence of the known template, then modeling will either be impossible or extremely unreliable. The second limitation is that all these widely used homology modeling-based methods are unable to determine the structural effects of point mutations.

The predicted structures were compared with the experimental structures derived from PDB. The work analysis was performed based on the TM-score metric (Jumper et al. 2021) and the RMSD metric. This study provides an overview of the performance of the two NN-based and homology modeling-based methods for phage structural proteins by showing the accuracy of AlphaFold2, ESMFold, and Phyre2 according to the average TM-score and RMSD value. When comparing the performance of two NN-based methods for the structure predictions it was found that AlphaFold2 predicted better than ESMFold. The individual TM-scores and RMSD values for each of the AlphaFold2 predicted models are quite higher than the ESMFold. The pLDDT (predicted Local Distance Difference Test) values of both NN- based models were also calculated. pLDDT values determined the confidence scores of the predicted models. pLDDT values greater than 90% indicate an accuracy in the position of the amino acid side chain comparable to that given by experimental crystal structures whereas the pLDDT values lower than 50% indicate a random position (Tunyasuvunakool et al. 2021). It further suggested that in case of Sfk20 protein structure predictions, AlphaFold2 was capable of predicting the models more confidently (the predicted structure contains more blue regions) than ESMFold (most of the predicted models belong to orange regions). While comparing the two NN-based methods with homology modeling-based methods it was found that AlphaFold2 and Phyre2 predicted models showed high similarity with the experimental models.



# CHAPTER 9

## Objective 3

*In vitro* phage-host interaction study  
by electron microscopy



### 9.1 INTRODUCTION

Understanding potential interactions between phages and their hosts is crucial to comprehend the functions of phages in nature. Phages can go through various life cycles, which determine their function in bacterial and archeal systems and how they interact with their physical environment. Based on their life cycles, phages are classified into lytic, lysogenic, and chronic. Virulent phages always follow the lytic cycle to infect the host bacteria. To initiate the infection process, the phage typically attaches to the surface via specific host cell surface receptors. After that through a cascade of conformational changes in various parts of the tail, phage particles inject their genetic material into the cytoplasm of the bacterial cell. The first step of phage infection is the precise identification of a receptor on the surface of the host cell by the RBPs (receptor binding proteins) of the phage located at the tip of the tail (Bertozzi Silva, Storms, and Sauvageau 2016; Letarov and Kulikov 2017). The successful identification of the cell surface receptor leads to the permanent adhesion of bacteriophage followed by a conduit formation that allows the injection of genetic material into the cell cytoplasm. Phage-encoded enzymes such as virion-associated peptidoglycan lysozyme are located in the tip of the phage tail and are responsible for the penetration of the genetic material. After entering the genome into the host cell, the lytic cycle gets activated for the lytic phages. Once the phage genome enters the host cell it hijacks the host replication machinery for rapid replication of the phage genome inside the host cell. The host cell supplies the molecular components and enzymes necessary for the reproduction of the phage genetic material. Thereafter the progeny phage particles are assembled, loaded with the genetic material, lysed the host cell membrane, and released into the surrounding environment. Endolysin and holin, two phage-encoded proteins, lyse the host cell from within. Small proteins called holins build up in the cytoplasmic membrane of the host, enabling endolysin to break down peptidoglycan and release the progeny phage to infect and eliminate nearby host bacteria in their surroundings. A benefit of using lytic phage in therapy is their ability to produce a large number of progenies. Lytic phages, however, only infect specific bacteria that have the specific receptor for the phages in their outer membrane. Therefore, phages have limited host ranges.

In the case of lysogenic phages, the phage genome is integrated into the host cell genome and remains as a prophage for a long time. This integrated phage DNA replicated normally with the host genome and these phage genome-carrying cells are divided during the cell division. The drawback of utilizing temperate phage in phage therapy is that some members of the phage

population can insert their genome into the chromosome of the host and either lay dormant or change the phenotype of the host. Unless the bacteria are exposed to stress or unfavourable environmental conditions, the lysogenic cycle can go on indefinitely. Although different bacteriophages respond to different induction signals, prophages are frequently produced when bacterial SOS responses are activated as a result of antibiotic treatment, oxidative stress, or DNA damage (Penadés et al. 2015). After the lysogenic cycle is finished, phage DNA expression follows, and the lytic cycle begins.

A third life cycle or a chronic life cycle is also seen in some archaeal viruses, filamentous and lysogenic phages. In this case, the newly formed phage virions are continuously released from the host cells without disrupting the cell (Munson-Mcgee, Snyder, and Young 2018) .

In this chapter phage host interaction study between phage Sfk20 and *Shigella flexneri 2a* bacteria and the lytic lifecycle of phage Sfk20 has been discussed. The early exponential phase culture of host bacteria was treated with phage Sfk20 at different time points and examined using transmission electron microscopy and scanning electron microscopy.

### 9.2. RESULTS

#### 9.2.1 The study of phage Sfk20 life cycle by transmission electron microscopy:

##### 9.2.1.1 Control bacteria cell:

The control experiment was performed without infecting with phage Sfk20 to visualize and examine the healthy bacteria. In brief, an exponential phase culture of *Shigella flexneri 2a* bacteria was fixed and the sample was then prepared for thin sectioning. The thin sections of the samples were examined under the transmission electron microscope. **Figure 9.1** showed the thin section of healthy bacteria with a prominent double-layered membrane. The internal materials are also intact.

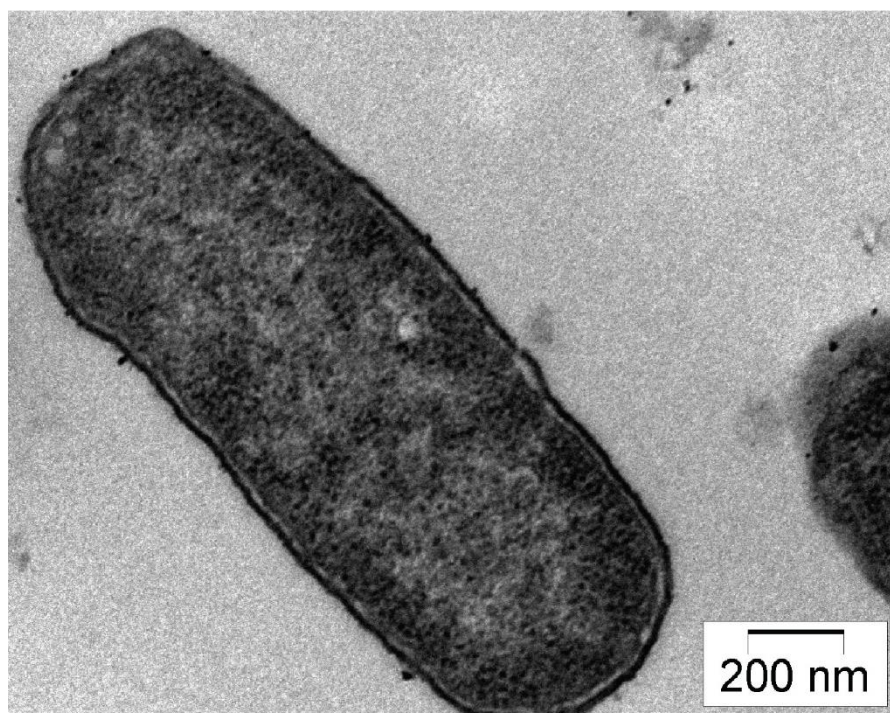


**Figure 9.1:** Thin section electron micrograph of control *Shigella flexneri 2a* bacteria without infecting with phage.



### 9.2.1.2 Phage attachment to the host cell:

Bacteriophage Sfk20 consists of a prolate head and a long contractile tail with a knob-like baseplate at the end. Upon infection, the phage attached to the host bacterial cell and injects its genomic material inside the cytoplasm. The host macromolecule synthesis also shuts off.

The early exponential phase culture of *Shigella flexneri 2a* was infected with Sfk20 bacteriophage for 15 minutes as described in the materials and methods section and samples were then fixed and prepared for the thin section microscopy. The thin section of the infected bacteria was visualized under a transmission electron microscope (FEI Tecnai 12 BioTwin). **Figure 9.2** showed the thin section of the infected bacterial cells. Within the first 15 minutes of infection, the phage particle is attached to the bacterial cell surface and the host nucleus started degrading and the cytoplasm looked like a homogeneous mass. Upon infection, the phage attached to the host bacterial cell and injects its genomic material inside the cytoplasm. The phage injects its genome inside the host cell and the empty phage heads are attached to the outer membrane of the host cell at the time of infection. The double-layered cell membrane and the intact internal materials are also seen in the image.

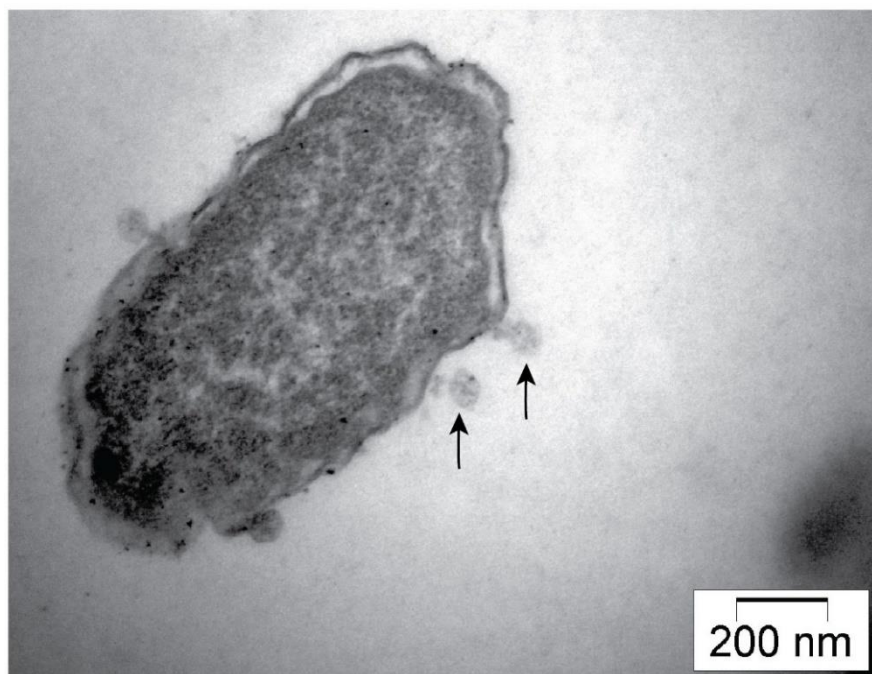


**Figure 9.2:** TEM images of the ultrathin section of *Shigella flexneri 2a* infected with isolated host-specific phage Sfk20 at a 15 minutes time point. Bacteriophage attachment was visible (black arrow indicates phage particles).

### 9.2.1.3 Intracellular development and loss of the internal material of phage Sfk20:

After the attachment of the phage particle to the bacterial cell it injects its genomic material inside the cell cytoplasm. Sfk20 DNA synthesis occurs inside the cell using host replication machinery. After the synthesis of the genomic material, the packaging of the DNA and the assembly of the phage begun. At the 30 minutes time point, the phage-infected bacterial cells were fixed and processed for thin sectioning. The processed sample was visualized under the transmission electron microscope. At this time duration, the infected cells were occupied by the DNA fibrils as phage DNA synthesis occurs at this point of time. DNA packaging and assembly were also started at this time point. The intracellular development of the phage heads was also found in **Figure 9.3. (A)**. In most of the infected cells between 30 - 60 minutes of infection, the outer membrane was intact, and the integrity of the inner membrane was lost. This might be due to the attachment of some concatemers to the inner membrane. The matured phage with the tail particles was found during this time and the loss of the internal materials was also visible as shown in **Figure 9.3 (B)** and **(C)**. The arrowheads of **Figure 9.3 (C)** showed the newly formed tail of the bacteriophage.

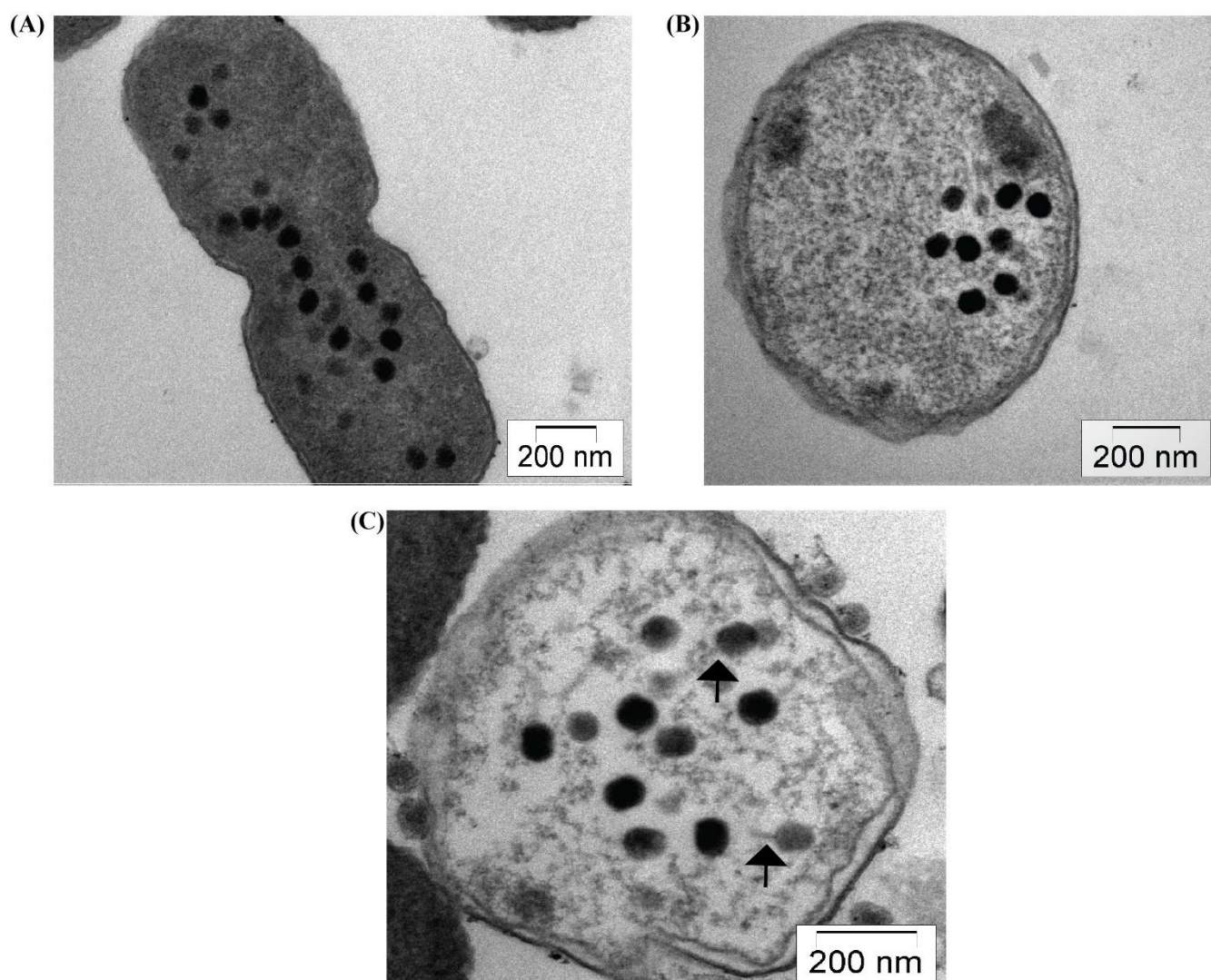


**Figure 9.3:** TEM images of the ultrathin section of *Shigella flexneri* 2a infected with isolated host-specific phage Sfk20 at 30 minutes points: **(A)** TEM image of 30 minutes showed intracellular phage development started, **(B)** the cytoplasmic material of the host cell was disorganized and **(C)** Intracellular fully developed phage, loss of internal material and membrane disorganization are visible. Black arrowheads indicate phage tail.

### 9.2.1.4 Lysis of the cell and release of progeny:

The log phase culture of *Shigella flexneri* 2a was infected with the phage Sfk20 for 60 minutes followed by glutaraldehyde fixation. The fixed sample was processed and visualized under the transmission electron microscope (FEI Tecnai 12 BioTwin). At this time point, the membrane of the bacteria was completely disrupted by the progeny phages, and the progeny phages were released from the lysed cell into the cellular environment as shown in **Figure 9.4**. The complete disruption of the bacterial cell was found and some debris were remaining.

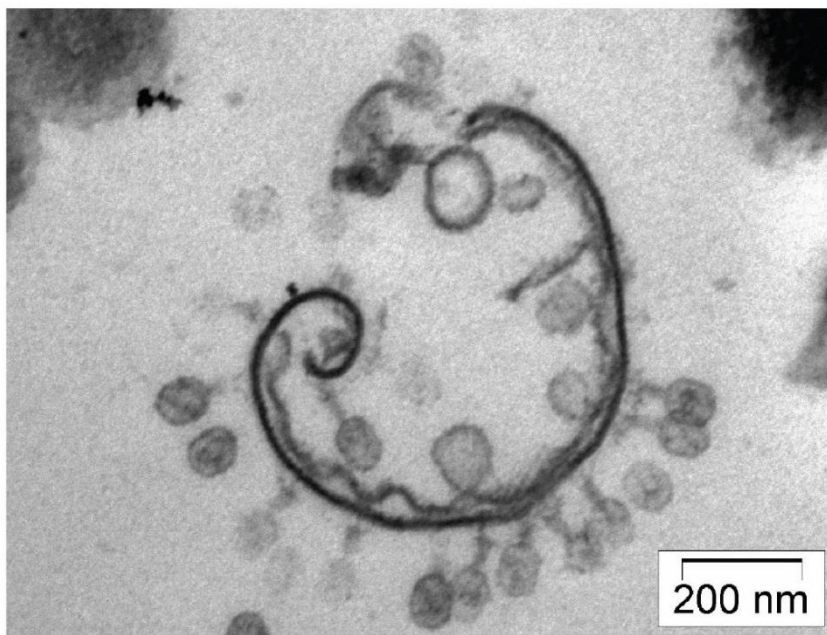


**Figure 9.4:** TEM images of the ultrathin section of *Shigella flexneri* 2a infected with isolated host-specific phage Sfk20 at 60 minutes time point. Complete lysis of bacteria cell is clearly shown at 60 minutes.

### 9.2.2 The study of phage-host interaction by scanning electron microscopy:

#### 9.2.2.1 Sfk20 bacteriophage sample:

Phage Sfk20 life cycle was also studied by scanning electron microscopy. For this purpose, the log phase culture of *Shigella flexneri 2a* was infected with phage Sfk20, and the sample was taken out from the early, mid, and late phases of the phage infection. The sample was then processed and examined under a scanning electron microscope. The Phage Sfk20 sample was also examined under the scanning electron microscope as shown in **Figure 9.5**. The head and the tail of the bacteriophage Sfk20 were clearly visible in the image.

#### 9.2.2.2 The early phase of the phage attachment:

In the early phase of phage infection, the phage particles were found attached to the host cell surface. In **Figure 9.6**, the intact phage particles and the initial step of phage attachment was shown. The structured membrane of the bacteria was also visualized. After the attachment of phage Sfk20 to the receptor on the cell surface membrane it injected its genome inside the host cell.

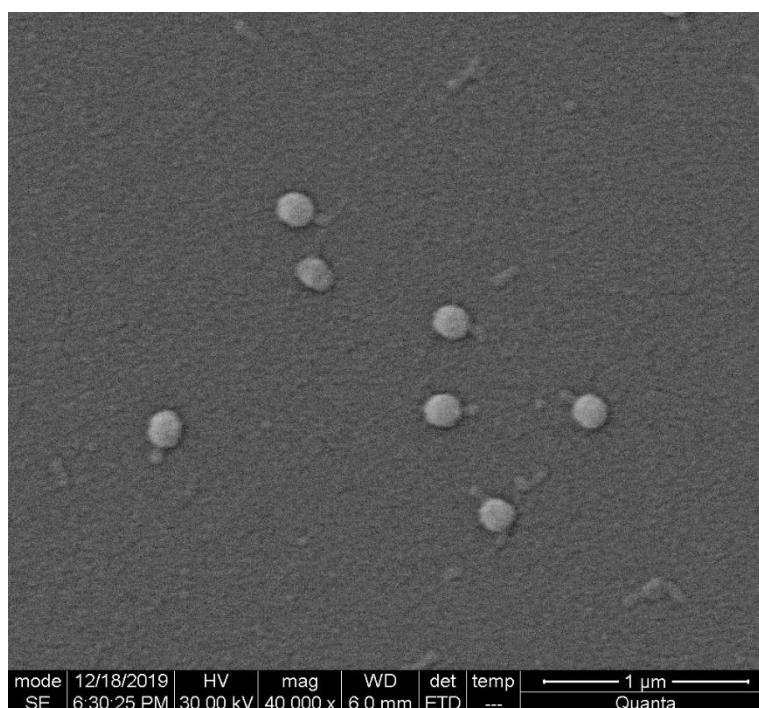


**Figure 9.5:** Scanning electron micrograph of the Sfk20 bacteriophage.



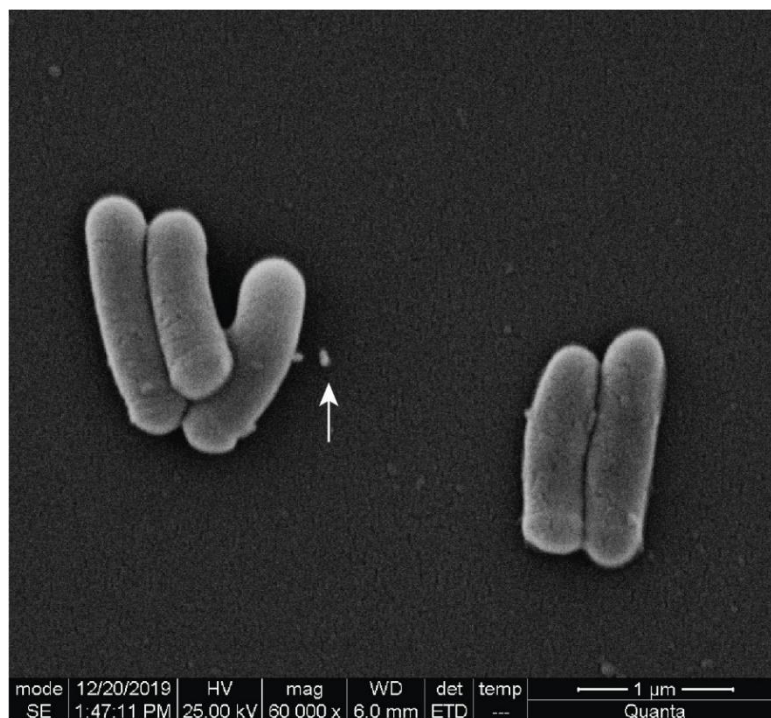


**Figure 9.6:** Scanning electron micrograph of the infected bacterial cell with phage Sfk20 at the early phase. In the early phase, few phage particles were attached to the bacterial cell (white arrow indicates phage particles attached)

### 9.2.2.3 The mid-phase of the phage attachment:

The infected sample was taken out from the mid-phase of the infection. At the mid-phase, most of the attached phages started injecting their genetic material inside the host cell and replicated inside the host cell using the host replication machinery. Moreover, the phage assembly also had been started. It was shown that the membrane started to disorganize. Finally, several phage particles attached to the bacteria, and the membrane of the bacteria started to deform as shown in **Figure 9.7**.

### 9.2.2.4 The late phase of the phage attachment:

At the late phase, the membrane of the bacterial cell was totally disorganized, and newly formed progeny phage particles were released as shown in **Figure 9.8**. Disorganized bacterial cells were quite clear in **Figure 9.8**.

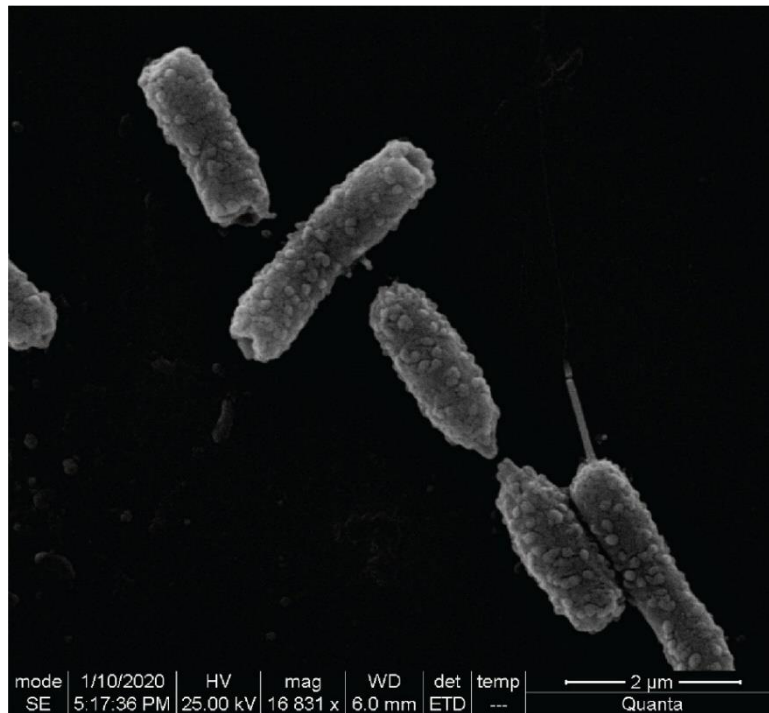


**Figure 9.7:** Scanning electron micrograph of the infected bacterial cell with phage Sfk20 at the mid-phase. Many phage particles were attached to bacterial cells at this phase.

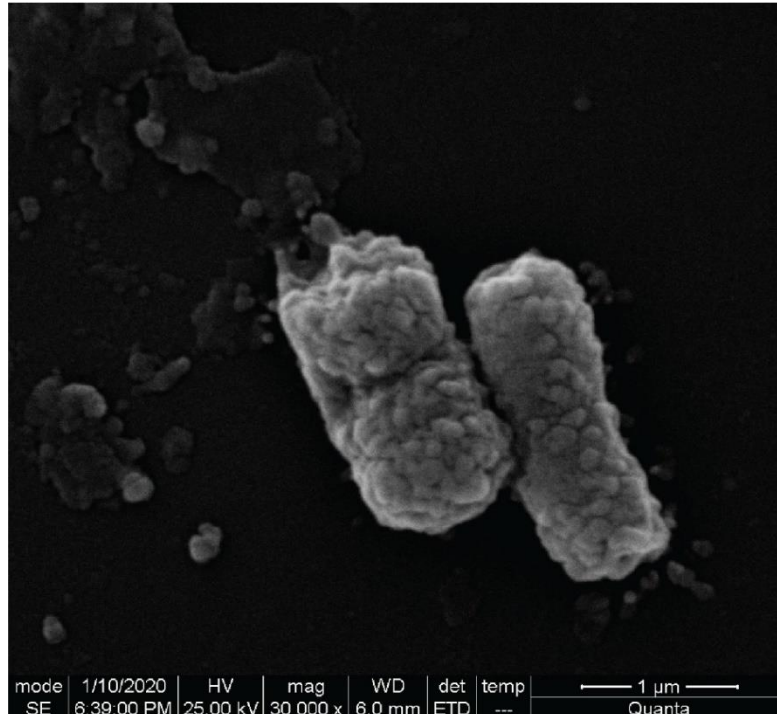


**Figure 9.8:** Scanning electron micrograph of the infected bacterial cell with phage Sfk20 at the late phase. Bacterial cell disruption was observed.

### 9.3 DISCUSSION

T4-like *Myoviridae* bacteriophage Sfk20 falls under the most complex-tailed bacteriophage group that infects *Shigella flexneri 2a* bacteria and followed strictly the lytic life cycle. In this work, the log phase culture of *Shigella flexneri 2a* was infected with the phage Sfk20 and the various phase of phage attachment, intracellular phage development, the loss of internal material of the host bacteria, finally, the lysis and the release of the progeny bacteriophages was captured and visualized by transmission electron microscopy and scanning electron microscopy. The first step of the infection begins with the attachment of the phage to the host cell via a specific host cell receptor. Initially, the phage infection is triggered by the attachment of the receptor-binding protein (RBP) located at the tip of the phage tail to the receptor present in the host cell surface (Bertozzi Silva et al. 2016). After the attachment, the baseplate of the phage tail changed its conformation from a high-energy dome-shaped structure to a low-energy star-shaped structure (Yap et al. 2016). The conformational change of the baseplate structure triggers the contraction of the tail sheath and the DNA is released from the needle-like tail tube in the host periplasm. In this work, the attachment of the phage Sfk20 to the host cell surface was shown in the first 15 minutes. It was reported in some other studies that during the infection the host DNA is completely degraded. After the infection, the phage DNA replication started inside the host cell. To start the replication mechanism inside the host cell the phages have to cross a variety of host cell surface boundaries. The capsular polysaccharide is a carbohydrate moiety that masks the host cell receptor (Labrie, Samson, and Moineau 2010; Mostowy and Holt 2018) and another moiety is the extracellular polysaccharides secreted by the host bacteria during the biofilm production (Labrie et al. 2010). Phage DNA encodes a variety of carbohydrate-active enzymes such as polysaccharide depolymerases (a common enzyme presents in the tailed bacteriophage (Yan et al. 2014) that help to recognize, bind and degrade the polysaccharides in the cell surface and get access to the cell surface receptor. At 30 minutes of the infection, the concatemeric DNA was converted into the monomeric unit, and the proheads were also developed inside the host cell. The monomeric DNA is packaged inside the heads. After 30 minutes, it was observed that the proheads started to develop and the matured phage particles were produced inside the host cell. During this time the host inner membrane and host internal material started to disrupt. At 60 minutes time point it was seen the newly formed Sfk20 phage particles were ready to lyse the cell membrane and the progeny phages were released into the environment. It was the last part of the lytic life cycle of phage Sfk20 where the newly formed tailed bacteriophages use the phage-encoded endolysin and



holin to disrupt the cell membrane (Latka et al. 2017). Endolysins are peptidoglycan layer degrading enzymes and it is synthesized at the late phase of the genome expression in the lytic lifecycle (Loessner et al. 2002). During lysis, endolysin degrades the cell wall of the host from within. Ultrastructural analysis of phage-infected bacteria and intracellular development of phages by transmission and scanning electron microscopic images confirmed the morphogenetic pathway of phage Sfk20 and further showed similarities with T4 phage (Kellenberger and Wunderli-Allenspach 1995). Understanding the interaction of the bacteria-bacteriophage system is an approach to considering bacteriophages for further uses.



# CHAPTER 10

## Objective 4

Antibiofilm activity of *Shigella* phage  
Sfk20 against host bacteria



### 10.1 INTRODUCTION

Biofilms are formed by some bacteria as a part of their survival mechanism in harsh environments and thus biofilms are ubiquitous in nature. Bacterial biofilms are formed on various surfaces such as medical devices, aquatic systems, living tissues, etc when the community of microorganisms is attached to each other or to the self-produced polymeric matrix. In 1683 Antoni van Leeuwenhoek observed the biofilm of his own teeth using his own light microscope (Høiby 2017). In the biofilm, the bacterial cells are aggregated in a self-produced extracellular polymeric matrix which is responsible for 90% of its biomass. This extracellular polymeric matrix is composed of exopolysaccharide (e.g., alginate), protein (fibrin) (Branda et al. 2006), flagella, pili, and other adhesive fibers (Cegelski et al., 2009), and extracellular DNA (eDNA) (Guiton et al. 2009). Nutrients are trapped inside the matrix of the biofilm for the metabolic utilization of residential bacteria and water is produced inside the matrix by the interaction of H-bond to the hydrophilic polysaccharide (Conrad et al. 2003; Flemming and Wingender 2010). Different enzymes are secreted by the bacteria present inside the biofilm that modifies the EPS composition of the biofilm in response to the availability of nutrients thereby helping to produce a structure of the biofilm in a specific environment (Gjermansen et al. 2010). Sometimes nutrition deficiency takes place within the biofilm due to altered metabolism, protein production, and gene expression. In that case, the cell division rate and the metabolic rate of the bacteria within the biofilm are reduced (Donlan and Costerton 2002; Hall-Stoodley and Stoodley 2009). Therefore, all these characteristics help to protect the biomass of the biofilm against anti-microbial agents, oxidizing agents, radiation, and other damaging agents (Flemming and Wingender 2010).

Biofilm formation is an important cause of the perseverance of food-borne pathogens (Kaoukab-Raji, Biskri, and Allaoui 2020). *Shigella flexneri* is one of the food-borne pathogens responsible for diarrheal disease in developing countries. Like other few Gram-negative bacteria *Shigella flexneri* is able to produce biofilm. The planktonic cell of *Shigella flexneri* produces the exopolysaccharide matrix in response to various environmental conditions thus producing the biofilm (O'Toole, Kaplan, and Kolter 2000). This assemblage is able to hide from the innate immune system of the body. Biofilms may cause tissue damage and acute infection. Some studies have shown that biofilm creates pathogenesis in the body by disrupting the host defense mechanism (Bai, Nakatsu, and Bhunia 2021). Studies have also shown that metabolically inactive non-dividing persister cells are present within the biofilm which makes

them resistant to the number of antibiotics and these cells are identical to the rest of the bacterial cells (Lewis 2005, 2008). The matrix of the biofilm protects the bacterial cells from antibiotics (Cerca et al. 2006; Jefferson, Goldmann, and Pier 2005). Therefore, the treatment process becomes quite difficult. Lytic bacteriophages have some unique properties that allow them to be applied as antibiofilm agents. Phage produces a depolymerase enzyme that can degrade the EPS matrix of the biofilm completely (Harper et al. 2014). Bacteriophages can also be used in combination with antibiotics for better treatment. Another approach that can be used for the removal of bacterial biofilm is the use of a phage cocktail.

Phage cocktails are made up of distinct phages that, when combined, can infect various bacterial species. The development of phage resistance could make single-phage therapy ineffective due to many reasons such as altered bacterial cell surface receptors, production of modified restriction enzymes that destroy phage DNA, and spontaneous mutation. On the other hand, phage cocktails, a mixture of phages, can be used to overcome the limitations of monophage therapy and to improve treatment outcomes. Therefore, phage cocktails can be used to reduce the production of altered phage-resistant strains and maximize the effectivity of phages to reduce bacterial biofilms. In addition, the cocktail is also able to broaden the host range and improves the lytic activity of phages.

In this chapter, the antibiofilm effect of phage Sfk20 alone and in combination with the antibiotic ampicillin, and in a phage cocktail to reduce the load of bacterial biofilm was discussed.

### 10.2 RESULTS

#### 10.2.1. Biofilm degradation study using phage Sfk20 and ampicillin combination:

##### 10.2.1.1 Biofilm formation and degradation study in 24 hours:

The *Shigella flexneri 2a* biofilm was grown in a controlled manner on coverslips for 24 hours at 37°C without shaking conditions. Thereafter the sample was treated with phage Sfk20, antibiotic ampicillin, and a combination of both Sfk20 and ampicillin. After 24 hours the samples were fixed and processed for scanning electron microscopy. **Figure 10.1 (A)** showed the image of 24 hours of biofilm where the matrix is not very prominent as the background matrix was not properly formed in 24 hours. **Figure 10.1 (B)** showed the SEM image of antibiotic-treated biofilm. The matrix of the biofilm was reduced a little compared to the control in the presence of the ampicillin and bacterial cells were elongated due to stress. The phage Sfk20-treated biofilm showed the degradation of the background matrix that results in a scattered bacterial distribution in **Figure 10.1 (C)**. The membrane of the bacterial cells also started to deform after the treatment of phage Sfk20. Therefore, it can be said that the efficiency of Sfk20 to destroy the biofilm is higher than that of antibiotics. **Figure 10.1 (D)** showed the image of the biofilm treated with phage Sfk20 and ampicillin combination. The scanning electron micrograph further revealed that the percentage of reduction of the bacterial cell is higher than that of Sfk20 and ampicillin alone. In this case, the bacterial cells also become elongated with part of the matrix remaining attached to the cells like thin appendages.

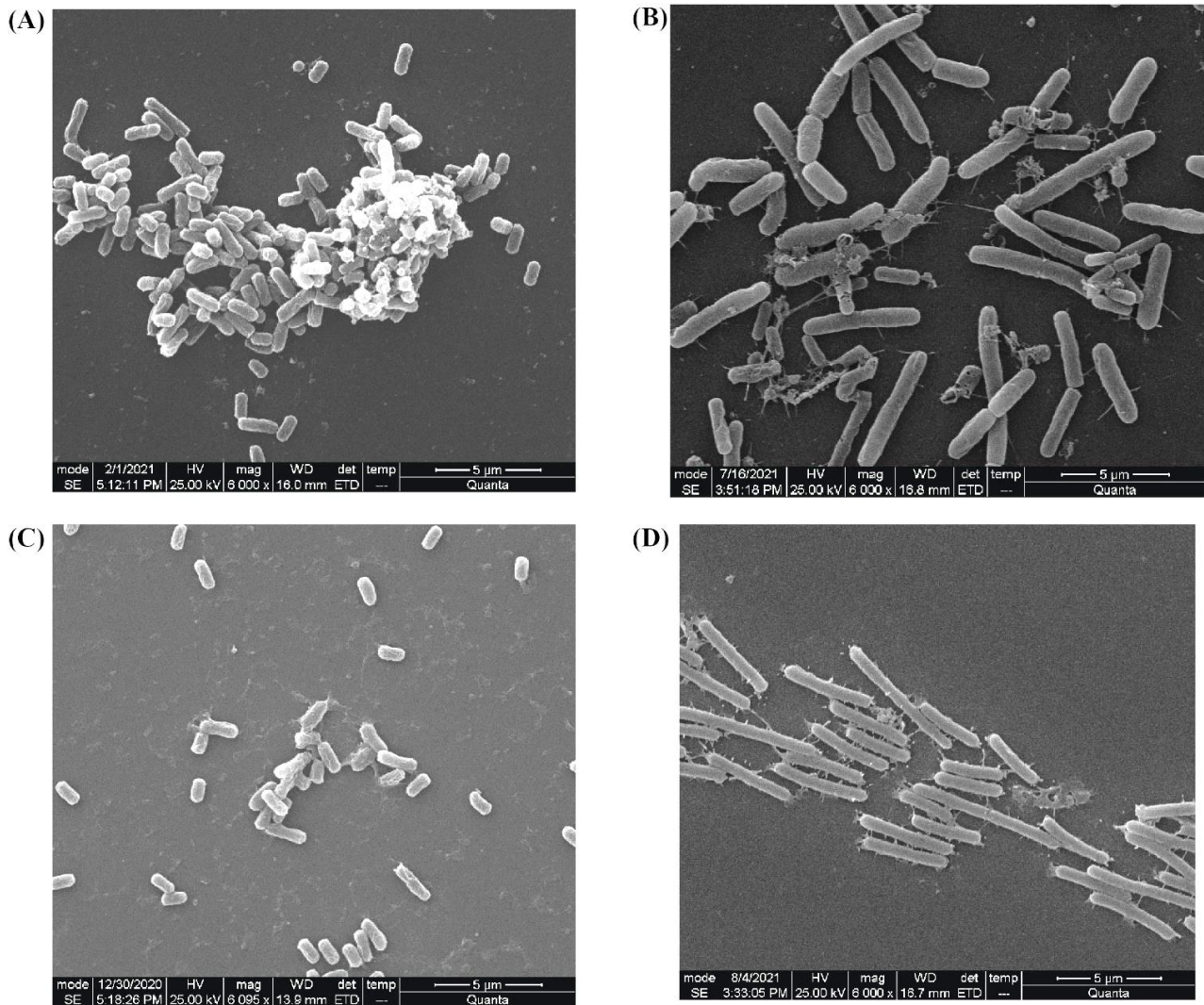


**Figure 10.1:** Scanning electron micrograph of the 24-hour biofilm formation and degradation assay: (A) 24-hour untreated control, (B) biofilm treated with antibiotic ampicillin, (C) biofilm treated with phage Sfk20 and (D) biofilm treated with the combination of Sfk20 and ampicillin.

### 10.2.1.2 Biofilm formation and degradation study in 48 hours:

The *Shigella flexneri* 2a biofilm was grown on a coverslip for 48 hours at 37°C without shaking conditions. After 48 hours the samples were washed and processed for scanning electron microscopy. The scanning electron micrograph showed that the formation of the biofilm is very prominent at 48 hours. The highly structured extracellular polysaccharide matrix consists of polysaccharides and proteins, and eDNA was formed in the background. The bacterial cells adhered to each other or to the matrix as shown in **Figure 10.2 (A)**. The scanning electron micrographs of the ampicillin-treated biofilm showed that the background matrix was reduced to some extent but not destroyed completely as shown in **Figure 10.2 (B)**. SEM image of the Sfk20 treated biofilm in **Figure 10.2(C)** showed that the clearance of the background matrix was quite prominent. The SEM analysis study revealed that Sfk20 was able to remove the background matrix more than the ampicillin alone. The membrane started to deform in some of the bacterial cells and some of them were lysed completely. The image of the 48-hour biofilm treated with the combination of Sfk20 and antibiotic was shown in **Figure 10.2 (D)**. These SEM images revealed a significant reduction in the load of the biofilm. The background matrix was lost completely. The lysed bacterial cells were in the background. Some of the bacterial cells were elongated as before. The membrane of most of the bacterial cells was deformed and there were holes in the membrane of bacterial cells.

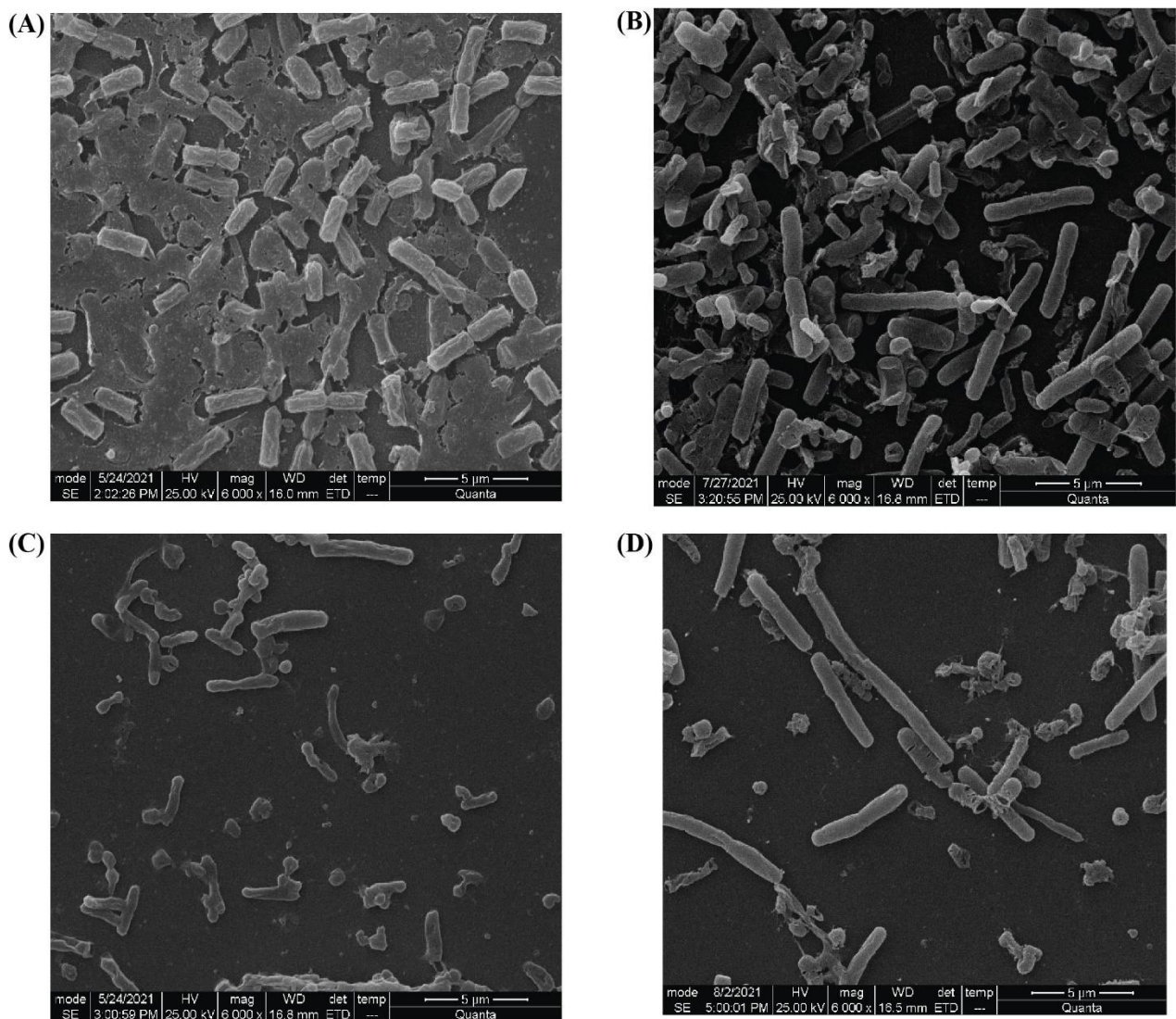


**Figure 10.2:** Scanning electron micrograph of the 48-hour biofilm formation and degradation assay: **(A)** 48-hour untreated control, **(B)** biofilm treated with antibiotic ampicillin, **(C)** biofilm treated with phage Sfk20 and **(D)** biofilm treated with the combination of Sfk20 and ampicillin.



### 10.2.1.3 Quantitative and qualitative assay of biofilm:

A quantitative assay of 48- hours of biofilm was performed on 96 well plates. After the biofilm formation, it was treated with both phage Sfk20 ( $10^{10}$  PFU/ml) and ampicillin (256  $\mu$ g/ml) alone, and a combination of Sfk20 and ampicillin to determine the synergistic effect if any. **Figure 10.3** showed that phage Sfk20 and ampicillin alone were able to remove 40% ( $P<0.001$ ) and 31% ( $P<0.001$ ) of the biofilm respectively when compared to the control. Whereas the combination of both Sfk20 and ampicillin was able to remove the biofilm up to 47% ( $P<0.01$ ) which is higher than the Sfk20 and ampicillin alone. Also, each pair of combinations showed a statistically significant reduction of biofilm. Therefore, a considerable synergistic effect was observed when biofilm is treated with both Sfk20 and ampicillin as shown in **Figure 10.3**.

This quantitative study was also supported by **Figure 10.4** where SEM images showed that the combination of ampicillin and phage Sfk20 can remove more biofilm than the Sfk20 and ampicillin alone. The quantitative and qualitative assays of biofilms were done simultaneously to assess the biofilm formation and removal activities.

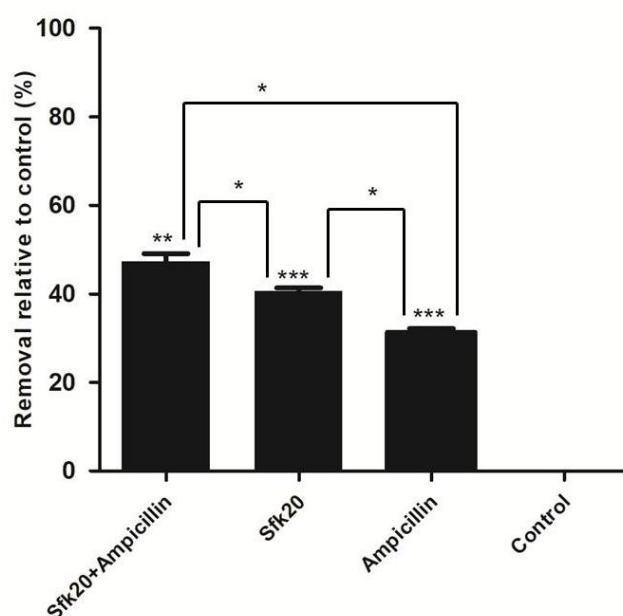


**Figure 10.3:** Percentage of biofilm removal with phage Sfk20, antibiotic ampicillin, and the combination of both with respect to untreated control. The values are shown as the mean  $\pm$  SD of the values; Asterisks indicate a significant reduction in biomass as measured by the two-way ANOVA test (\*\*\* $P<0.001$ ; \*\* $P<0.01$ ; \* $P<0.05$ ).

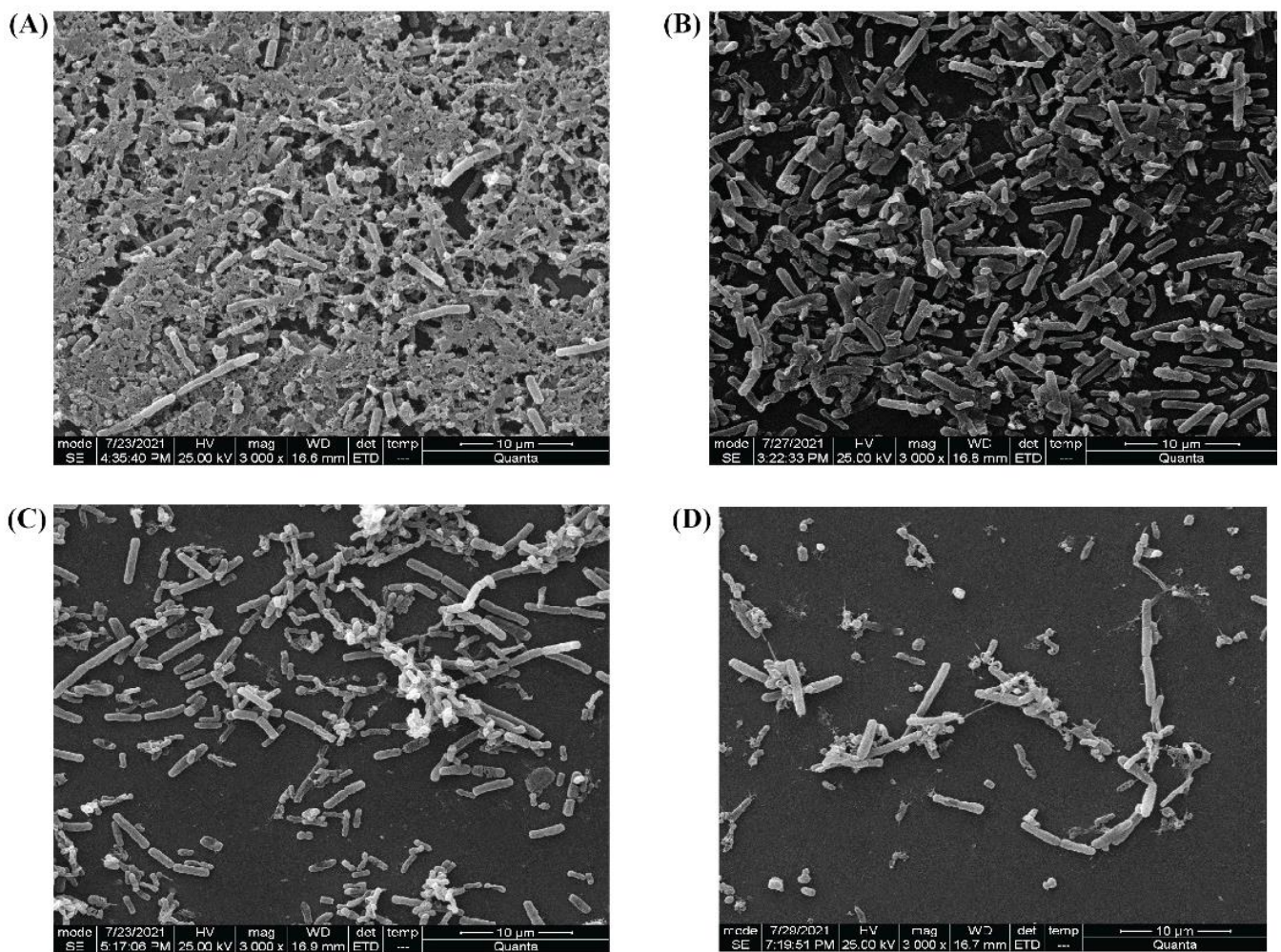


**Figure 10.4:** Scanning electron micrograph of biofilm formation and degradation assay: (A) 48-hour control biofilm, (B) biofilm treated with ampicillin, (C) biofilm treated with phage Sfk20 and (D) biofilm treated with the combination of Sfk20 and ampicillin.

### 10.2.2 Biofilm degradation assay using *Shigella* phage cocktail:

#### 10.2.2.1 Morphology, host range, and E.O.P determination of a new *Shigella* phage Sfk23, used for phage cocktail preparation along with Sfk20:

For the preparation of the phage cocktail, another newly isolated *Shigella* phage was chosen from our laboratory and its morphology was determined using transmission electron microscopy. The transmission electron micrograph revealed that the phage had a prolate-shaped head and a long contractile tail. Based on the morphology this new phage was also classified as a member of the *Myoviridae* family and *Caudovirale* order. The newly isolated phage was named Sfk23 following the rules of phage nomenclature. The transmission electron micrograph of intact phage Sfk23 was shown in **Figure 10.5**.

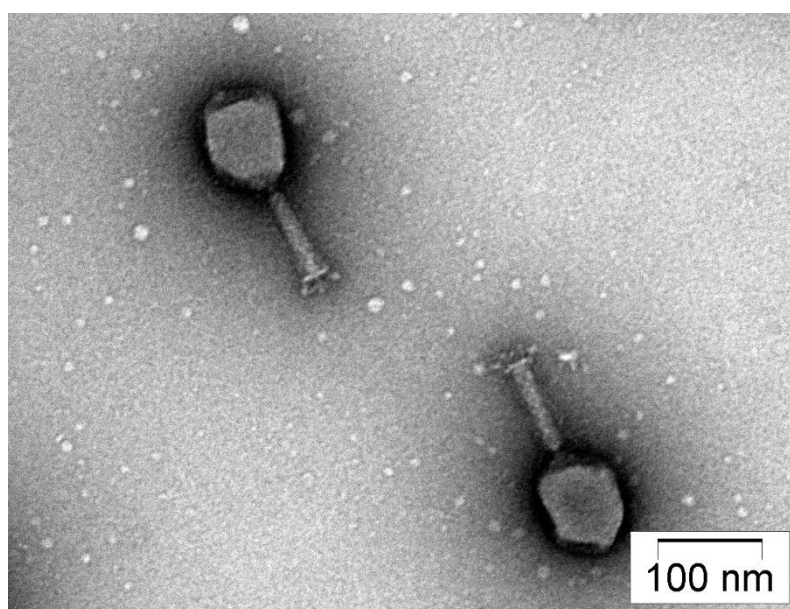


**Figure 10.5:** Transmission electron micrograph of the bacteriophage Sfk23.

Around eight strains: *Shigella flexneri* 2a, *Shigella flexneri* 3a, *Shigella flexneri* 1b, *Shigella flexneri* 4, *Shigella flexneri* 6, *Shigella sonnei*, *Shigella dysenteriae* 1, *Shigella boydii*, two typhoidal *Salmonella* strains: *Salmonella typhi*, two non-typhoidal *Salmonella* strains: *Salmonella typhimurium*, *Salmonella enteritidis*, and one *Vibrio cholerae* O1, one *E. coli* strain *ETEC* were used to analyze the host range of phage Sfk23. This study revealed that Sfk23 can infect and lyse different *Shigella flexneri* serotypes: 1b, 2a, 3a, *Shigella dysenteriae* 1, and *Shigella sonnei* but could not infect *Shigella flexneri* serotype: 4, 6 and *Shigella boydii*, Phage

Sfk20 could also infect and lyse *Salmonella typhimurium*, *Salmonella enteritidis* but could not infect *Salmonella typhi*, *ETEC*, and *Vibrio cholerae O1* (**Table 10.1**). The Efficiency of Plating (EOP) of *Shigella flexneri 2a* showed the highest value for phage Sfk23 (**Table 10.1**). The value of EOP was also higher for other *Shigella* strains such as *Shigella flexneri 1b*, *Shigella flexneri 3a*, *Shigella sonnei*, and *Shigella dysenteriae 1* compared to the *Salmonella typhimurium* and *Salmonella enteritidis* strains. This study further indicated that *Shigella flexneri 2a* was the most suitable host strain of phage Sfk23 and it was a *Shigella* phage.

**Table 10.1:** Host range analysis of phage Sfk23.

Bacterial species	Strain no.	Infectivity	EOP value
<i>Shigella flexneri 2a</i>	2457T	+	1
<i>Shigella flexneri 3a</i>	UB811	+	0.0032
<i>Shigella flexneri 1b</i>	03075/19	+	0.64
<i>Shigella flexneri 4</i>	C2529	-	-
<i>Shigella flexneri 6</i>	UB812	-	-
<i>Shigella sonnei</i>	IDH00968	+	0.36
<i>Shigella dysenteriae 1</i>	NT4907	+	0.79
<i>Shigella boydii 1</i>	NK02379	-	-
<i>Salmonella enteritidis</i>	520833	+	0.00026
<i>Salmonella typhimurium</i>	PH-94	+	0.00017
<i>Salmonella typhi</i>	KOL 551	-	-
<i>ETEC</i>	IDH07942	-	-
<i>Vibrio cholerae O1</i>	MAK757	-	-

### 10.2.2.2. Biofilm degradation capability of phage cocktail in microtiter plate:

The biofilm degradation assay of the phage cocktail was performed on the microtiter plate. In this study, a phage cocktail was prepared using two *Shigella* bacteriophages Sfk20 and Sfk23, which is capable of lysing most of the *Shigella* strains based on the efficiency of plating for each individual phage. The matured biofilm was grown on the microtiter plate for 48 hours. After the formation of the biofilm, it was treated with phage Sfk20 ( $1 \times 10^{11}$  PFU/ml), phage Sfk23 ( $1 \times 10^{11}$  PFU/ml), and their cocktail ( $2.2 \times 10^{11}$  pfu/ml) to see their effect on the biofilm. The result was shown in a graphical representation in **Figure 10.6**. The result showed that phage Sfk20 and Sfk23 alone were able to remove the biofilm up to 37% ( $P < 0.01$ ) and 31% ( $P < 0.001$ ) respectively when compared to the control. Whereas the cocktail was capable of 57% ( $P < 0.001$ ) removal of biofilm which is quite higher than the individual phages. Therefore, it can be concluded that the phage cocktail of Sfk20 and Sfk23 was more efficient than single phages to remove bacterial biofilm possibly due to the synergistic effect of the two phages.

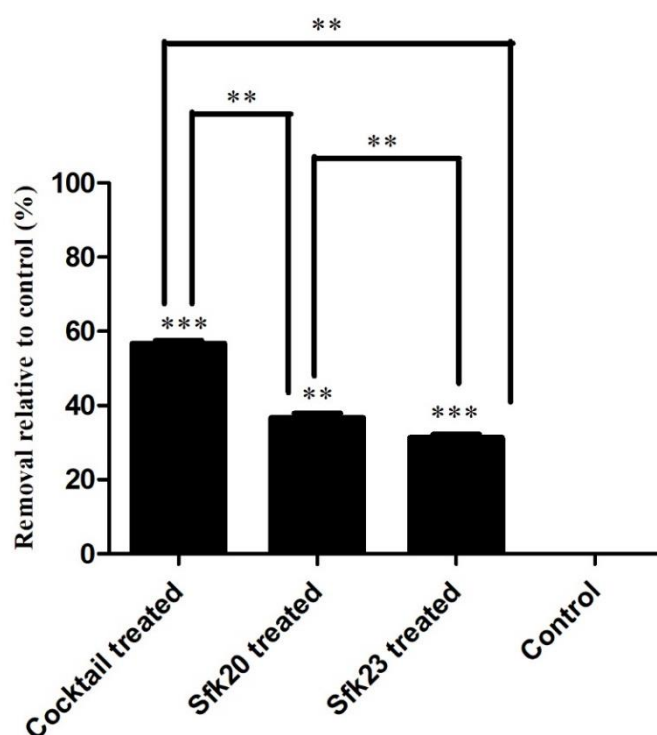


**Figure 10.6:** Percentage of biofilm removal with phage Sfk20, Sfk23, and the combination of both with respect to untreated control. The values are shown as the mean  $\pm$  SD of the values; Asterisks indicate a significant reduction in biomass as measured by the two-way ANOVA test (\*\*\* $P < 0.001$ ; \*\* $P < 0.01$ ; \* $P < 0.05$ ).

### 10.3 DISCUSSION

Biofilms can adhere to any of the biotic or abiotic surfaces. It can be found in every natural system such as lakes, streams oceans as well as in medical devices, and in human tissue also (Hall-Stoodley, Costerton, and Stoodley 2004). Some recent reports suggested that bacterial biofilms can be formed in extreme environments. The widespread occurrence of biofilm represents a serious threat of infectious disease and economic loss. Antibiotic resistance activity of the biofilm is another major threat for society and it produces a serious infection. The antibiotic susceptibility of the biofilm-containing microorganisms decreases 1000-fold compared to normal planktonic cells (Malheiro and Simões 2017). Therefore, conventional antibiotic therapy to eradicate, bacterial biofilm is inadequate. The matrix of the bacterial biofilm protects the microorganisms from physical, chemical, and biological stress and it also inactivates antibiotic molecules to spread through the polymeric matrix (Ciofu et al. 2017). Due to the diversity of the bacteria within the biofilm matrix and also the lack of permeability, antibiotics usually fail during the treatment of biofilm-mediated infections. The bacteriophages can be a potential alternative because the phage works in a different mechanism than antibiotics and is able to produce the depolymerase enzyme to degrade the biofilm layer.

In the current work, the *Shigella flexneri 2a* biofilm was formed on glass coverslips. The degradation activity of phage Sfk20 alone and in combination with ampicillin was analyzed by scanning electron microscopy. Penetration, diffusion, and propagation are three important steps to using single phages or phage cocktails to remove biofilms (Ferriol-González and Domingo-Calap 2020). The results show phage Sfk20 could fulfill the criteria to a significant extent by degrading the biofilm of its host indicator bacteria *Shigella flexneri 2a*. The phage-ampicillin combination showed a synergistic effect in the removal of *Shigella* biofilm though not complete removal. To the best of our knowledge, Sfk20 is reported as one of the first lytic, tailed *Shigella* phages capable of degrading the biofilm formed by the *Shigella flexneri 2a* strain in laboratory conditions. The phage depolymerase enzyme is able to digest the exopolysaccharide layer of the biofilm and some studies also revealed that this protein is encoded by the structural gene (tail fibers or baseplate) of the phage genome (Knecht, Veljkovic, and Fieseler 2020). These phage-encoded enzymes were able to recognize, bind, and digest the bacterial cell wall polysaccharide compound. Tailed phages can invade the matrix layer by the hydrolytic activity of depolymerase enzymes present in their tail spike proteins (Pires et al. 2016). After that probably phages diffuse through the biofilm to infect and destroy bacteria in the deeper layer

(Parasion et al. 2014). Sfk20 with its long contractile tail might help to remove the external matrix by its enzymatic activity. The other possible reasons for Sfk20 efficacy in biofilm removal are the presence of endolysins and virion-associated peptidoglycan hydrolases (VAPGHs) that either disrupt or make a small hole in the cell (Fischetti 2008; Rodríguez-Rubio et al. 2013). Moreover, a small percentage of stress-tolerant cells are usually present in biofilm and a recent study suggests phage lytic proteins can remove that cell (Gutiérrez et al. 2014). It could probably facilitate the dispersion of the biofilm matrix. This study indicated structural characteristics and spatial information of the bacterial biofilm and qualitative observation of the disruption of the biofilm through direct imaging. With the discovery of the activity of phage depolymerase enzymes to degrade the exopolysaccharide (EPS) components of the biofilm, phages can be used as an alternative to antibiotics for the treatment of biofilm-mediated infections. Phage depolymerases are very much specific to the host unlike antibiotics and therefore the natural bacterial flora remains undisturbed. The biofilm degradation capacity of Sfk20 revealed that it could be used in the future as a single phage or in a phage cocktail or phage-antibiotic combination as a therapeutic agent against biofilm-mediated diseases.

We have also done a quantitative experiment to address the eradication efficacy. Sometimes the phage-encoded depolymerase alone is not sufficient to remove the biofilm. In that case, it is recommended to use a combination of phage and antibiotics. The use of bacteriophage Sfk20 ( $10^{10}$  PFU/ml) with ampicillin at a high concentration (256 µg/ml) exhibited a better biofilm removal activity compared to the phage or antibiotic alone. This could be due to the presence and enzymatic activity of depolymerase in the phage tail. It might have degraded the extracellular capsular polysaccharide parts of the biofilm and phages could diffuse easily inside the biofilm to target bacteria in the deeper layer creating a free path for a higher dose of antibiotics to reach inside the biofilm. Thus, a combination of phage plus antibiotic showed faster destruction of the biofilm matrix and the associated bacteria. Similar results were reported in other studies of phage-antibiotic combination therapy (Bedi, Verma, and Chhibber 2009; Harper et al. 2014). Phage-antibiotic synergism is observed in most of the infections caused by biofilm-producing bacteria (Chaudhry et al. 2017). In this study, phage Sfk20 alone can remove at least 40% of the total biofilm and in combination with ampicillin, the removal percentage of biofilm was 47%. It confirmed the synergistic effect of the Sfk20-ampicillin combination.

Bacteriophages are highly selective in their host cell targeting, infection, and lysing. Bacteriophage treatments can be classified as either mono-phage treatments or phage mixtures

(phage cocktails). Monophage treatment consists of one singular phage type and is used to target to reduce the load of the biofilm alone. Whereas phage cocktail preparations are a mixture of multiple phage types and are able to infect many bacteria. In this study, the matured biofilm of *Shigella flexneri 2a* was treated with two mono phages: Sfk20 ( $10^{11}$  PFU/ml) and Sfk23 ( $10^{11}$  PFU/ml), and their cocktail ( $2 \times 10^{11}$  PFU/ml). It was found that the phage cocktails are able to remove the biofilm more effectively than the monophages. This might be because the phage cocktail preparation boosts the effectiveness of such pairings by expanding their field of effect (Kifelew et al. 2020). The most frequent defense mechanism employed by host cells to prevent bacteriophage attachment has been hypothesized to be the surface modification of bacterial receptors (Labrie et al. 2010). The use of a single phage type may stimulate the development of resistant mutants whereas the cocktail of two or more phages can overcome the limitation of the monophage effect. This study showed that the phage Sfk20 and Sfk23 alone results in 37% and 31% reduction of the biofilm whereas the cocktail is able to reduce 57% load of biofilm. Therefore, the cocktail of two phages is proved to be more efficient to reduce the load of the biofilm.





# CHAPTER 11

## **General Discussion**



### 11.1 DISCUSSION

It has been observed over the past 25 years that the prevalence of diarrheal disease has significantly decreased globally as a result of better nutrition, access to clean water, and rotavirus vaccination programs. However, the enteric infection rates particularly those caused by human-restricted bacterial pathogens are still high. *Shigella* continues to be the third-leading cause of fatalities from diarrhea in children under the age of five and the second-leading cause of all deaths from diarrhea (Kotloff, 2017). Lack of effective vaccination and the increasing trend of antibiotic-resistant strains are two current obstacles to treating diarrheal illnesses (Barry et al. 2013; Pitisuttithum et al. 2016). The lack of sufficient preclinical animal model knowledge and the poor understanding of pathophysiology have hindered the development of better vaccines (Kim et al. 2013). To develop effective treatments against intestinal pathogens such as *Shigella*, innovative alternative strategies are desperately needed.

Bacteriophages (phages) are the most prevalent bacterial viruses on this planet. They are specifically present wherever their host survives. Since phages are bacteria's natural enemies, they play a crucial role in managing the bacterial population in a range of settings, including wastewater treatment and medicinal uses (Batinovic et al., 2019; Clokie et al., 2011). Felix d'Herelle first identified phages in 1917 and also tested the possibility of phage therapy. Though other researchers namely Hankin, Gamaleya, and Twort also observed phages with antibacterial or healing activity in 1896, 1898, and 1915, respectively. Once the antibacterial properties of phages were confirmed, the scientific community was quite excited about the possibility of using them to treat bacterial illnesses. But with the development of antibiotics, phage therapy has been largely superseded, which has a broad spectrum of activity and can be manufactured to a specific quality (Lin, Koskella, and Lin 2017). Additionally, biogeographical variations may be detrimental to the antibacterial efficacy of phages (Bhetwal et al. 2017). A phage obtained from one geographic location may not have the same antibacterial effects on another strain of the same species isolated from a different location. These factors have led to phage therapy's significant decline in use since the first half of the 20th century. However, the steady rise in bacterial strains with multidrug resistance (MDR) and the failure of the current antibiotics to effectively treat infectious diseases have prompted efforts to find substitutes to mitigate antimicrobial resistance. It is necessary to discover new antibiotics to stop the emergence and spread of resistance. However, despite the discovery of new antibiotics, the selective pressure of antibiotics may mean that resistance development among bacteria cannot

be entirely avoided (Davies and Davies 2010). Phage therapy can be a possible alternative to antibiotics, but since this century-old concept has recently been revived, there is an upsurge in studies to isolate and characterize new bacteriophages and explore their applications. Specific requirements must be met for phage therapy to be effective, including having a large collection of bacteriophages, using obligately lytic phages rather than temperate phages, having a wide range of hosts, and screening phage genomes for the presence of toxin genes (Weber-Dabrowska et al. 2016). Utilizing phages that can effectively bind to host cells, multiply quickly, have a large burst size, and can quickly eradicate target bacteria is also advantageous.

In this study, a lytic *Shigella* bacteriophage Sfk20 was isolated from the environmental water of a diarrheal outbreak area against host bacteria *Shigella flexneri* 2a 2457T strain. Environmental water is rich habitats from which lytic phages can readily be isolated with their respective host bacteria. Additionally, clinically significant bacterial pathogens and associated lytic phages can be found in the environmental water in good numbers (Sharma et al. 2020). Based on the morphological features phage Sfk20 isolated in this study belongs to the family of *Myoviridae*, *Caudovirale* order. The host range analysis and efficiency of the plating study revealed that phage Sfk20 is effective against various *Shigella* strains *Shigella flexneri* serotypes 1b, 2a, 3a, *Shigella sonnei* and *Shigella dysenteriae* 1. The isolated phage was also found to be effective against two non-typhoidal *Salmonella* strains: *Salmonella enteritidis* and *Salmonella typhimurium*. Phage Sfk20 appeared to be highly stable in the range of 4–37°C and for at least up to six months without losing viability in the usual storage temperature of 4°C. Phage Sfk20 also remains stable up to the pH 7–9 range. At 0–5% salt concentration phage Sfk20 remains activated for up to 28 days. For the large-scale biocontrol of host bacteria, the employment of phages with strong lytic activity against several targeted bacterial populations is essential. This characteristic is connected to the large burst size. One of the essential qualities of a therapy candidate bacteriophage is associated with a large burst size since this quality is strongly linked to phage growth (Gallet, Kannoly, and Wang 2011). The one-step growth curve study revealed that bacteriophage Sfk20 has a short latent period (20 min) and large burst size (123 PFU/infected cell). Large burst-size phages may have a selective advantage as an antibacterial agent as they can dramatically increase the initial dose several hundred-fold in a short period of time (Choi et al., 2010; Nilsson, 2014). Phages unlike antibiotics follow a different mode of action that is receptor-mediated interaction with host bacteria to infect and lyse the cell eventually. Therefore, the adsorption of phage to the host cell surface receptor is a vital step to initiate the infection process. Due to the fact that *Shigella* spp. are gram-negative

bacteria, the outer membrane carbohydrate (LPS) or protein may serve as the particular receptor for phage infection. This study revealed phage Sfk20 uses LPS as a receptor to infect *Shigella flexneri* 2a. The study of bacteriolytic activity showed the growth of the host bacteria was reduced at MOI 1 and 100.

The genome of the Sfk20 bacteriophage was isolated and digested with restriction enzymes to confirm the presence of a double-stranded DNA genome in phage Sfk20. Genome sequencing, analysis, and complete annotation as well as proteomic study provide sufficient information on the phage Sfk20 genome and proteome. Phage Sfk20 had a double-stranded DNA genome of 164878 bp in length with a GC content of 35.62%. Analysis of the phage Sfk20 genome confirmed the presence of lytic proteins and the absence of any lysogenic, toxin, or antibiotic resistance genes suggesting that the phage could be used as a safe biocontrol agent for its host enteric bacteria. Holin and endolysin genes encode proteins responsible for progeny phage release at the end of a lytic cycle. The presence of both genes in the sequence of the phage Sfk20 genome can confirm its lytic nature. Phage Sfk20 showed sequence similarity with T-4 like *Myoviridae Shigella* bacteriophages such as pSs-1, SH7, SfPhi01, Sf21, and Sf23. The phylogenetic trees of the baseplate wedge subunit and terminase large subunit both confirmed that the phage Sfk20 is closely related to the other T4 like *Myoviridae Shigella* and *E. coli* phages and probably evolved from the common ancestors. Following the LC-MS/MS forty different proteins were identified. Among them seventeen structural proteins, three functional proteins, and twenty hypothetical proteins.

Structural studies of the currently known tailed phages have shown a common organization, which implies that they have a single ancestor and diversity has arisen through evolution (Bamford, Grimes, and Stuart 2005). In this study, a tailed *Myoviridae* phage structure and its structural proteins were characterized. The phage Sfk20 intact structure including capsid, tail connector, and tail components was determined using single-particle cryo-electron microscopy and image processing. We have discussed in previous sections that Sfk20 is a T4-like *Myoviridae* tailed phage consisting of a prolate-shaped head, a head-to-tail connector, a long contractile tail, and a baseplate. In this study, the images of intact phage particles were collected and the four different parts were separately reconstructed. The mature phage particle has a prolate-shaped head that encapsidates the genome. The head is first assembled as an empty capsid that is subsequently packaged with DNA by an ATP-dependent packaging device. This device attaches to the same unique pentameric vertex that is later occupied by the phage tail. The head is prolate, meaning that it has two icosahedral ends and a cylindrical mid-section.

The filled head is attached to the tail via a phage neck structure. The tail is made up of a tail tube and a helical sheath. The baseplate's dome-shaped end opposite the head is where the tube and sheath are joined. Assembly of the tail begins with the connector of the six wedges and a central hub. These together form the baseplate that then nucleates the assembly of the tail tube around which the sheath assembles (Yap and Rossmann 2014). The baseplate goes through a significant conformational change during the infection process that relaxes the high-energy dome-shaped structure to a low-energy star-shaped structure (Leiman et al., 2004).

Six structurally relevant phage proteins were selected and their structure was predicted using two NN-based methods (AlphaFold2 and ESMFold) and a homology-based modeling method (Phyre2). The predicted structures were aligned with the experimental structure collected from the PDB. Later the predicted structures were compared based on various metrics such as TM-score and RMSD values. It was a comparative study to understand which software can predict the structure more accurately. It was found that AlphaFold2 and Phyre2 predicted the protein structures of phage Sfk20 more accurately than the ESMFold. The major drawback of using Phyre2 is that a template is required for the predicting structure. If the template is not available the phyre2 is not capable to produce the structure.

The organization of microbial communities is significantly shaped by complex interactions between bacteriophages and their bacterial hosts, which can alter bacterial gene expression patterns as well as transduce genetic material. The ability of the phages to infect their bacterial hosts, particularly during phage entry, is their main means of survival. Bacteriophage diversity and abundance are determined by bacteriophages' capacity for dynamic adaptability in the face of selective forces such as host adaptation and resistance. Understanding the interaction of the bacteria-bacteriophage system is an approach to considering bacteriophages as biocontrol agents. In this study, the lytic life cycle of the phage Sfk20 was studied using electron microscopy. Ultrastructural analysis of phage-infected bacteria and intracellular development of phages by transmission and scanning electron microscopic images confirms the morphogenetic pathway of phage Sfk20 and further showed similarities with T4 phage. Further, the different forms of the infected cells indicated that the extent of intracellular phage development depends on the multiplicity of infection of an individual particle.

Biofilm is a complex integrated aggregation of bacterial cells adhered to both biotic and abiotic surfaces. Biofilm formation is considered a virulence factor (Musk Jr. and Hergenrother 2006). One of the most crucial survival mechanisms for bacteria in extreme conditions is the

production of biofilms, which improves their virulence and makes them more resilient and, as a result, increases their tolerance to most of antibiotics. Therefore, antibiotic treatments are not always suitable for removing biofilms, mainly because of the increased level of tolerance of the bacteria within the biofilms. Moreover, the innermost cells of the biofilms are metabolically inactive and therefore less affected by antibiotics. While tolerance is a phenotypically defined process by which bacteria survive the effects of a particular antibiotic in a specific environment, drug resistance is frequently described as a genetic process occurring from spontaneous mutations or horizontal gene transfer (Mah 2012). There is a need for new treatment methods that could aim to eradicate biofilms, and bacteriophage may be a promising alternative. Phages are equipped with a special enzyme depolymerase that degrades the exopolysaccharide matrix of the biofilm. Therefore, Phages can reach the inner layers of a biofilm by diffusing through its water channels (Pires et al. 2017). The effect of the antibiotics can be stimulated by bacteriophages. This phenomenon is referred to as phage-antibiotic synergy. In current study, the *Shigella flexneri* 2a biofilm was treated with the phage Sfk20 and ampicillin alone and also in combination. Thereafter removal of biofilm was analyzed by scanning electron microscopy which showed better results in phage-antibiotic combination. During treatment phage and antibiotics are often used in conjunction because it was observed that applying two different selective pressures increase the efficacy more compared to using them separately (Torres-Barceló and Hochberg 2016). A quantitative experiment was also performed on a microtiter plate to address the eradication efficacy. In both of the cases, it was found that combination therapy can effectively remove the biofilm.

Another newly emerged method to treat bacterial biofilm is using a phage cocktail which consists of two or more bacteriophages. Cocktails effectively overcome the limitations of monophage therapy and improve treatment outcomes. Nowadays the demand for phage cocktails has increased because the phage resistant mutant of the host bacteria is continuously increasing. Therefore, phage cocktails may delay or postpone the establishment of phage-resistant bacteria with the inclusion of more than one phage type (Domingo-Calap and Delgado-Martínez 2018). Additionally, many phage strains may complement one another by delivering the essential antibacterial components that another may lack. In this study, a phage cocktail was prepared using one more lytic *Shigella* phage Sfk23 along with the studied phage Sfk20. The phage cocktail was used to treat the bacterial biofilm in a microtiter well plate. It was found that the phage cocktail eradicated the bacterial biofilm more effectively than the individual phages.



# CHAPTER 12

## **Conclusion,** **Significance & Future** **prospect**



### 12.1 CONCLUSION

The century-old phage therapy got revived as an alternative therapy choice to control the growing number of multidrug-resistant strains of pathogenic bacteria. A continuous search for novel lytic bacteriophages during a seasonal upsurge of the diarrheal outbreak could indicate the presence of related virulent bacteria in the environment. In this work, a novel lytic *Shigella* bacteriophage Sfk20 was isolated from the environmental water of a diarrheal outbreak area, Kolkata. The morphological study revealed that phage Sfk20 belongs to the family of *Myoviridae*, *Caudovirale* order. Phage Sfk20 was capable of inhibiting the growth of many *Shigella* spp. and two nontyphoidal *Salmonella* species. Environmental factors can strongly influence the efficiency of phages as therapeutic agents. Therefore, a study on phage stability was conducted at different temperatures, pH, and saline conditions that revealed Sfk20 remains active at a range of temperatures and pH but became inactive at high saline conditions. The attachment of phages to the host bacterial membrane occurs through the binding of phage particles to a specific host cell surface receptor. Therefore, host receptor identification is necessary to better understand the infection process of any phage. A study on identifying the nature of the phage Sfk20 host receptor showed that the bacterial outer membrane LPS of the *Shigella flexneri* 2a acts as a receptor for the phage Sfk20. Lytic phages always show a significant level of bacteriolytic activities very similar to antibiotics but using a different mechanism. The bacteriolytic activity of phage Sfk20 at various MOI studies revealed that at high MOI the growth of the host bacteria became restricted, one of the essential criteria to qualify as a potential biocontrol agent. The whole genome sequencing and the comparative genomic study revealed that the phage Sfk20 carries genes for lysis proteins holin and endolysin, but the lysogeny genes and virulence genes were absent in the genome. This further confirmed the lytic nature of the phage Sfk20. The phylogenetic analysis revealed that the bacteriophage belongs to the T4-like bacteriophage family. Phage protein identification is valuable to understand the relationship between closely related phages, and the structure-function relationship. A nano LC-MS/MS technique was used here to analyze and detect the Sfk20 phage proteins based on specific peptides. The structural characterization by single particle cryo-electron microscopy and image processing further expanded our knowledge of detailed phage structure. To our knowledge, this is the first cryo-EM study of long-tailed *Shigella* phage in India. The important protein structures were predicted using two deep learning-based and one homology-based method. After comparing the protein structures based on their TM-score and RMSD values, it was concluded that AlphaFold2 and Phyre2 performed



better than ESMFold in the case of phage Sfk20 proteins. The *in vitro* phage host interaction and complete lytic cycle study also confirmed the lytic nature of this phage. The antibiofilm activity of phage Sfk20 against *Shigella* bacteria both alone and in combination with antibiotic ampicillin showed the synergistic effect of phage Sfk20 because along with ampicillin it removed the biofilm more effectively. The use of a phage cocktail of Sfk20 with another *Shigella* phage Sfk23 was found more effective as an antibiofilm agent compared to the individual bacteriophages and it also reduced the risk of phage resistance. Altogether, the promising findings facilitated the understanding of general phage biology and made the phage Sfk20 a potential biocontrol and therapeutic agent.

### 12.2 Significance and Impact

Phage isolation and characterization is highly significant to search for stable phages with a wide host range. These phages could be potential phage therapy candidates to control antibiotic-resistant bacterial infections. Moreover, a better understanding of phage biology has opened up new fields of phage application such as vaccine development, medical sciences, food industries, surface decontaminators, bacterial detection systems, etc. We have isolated a lytic *Shigella* phage Sfk20 and characterized it in detail to better understand the phage before proposing it as a promising alternative therapeutic candidate. The in-vitro biofilm removal activity of phage Sfk20 alone and in combination with antibiotics showed the antimicrobial synergy of phage and antibiotic. The strength of a phage cocktail had also been shown by the antibiofilm activity. Altogether phages have an immense impact on human health as well as the environment. It can be a viable alternative in health sciences to control the antibiotic-resistant bacteria in the era of the AMR crisis and reduces the economic loss due to the wastage of food.

### 12.3 Future prospect

All the results generated through this study suggested that phage Sfk20 could be a great alternative agent to treat Shigellosis. In the near future, phage Sfk20 can be useable as a potential therapy candidate. Phage therapy has the potential to go beyond merely treating an infection in a patient to minimize its causes and prevent further complications that require additional studies and confirmation. The development of phage-based products may increase the safety of food products leading to a decreased economic burden of foodborne pathogens in the food industry.



# CHAPTER 13

## **Bibliography**



- . d'Herelle F. 1931. "Bacteriophages as a Treatment in Acute Medical and Surgical Infections."
- Abedon, Stephen T. 2006. "Phage Ecology on Wikipedia." *Technology* 1–109.
- Abedon, Stephen T., Sarah J. Kuhl, Bob G. Blasdel, and Elizabeth Martin Kutter. 2011. "Phage Treatment of Human Infections." *Bacteriophage* 1(2):66–85. doi: 10.4161/BACT.1.2.15845.
- Abril, Ana G., Mónica Carrera, Karola Böhme, Jorge Barros-Velázquez, Benito Cañas, Jose L. R. Rama, Tomás G. Villa, and Pilar Calo-Mata. 2020. "Characterization of Bacteriophage Peptides of Pathogenic Streptococcus by LC-ESI-MS/MS: Bacteriophage Phylogenomics and Their Relationship to Their Host." *Frontiers in Microbiology* 11. doi: 10.3389/FMICB.2020.01241.
- Ackermann, H. W. 2007. "5500 Phages Examined in the Electron Microscope." *Archives of Virology* 152(2):227–43. doi: 10.1007/S00705-006-0849-1/METRICS.
- Ackermann, H. W., and H. M. Krisch. 1997. "A Catalogue of T4-Type Bacteriophages." *Archives of Virology* 142(12):2329–45. doi: 10.1007/S007050050246.
- Ackermann, Hans-W. 2011. "Phage or Phages." [Http://Dx.Doi.Org/10.4161/Bact.1.1.14354](http://Dx.Doi.Org/10.4161/Bact.1.1.14354) 1(1):52–53. doi: 10.4161/BACT.1.1.14354.
- Adams, M. H. 1959. "Bacteriophages." *Bacteriophages*.
- Adriaenssens, Evelien M., Hans Wolfgang Ackermann, Hany Anany, Bob Blasdel, Ian F. Connerton, David Goulding, Mansel W. Griffiths, Steven P. Hooton, Elizabeth M. Kutter, Andrew M. Kropinski, Ju Hoon Lee, Martine Maes, Derek Pickard, Sangryeol Ryu, Zargham Sepehrizadeh, S. Sabouri Shahrababak, Ana L. Toribio, and Rob Lavigne. 2012. "A Suggested New Bacteriophage Genus: 'Viunalikevirus.'" *Archives of Virology* 157(10):2035–46. doi: 10.1007/S00705-012-1360-5/FIGURES/6.
- Adriaenssens, Evelien M., and J. Rodney Brister. 2017. "How to Name and Classify Your Phage: An Informal Guide." *Viruses* 9(4). doi: 10.3390/V9040070.
- Adrian, Marc, Jacques Dubochet, Jean Lepault, and Alasdair W. McDowall. 1984. "Cryo-Electron Microscopy of Viruses." *Nature* 1984 308:5954 308(5954):32–36. doi: 10.1038/308032a0.
- Ahamed, S. K. Tousif, Banibrata Roy, Utpal Basu, Shanta Dutta, A. N. Ghosh, Boudhayan Bandyopadhyay, and Nabanita Giri. 2019. "Genomic and Proteomic Characterizations of Sfin-1, a Novel Lytic Phage Infecting Multidrug-Resistant Shigella Spp. and Escherichia Coli C." *Frontiers in Microbiology* 10(AUG). doi: 10.3389/FMICB.2019.01876.
- Aksyuk, Anastasia A., Petr G. Leiman, Lidia P. Kurochkina, Mikhail M. Shneider, Victor A. Kostyuchenko, Vadim V. Mesyanzhinov, and Michael G. Rossmann. 2009. "The Tail Sheath Structure of Bacteriophage T4: A Molecular Machine for Infecting Bacteria." *The EMBO Journal* 28(7):821–29. doi: 10.1038/EMBOJ.2009.36.
- Aksyuk, Anastasia A., Petr G. Leiman, Mikhail M. Shneider, Vadim V. Mesyanzhinov, and Michael G. Rossmann. 2009. "The Structure of Gene Product 6 of Bacteriophage T4, the Hinge-Pin of the Baseplate." *Structure* 17(6):800–808. doi: 10.1016/J.STR.2009.04.005.

- Akter, Mahmuda, Nathan Brown, Martha Clokie, Mahmuda Yeasmin, Tokee M. Tareq, Ramani Baddam, Muhammad A. K. Azad, Amar N. Ghosh, Niyaz Ahmed, and Kaisar A. Talukder. 2019. "Prevalence of *Shigella* *Boydii* in Bangladesh: Isolation and Characterization of a Rare Phage MK-13 That Can Robustly Identify Shigellosis Caused by *Shigella* *Boydii* Type 1." *Frontiers in Microbiology* 10. doi: 10.3389/FMICB.2019.02461.
- Albers, Suki, and Andreas Czech. 2016. "Exploiting TRNAs to Boost Virulence." *Life (Basel, Switzerland)* 6(1). doi: 10.3390/LIFE6010004.
- Al-Hendy, Ayman, Paavo Toivanen, and Mikael Skurnik. 1991. "Expression Cloning of *Yersinia* *Enterocolitica* O:3 Rfb Gene Cluster in *Escherichia* *Coli* K12." *Microbial Pathogenesis* 10(1):47–59. doi: 10.1016/0882-4010(91)90065-I.
- Almeida, Adelaide, Ângela Cunha, Newton C. M. Gomes, Eliana Alves, Liliana Costa, and Maria A. F. Faustino. 2009. "Phage Therapy and Photodynamic Therapy: Low Environmental Impact Approaches to Inactivate Microorganisms in Fish Farming Plants." *Marine Drugs* 7(3):268. doi: 10.3390/MD7030268.
- Amitsur, M., R. Levitz, and G. Kaufmann. 1987. "Bacteriophage T4 Anticodon Nuclease, Polynucleotide Kinase and RNA Ligase Reprocess the Host Lysine tRNA." *The EMBO Journal* 6(8):2499–2503. doi: 10.1002/J.1460-2075.1987.TB02532.X.
- Anpilov, L. I., and A. A. Prokudin. 1984. "[Preventive Effectiveness of Dried Polyvalent *Shigella* Bacteriophage in Organized Collective Farms]." *Voenno-Meditsinskii Zhurnal* (5):39–40.
- Anteneh, Zelalem Alamrew, Kassawmar Andargie, and Molalign Tarekegn. 2017. "Prevalence and Determinants of Acute Diarrhea among Children Younger than Five Years Old in Jabithennan District, Northwest Ethiopia, 2014." *BMC Public Health* 17(1):1–8. doi: 10.1186/S12889-017-4021-5.
- Ashkenazi, Shai, Itzhak Levy, Vered Kazaronovski, and Zmira Samra. 2003. "Growing Antimicrobial Resistance of *Shigella* Isolates." *The Journal of Antimicrobial Chemotherapy* 51(2):427–29. doi: 10.1093/JAC/DKG080.
- Babalova, E. G., K. Katsitadze, L. A. Sakvarelidze, N. S. Imnaishvili, T. G. Sharashidze, V. A. Badashvili, G. P. Kiknadze, A. N. Mešpariani, N. D. Gendzekhadze, E. V. Machavariani, K. L. Gogoberidze, E. I. Gozalov, and N. G. Dekanosidze. 1968. "[Preventive Value of Dried Dysentery Bacteriophage]." *Zhurnal Mikrobiologii, Epidemiologii, i Immunobiologii*.
- Bai, Xingjian, Cindy H. Nakatsu, and Arun K. Bhunia. 2021. "Bacterial Biofilms and Their Implications in Pathogenesis and Food Safety." *Foods (Basel, Switzerland)* 10(9). doi: 10.3390/FOODS10092117.
- Baker, Matthew L., Wen Jiang, Frazer J. Rixon, and Wah Chiu. 2005. "Common Ancestry of Herpesviruses and Tailed DNA Bacteriophages." *Journal of Virology* 79(23):14967–70. doi: 10.1128/JVI.79.23.14967-14970.2005.
- Baker, Timothy S., and John E. Johnson. 1996. "Low Resolution Meets High: Towards a Resolution Continuum from Cells to Atoms." *Current Opinion in Structural Biology* 6(5):585–94. doi: 10.1016/S0959-440X(96)80023-6.

- Bamford, Dennis H., Jonathan M. Grimes, and David I. Stuart. 2005. "What Does Structure Tell Us about Virus Evolution?" *Current Opinion in Structural Biology* 15(6):655–63. doi: 10.1016/J.SBI.2005.10.012.
- Bardhan, Pradip, A. S. G. Faruque, Aliya Naheed, and David A. Sack. 2010. "Decrease in Shigellosis-Related Deaths without Shigella Spp.-Specific Interventions, Asia." *Emerging Infectious Diseases* 16(11):1718–23. doi: 10.3201/EID1611.090934.
- Barrow, Paul A., and James S. Soothill. 1997. "Bacteriophage Therapy and Prophylaxis: Rediscovery and Renewed Assessment of Potential." *Trends in Microbiology* 5(7):268–71. doi: 10.1016/S0966-842X(97)01054-8.
- Barry, Eileen M., Marcela F. Pasetti, Marcelo B. Sztein, Alessio Fasano, Karen L. Kotloff, and Myron M. Levine. 2013. "Progress and Pitfalls in Shigella Vaccine Research." *Nature Reviews. Gastroenterology & Hepatology* 10(4):245–55. doi: 10.1038/NRGASTRO.2013.12.
- Barylski, Jakub, François Enault, Bas E. Dutilh, Margo B. P. Schuller, Robert A. Edwards, Annika Gillis, Jochen Klumpp, Petar Knezevic, Mart Krupovic, Jens H. Kuhn, Rob Lavigne, Hanna M. Oksanen, Matthew B. Sullivan, Ho B. I. N. Jang, Peter Simmonds, Pakorn Aiewsakun, Johannes Wittmann, Igor Tolstoy, J. Rodney Brister, Andrew M. Kropinski, and Evelien M. Adriaenssens. 2020. "Analysis of Spounaviruses as a Case Study for the Overdue Reclassification of Tailed Phages." *Systematic Biology* 69(1):110–23. doi: 10.1093/SYSBIO/SYZ036.
- Batchelor, B. I. F., J. N. Kimari, and R. J. Brindle. 1996. "Microbiology of HIV Associated Bacteraemia and Diarrhoea in Adults from Nairobi, Kenya." *Epidemiology and Infection* 117(1):139–44. doi: 10.1017/S0950268800001230.
- Batinovic, Steven, Flavia Wassef, Sarah A. Knowler, Daniel T. F. Rice, Cassandra R. Stanton, Jayson Rose, Joseph Tucci, Tadashi Nittami, Antony Vinh, Grant R. Drummond, Christopher G. Sobey, Hiu Tat Chan, Robert J. Seviour, Steve Petrovski, and Ashley E. Franks. 2019. "Bacteriophages in Natural and Artificial Environments." *Pathogens (Basel, Switzerland)* 8(3). doi: 10.3390/PATHOGENS8030100.
- Baxa, Ulrich, Stefan Steinbacher, Stefan Miller, Andrej Weintraub, Robert Huber, and Robert Seckler. 1996. "Interactions of Phage P22 Tails with Their Cellular Receptor, Salmonella O-Antigen Polysaccharide." *Biophysical Journal* 71(4):2040–48. doi: 10.1016/S0006-3495(96)79402-X.
- Bedi, Manmeet Sakshi, Vivek Verma, and Sanjay Chhibber. 2009. "Amoxicillin and Specific Bacteriophage Can Be Used Together for Eradication of Biofilm of Klebsiella Pneumoniae B5055." *World Journal of Microbiology and Biotechnology* 25(7):1145–51. doi: 10.1007/S11274-009-9991-8/METRICS.
- Bell, James M., Muyuan Chen, Philip R. Baldwin, and Steven J. Ludtke. 2016. "High Resolution Single Particle Refinement in EMAN2.1." *Methods (San Diego, Calif.)* 100:25–34. doi: 10.1016/J.YMETH.2016.02.018.
- Bennish, Michael L., and Sabeena Ahmed. 2020. "Shigellosis." *Hunter's Tropical Medicine and Emerging Infectious Diseases* 492–99. doi: 10.1016/B978-0-323-55512-8.00048-X.

- Bennish, Michael L., Mohammed A. Salam, Rukhsana Haider, and Michael Barza. 1990. "Therapy for Shigellosis. II. Randomized, Double-Blind Comparison of Ciprofloxacin and Ampicillin." *The Journal of Infectious Diseases* 162(3):711–16. doi: 10.1093/INFDIS/162.3.711.
- Benny, Edwin, Kelly Mesere, Boris I. Pavlin, Logan Yakam, Rebecca Ford, Miton Yoannes, Debbie Kisa, Mohammad Y. Abdad, Lincoln Menda, Andrew R. Greenhill, and Paul F. Horwood. 2014. "A Large Outbreak of Shigellosis Commencing in an Internally Displaced Population, Papua New Guinea, 2013." *Western Pacific Surveillance and Response Journal : WPSAR* 5(3):18–21. doi: 10.5365/WPSAR.2014.5.2.003.
- Benson, Stacy D., Jaana K. H. Bamford, Dennis H. Bamford, and Roger M. Burnett. 1999. "Viral Evolution Revealed by Bacteriophage PRD1 and Human Adenovirus Coat Protein Structures." *Cell* 98(6):825–33. doi: 10.1016/S0092-8674(00)81516-0.
- Bergh, Øivind, Knut Yngve Børsheim, Gunnar Bratbak, and Mikal Heldal. 1989a. "High Abundance of Viruses Found in Aquatic Environments." *Nature* 340(6233):467–68. doi: 10.1038/340467A0.
- Bergh, Øivind, Knut Yngve Børsheim, Gunnar Bratbak, and Mikal Heldal. 1989b. "High Abundance of Viruses Found in Aquatic Environments." *Nature* 340(6233):467–68. doi: 10.1038/340467A0.
- Bergmans, L., P. Moisiadis, B. Van Meerbeek, M. Quirynen, and P. Lambrechts. 2005. "Microscopic Observation of Bacteria: Review Highlighting the Use of Environmental SEM." *International Endodontic Journal* 38(11):775–88. doi: 10.1111/J.1365-2591.2005.00999.X.
- Bernardini, M. L., J. Mounier, H. D’Hauteville, M. Coquis-Rondon, and P. J. Sansonetti. 1989. "Identification of IcsA, a Plasmid Locus of *Shigella Flexneri* That Governs Bacterial Intra- and Intercellular Spread through Interaction with F-Actin." *Proceedings of the National Academy of Sciences* 86(10):3867–71. doi: 10.1073/PNAS.86.10.3867.
- Bertoizzi Silva, Juliano, Zachary Storms, and Dominic Sauvageau. 2016. "Host Receptors for Bacteriophage Adsorption." *FEMS Microbiology Letters* 363(4). doi: 10.1093/FEMSLE/FNW002.
- Bhattacharya, D., H. Bhattacharya, D. S. Sayi, A. P. Bharadwaj, M. Singhanian, A. P. Sugunan, and S. Roy. 2015. "Changing Patterns and Widening of Antibiotic Resistance in *Shigella* Spp. over a Decade (2000-2011), Andaman Islands, India." *Epidemiology and Infection* 143(3):470–77. doi: 10.1017/S0950268814000958.
- Bhattacharya, S., P. Datta, D. Datta, M. Bhattacharya, D. Sen, M. Saha, G. Nair, P. Das, S. Sikdar, and R. Bose. 1987. "Relative Efficacy of Trimethoprim-Sulfamethoxazole and Nalidixic Acid for Acute Invasive Diarrhea." *Antimicrobial Agents and Chemotherapy* 31(5):837. doi: 10.1128/AAC.31.5.837.
- Bhattacharya, S. K., M. K. Bhattacharya, P. Dutta, D. Sen, R. Rasaily, A. Moitra, and S. C. Pal. 1991. "Randomized Clinical Trial of Norfloxacin for Shigellosis." *American Journal of Tropical Medicine and Hygiene* 45(6):683–87. doi: 10.4269/ajtmh.1991.45.683.

- Bhetwal, Anjeela, Anjila Maharjan, Shreena Shakya, Deepa Satyal, Sumitra Ghimire, Puspa Raj Khanal, and Narayan Prasad Parajuli. 2017. "Isolation of Potential Phages against Multidrug-Resistant Bacterial Isolates: Promising Agents in the Rivers of Kathmandu, Nepal." *BioMed Research International* 2017. doi: 10.1155/2017/3723254.
- Blaser, M. J., R. A. Pollard, and R. A. Feldman. 1983. "Shigella Infections in the United States, 1974-1980." *The Journal of Infectious Diseases* 147(4):771-75. doi: 10.1093/INFDIS/147.4.771.
- Bolger-Munro, Madison, Kelvin Cheung, Anne Fang, and Lisa Wang. 2013. "T4 Bacteriophage Average Burst Size Varies with Escherichia Coli B23 Cell Culture Age." *Journal of Experimental Microbiology and Immunology (JEMI)* 17:115-19.
- Bowen, Anna, Jacqueline Hurd, Cora Hoover, Yvette Khachadourian, Elizabeth Traphagen, Emily Harvey, Tanya Libby, Sara Ehlers, Melissa Ongpin, J. Corbin Norton, Amelia Bicknese, Akiko Kimura, and Centers for Disease Control and Prevention (CDC). 2015. "Importation and Domestic Transmission of Shigella Sonnei Resistant to Ciprofloxacin — United States, May 2014–February 2015." *Morbidity and Mortality Weekly Report* 64(12):318.
- Boyd, J. S. K., and B. Portnoy. 1944. "Bacteriophage Therapy in Bacillary Dysentery." *Transactions of The Royal Society of Tropical Medicine and Hygiene* 37(4):243-62. doi: 10.1016/S0035-9203(44)90037-4.
- Branda, Steven S., Frances Chu, Daniel B. Kearns, Richard Losick, and Roberto Kolter. 2006. "A Major Protein Component of the Bacillus Subtilis Biofilm Matrix." *Molecular Microbiology* 59(4):1229-38. doi: 10.1111/J.1365-2958.2005.05020.X.
- Bratoeva, M. P., J. F. John, and N. L. Barg. 1992. "Molecular Epidemiology of Trimethoprim-Resistant Shigella Boydii Serotype 2 Strains from Bulgaria." *Journal of Clinical Microbiology* 30(6):1428-31. doi: 10.1128/JCM.30.6.1428-1431.1992.
- Breitbart, Mya, Chelsea Bonnain, Kema Malki, and Natalie A. Sawaya. 2018. "Phage Puppet Masters of the Marine Microbial Realm." *Nature Microbiology* 3(7):754-66. doi: 10.1038/S41564-018-0166-Y.
- Breitbart, Mya, Ian Hewson, Ben Felts, Joseph M. Mahaffy, James Nulton, Peter Salamon, and Forest Rohwer. 2003. "Metagenomic Analyses of an Uncultured Viral Community from Human Feces." *Journal of Bacteriology* 185(20):6220-23. doi: 10.1128/JB.185.20.6220-6223.2003.
- Breitbart, Mya, Peter Salamon, Bjarne Andresen, Joseph M. Mahaffy, Anca M. Segall, David Mead, Farooq Azam, and Forest Rohwer. 2002. "Genomic Analysis of Uncultured Marine Viral Communities." *Proceedings of the National Academy of Sciences of the United States of America* 99(22):14250-55. doi: 10.1073/PNAS.202488399.
- Brenner, S., and R. W. Horne. 1959. "A Negative Staining Method for High Resolution Electron Microscopy of Viruses." *Biochimica et Biophysica Acta* 34(C):103-10. doi: 10.1016/0006-3002(59)90237-9.
- Brilot, Axel F., James Z. Chen, Anchi Cheng, Junhua Pan, Stephen C. Harrison, Clinton S. Potter, Bridget Carragher, Richard Henderson, and Nikolaus Grigorieff. 2012. "Beam-

- Induced Motion of Vitrified Specimen on Holey Carbon Film.” *Journal of Structural Biology* 177(3):630–37. doi: 10.1016/J.JSB.2012.02.003.
- Brown, Christopher M., and Kay D. Bidle. 2014. “Attenuation of Virus Production at High Multiplicities of Infection in *Aureococcus Anophagefferens*.” *Virology* 466–467:71–81. doi: 10.1016/J.VIROL.2014.07.023.
- Brum, Jennifer R., J. Cesar Ignacio-Espinoza, Simon Roux, Guilhem Doulier, Silvia G. Acinas, Adriana Alberti, Samuel Chaffron, Corinne Cruaud, Colomban De Vargas, Josep M. Gasol, Gabriel Gorsky, Ann C. Gregory, Lionel Guidi, Pascal Hingamp, Daniele Iudicone, Fabrice Not, Hiroyuki Ogata, Stéphane Pesant, Bonnie T. Poulos, Sarah M. Schwenck, Sabrina Speich, Celine Dimier, Stefanie Kandels-Lewis, Marc Picheral, Sarah Searson, Peer Bork, Chris Bowler, Shinichi Sunagawa, Patrick Wincker, Eric Karsenti, Matthew B. Sullivan, Emmanuel Boss, Michael Follows, Nigel Grimsley, Olivier Jaillon, Lee Karp-Boss, Uros Krzic, Jeroen Raes, Emmanuel G. Reynaud, Christian Sardet, Mike Sieracki, Lars Stemmann, Didier Velayoudon, and Jean Weissenbach. 2015. “Patterns and Ecological Drivers of Ocean Viral Communities.” *Science* 348(6237):1261498. doi: 10.1126/SCIENCE.1261498.
- Brum, Jennifer R., and Matthew B. Sullivan. 2015. “Rising to the Challenge: Accelerated Pace of Discovery Transforms Marine Virology.” *Nature Reviews. Microbiology* 13(3):147–59. doi: 10.1038/NRMICRO3404.
- Callaway, Ewen. 2015. “The Revolution Will Not Be Crystallized: A New Method Sweeps through Structural Biology.” *Nature* 525(7568):172–74. doi: 10.1038/525172A.
- Campoy, Susana, Jesús Aranda, Gerard Álvarez, Jordi Barbé, and Montserrat Llagostera. 2006. “Isolation and Sequencing of a Temperate Transducing Phage for *Pasteurella Multocida*.” *Applied and Environmental Microbiology* 72(5):3154–60. doi: 10.1128/AEM.72.5.3154-3160.2006.
- Caramia, Giuseppe, Stefania Silvi, Maria Cristina Verdenelli, and Maria Magdalena Coman. 2015. “Treatment of Acute Diarrhoea: Past and Now.” *International Journal of Enteric Pathogens* 3(4). doi: 10.17795/IJEP28612.
- Cardarelli, Lia, Lisa G. Pell, Philipp Neudecker, Nawaz Pirani, Amanda Liu, Lindsay A. Baker, John L. Rubinstein, Karen L. Maxwell, and Alan R. Davidson. 2010. “Phages Have Adapted the Same Protein Fold to Fulfill Multiple Functions in Virion Assembly.” *Proceedings of the National Academy of Sciences of the United States of America* 107(32):14384–89. doi: 10.1073/PNAS.1005822107/SUPPL\_FILE/PNAS.201005822SI.PDF.
- Carmody, Caitlin M., Julie M. Goddard, and Sam R. Nugen. 2021. “Bacteriophage Capsid Modification by Genetic and Chemical Methods.” *Bioconjugate Chemistry* 32(3):466–81. doi: 10.1021/ACS.BIOCONJCHEM.1C00018.
- Casjens, Sherwood R. 2011. “The DNA-Packaging Nanomotor of Tailed Bacteriophages.” *Nature Reviews. Microbiology* 9(9):647–57. doi: 10.1038/NRMICRO2632.
- Cegelski, Lynette, Jerome S. Pinkner, Neal D. Hammer, Corinne K. Cusumano, Chia S. Hung, Erik Chorell, Veronica Åberg, Jennifer N. Walker, Patrick C. Seed, Fredrik Almqvist,



- Matthew R. Chapman, and Scott J. Hultgren. 2009. "Small-Molecule Inhibitors Target Escherichia Coli Amyloid Biogenesis and Biofilm Formation." *Nature Chemical Biology* 5(12):913–19. doi: 10.1038/NCHEMBIO.242.
- Cerca, Nuno, Kimberly K. Jefferson, Rosario Oliveira, Gerald B. Pier, and Joana Azeredo. 2006. "Comparative Antibody-Mediated Phagocytosis of Staphylococcus Epidermidis Cells Grown in a Biofilm or in the Planktonic State." *Infection and Immunity* 74(8):4849. doi: 10.1128/IAI.00230-06.
- Cerritelli, Mario E., James F. Conway, Naiqian Cheng, Benes L. Trus, and Alasdair C. Steven. 2003. "Molecular Mechanisms in Bacteriophage T7 Procapsid Assembly, Maturation, and DNA Containment." *Advances in Protein Chemistry* 64:301–23. doi: 10.1016/S0065-3233(03)01008-8.
- Chanishvili, Nina. 2012. "Phage Therapy--History from Twort and d'Herelle through Soviet Experience to Current Approaches." *Advances in Virus Research* 83:3–40. doi: 10.1016/B978-0-12-394438-2.00001-3.
- Chaudhry, Waqas Nasir, Jeniffer Concepcion-Acevedo, Taehyun Park, Saadia Andleeb, James J. Bull, and Bruce R. Levin. 2017. "Synergy and Order Effects of Antibiotics and Phages in Killing Pseudomonas Aeruginosa Biofilms." *PloS One* 12(1). doi: 10.1371/JOURNAL.PONE.0168615.
- Chen, James Z., and Nikolaus Grigorieff. 2007. "SIGNATURE: A Single-Particle Selection System for Molecular Electron Microscopy." *Journal of Structural Biology* 157(1):168–73. doi: 10.1016/J.JSB.2006.06.001.
- Chen, Ling, Jiqiang Fan, Tingwei Yan, Quan Liu, Shengjian Yuan, Haoran Zhang, Jinfang Yang, Deng Deng, Shuqiang Huang, and Yingfei Ma. 2019. "Isolation and Characterization of Specific Phages to Prepare a Cocktail Preventing Vibrio Sp. Va-F3 Infections in Shrimp ( Litopenaeus Vannamei)." *Frontiers in Microbiology* 10. doi: 10.3389/FMICB.2019.02337.
- Chen, Zhenguo, Lei Sun, Zhihong Zhang, Andrei Fokine, Victor Padilla-Sanchez, Dorit Hanein, Wen Jiang, Michael G. Rossmann, and Venigalla B. Rao. 2017. "Cryo-EM Structure of the Bacteriophage T4 Isometric Head at 3.3-Å Resolution and Its Relevance to the Assembly of Icosahedral Viruses." *Proceedings of the National Academy of Sciences of the United States of America* 114(39):E8184–93. doi: 10.1073/PNAS.1708483114.
- Cheng, Lingpeng, Jiang Zhu, Wong Hoi Hui, Xiaokang Zhang, Barry Honig, Qin Fang, and Z. Hong Zhou. 2010. "Backbone Model of an Aquareovirus Virion by Cryo-Electron Microscopy and Bioinformatics." *Journal of Molecular Biology* 397(3):852–63. doi: 10.1016/J.JMB.2009.12.027.
- Chipman, Paul R., Mavis Agbandje-McKenna, Joël Renaudin, Timothy S. Baker, and Robert McKenna. 1998. "Structural Analysis of the Spiroplasma Virus, SpV4: Implications for Evolutionary Variation to Obtain Host Diversity among the Microviridae." *Structure (London, England : 1993)* 6(2):135–45. doi: 10.1016/S0969-2126(98)00016-1.

- Choi, Charles, Eugene Kuatsjah, Elizabeth Wu, and Serena Yuan. 2010. "The Effect of Cell Size on the Burst Size of T4 Bacteriophage Infections of Escherichia Coli B23." *Journal of Experimental Microbiology and Immunology (JEMI)* 14:85–91.
- Christopher, Prince Rh, Kirubah V David, Sushil M. John, and Venkatesan Sankarapandian. 2010. "Antibiotic Therapy for Shigella Dysentery." *The Cochrane Database of Systematic Reviews* 2010(8):CD006784. doi: 10.1002/14651858.CD006784.pub4.
- Christopher, Prince Rh, Kirubah v David, Sushil M. John, and Venkatesan Sankarapandian. 2010. "Antibiotic Therapy for Shigella Dysentery." *The Cochrane Database of Systematic Reviews* 2010(8):CD006784. doi: 10.1002/14651858.CD006784.pub4.
- Chua, James E. H., Paul A. Manning, and Renato Morona. 1999. "The Shigella Flexneri Bacteriophage Sf6 Tailspike Protein (TSP)/Endorhamnosidase Is Related to the Bacteriophage P22 TSP and Has a Motif Common to Exo- and Endoglycanases, and C-5 Epimerases." *Microbiology* 145(7):1649–59. doi: 10.1099/13500872-145-7-1649/CITE/REFWORKS.
- Chung, Jae-Hee, and Ho Min Kim. 2017. "The Nobel Prize in Chemistry 2017: High-Resolution Cryo-Electron Microscopy." *Applied Microscopy* 47(4):218–22. doi: 10.9729/AM.2017.47.4.218.
- Ciofu, Oana, Estrella Rojo-Molinero, María D. Macià, and Antonio Oliver. 2017. "Antibiotic Treatment of Biofilm Infections." *APMIS: Acta Pathologica, Microbiologica, et Immunologica Scandinavica* 125(4):304–19. doi: 10.1111/APM.12673.
- Clark, Jason R., and John B. March. 2006. "Bacteriophages and Biotechnology: Vaccines, Gene Therapy and Antibacterials." *Trends in Biotechnology* 24(5):212–18. doi: 10.1016/J.TIBTECH.2006.03.003.
- CLEMENS, JOHN D., BONITA STANTON, BARBARA STOLL, NIGAR S. SHAHID, HASINA BANU, and A. K. M. ALAUDDIN CHOWDHURY. 1986. "Breast Feeding As a Determinant of Severity in Shigellosis." *American Journal of Epidemiology* 123(4):710–20. doi: 10.1093/oxfordjournals.aje.a114291.
- Clokier, Martha R. J., Andrew D. Millard, Andrey V. Letarov, and Shaun Heaphy. 2011a. "Phages in Nature." *Bacteriophage* 1(1):31–45. doi: 10.4161/bact.1.1.14942.
- Clokier, Martha R. J., Andrew D. Millard, Andrey V. Letarov, and Shaun Heaphy. 2011b. "Phages in Nature." *Bacteriophage* 1(1):31–45. doi: 10.4161/BACT.1.1.14942.
- Conrad, Arnaud, Merja Kontro, Minna M. Keinänen, Aurore Cadoret, Pierre Faure, Laurence Mansuy-Huault, and Jean Claude Block. 2003. "Fatty Acids of Lipid Fractions in Extracellular Polymeric Substances of Activated Sludge Flocs." *Lipids* 38(10):1093–1105. doi: 10.1007/S11745-006-1165-Y/METRICS.
- Conway, J. F., W. R. Wikoff, N. Cheng, R. L. Duda, R. W. Hendrix, J. E. Johnson, and A. C. Steven. 2001. "Virus Maturation Involving Large Subunit Rotations and Local Refolding." *Science* 292(5517):744–48. doi: 10.1126/SCIENCE.1058069.

- 227 | Page

- d'Herelle, F. 1931. "Annual Graduate Fortnight. Medical and Surgical Aspects of Acute Bacterial Infections, October 20 to 31, 1930: Bacteriophage as a Treatment in Acute Medical and Surgical Infections." *Bulletin of the New York Academy of Medicine* 7(5):329.
- D'Herelle, M. F. 1961. "Sur Un Microbe Invisible Antagoniste Des Bacilles Dysenteriques."
- D'herelle, Mr F., and Mr Roux. n.d. "On an Invisible Microbe Antagonistic toward Dysenteric Bacilli: Brief Note." doi: 10.1016/j.resmic.2007.07.005.
- Ding, Tongyan, Huzhi Sun, Qiang Pan, Feiyang Zhao, Zhaozuo Zhang, and Huiying Ren. 2020. "Isolation and Characterization of Vibrio Parahaemolyticus Bacteriophage VB\_VpaS\_PG07." *Virus Research* 286. doi: 10.1016/J.VIRUSRES.2020.198080.
- Dini, Cecilia, Germán A. Islan, Patricio J. de Urreaza, and Guillermo R. Castro. 2012. "Novel Biopolymer Matrices for Microencapsulation of Phages: Enhanced Protection against Acidity and Protease Activity." *Macromolecular Bioscience* 12(9):1200–1208. doi: 10.1002/MABI.201200109.
- Dion, Moïra B., Frank Oechslin, and Sylvain Moineau. 2020. "Phage Diversity, Genomics and Phylogeny." *Nature Reviews. Microbiology* 18(3):125–38. doi: 10.1038/S41579-019-0311-5.
- Domingo-Calap, Pilar, and Jennifer Delgado-Martínez. 2018. "Bacteriophages: Protagonists of a Post-Antibiotic Era." *Antibiotics (Basel, Switzerland)* 7(3). doi: 10.3390/ANTIBIOTICS7030066.
- Donate, Luis E., L. Herranz, Juan P. Secilla, JoséM M. Carazo, Hisao Fujisawa, and JoséL L. Carrascosa. 1988. "Bacteriophage T3 Connector: Three-Dimensional Structure and Comparison with Other Viral Head-Tail Connecting Regions." *Journal of Molecular Biology* 201(1):91–100. doi: 10.1016/0022-2836(88)90441-X.
- Donlan, Rodney M., and J. William Costerton. 2002. "Biofilms: Survival Mechanisms of Clinically Relevant Microorganisms." *Clinical Microbiology Reviews* 15(2):167–93. doi: 10.1128/CMR.15.2.167-193.2002.
- Duarte, Carlos M. 2015. "Seafaring in the 21St Century: The Malaspina 2010 Circumnavigation Expedition." *Limnology and Oceanography Bulletin* 24(1):11–14. doi: 10.1002/LOB.10008.
- Duda, Robert L., and Carolyn M. Teschke. 2019. "The Amazing HK97 Fold: Versatile Results of Modest Differences." *Current Opinion in Virology* 36:9–16. doi: 10.1016/J.COVIRO.2019.02.001.
- Dunn, John J., F. William Studier, and M. Gottesman. 1983. "Complete Nucleotide Sequence of Bacteriophage T7 DNA and the Locations of T7 Genetic Elements." *Journal of Molecular Biology* 166(4):477–535. doi: 10.1016/S0022-2836(83)80282-4.
- Dutilh, Bas E., Noriko Cassman, Katelyn McNair, Savannah E. Sanchez, Genivaldo G. Z. Silva, Lance Boling, Jeremy J. Barr, Daan R. Speth, Victor Seguritan, Ramy K. Aziz, Ben Felts, Elizabeth A. Dinsdale, John L. Mokili, and Robert A. Edwards. 2014. "A Highly Abundant Bacteriophage Discovered in the Unknown Sequences of Human Faecal Metagenomes." *Nature Communications* 2014 5:1 5(1):1–11. doi: 10.1038/ncomms5498.

- Dutta, Moumita, and Amar N. Ghosh. 2007. "Physicochemical Characterization of El Tor Vibriophage S20." *Intervirology* 50(4):264–72. doi: 10.1159/000102469.
- Düzgüneş, Nejat, Melike Sessevmez, and Metin Yildirim. 2021. "Bacteriophage Therapy of Bacterial Infections: The Rediscovered Frontier." *Pharmaceuticals (Basel, Switzerland)* 14(1):1–16. doi: 10.3390/PH14010034.
- E., GOLDBERG. 1994a. "Recognition Attachment, and Injection." *Molecular Biology of Bacteriophage T4* 347–56.
- E., GOLDBERG. 1994b. "Recognition Attachment, and Injection." *Molecular Biology of Bacteriophage T4* 347–56.
- Earnshaw, William C., and Sherwood R. Casjens. 1980. "DNA Packaging by the Double-Stranded DNA Bacteriophages." *Cell* 21(2):319–31. doi: 10.1016/0092-8674(80)90468-7.
- Eisenstein, Michael. 2012. "Oxford Nanopore Announcement Sets Sequencing Sector Abuzz." *Nature Biotechnology* 30(4):295–96. doi: 10.1038/NBT0412-295.
- Elbreki, Mohamed, R. Paul Ross, Colin Hill, Jim O'Mahony, Olivia McAuliffe, and Aidan Coffey. 2014. "Bacteriophages and Their Derivatives as Biotherapeutic Agents in Disease Prevention and Treatment." *Journal of Viruses* 2014:1–20. doi: 10.1155/2014/382539.
- Elmlund, Dominika, and Hans Elmlund. 2012. "SIMPLE: Software for Ab Initio Reconstruction of Heterogeneous Single-Particles." *Journal of Structural Biology* 180(3):420–27. doi: 10.1016/J.JSB.2012.07.010.
- Fasano, A., F. R. Noriega, F. M. Liao, W. Wang, and M. M. Levine. 1997. "Effect of Shigella Enterotoxin 1 (ShET1) on Rabbit Intestine in Vitro and in Vivo." *Gut* 40(4):505–11. doi: 10.1136/GUT.40.4.505.
- Fennema, Owen R. 1996. "Food Chemistry, Third Edition (Google EBook)." 1067.
- Fernandez-Prada, C. M., M. M. Venkatesan, A. A. Franco, C. F. Lanata, R. B. Sack, A. B. Hartman, and W. Spira. 2004. "Molecular Epidemiology of Shigella Flexneri in a Diarrhoea-Endemic Area of Lima, Peru." *Epidemiology and Infection* 132(2):303–16. doi: 10.1017/S0950268803001560.
- Ferreccio, Catherine, Valeria Prado, Alicia Ojeda, Marisol Cayyazo, Paulina Abrego, Linda Guers, and Myron M. Levine. 1991. "Epidemiologic Patterns of Acute Diarrhea and Endemic Shigella Infections in Children in a Poor Periurban Setting in Santiago, Chile." *American Journal of Epidemiology* 134(6):614–27. doi: 10.1093/OXFORDJOURNALS.AJE.A116134.
- Ferriol-González, Celia, and Pilar Domingo-Calap. 2020. "Phages for Biofilm Removal." *Antibiotics (Basel, Switzerland)* 9(5). doi: 10.3390/ANTIBIOTICS9050268.
- Financsek, I., I. Ketyi, W. Sasak, W. Jankowski, E. Janczura, and T. Chojnacki. 1976. "Phage-Dependent Changes in Shigella Flexneri Type Antigen Synthesis." *Infection and Immunity* 14(6):1290. doi: 10.1128/IAI.14.6.1290-1292.1976.

- Fineran, Peter C., Tim R. Blower, Ian J. Foulds, David P. Humphreys, Kathryn S. Lilley, and George P. C. Salmond. 2009. "The Phage Abortive Infection System, ToxIN, Functions as a Protein-RNA Toxin-Antitoxin Pair." *Proceedings of the National Academy of Sciences of the United States of America* 106(3):894–99. doi: 10.1073/PNAS.0808832106.
- Fischetti, Vincent A. 2001. "Phage Antibacterials Make a Comeback." *Nature Biotechnology* 2001 19:8 19(8):734–35. doi: 10.1038/90777.
- Fischetti, Vincent A. 2008. "Bacteriophage Lysins as Effective Antibacterials." *Current Opinion in Microbiology* 11(5):393–400. doi: 10.1016/J.MIB.2008.09.012.
- Flemming, Hans Curt, and Jost Wingender. 2010. "The Biofilm Matrix." *Nature Reviews. Microbiology* 8(9):623–33. doi: 10.1038/NRMICRO2415.
- Frost, Laura S., Raphael Leplae, Anne O. Summers, and Ariane Toussaint. 2005. "Mobile Genetic Elements: The Agents of Open Source Evolution." *Nature Reviews Microbiology* 2005 3:9 3(9):722–32. doi: 10.1038/nrmicro1235.
- Fruciano, Emiliano, and Shawna Bourne. 2007. "Phage as an Antimicrobial Agent: D'Herelle's Heretical Theories and Their Role in the Decline of Phage Prophylaxis in the West." *The Canadian Journal of Infectious Diseases & Medical Microbiology = Journal Canadien Des Maladies Infectieuses et de La Microbiologie Medicale* 18(1):19–26. doi: 10.1155/2007/976850.
- Gallet, Romain, Sherin Kannoly, and Ing Nang Wang. 2011. "Effects of Bacteriophage Traits on Plaque Formation." *BMC Microbiology* 11:181. doi: 10.1186/1471-2180-11-181.
- Gaynor, Kate, S. Y. Park, R. Kanenaka, R. Colindres, E. Mintz, P. K. Ram, P. Kitsutani, M. Nakata, S. Wedel, D. Boxrud, D. Jennings, H. Yoshida, N. Tosaka, H. He, M. Ching-Lee, and P. V. Effler. 2009. "International Foodborne Outbreak of Shigella Sonnei Infection in Airline Passengers." *Epidemiology and Infection* 137(3):335–41. doi: 10.1017/S0950268807000064.
- Geredew Kifelew, Legesse, James G. Mitchell, and Peter Speck. 2019. "Mini-Review: Efficacy of Lytic Bacteriophages on Multispecies Biofilms." <https://doi.org/10.1080/08927014.2019.1613525> 35(4):472–81. doi: 10.1080/08927014.2019.1613525.
- Gill, Jason, and Paul Hyman. 2010. "Phage Choice, Isolation, and Preparation for Phage Therapy." *Current Pharmaceutical Biotechnology* 11(1):2–14. doi: 10.2174/138920110790725311.
- Girardin, Stephen E., Ivo G. Boneca, Leticia A. M. Carneiro, Aude Antignac, Muguette Jéhanno, Jérôme Viala, Karsten Tedin, Muhamed-Kheir Taha, Agnès Labigne, Ulrich Zähringer, Anthony J. Coyle, Peter S. DiStefano, John Bertin, Philippe J. Sansonetti, Dana J. Philpott, Stephen E. Girardin, Ivo G. Boneca, Leticia A. M. Carneiro, Aude Antignac, Muguette Jéhanno, Jérôme Viala, Karsten Tedin, Muhamed-Kheir Taha, Agnès Labigne, Ulrich Zähringer, Anthony J. Coyle, Peter S. DiStefano, John Bertin, Philippe J. Sansonetti, and Dana J. Philpott. 2003. "Nod1 Detects a Unique Muropeptide from Gram-Negative Bacterial Peptidoglycan." *Sci* 300(5625):1584–87. doi: 10.1126/SCIENCE.1084677.

- Gjermansen, Morten, Martin Nilsson, Liang Yang, and Tim Tolker-Nielsen. 2010. "Characterization of Starvation-Induced Dispersion in *Pseudomonas Putida* Biofilms: Genetic Elements and Molecular Mechanisms." *Molecular Microbiology* 75(4):815–26. doi: 10.1111/J.1365-2958.2009.06793.X.
- Goldsmith, Cynthia S., and Sara E. Miller. 2009. "Modern Uses of Electron Microscopy for Detection of Viruses." *Clinical Microbiology Reviews* 22(4):552–63. doi: 10.1128/CMR.00027-09.
- Goodridge, Lawrence D. 2013. "Bacteriophages for Managing *Shigella* in Various Clinical and Non-Clinical Settings." *Bacteriophage* 3(1):e25098. doi: 10.4161/BACT.25098.
- Goulet, Adeline, and Christian Cambillau. 2022. "Present Impact of AlphaFold2 Revolution on Structural Biology, and an Illustration With the Structure Prediction of the Bacteriophage J-1 Host Adhesion Device." *Frontiers in Molecular Biosciences* 9. doi: 10.3389/FMOLB.2022.907452.
- Greenberg, N., and S. Rottem. 1979. "Composition and Molecular Organization of Lipids and Proteins in the Envelope of Mycoplasma virus MVL2." *Journal of Virology* 32(3):717. doi: 10.1128/JVI.32.3.717-726.1979.
- Grose, Julianne H., and Sherwood R. Casjens. 2014. "Understanding the Enormous Diversity of Bacteriophages: The Tailed Phages That Infect the Bacterial Family Enterobacteriaceae." *Virology* 468–470:421–43. doi: 10.1016/J.VIROL.2014.08.024.
- Gu, Bing, Yan Cao, Shiyang Pan, Ling Zhuang, Rongbin Yu, Zhihang Peng, Huimin Qian, Yongyue Wei, Lianying Zhao, Genyan Liu, and Mingqing Tong. 2012. "Comparison of the Prevalence and Changing Resistance to Nalidixic Acid and Ciprofloxacin of *Shigella* between Europe-America and Asia-Africa from 1998 to 2009." *International Journal of Antimicrobial Agents* 40(1):9–17. doi: 10.1016/j.ijantimicag.2012.02.005.
- Guiton, Pascale S., Chia S. Hung, Kimberly A. Kline, Robyn Roth, Andrew L. Kau, Ericka Hayes, John Heuser, Karen W. Dodson, Michael G. Caparon, and Scott J. Hultgren. 2009. "Contribution of Autolysin and Sortase a during *Enterococcus Faecalis* DNA-Dependent Biofilm Development." *Infection and Immunity* 77(9):3626–38. doi: 10.1128/IAI.00219-09.
- Gutiérrez, Diana, Patricia Ruas-Madiedo, Beatriz Martínez, Ana Rodríguez, and Pilar García. 2014. "Effective Removal of Staphylococcal Biofilms by the Endolysin LysH5." *PloS One* 9(9). doi: 10.1371/JOURNAL.PONE.0107307.
- Hacking, Sean, and Vanesa Bijol. 2021. "Deep Learning for the Classification of Medical Kidney Disease: A Pilot Study for Electron Microscopy." *Ultrastructural Pathology* 45(2):118–27. doi: 10.1080/01913123.2021.1882628.
- Hagen, E. W., B. E. Reilly, M. E. Tosi, and D. L. Anderson. 1976. "Analysis of Gene Function of Bacteriophage Phi 29 of *Bacillus Subtilis*: Identification of Cistrons Essential for Viral Assembly." *Journal of Virology* 19(2):501–17. doi: 10.1128/JVI.19.2.501-517.1976.
- Haler, David. 1938. "Use of the Bacteriophage in an Outbreak of Dysentery." *British Medical Journal* 2(4056):698–700. doi: 10.1136/BMJ.2.4056.698.

HALL, C. E. 1966. "INTRODUCTION TO ELECTRON MICROSCOPY."

Hall-Stoodley, Luanne, J. William Costerton, and Paul Stoodley. 2004. "Bacterial Biofilms: From the Natural Environment to Infectious Diseases." *Nature Reviews. Microbiology* 2(2):95–108. doi: 10.1038/NRMICRO821.

Hall-Stoodley, Luanne, and Paul Stoodley. 2009. "Evolving Concepts in Biofilm Infections." *Cellular Microbiology* 11(7):1034–43. doi: 10.1111/J.1462-5822.2009.01323.X.

Haltalin, Kenneth C., John D. Nelson, Helen T. Kusmiesz, and Lula V. Hinton. 1968. "Comparison of Intramuscular and Oral Ampicillin Therapy for Shigellosis." *The Journal of Pediatrics* 73(4):617–22. doi: 10.1016/S0022-3476(68)80282-3.

Hao, Guijuan, Chaoqun Yuan, Rundong Shu, Yuanqi Jia, Suqin Zhao, Saijun Xie, Ming Liu, Haijian Zhou, Shuhong Sun, and Hui Wang. 2021. "O-Antigen Serves as a Two-Faced Host Factor for Bacteriophage NJS1 Infecting Nonmucoid *Klebsiella Pneumoniae*." *Microbial Pathogenesis* 155. doi: 10.1016/J.MICPATH.2021.104897.

Harper, David R., Helena M. R. T. Parracho, James Walker, Richard Sharp, Gavin Hughes, Maria Werthén, Susan Lehman, and Sandra Morales. 2014. "Bacteriophages and Biofilms." *Antibiotics* 3(3):270–84. doi: 10.3390/ANTIBIOTICS3030270.

Harris, J. Robin, and Sacha De Carlo. 2014. "Negative Staining and Cryo-Negative Staining: Applications in Biology and Medicine." *Methods in Molecular Biology* 1117:215–58. doi: 10.1007/978-1-62703-776-1\_11/COVER.

Harrison, S. C., A. J. Olson, C. E. Schutt, F. K. Winkler, and G. Bricogne. 1978. "Tomato Bushy Stunt Virus at 2.9 Å Resolution." *Nature* 1978 276:5686 276(5686):368–73. doi: 10.1038/276368a0.

Hatfull, Graham F., and Roger W. Hendrix. 2011. "Bacteriophages and Their Genomes." *Current Opinion in Virology* 1(4):298–303. doi: 10.1016/J.COVIRO.2011.06.009.

Hatfull, Graham F., and Gary J. Sarkis. 1993. "DNA Sequence, Structure and Gene Expression of Mycobacteriophage L5: A Phage System for Mycobacterial Genetics." *Molecular Microbiology* 7(3):395–405. doi: 10.1111/J.1365-2958.1993.TB01131.X.

Hayani, K. C., M. L. Guerrero, G. M. Ruiz-Palacios, H. F. Gomez, and T. G. Cleary. 1991. "Evidence for Long-Term Memory of the Mucosal Immune System: Milk Secretory Immunoglobulin A against *Shigella* Lipopolysaccharides." *Journal of Clinical Microbiology* 29(11):2599–2603. doi: 10.1128/jcm.29.11.2599-2603.1991.

He, Fan, Ke Han, Lunguang Liu, Wei Sun, Lijie Zhang, Baoping Zhu, and Huilai Ma. 2012. "Shigellosis Outbreak Associated with Contaminated Well Water in a Rural Elementary School: Sichuan Province, China, June 7–16, 2009." *PLOS ONE* 7(10):e47239. doi: 10.1371/JOURNAL.PONE.0047239.

He, Shaoda, and Sjors H. W. Scheres. 2017. "Helical Reconstruction in RELION." *Journal of Structural Biology* 198(3):163–76. doi: 10.1016/J.JSB.2017.02.003.

Van Heel, Marin, Brent Gowen, Rishi Matadeen, Elena V. Orlova, Robert Finn, Tillmann Pape, Dana Cohen, Holger Stark, Ralf Schmidt, Michael Schatz, and Ardan Patwardhan. 2000.



- “Single-Particle Electron Cryo-Microscopy: Towards Atomic Resolution.” *Quarterly Reviews of Biophysics* 33(4):307–69. doi: 10.1017/S0033583500003644.
- HL, DuPont. 2010. *Shigella Species (Bacillary Dysentery)*. Elsevier: Philadelphia;
- HL, DuPont, Levine MM, Hornick RB, and Formal SB. 1989. “Inoculum Size in Shigellosis and Implications for Expected Mode of Transmission.” *The Journal of Infectious Diseases* 159(6):1126–28. doi: 10.1093/INFDIS/159.6.1126.
- Hobbs, Zack, and Stephen T. Abedon. 2016. “Diversity of Phage Infection Types and Associated Terminology: The Problem with ‘Lytic or Lysogenic.’” *FEMS Microbiology Letters* 363(7). doi: 10.1093/FEMSLE/FNW047.
- Høiby, Niels. 2017. “A Short History of Microbial Biofilms and Biofilm Infections.” *APMIS* 125(4):272–75. doi: 10.1111/APM.12686.
- Holm, Liisa. 2022. “Dali Server: Structural Unification of Protein Families.” *Nucleic Acids Research* 50(W1):W210–15. doi: 10.1093/NAR/GKAC387.
- Hoyle, Naomi, and Elizabeth Kutter. 2021. “Phage Therapy: Bacteriophages as Natural, Self-Replicating Antimicrobials.” *Practical Handbook of Microbiology* 801–24. doi: 10.1201/9781003099277-57.
- Huang, Liang, and Ye Xiang. 2020. “Structures of the Tailed Bacteriophages That Infect Gram-Positive Bacteria.” *Current Opinion in Virology* 45:65–74. doi: 10.1016/J.COVIRO.2020.09.002.
- Hurwitz, B. L., and M. B. Sullivan. 2013. “The Pacific Ocean Virome (POV): A Marine Viral Metagenomic Dataset and Associated Protein Clusters for Quantitative Viral Ecology) The Pacific Ocean Virome (POV): A Marine Viral Metagenomic Dataset and Associated Protein Clusters for Quantitative Viral Ecology.” *PLoS ONE* 8(2):57355. doi: 10.1371/journal.pone.0057355.
- Islam, Dilara, Lisa Bandholtz, Jakob Nilsson, Hans Wigzell, Birger Christensson, Birgitta Agerberth, and Gudmundur H. Gudmundsson. 2001. “Downregulation of Bactericidal Peptides in Enteric Infections: A Novel Immune Escape Mechanism with Bacterial DNA as a Potential Regulator.” *Nature Medicine* 7(2):180–85. doi: 10.1038/84627.
- Islam, Dilara, Béla Veress, Pradip Kumar Bardhan, Alf A. Lindberg, and Birger Christensson. 1997. “In Situ Characterization of Inflammatory Responses in the Rectal Mucosae of Patients with Shigellosis.” *Infection and Immunity* 65(2):739–49. doi: 10.1128/IAI.65.2.739-749.1997.
- Jamal, Muhsin, Waqas Nasir Chaudhry, Tahir Hussain, Chythanya Rajanna Das, and Saadia Andleeb. 2015. “Characterization of New Myoviridae Bacteriophage WZ1 against Multi-Drug Resistant (MDR) *Shigella Dysenteriae*.” *Journal of Basic Microbiology* 55(4):420–31. doi: 10.1002/JOBM.201400688.
- Jefferson, Kimberly K., Donald A. Goldmann, and Gerald B. Pier. 2005. “Use of Confocal Microscopy to Analyze the Rate of Vancomycin Penetration through *Staphylococcus Aureus* Biofilms.” *Antimicrobial Agents and Chemotherapy* 49(6):2467–73. doi: 10.1128/AAC.49.6.2467-2473.2005.

- Jiang, Wen, Juan Chang, Joanita Jakana, Peter Weigele, Jonathan King, and Wah Chiu. 2006. "Structure of Epsilon15 Bacteriophage Reveals Genome Organization and DNA Packaging/Injection Apparatus." *Nature* 439(7076):612–16. doi: 10.1038/NATURE04487.
- Jończyk, E., M. Kłak, R. Międzybrodzki, and A. Górski. 2011. "The Influence of External Factors on Bacteriophages--Review." *Folia Microbiologica* 56(3):191–200. doi: 10.1007/S12223-011-0039-8.
- Jordan, Tuajuanda C., Sandra H. Burnett, Susan Carson, Steven M. Caruso, Kari Clase, Randall J. DeJong, John J. Dennehy, Dee R. Denver, David Dunbar, Sarah C. R. Elgin, Ann M. Findley, Chris R. Gissendanner, Urszula P. Golebiewska, Nancy Guild, Grant A. Hartzog, Wendy H. Grillo, Gail P. Hollowell, Lee E. Hughes, Allison Johnson, Rodney A. King, Lynn O. Lewis, Wei Li, Frank Rosenzweig, Michael R. Rubin, Margaret S. Saha, James Sandoz, Christopher D. Shaffer, Barbara Taylor, Louise Temple, Edwin Vazquez, Vassie C. Ware, Lucia P. Barker, Kevin W. Bradley, Deborah Jacobs-Sera, Welkin H. Pope, Daniel A. Russell, Steven G. Cresawn, David Lopatto, Cheryl P. Bailey, and Graham F. Hatfull. 2014. "A Broadly Implementable Research Course in Phage Discovery and Genomics for First-Year Undergraduate Students." *MBio* 5(1). doi: 10.1128/MBIO.01051-13.
- Jumper, John, Richard Evans, Alexander Pritzel, Tim Green, Michael Figurnov, Olaf Ronneberger, Kathryn Tunyasuvunakool, Russ Bates, Augustin Židek, Anna Potapenko, Alex Bridgland, Clemens Meyer, Simon A. A. Kohl, Andrew J. Ballard, Andrew Cowie, Bernardino Romera-Paredes, Stanislav Nikolov, Rishub Jain, Jonas Adler, Trevor Back, Stig Petersen, David Reiman, Ellen Clancy, Michal Zielinski, Martin Steinegger, Michalina Pacholska, Tamas Berghammer, Sebastian Bodenstein, David Silver, Oriol Vinyals, Andrew W. Senior, Koray Kavukcuoglu, Pushmeet Kohli, and Demis Hassabis. 2021. "Highly Accurate Protein Structure Prediction with AlphaFold." *Nature* 2021 596:7873 596(7873):583–89. doi: 10.1038/s41586-021-03819-2.
- Junqueira, Magno, Victor Spirin, Tiago Santana Balbuena, Henrik Thomas, Ivan Adzhubei, Shamil Sunyaev, and Andrej Shevchenko. 2008. "Protein Identification Pipeline for the Homology-Driven Proteomics." *Journal of Proteomics* 71(3):346–56. doi: 10.1016/J.JPROT.2008.07.003.
- Kania, Dane A., Tracy H. Hazen, Anowar Hossain, James P. Nataro, and David A. Rasko. 2016. "Genome Diversity of *Shigella* *Boydii*." *Pathogens and Disease* 74(4):ftw027. doi: 10.1093/FEMSPD/FTW027.
- Kaoukab-Raji, Abdelmoughit, Latéfa Biskri, and Abdelmounaaim Allaoui. 2020. "Inactivation of the Sfgtr4 Gene of *Shigella* *Flexneri* Induces Biofilm Formation and Affects Bacterial Pathogenicity." *Microorganisms* 8(6). doi: 10.3390/MICROORGANISMS8060841.
- Karam, Jim D., and Eric S. Miller. 2010. "Bacteriophage T4 and Its Relatives." *Virology Journal* 7(1):1–4. doi: 10.1186/1743-422X-7-293/METRICS.
- Kauffman, Kathryn M., Fatima A. Hussain, Joy Yang, Philip Arevalo, Julia M. Brown, William K. Chang, David Vaninsberghe, Joseph Elsherbini, Radhey S. Sharma, Michael B. Cutler, Libusha Kelly, and Martin F. Polz. 2018. "A Major Lineage of Non-Tailed DsDNA Viruses

- as Unrecognized Killers of Marine Bacteria.” *Nature* 2018 554:7690 554(7690):118–22. doi: 10.1038/nature25474.
- Kausche, G. A., E. Pfankuch, and H. Ruska. 1939. “Die Sichtbarmachung von Pflanzlichem Virus Im Übermikroskop.” *Die Naturwissenschaften* 27(18):292–99. doi: 10.1007/BF01493353/METRICS.
- Kellenberger, Eduard, and Heidi Wunderli-Allenspach. 1995. “Electron Microscopic Studies on Intracellular Phage Development—History and Perspectives.” *Micron* 26(3):213–45. doi: 10.1016/0968-4328(94)00051-Q.
- Kelley, Lawrence A., Stefans Mezulis, Christopher M. Yates, Mark N. Wass, and Michael J. E. Sternberg. 2015. “The Phyre2 Web Portal for Protein Modeling, Prediction and Analysis.” *Nature Protocols* 2015 10:6 10(6):845–58. doi: 10.1038/nprot.2015.053.
- Kemp, Priscilla, L. René Garcia, and Ian J. Molineux. 2005. “Changes in Bacteriophage T7 Virion Structure at the Initiation of Infection.” *Virology* 340(2):307–17. doi: 10.1016/J.VIROL.2005.06.039.
- Khan, Wasif A., Jeffrey K. Griffiths, and Michael L. Bennish. 2013. “Gastrointestinal and Extra-Intestinal Manifestations of Childhood Shigellosis in a Region Where All Four Species of Shigella Are Endemic.” *PLOS ONE* 8(5):e64097. doi: 10.1371/JOURNAL.PONE.0064097.
- Khatami, Ameneh, David A. Foley, Morgyn S. Warner, Elizabeth H. Barnes, Anton Y. Peleg, Jian Li, Stephen Stick, Nettie Burke, Ruby C. Y. Lin, Julia Warning, Thomas L. Snelling, Steven Y. C. Tong, and Jonathan Iredell. 2022. “Standardised Treatment and Monitoring Protocol to Assess Safety and Tolerability of Bacteriophage Therapy for Adult and Paediatric Patients (STAMP Study): Protocol for an Open-Label, Single-Arm Trial.” *BMJ Open* 12(12). doi: 10.1136/BMJOPEN-2022-065401.
- Kifelew, Legesse Garedew, Morgyn S. Warner, Sandra Morales, Nicky Thomas, David L. Gordon, James G. Mitchell, and Peter G. Speck. 2020. “Efficacy of Lytic Phage Cocktails on Staphylococcus Aureus and Pseudomonas Aeruginosa in Mixed-Species Planktonic Cultures and Biofilms.” *Viruses* 12(5). doi: 10.3390/V12050559.
- Kiljunen, Saija, Neeta Datta, Svetlana v. Dentovskaya, Andrey P. Anisimov, Yuriy A. Knirel, José A. Bengoechea, Otto Holst, and Mikael Skurnik. 2011. “Identification of the Lipopolysaccharide Core of Yersinia Pestis and Yersinia Pseudotuberculosis as the Receptor for Bacteriophage  $\Phi$ A1122.” *Journal of Bacteriology* 193(18):4963–72. doi: 10.1128/JB.00339-11.
- Kiljunen, Saija, Kristo Hakala, Elise Pinta, Suvi Huttunen, Patrycja Pluta, Aneta Gador, Harri Lönnberg, and Mikael Skurnik. 2005. “Yersiniophage  $\Phi$ R1-37 Is a Tailed Bacteriophage Having a 270 Kb DNA Genome with Thymidine Replaced by Deoxyuridine.” *Microbiology* 151(12):4093–4102. doi: 10.1099/MIC.0.28265-0/CITE/REFWORKS.
- Kim, Min Soo, and Jin Woo Bae. 2018. “Lysogeny Is Prevalent and Widely Distributed in the Murine Gut Microbiota.” *The ISME Journal* 2018 12:4 12(4):1127–41. doi: 10.1038/s41396-018-0061-9.

- Kim, Yeon-Jeong, Sang-Gu Yeo, Jae-Hak Park, and Hyun-Jeong Ko. 2013. "Shigella Vaccine Development: Prospective Animal Models and Current Status." *Current Pharmaceutical Biotechnology* 14(10):903–12. doi: 10.2174/1389201014666131226123900.
- King, Gareth, and Noreen E. Murray. 1994. "Restriction Enzymes in Cells, Not Eppendorfs." *Trends in Microbiology* 2(12):465–69. doi: 10.1016/0966-842X(94)90649-1.
- Klontz, Karl C., and Nalini Singh. 2015. "Treatment of Drug-Resistant Shigella Infections." *Expert Review of Anti-Infective Therapy* 13(1):69–80. doi: 10.1586/14787210.2015.983902.
- Klug, A., and J. T. Finch. 1965. "STRUCTURE OF VIRUSES OF THE PAPILLOMA-POLYOMA TYPE. I. HUMAN WART VIRUS." *Journal of Molecular Biology* 11(2):403–23. doi: 10.1016/S0022-2836(65)80066-3.
- Knecht, Leandra E., Marjan Veljkovic, and Lars Fieseler. 2020. "Diversity and Function of Phage Encoded Depolymerases." *Frontiers in Microbiology* 10. doi: 10.3389/FMICB.2019.02949.
- Knoll, M., and E. Ruska. 1932. "Das Elektronenmikroskop." *Zeitschrift Für Physik* 78(5–6):318–39. doi: 10.1007/BF01342199/METRICS.
- Ko, Ching Fen, Nien Tsung Lin, Chien Shun Chiou, Li Yu Wang, Ming Ching Liu, Chiou Ying Yang, and Yeong Sheng Lee. 2013. "Infrequent Cross-Transmission of Shigella Flexneri 2a Strains among Villages of a Mountainous Township in Taiwan with Endemic Shigellosis." *BMC Infectious Diseases* 13(1):354–354. doi: 10.1186/1471-2334-13-354.
- Kocharunchitt, C., T. Ross, and D. L. McNeil. 2009. "Use of Bacteriophages as Biocontrol Agents to Control Salmonella Associated with Seed Sprouts." *International Journal of Food Microbiology* 128(3):453–59. doi: 10.1016/J.IJFOODMICRO.2008.10.014.
- Koebnik, Ralf, Kaspar P. Locher, and Patrick Van Gelder. 2000. "Structure and Function of Bacterial Outer Membrane Proteins: Barrels in a Nutshell." *Molecular Microbiology* 37(2):239–53. doi: 10.1046/J.1365-2958.2000.01983.X.
- Koning, Roman I., Josue Gomez-Blanco, Inara Akopjana, Javier Vargas, Andris Kazaks, Kaspars Tars, José María Carazo, and Abraham J. Koster. 2016. "Asymmetric Cryo-EM Reconstruction of Phage MS2 Reveals Genome Structure in Situ." *Nature Communications* 7. doi: 10.1038/NCOMMS12524.
- Koonin, Eugene v. 2005. "Virology: Gulliver among the Lilliputians." *Current Biology: CB* 15(5). doi: 10.1016/J.CUB.2005.02.042.
- Koonin, Eugene v., Tatiana G. Senkevich, and Valerian v. Dolja. 2009. "Compelling Reasons Why Viruses Are Relevant for the Origin of Cells." *Nature Reviews Microbiology* 2009 7:8 7(8):615–615. doi: 10.1038/nrmicro2108-c5.
- Koskella, Britt, and Sean Meaden. 2013. "Understanding Bacteriophage Specificity in Natural Microbial Communities." *Viruses* 5(3):806–23. doi: 10.3390/V5030806.

- Kostrzewski, J., and Stypulkowska-Misiurewicz. 1968. "Changes in the Epidemiology of Dysentery in Poland and the Situation in Europe." *Archivum Immunologiae et Therapiae Experimentalis* 16(3):429–51.
- Kostyuchenko, Victor A., Paul R. Chipman, Petr G. Leiman, Fumio Arisaka, Vadim V. Mesyanzhinov, and Michael G. Rossmann. 2005. "The Tail Structure of Bacteriophage T4 and Its Mechanism of Contraction." *Nature Structural & Molecular Biology* 12(9):810–13. doi: 10.1038/NSMB975.
- Kotloff, K. L., J. P. Winickoff, B. Ivanoff, J. D. Clemens, D. L. Swerdlow, P. J. Sansonetti, G. K. Adak, and M. M. Levine. 1999. "Global Burden of Shigella Infections: Implications for Vaccine Development and Implementation of Control Strategies." *Bulletin of the World Health Organization* 77(8):651–66.
- Kotloff, K., J. Winickoff, B. Ivanoff, J. Clemens, D. Swerdlow, P. Sansonetti, G. Adak, and M. Levine. 1999. "Global Burden of Shigella Infections: Implications for Vaccine Development and Implementation of Control Strategies." *Bulletin of the World Health Organization*.
- Kotloff, Karen L. 2017. "Shigella Infection in Children and Adults: A Formidable Foe." *The Lancet. Global Health* 5(12):e1166–67. doi: 10.1016/S2214-109X(17)30431-X.
- Kotloff, Karen L., James P. Nataro, Genevieve A. Losonsky, Steven S. Wasserman, Thomas L. Hale, David N. Taylor, Jerald C. Sadoff, and Myron M. Levine. 1995. "A Modified Shigella Volunteer Challenge Model in Which the Inoculum Is Administered with Bicarbonate Buffer: Clinical Experience and Implications for Shigella Infectivity." *Vaccine* 13(16):1488–94. doi: 10.1016/0264-410X(95)00102-7.
- Kotloff, Karen L., Mark S. Riddle, James A. Platts-Mills, Patricia Pavlinac, and Anita K. M. Zaidi. 2018. "Shigellosis." *Lancet (London, England)* 391(10122):801–12. doi: 10.1016/S0140-6736(17)33296-8.
- Kozyreva, Varvara K., Guillaume Jospin, Alexander L. Greninger, James P. Watt, Jonathan A. Eisen, and Vishnu Chaturvedi. 2016. "Recent Outbreaks of Shigellosis in California Caused by Two Distinct Populations of Shigella Sonnei with Either Increased Virulence or Fluoroquinolone Resistance." *MSphere* 1(6):e00344-16. doi: 10.1128/MSPHERE.00344-16.
- Krueger, Albert Paul, and E. Jane Scribner. 1941. "THE BACTERIOPHAGE: ITS NATURE AND ITS THERAPEUTIC USE." *JAMA* 116(20):2269–77. doi: 10.1001/JAMA.1941.62820200013011.
- Krüger, D. H., and C. Schroeder. 1981. "Bacteriophage T3 and Bacteriophage T7 Virus-Host Cell Interactions." *Microbiological Reviews* 45(1):9–51. doi: 10.1128/MR.45.1.9-51.1981.
- Krupovic, Mart. 2018. "ICTV Virus Taxonomy Profile: Plasmaviridae." *Journal of General Virology* 99(5):617–18. doi: 10.1099/JGV.0.001060/CITE/REFWORKS.
- Krupovič, Mart, and Dennis H. Bamford. 2008. "Virus Evolution: How Far Does the Double Beta-Barrel Viral Lineage Extend?" *Nature Reviews. Microbiology* 6(12):941–48. doi: 10.1038/NRMICRO2033.

- Kühlbrandt, Werner. 2014. "Cryo-EM Enters a New Era." *ELife* 3:e03678. doi: 10.7554/ELIFE.03678.
- Kumari, Seema, Kusum Harjai, and Sanjay Chhibber. 2011. "Bacteriophage versus Antimicrobial Agents for the Treatment of Murine Burn Wound Infection Caused by *Klebsiella Pneumoniae* B5055." *Journal of Medical Microbiology* 60(2):205–10. doi: 10.1099/jmm.0.018580-0.
- Kuo, Hung Wei, Sabine Kasper, Sandra Jelovcan, Gerda Höger, Ingeborg Lederer, Christoph König, Gerda Pridnig, Anita Luckner-Hornischer, Franz Allerberger, and Daniela Schmid. 2009. "A Food-Borne Outbreak of *Shigella Sonnei* Gastroenteritis, Austria, 2008." *Wiener Klinische Wochenschrift* 121(3–4):157–63. doi: 10.1007/S00508-008-1141-7.
- Kutter, Elizabeth. 2009. "Phage Host Range and Efficiency of Plating." *Methods in Molecular Biology (Clifton, N.J.)* 501:141–49. doi: 10.1007/978-1-60327-164-6\_14.
- Kwan, Tony, Jing Liu, Michael DuBow, Philippe Gros, and Jerry Pelletier. 2006. "Comparative Genomic Analysis of 18 *Pseudomonas Aeruginosa* Bacteriophages." *Journal of Bacteriology* 188(3):1184–87. doi: 10.1128/JB.188.3.1184-1187.2006.
- De la Fuente-Núñez, César, Fany Reffuveille, Lucía Fernández, and Robert E. W. Hancock. 2013. "Bacterial Biofilm Development as a Multicellular Adaptation: Antibiotic Resistance and New Therapeutic Strategies." *Current Opinion in Microbiology* 16(5):580–89. doi: 10.1016/J.MIB.2013.06.013.
- de la Rosa-Trevín, J. M., A. Quintana, L. del Cano, A. Zaldívar, I. Foche, J. Gutiérrez, J. Gómez-Blanco, J. Burguet-Castell, J. Cuenca-Alba, V. Abrishami, J. Vargas, J. Otón, G. Sharov, J. L. Vilas, J. Navas, P. Conesa, M. Kazemi, R. Marabini, C. O. S. Sorzano, and J. M. Carazo. 2016. "Scipion: A Software Framework toward Integration, Reproducibility and Validation in 3D Electron Microscopy." *Journal of Structural Biology* 195(1):93–99. doi: 10.1016/J.JSB.2016.04.010.
- Labrie, Simon J., Julie E. Samson, and Sylvain Moineau. 2010. "Bacteriophage Resistance Mechanisms." *Nature Reviews. Microbiology* 8(5):317–27. doi: 10.1038/NRMICRO2315.
- Laemmli, U. K. 1970. "Cleavage of Structural Proteins during the Assembly of the Head of Bacteriophage T4." *Nature* 227(5259):680–85. doi: 10.1038/227680A0.
- Laohachai, Karina N., Randa Bahadi, Maria B. Hardo, Phillip G. Hardo, and Joseph I. Kourie. 2003. "The Role of Bacterial and Non-Bacterial Toxins in the Induction of Changes in Membrane Transport: Implications for Diarrhea." *Toxicon* 42(7):687–707. doi: 10.1016/j.toxicon.2003.08.010.
- Laslett, Dean, and Bjorn Canback. 2004. "ARAGORN, a Program to Detect tRNA Genes and tmRNA Genes in Nucleotide Sequences." *Nucleic Acids Research* 32(1):11–16. doi: 10.1093/NAR/GKH152.
- Latka, Agnieszka, Barbara Maciejewska, Grazyna Majkowska-Skrobek, Yves Briers, and Zuzanna Drulis-Kawa. 2017. "Bacteriophage-Encoded Virion-Associated Enzymes to Overcome the Carbohydrate Barriers during the Infection Process." *Applied Microbiology and Biotechnology* 2017 101:8 101(8):3103–19. doi: 10.1007/S00253-017-8224-6.

- Lee, Gwenyth, Maribel Paredes Olortegui, Pablo Peñataro Yori, Robert E. Black, Laura Caulfield, Cesar Banda Chavez, Eric Hall, William K. Pan, Rina Meza, and Margaret Kosek. 2014. "Effects of Shigella-, Campylobacter- and ETEC-Associated Diarrhea on Childhood Growth." *The Pediatric Infectious Disease Journal* 33(10):1004–9. doi: 10.1097/INF.0000000000000351.
- Leiman, Petr G., Paul R. Chipman, Victor A. Kostyuchenko, Vadim V. Mesyanzhinov, and Michael G. Rossmann. 2004a. "Three-Dimensional Rearrangement of Proteins in the Tail of Bacteriophage T4 on Infection of Its Host." *Cell* 118(4):419–29. doi: 10.1016/j.cell.2004.07.022.
- Leiman, Petr G., Paul R. Chipman, Victor A. Kostyuchenko, Vadim V. Mesyanzhinov, and Michael G. Rossmann. 2004b. "Three-Dimensional Rearrangement of Proteins in the Tail of Bacteriophage T4 on Infection of Its Host." *Cell* 118(4):419–29. doi: 10.1016/j.cell.2004.07.022.
- Leiman, Petr G, Paul R. Chipman, Victor A. Kostyuchenko, Vadim V Mesyanzhinov, Michael G. Rossmann, West State Street, and West Lafayette. 2004. "Three-Dimensional Rearrangement of Proteins in the Tail of Bacteriophage T4 on Infection of Its Host." 118:419–29.
- Letarov, A. V., and E. E. Kulikov. 2017. "Adsorption of Bacteriophages on Bacterial Cells." *Biochemistry (Moscow)* 82(13):1632–58. doi: 10.1134/S0006297917130053.
- Lewis, K. 2005. "Persister Cells and the Riddle of Biofilm Survival." *Biochemistry. Biokhimiia* 70(2):267–74. doi: 10.1007/S10541-005-0111-6.
- Lewis, K. 2008. "Multidrug Tolerance of Biofilms and Persister Cells." *Current Topics in Microbiology and Immunology* 322:107–31. doi: 10.1007/978-3-540-75418-3\_6/COVER.
- Li, Xueming, Shawn Zheng, David A. Agard, and Yifan Cheng. 2015. "Asynchronous Data Acquisition and On-the-Fly Analysis of Dose Fractionated CryoEM Images by UCSFImage." *Journal of Structural Biology* 192(2):174–78. doi: 10.1016/J.JSB.2015.09.003.
- Liang, Lingfei, Haiyan Zhao, Bowen An, and Liang Tang. 2017. "High-Resolution Structure of Podovirus Tail Adaptor Suggests Repositioning of an Octad Motif That Mediates the Sequential Tail Assembly." *Proceedings of the National Academy of Sciences of the United States of America* 115(2):313–18. doi: 10.1073/PNAS.1706846115/SUPPL\_FILE/PNAS.201706846SI.PDF.
- Lin, Derek M., Britt Koskella, and Henry C. Lin. 2017. "Phage Therapy: An Alternative to Antibiotics in the Age of Multi-Drug Resistance." *World Journal of Gastrointestinal Pharmacology and Therapeutics* 8(3):162. doi: 10.4292/WJGPT.V8.I3.162.
- Lin, Zeming, Halil Akin, Roshan Rao, B. Hie, Zhongkai Zhu, Wenting Lu, Nikita Smetanin, Robert Verkuil, Ori Kabeli, Y. Shmueli, Allan dos Santos Costa, M. Fazel-Zarandi, Tom Sercu, Salvatore Candido, and Alexander Rives. 2022. "Evolutionary-Scale Prediction of Atomic Level Protein Structure with a Language Model." *BioRxiv*. doi: 10.1101/2022.07.20.500902.

- Lindberg, A. A. 2003. "Bacteriophage Receptors." *Https://Doi.Org/10.1146/Annurev.Mi.27.100173.001225* 27:205–41. doi: 10.1146/ANNUREV.MI.27.100173.001225.
- Lionnet, Timothée, Michelle M. Spiering, Stephen J. Benkovic, David Bensimon, and Vincent Croquette. 2007. "Real-Time Observation of Bacteriophage T4 Gp41 Helicase Reveals an Unwinding Mechanism." *Proceedings of the National Academy of Sciences of the United States of America* 104(50):19790–95. doi: 10.1073/PNAS.0709793104/SUPPL\_FILE/IMAGE48.GIF.
- Liu, Jing, Mohammed Dehbi, Greg Moeck, Francis Arhin, Pascale Banda, Dominique Bergeron, Mario Callejo, Vincent Ferretti, Nhuan Ha, Tony Kwan, John McCarty, Ramakrishnan Srikumar, Dan Williams, Jinzi J. Wu, Philippe Gros, Jerry Pelletier, and Michael DuBow. 2004. "Antimicrobial Drug Discovery through Bacteriophage Genomics." *Nature Biotechnology* 22(2):185–91. doi: 10.1038/NBT932.
- Liu, Yi Yun, Yang Wang, Timothy R. Walsh, Ling Xian Yi, Rong Zhang, James Spencer, Yohei Doi, Guobao Tian, Baolei Dong, Xianhui Huang, Lin Feng Yu, Danxia Gu, Hongwei Ren, Xiaojie Chen, Luchao Lv, Dandan He, Hongwei Zhou, Zisen Liang, Jian Hua Liu, and Jianzhong Shen. 2016. "Emergence of Plasmid-Mediated Colistin Resistance Mechanism MCR-1 in Animals and Human Beings in China: A Microbiological and Molecular Biological Study." *The Lancet. Infectious Diseases* 16(2):161–68. doi: 10.1016/S1473-3099(15)00424-7.
- Livio, Sofie, Nancy A. Strockbine, Sandra Panchalingam, Sharon M. Tennant, Eileen M. Barry, Mark E. Marohn, Martin Antonio, Anowar Hossain, Inacio Mandomando, John B. Ochieng, Joseph O. Oundo, Shahida Qureshi, Thandavarayan Ramamurthy, Boubou Tamboura, Richard A. Adegbola, Mohammed Jahangir Hossain, Debasish Saha, Sunil Sen, Abu Syed Golam Faruque, Pedro L. Alonso, Robert F. Breiman, Anita K. M. Zaidi, Dipika Sur, Samba O. Sow, Lynette Y. Berkeley, Ciara E. O'Reilly, Eric D. Mintz, Kousick Biswas, Dani Cohen, Tamer H. Farag, Dilruba Nasrin, Yukun Wu, William C. Blackwelder, Karen L. Kotloff, James P. Nataro, and Myron M. Levine. 2014. "Shigella Isolates from the Global Enteric Multicenter Study Inform Vaccine Development." *Clinical Infectious Diseases : An Official Publication of the Infectious Diseases Society of America* 59(7):933–41. doi: 10.1093/CID/CIU468.
- Łobocka, Małgorzata B., Aleksandra Głowacka, and Piotr Golec. 2018. "Methods for Bacteriophage Preservation." *Methods in Molecular Biology (Clifton, N.J.)* 1693:219–30. doi: 10.1007/978-1-4939-7395-8\_17.
- Loc-Carrillo, Catherine, and Stephen T. Abedon. 2011. "Pros and Cons of Phage Therapy." *Bacteriophage* 1(2):111–14. doi: 10.4161/BACT.1.2.14590.
- Loeffler, J. M., D. Nelson, and V. A. Fischetti. 2001. "Rapid Killing of Streptococcus Pneumoniae with a Bacteriophage Cell Wall Hydrolase." *Science (New York, N.Y.)* 294(5549):2170–72. doi: 10.1126/SCIENCE.1066869.
- Loessner, Martin J., Karl Kramer, Frank Ebel, and Siegfried Scherer. 2002. "C-Terminal Domains of Listeria Monocytogenes Bacteriophage Murein Hydrolases Determine



- Specific Recognition and High-Affinity Binding to Bacterial Cell Wall Carbohydrates.” *Molecular Microbiology* 44(2):335–49. doi: 10.1046/J.1365-2958.2002.02889.X.
- Löfdahl, M., S. Ivarsson, S. Andersson, J. Långmark, and L. Plym-Forsell. 2009. “An Outbreak of *Shigella Dysenteriae* in Sweden, May-June 2009, with Sugar Snaps as the Suspected Source.” *Euro Surveillance: Bulletin Européen Sur Les Maladies Transmissibles = European Communicable Disease Bulletin* 14(28):19268. doi: 10.2807/ESE.14.28.19268-EN/CITE/PLAINTEXT.
- Lubbers, M. W., N. R. Waterfield, T. P. J. Beresford, R. W. F. Le Page, and A. W. Jarvis. 1995. “Sequencing and Analysis of the Prolate-Headed Lactococcal Bacteriophage C2 Genome and Identification of the Structural Genes.” *Applied and Environmental Microbiology* 61(12):4348–56. doi: 10.1128/AEM.61.12.4348-4356.1995.
- Ludmir, Ethan B., and Lynn W. Enquist. 2009. “Viral Genomes Are Part of the Phylogenetic Tree of Life.” *Nature Reviews Microbiology* 2009 7:8 7(8):615–615. doi: 10.1038/nrmicro2108-c4.
- Ludtke, Steven J., Philip R. Baldwin, and Wah Chiu. 1999. “EMAN: Semiautomated Software for High-Resolution Single-Particle Reconstructions.” *Journal of Structural Biology* 128(1):82–97. doi: 10.1006/JSBI.1999.4174.
- Ly-Chatain, Mai Huong. 2014. “The Factors Affecting Effectiveness of Treatment in Phages Therapy.” *Frontiers in Microbiology* 5(FEB). doi: 10.3389/FMICB.2014.00051.
- Maghsoodi, Ameneh, Anupam Chatterjee, Ioan Andricioaei, and Noel C. Perkins. 2019. “How the Phage T4 Injection Machinery Works Including Energetics, Forces, and Dynamic Pathway.” *Proceedings of the National Academy of Sciences of the United States of America* 116(50):25097–105. doi: 10.1073/PNAS.1909298116.
- Magiorakos, A. P., A. Srinivasan, R. B. Carey, Y. Carmeli, M. E. Falagas, C. G. Giske, S. Harbarth, J. F. Hindler, G. Kahlmeter, B. Olsson-Liljequist, D. L. Paterson, L. B. Rice, J. Stelling, M. J. Struelens, A. Vatopoulos, J. T. Weber, and D. L. Monnet. 2012. “Multidrug-Resistant, Extensively Drug-Resistant and Pandrug-Resistant Bacteria: An International Expert Proposal for Interim Standard Definitions for Acquired Resistance.” *Clinical Microbiology and Infection* 18(3):268–81. doi: 10.1111/j.1469-0691.2011.03570.x.
- Mah, Thien Fah. 2012. “Biofilm-Specific Antibiotic Resistance.” *Future Microbiology* 7(9):1061–72. doi: 10.2217/FMB.12.76.
- Majumdar, Sabita, Sailendra N. Dey, Rukhsana Chowdhury, Chitra Dutta, and Jyotirmoy Das. 1988. “Intracellular Development of Cholera phage Phi 149 under Permissive and Nonpermissive Conditions: An Electron Microscopic Study.” *Intervirology* 29(1):27–38. doi: 10.1159/000150026.
- Malheiro, J., and M. Simões. 2017. “Antimicrobial Resistance of Biofilms in Medical Devices.” *Biofilms and Implantable Medical Devices: Infection and Control* 97–113. doi: 10.1016/B978-0-08-100382-4.00004-6.
- Malik, Danish J., Ilya J. Sokolov, Gurinder K. Vinner, Francesco Mancuso, Salvatore Cinquerrui, Goran T. Vladislavljevic, Martha R. J. Clokie, Natalie J. Garton, Andrew G. F. Stapley, and Anna Kirpichnikova. 2017. “Formulation, Stabilisation and Encapsulation of

- Bacteriophage for Phage Therapy.” *Advances in Colloid and Interface Science* 249:100–133. doi: 10.1016/J.CIS.2017.05.014.
- Mallick, Bani, Payel Mondal, and Moumita Dutta. 2021. “Morphological, Biological, and Genomic Characterization of a Newly Isolated Lytic Phage Sfk20 Infecting *Shigella Flexneri*, *Shigella Sonnei*, and *Shigella Dysenteriae*1.” *Scientific Reports* 11(1):1–12. doi: 10.1038/s41598-021-98910-z.
- Mani, Sachin, Thomas Wierzba, and Richard I. Walker. 2016. “Status of Vaccine Research and Development for *Shigella*.” *Vaccine* 34(26):2887–94. doi: 10.1016/J.VACCINE.2016.02.075.
- Marinelli, Laura J., Graham F. Hatfull, and Mariana Piuri. 2012. “Recombineering: A Powerful Tool for Modification of Bacteriophage Genomes.” *Bacteriophage* 2(1):5–14. doi: 10.4161/BACT.18778.
- Marinelli, Laura J., Mariana Piuri, Zuzana Swigoňová, Amrita Balachandran, Lauren M. Oldfield, Julia C. van Kessel, and Graham F. Hatfull. 2008. “BRED: A Simple and Powerful Tool for Constructing Mutant and Recombinant Bacteriophage Genomes.” *PLOS ONE* 3(12):e3957. doi: 10.1371/JOURNAL.PONE.0003957.
- Mastronarde, David N. 2005. “Automated Electron Microscope Tomography Using Robust Prediction of Specimen Movements.” *Journal of Structural Biology* 152(1):36–51. doi: 10.1016/J.JSB.2005.07.007.
- Matsuzaki, Shigenobu, Mohammad Rashel, Jumpei Uchiyama, Shingo Sakurai, Takako Ujihara, Masayuki Kuroda, Masahiko Ikeuchi, Toshikazu Tani, Mikiya Fujieda, Hiroshi Wakiguchi, and Shosuke Imai. 2005. “Bacteriophage Therapy: A Revitalized Therapy against Bacterial Infectious Diseases.” *Journal of Infection and Chemotherapy : Official Journal of the Japan Society of Chemotherapy* 11(5):211–19. doi: 10.1007/S10156-005-0408-9.
- Mavrich, Travis N., and Graham F. Hatfull. 2017. “Bacteriophage Evolution Differs by Host, Lifestyle and Genome.” *Nature Microbiology* 2:9 2(9):1–9. doi: 10.1038/nmicrobiol.2017.112.
- McCormick, Beth A., Andrew M. Siber, and Anthony T. Maurelli. 1998. “Requirement of the *Shigella Flexneri* Virulence Plasmid in the Ability to Induce Trafficking of Neutrophils across Polarized Monolayers of the Intestinal Epithelium.” *Infection and Immunity* 66(9):4237–43. doi: 10.1128/IAI.66.9.4237-4243.1998.
- McMahon, Stephen A., Gareth A. Roberts, Kenneth A. Johnson, Laurie P. Cooper, Huanting Liu, John H. White, Lester G. Carter, Bansi Sanghvi, Muse Oke, Malcolm D. Walkinshaw, Garry W. Blakely, James H. Naismith, and David T. F. Dryden. 2009. “Extensive DNA Mimicry by the *ArdA* Anti-Restriction Protein and Its Role in the Spread of Antibiotic Resistance.” *Nucleic Acids Research* 37(15):4887–97. doi: 10.1093/NAR/GKP478.
- Mead, P. S., E. F. Dunne, L. Graves, M. Wiedmann, M. Patrick, S. Hunter, E. Salehi, F. Mostashari, A. Craig, P. Mshar, T. Bannerman, B. D. Sauders, P. Hayes, W. Dewitt, P. Sparling, P. Griffin, D. Morse, L. Slutsker, B. Swaminathan, Kathryn Boor, William Bibb, Tim Cote, Thomas Donkar, Sietske de Fitjer, Ruth Etzel, Elizabeth Koch, Stan Kondracki,

- Jeremy Miller, Forrest Smith, Robert Taylor, and Shelley Zansky. 2006. “Nationwide Outbreak of Listeriosis Due to Contaminated Meat.” *Epidemiology and Infection* 134(4):744–51. doi: 10.1017/S0950268805005376.
- Medhekar, Bob, and Jeff F. Miller. 2007. “Diversity-Generating Retroelements.” *Current Opinion in Microbiology* 10(4):388–95. doi: 10.1016/J.MIB.2007.06.004.
- Mesyanzhinov, Vadim v. 2004. “Bacteriophage T4: Structure, Assembly, and Initiation Infection Studied in Three Dimensions” 1 Dedicated to Professor Eduard Kellenberger on Occasion of the 50th Anniversary of His Pioneering Research on Bacteriophage T4 Structure and Morphogenesis.” *Advances in Virus Research* 63:287–352. doi: 10.1016/S0065-3527(04)63005-3.
- Metters, Andrew, and Jeffrey Hubbell. 2005. “Network Formation and Degradation Behavior of Hydrogels Formed by Michael-Type Addition Reactions.” *Biomacromolecules* 6(1):290–301. doi: 10.1021/BM049607O.
- Miller, Eric S., Elizabeth Kutter, Gisela Mosig, Fumio Arisaka, Takashi Kunisawa, and Wolfgang R  ger. 2003. “Bacteriophage T4 Genome.” *Microbiology and Molecular Biology Reviews : MMBR* 67(1):86–156. doi: 10.1128/MMBR.67.1.86-156.2003.
- Milyutina, L. N., and N. V. Vorotyntseva. 1993. “[Current Strategy and Tactics of Etiotropic Therapy of Acute Intestinal Infections in Children].” *Antibiotiki i Khimioterapiia = Antibiotics and Chemotherapy [Sic]* 38(1):46–53.
- Mirdita, Milot, Konstantin Sch  tze, Yoshitaka Moriwaki, Lim Heo, Sergey Ovchinnikov, and Martin Steinegger. 2022. “ColabFold: Making Protein Folding Accessible to All.” *Nature Methods* 19(6):679–82. doi: 10.1038/S41592-022-01488-1.
- Monack, Denise M., and Julie A. Theriot. 2001. “Actin-Based Motility Is Sufficient for Bacterial Membrane Protrusion Formation and Host Cell Uptake.” *Cellular Microbiology* 3(9):633–47. doi: 10.1046/J.1462-5822.2001.00143.X.
- Moody, M. F., and L. Makowski. 1981. “X-Ray Diffraction Study of Tail-Tubes from Bacteriophage T2L.” *Journal of Molecular Biology* 150(2):217–44. doi: 10.1016/0022-2836(81)90450-2.
- Morgan, Oliver, Paul Crook, Tom Cheasty, Brian Jiggle, Isabelle Giraudon, Harriett Hughes, Stephen Morris Jones, and Helen Maguire. 2006. “Shigella Sonnei Outbreak among Homosexual Men, London [2].” *Emerging Infectious Diseases* 12(9):1458–60. doi: 10.3201/eid1209.060282.
- Mostowy, Rafa   J., and Kathryn E. Holt. 2018. “Diversity-Generating Machines: Genetics of Bacterial Sugar-Coating.” *Trends in Microbiology* 26(12):1008–21. doi: 10.1016/J.TIM.2018.06.006.
- Muller, L., T. Jensen, R. F. Petersen, K. M  lbak, and S. Ethelberg. 2009. “Imported Fresh Sugar Peas as Suspected Source of an Outbreak of Shigella Sonnei in Denmark, April-May 2009.” *Euro Surveillance : Bulletin European Sur Les Maladies Transmissibles = European Communicable Disease Bulletin* 14(24). doi: 10.2807/ESE.14.24.19241-EN.

- Munshi, M. H., Khaleda Haider, M. M. Rahaman, David A. Sack, Zia U. Ahmed, and M. G. Morshed. 1987. "Plasmid-Mediated Resistance to Nalidixic Acid in *Shigella Dysenteriae* Type 1." *Lancet (London, England)* 2(8556):419–21. doi: 10.1016/S0140-6736(87)90957-3.
- Munson-Mcgee, Jacob H., Jamie C. Snyder, and Mark J. Young. 2018. "Archaeal Viruses from High-Temperature Environments." *Genes* 9(3). doi: 10.3390/GENES9030128.
- Musk Jr., Dinty, and Paul Hergenrother. 2006. "Chemical Countermeasures for the Control of Bacterial Biofilms: Effective Compounds and Promising Targets." *Current Medicinal Chemistry* 13(18):2163–77. doi: 10.2174/092986706777935212.
- Nagel, Tobi E., Benjamin K. Chan, Daniel De Vos, Ayman El-Shibiny, Erastus K. Kang'ethe, Angela Makumi, and Jean Paul Pirnay. 2016. "The Developing World Urgently Needs Phages to Combat Pathogenic Bacteria." *Frontiers in Microbiology* 7(JUN):882–882. doi: 10.3389/FMICB.2016.00882.
- Nagel, Tobi E., Benjamin K. Chan, Daniel De Vos, Ayman El-Shibiny, Erastus K. Kang'ethe, Angela Makumi, and Jean-Paul Pirnay. 2016. "The Developing World Urgently Needs Phages to Combat Pathogenic Bacteria." *Frontiers in Microbiology* 7:882. doi: 10.3389/FMICB.2016.00882.
- Naheed, A., P. Kalluri, K. A. Talukder, A. S. G. Faruque, F. Khatun, G. B. Nair, E. D. Mintz, and R. F. Breiman. 2004. "Fluoroquinolone-Resistant *Shigella Dysenteriae* Type 1 in Northeastern Bangladesh." *Lancet Infectious Diseases* 4(10):607–8. doi: 10.1016/S1473-3099(04)01143-0.
- Nataro, J. P., J. Seriwatana, A. Fasano, D. R. Maneval, L. D. Guers, F. Noriega, F. Dubovsky, M. M. Levine, and J. G. Morris. 1995. "Identification and Cloning of a Novel Plasmid-Encoded Enterotoxin of Enteroinvasive *Escherichia Coli* and *Shigella* Strains." *Infection and Immunity* 63(12):4721–28. doi: 10.1128/IAI.63.12.4721-4728.1995.
- Nelson, J. D., and K. C. Haltalin. 1974. "Amoxicillin Less Effective than Ampicillin against *Shigella* in Vitro and in Vivo: Relationship of Efficacy to Activity in Serum." *The Journal of Infectious Diseases* 129(Supplement\_2):S222–27. doi: 10.1093/INFDIS/129.SUPPLEMENT\_2.S222.
- Nelson, John D., Helen Kusmiesz, and Lula Hinton Jackson. 1976. "Comparison of Trimethoprim-Sulfamethoxazole and Ampicillin Therapy for Shigellosis in Ambulatory." *The Journal of Pediatrics* 89(3):491–93. doi: 10.1016/S0022-3476(76)80561-6.
- Nelson, John D., Helen Kusmiesz, and Sharon Shelton. 1982. "Oral or Intravenous Trimethoprim-Sulfamethoxazole Therapy for Shigellosis." *Reviews of Infectious Diseases* 4(2):546–50. doi: 10.1093/CLINIDS/4.2.546.
- Nesper, J., D. Kapfhammer, K. E. Klose, H. Merkert, and J. Reidl. 2000. "Characterization of *Vibrio Cholerae* O1 Antigen as the Bacteriophage K139 Receptor and Identification of IS1004 Insertions Aborting O1 Antigen Biosynthesis." *Journal of Bacteriology* 182(18):5097. doi: 10.1128/JB.182.18.5097-5104.2000.

- Newcomb, William W., Rachel M. Juhas, Darrell R. Thomsen, Fred L. Homa, April D. Burch, Sandra K. Weller, and Jay C. Brown. 2001. "The UL6 Gene Product Forms the Portal for Entry of DNA into the Herpes Simplex Virus Capsid." *Journal of Virology* 75(22):10923–32. doi: 10.1128/JVI.75.22.10923-10932.2001.
- Nichter, Mark, Cecilia S. Acuin, and Alberta Vargas. 2008. "Introducing Zinc in a Diarrhoeal Disease Control Programme Guide to Conducting Formative Research."
- Nickerson, Kourtney P., Rachael B. Chanin, Jeticia R. Sistrunk, David A. Rasko, Peter J. Fink, Eileen M. Barry, James P. Nataro, and Christina S. Faherty. 2017. "Analysis of *Shigella Flexneri* Resistance, Biofilm Formation, and Transcriptional Profile in Response to Bile Salts." doi: 10.1128/IAI.01067-16.
- Nigro, Olivia D., Sean P. Jungbluth, Huei Ting Lin, Chih Chiang Hsieh, Jaclyn A. Miranda, Christopher R. Schvarcz, Michael S. Rappé, and Grieg F. Steward. 2017. "Viruses in the Oceanic Basement." *MBio* 8(2). doi: 10.1128/MBIO.02129-16.
- Nilsson, Anders S. 2014. "Phage Therapy--Constraints and Possibilities." *Upsala Journal of Medical Sciences* 119(2):192–98. doi: 10.3109/03009734.2014.902878.
- Nobrega, Franklin L., Ana Rita Costa, José F. Santos, Melvin F. Siliakus, Jan W. M. Van Lent, Servé W. M. Kengen, Joana Azeredo, and Leon D. Kluskens. 2016. "Genetically Manipulated Phages with Improved PH Resistance for Oral Administration in Veterinary Medicine." *Scientific Reports* 6. doi: 10.1038/SREP39235.
- Ofir, Gal, and Rotem Sorek. 2018. "Contemporary Phage Biology: From Classic Models to New Insights." *Cell* 172(6):1260–70. doi: 10.1016/J.CELL.2017.10.045.
- O’Flaherty, Sarah, R. Paul Ross, and Aidan Coffey. 2009. "Bacteriophage and Their Lysins for Elimination of Infectious Bacteria." *FEMS Microbiology Reviews* 33(4):801–19. doi: 10.1111/J.1574-6976.2009.00176.X.
- Okame, Michio, Eisuke Adachi, Hidenori Sato, Shoichi Shimizu, Tadashi Kikuchi, Naoko Miyazaki, Michiko Koga, Hitomi Nakamura, Masato Suzuki, Naoki Oyaizu, Takeshi Fujii, Aikichi Iwamoto, and Tomohiko Koibuchi. 2012. "Shigella Sonnei Outbreak among Men Who Have Sex with Men in Tokyo." *Japanese Journal of Infectious Diseases* 65(3):277–78. doi: 10.7883/yoken.65.277.
- Olsen, Jesper V., Lyris M. F. de Godoy, Guoqing Li, Boris Macek, Peter Mortensen, Reinhold Pesch, Alexander Makarov, Oliver Lange, Stevan Horning, and Matthias Mann. 2005. "Parts per Million Mass Accuracy on an Orbitrap Mass Spectrometer via Lock Mass Injection into a C-Trap." *Molecular & Cellular Proteomics : MCP* 4(12):2010–21. doi: 10.1074/MCP.T500030-MCP200.
- Olson, Matthew R., Richard P. Axler, and Randall E. Hicks. 2004. "Effects of Freezing and Storage Temperature on MS2 Viability." *Journal of Virological Methods* 122(2):147–52. doi: 10.1016/J.JVIROMET.2004.08.010.
- Olson, Scott, Alexis Hall, Mark S. Riddle, and Chad K. Porter. 2019. "Travelers’ Diarrhea: Update on the Incidence, Etiology and Risk in Military and Similar Populations - 1990-2005 versus 2005-2015, Does a Decade Make a Difference?" *Tropical Diseases, Travel Medicine and Vaccines* 5(1). doi: 10.1186/S40794-018-0077-1.

- O'Neill, J. 2016. "Tackling Drug-Resistant Infections Globally: Final Report and Recommendations."
- Ongena, Véronique, Ariane Briegel, and Dennis Claessen. 2021. "Cell Wall Deficiency as an Escape Mechanism from Phage Infection." *Open Biology* 11(9). doi: 10.1098/RSOB.210199/.
- Onsea, Jolien, Saartje Uyttebroek, Baixing Chen, Jeroen Wagemans, Cédric Lood, Laura Van Gerven, Isabel Spriet, David Devolder, Yves Debaveye, Melissa Depypere, Lieven Dupont, Paul De Munter, Willy E. Peetermans, Vera van Noort, Maia Merabishvili, Jean Paul Pirnay, Rob Lavigne, and Willem Jan Metsemakers. 2021. "Bacteriophage Therapy for Difficult-to-Treat Infections: The Implementation of a Multidisciplinary Phage Task Force ( The PHAGEFORCE Study Protocol)." *Viruses* 13(8). doi: 10.3390/V13081543.
- Orlova, E. V., P. Dube, E. Beckmann, F. Zemlin, R. Lurz, T. A. Trautner, P. Tavares, and M. Van Heel. 1999. "Structure of the 13-Fold Symmetric Portal Protein of Bacteriophage SPP1." *Nature Structural Biology* 1999 6:9 6(9):842–46. doi: 10.1038/12303.
- Orlova, E. V., and H. R. Saibil. 2011. "Structural Analysis of Macromolecular Assemblies by Electron Microscopy." *Chemical Reviews* 111(12):7710–48. doi: 10.1021/CR100353T.
- Orlova, Elena V., Brent Gowen, Anja Dröge, Asita Stiege, Frank Weise, Rudi Lurz, Marin Van Heel, and Paulo Tavares. 2003. "Structure of a Viral DNA Gatekeeper at 10 Å Resolution by Cryo-Electron Microscopy." *The EMBO Journal* 22(6):1255. doi: 10.1093/EMBOJ/CDG123.
- O'Toole, G., H. B. Kaplan, and R. Kolter. 2000. "Biofilm Formation as Microbial Development." *Annual Review of Microbiology* 54:49–79. doi: 10.1146/ANNUREV.MICRO.54.1.49.
- Pajunen, M., S. Kiljunen, and M. Skurnik. 2000. "Bacteriophage ΦYeO3-12, Specific for Yersinia Enterocolitica Serotype O:3, Is Related to Coliphages T3 and T7." *Journal of Bacteriology* 182(18):5114. doi: 10.1128/JB.182.18.5114-5120.2000.
- Parasion, Sylwia, Magdalena Kwiatek, Romuald Gryko, Lidia Mizak, and Anna Malm. 2014. "Bacteriophages as an Alternative Strategy for Fighting Biofilm Development." *Polish Journal of Microbiology* 63(2):137–45. doi: 10.33073/PJM-2014-019.
- Pazhani, G. P., T. Ramamurthy, U. Mitra, S. K. Bhattacharya, and S. K. Niyogi. 2005. "Species Diversity and Antimicrobial Resistance of Shigella Spp. Isolated between 2001 and 2004 from Hospitalized Children with Diarrhoea in Kolkata (Calcutta), India." *Epidemiology and Infection* 133(6):1089–95. doi: 10.1017/S0950268805004498.
- Peabody, D. S. 1993. "The RNA Binding Site of Bacteriophage MS2 Coat Protein." *The EMBO Journal* 12(2):595–600. doi: 10.1002/J.1460-2075.1993.TB05691.X.
- Pédrón, Thierry, Christelle Thibault, and Philippe J. Sansonetti. 2003. "The Invasive Phenotype of Shigella Flexneri Directs a Distinct Gene Expression Pattern in the Human Intestinal Epithelial Cell Line Caco-2." *Journal of Biological Chemistry* 278(36):33878–86. doi: 10.1074/jbc.M303749200.

- Pell, Lisa G., Voula Kanelis, Logan W. Donaldson, P. Lynne Howell, and Alan R. Davidson. 2009. "The Phage Lambda Major Tail Protein Structure Reveals a Common Evolution for Long-Tailed Phages and the Type VI Bacterial Secretion System." *Proceedings of the National Academy of Sciences of the United States of America* 106(11):4160–65. doi: 10.1073/PNAS.0900044106.
- Penadés, José R., John Chen, Nuria Quiles-Puchalt, Nuria Carpena, and Richard P. Novick. 2015. "Bacteriophage-Mediated Spread of Bacterial Virulence Genes." *Current Opinion in Microbiology* 23:171–78. doi: 10.1016/J.MIB.2014.11.019.
- Peralta, Bibiana, David Gil-Carton, Daniel Castaño-Díez, Aurelie Bertin, Claire Boulogne, Hanna M. Oksanen, Dennis H. Bamford, and Nicola G. A. Abrescia. 2013. "Mechanism of Membranous Tunnelling Nanotube Formation in Viral Genome Delivery." *PLoS Biology* 11(9). doi: 10.1371/JOURNAL.PBIO.1001667.
- Perdomo, Juana J., Pierre Gounon, and Philippe J. Sansonetti. 1994. "Polymorphonuclear Leukocyte Transmigration Promotes Invasion of Colonic Epithelial Monolayer by *Shigella Flexneri*." *The Journal of Clinical Investigation* 93(2):633–43. doi: 10.1172/JCI117015.
- Perdomo, O. J. J., J. M. Cavaillon, M. Huerre, H. Ohayon, P. Gounon, and P. J. Sansonetti. 1994. "Acute Inflammation Causes Epithelial Invasion and Mucosal Destruction in Experimental Shigellosis." *The Journal of Experimental Medicine* 180(4):1307–19. doi: 10.1084/JEM.180.4.1307.
- Perros, Manos. 2015. "A Sustainable Model for Antibiotics." *Science* 347(6226):1062–64. doi: 10.1126/SCIENCE.AAA3048.
- Pettersen, Eric F., Thomas D. Goddard, Conrad C. Huang, Gregory S. Couch, Daniel M. Greenblatt, Elaine C. Meng, and Thomas E. Ferrin. 2004. "UCSF Chimera--a Visualization System for Exploratory Research and Analysis." *Journal of Computational Chemistry* 25(13):1605–12. doi: 10.1002/JCC.20084.
- Pettersen, Eric F., Thomas D. Goddard, Conrad C. Huang, Elaine C. Meng, Gregory S. Couch, Tristan I. Croll, John H. Morris, and Thomas E. Ferrin. 2021. "UCSF ChimeraX: Structure Visualization for Researchers, Educators, and Developers." *Protein Science: A Publication of the Protein Society* 30(1):70–82. doi: 10.1002/PRO.3943.
- Phalipon, Armelle, and Philippe J. Sansonetti. 2007. "Shigella's Ways of Manipulating the Host Intestinal Innate and Adaptive Immune System: A Tool Box for Survival?" *Immunology and Cell Biology* 85(2):119–29. doi: 10.1038/SJ.ICB7100025.
- Philpott, Dana J., Shoji Yamaoka, Alain Israël, and Philippe J. Sansonetti. 2000. "Invasive *Shigella Flexneri* Activates NF-Kappa B through a Lipopolysaccharide-Dependent Innate Intracellular Response and Leads to IL-8 Expression in Epithelial Cells." *Journal of Immunology (Baltimore, Md. : 1950)* 165(2):903–14. doi: 10.4049/JIMMUNOL.165.2.903.
- Pinta, Elise, Katarzyna Anna Duda, Anna Hanuszkiewicz, Tiina A. Salminen, José Antonio Bengoechea, Heidi Hyytiäinen, Buko Lindner, Joanna Radziejewska-Lebrecht, Otto Holst, and Mikael Skurnik. 2010. "Characterization of the Six Glycosyltransferases

- Involved in the Biosynthesis of *Yersinia Enterocolitica* Serotype O:3 Lipopolysaccharide Outer Core.” *Journal of Biological Chemistry* 285(36):28333–42. doi: 10.1074/JBC.M110.111336.
- Pires, D. P., L. D. R. Melo, D. Vilas Boas, S. Sillankorva, and J. Azeredo. 2017. “Phage Therapy as an Alternative or Complementary Strategy to Prevent and Control Biofilm-Related Infections.” *Current Opinion in Microbiology* 39:48–56. doi: 10.1016/J.MIB.2017.09.004.
- Pires, Diana P., Hugo Oliveira, Luís D. R. Melo, Sanna Sillankorva, and Joana Azeredo. 2016. “Bacteriophage-Encoded Depolymerases: Their Diversity and Biotechnological Applications.” *Applied Microbiology and Biotechnology* 100(5):2141–51. doi: 10.1007/S00253-015-7247-0.
- Pitisuttithum, Punnee, Dilara Islam, Supat Chamnanchanunt, Nattaya Ruamsap, Patchariya Khantapura, Jaranit Kaewkungwal, Chatporn Kittitrakul, Viravarn Luvira, Jittima Dhitavat, Malabi M. Venkatesan, Carl J. Mason, and Ladaporn Bodhidatta. 2016. “Clinical Trial of an Oral Live *Shigella Sonnei* Vaccine Candidate, WRSS1, in Thai Adults.” *Clinical and Vaccine Immunology : CVI* 23(7):564–75. doi: 10.1128/CVI.00665-15.
- Plisson, Celia, Helen E. White, Isabelle Auzat, Amineh Zafarani, Carlos São-José, Sophie Lhuillier, Paulo Tavares, and Elena v. Orlova. 2007. “Structure of Bacteriophage SPP1 Tail Reveals Trigger for DNA Ejection.” *The EMBO Journal* 26(15):3720–28. doi: 10.1038/SJ.EMBOJ.7601786.
- Porter, Keith R., Albert Claude, and Ernest F. Fullam. 1945. “A STUDY OF TISSUE CULTURE CELLS BY ELECTRON MICROSCOPY: METHODS AND PRELIMINARY OBSERVATIONS.” *The Journal of Experimental Medicine* 81(3):233–46. doi: 10.1084/JEM.81.3.233.
- Prehm, P., B. Jann, K. Jann, G. Schmidt, and S. Stirm. 1976. “On a Bacteriophage T3 and T4 Receptor Region within the Cell Wall Lipopolysaccharide of *Escherichia Coli* B.” *Journal of Molecular Biology* 101(2):277–81. doi: 10.1016/0022-2836(76)90377-6.
- Prendergast, Andrew J., and Paul Kelly. 2016. “Interactions between Intestinal Pathogens, Enteropathy and Malnutrition in Developing Countries.” *Current Opinion in Infectious Diseases* 29(3):229–36. doi: 10.1097/QCO.0000000000000261.
- PRICE, W. H. 2003. “BACTERIAL VIRUSES.” *https://doi.org/10.1146/Annurev.Mi.12.100158.000331* 67(2):124–27. doi: 10.1146/ANNUREV.MI.12.100158.000331.
- Prokhorov, Nikolai S., Cristian Riccio, Evelina L. Zdrovenko, Mikhail M. Shneider, Christopher Browning, Yuriy A. Knirel, Petr G. Leiman, and Andrey v. Letarov. 2017. “Function of Bacteriophage G7C Esterase Tailspike in Host Cell Adsorption.” *Molecular Microbiology* 105(3):385–98. doi: 10.1111/MMI.13710.
- Puzari, Minakshi, Mohan Sharma, and Pankaj Chetia. 2017. “Emergence of Antibiotic Resistant *Shigella* Species: A Matter of Concern.” *Journal of Infection and Public Health* 11(4):451–54. doi: 10.1016/J.JIPH.2017.09.025.



- Puzari, Minakshi, Mohan Sharma, and Pankaj Chetia. 2018. "Emergence of Antibiotic Resistant Shigella Species: A Matter of Concern." *Journal of Infection and Public Health* 11(4):451–54. doi: 10.1016/J.JIPH.2017.09.025.
- Qiu, Shaofu, Yong Wang, Xuebin Xu, Peng Li, Rongzhang Hao, Chaojie Yang, Nan Liu, Zhenjun Li, Zhongqiang Wang, Jian Wang, Zhihao Wu, Wenli Su, Guang Yang, Huiming Jin, Ligui Wang, Yansong Sun, Zhengan Yuan, Liuyu Huang, and Hongbin Song. 2013. "Multidrug-Resistant Atypical Variants of Shigella Flexneri in China." *Emerging Infectious Diseases* 19(7):1147–50. doi: 10.3201/EID1907.111221.
- Rakonjac, Jasna, Marjorie Russel, Sofia Khanum, Sam J. Brooke, and Marina Rajič. 2017. "Filamentous Phage: Structure and Biology." *Advances in Experimental Medicine and Biology* 1053:1–20. doi: 10.1007/978-3-319-72077-7\_1/COVER.
- Ram, Sripad, E. Sally Ward, and Raimund J. Ober. 2006. "Beyond Rayleigh's Criterion: A Resolution Measure with Application to Single-Molecule Microscopy." *Proceedings of the National Academy of Sciences of the United States of America* 103(12):4457–62. doi: 10.1073/PNAS.0508047103/SUPPL\_FILE/08047SUPPORTINGTEXT.PDF.
- Ranea, Juan A. G., Antonio Sillero, Janet M. Thornton, and Christine A. Orengo. 2006. "Protein Superfamily Evolution and the Last Universal Common Ancestor (LUCA)." *Journal of Molecular Evolution* 63(4):513–25. doi: 10.1007/S00239-005-0289-7/METRICS.
- Ranjbar, Reza, Mohammad Javad Hosseini, Ali Reza Kaffashian, and Shohreh Farshad. 2010. "An Outbreak of Shigellosis Due to Shigella Flexneri Serotype 3a in a Prison in Iran." *Archives of Iranian Medicine* 13(5):413–16. doi: 010135/aim.008.
- Ranjbar, Reza, Caterina Mammina, Mohammad R. Pourshafie, and Mohammad M. Soltan-Dallal. 2008. "Characterization of Endemic Shigella Boydii Strains Isolated in Iran by Serotyping, Antimicrobial Resistance, Plasmid Profile, Ribotyping and Pulsed-Field Gel Electrophoresis." *BMC Research Notes* 1. doi: 10.1186/1756-0500-1-74.
- Rao, Venigalla B., Vishakha Thaker, and Lindsay W. Black. 1992. "A Phage T4 in Vitro Packaging System for Cloning Long DNA Molecules." *Gene* 113(1):25–33. doi: 10.1016/0378-1119(92)90666-D.
- Raoult, Didier, Stéphane Audic, Catherine Robert, Chantal Abergel, Patricia Renesto, Hiroyuki Ogata, Bernard la Scola, Marie Suzan, and Jean Michel Claverie. 2004. "The 1.2-Megabase Genome Sequence of Mimivirus." *Science (New York, N.Y.)* 306(5700):1344–50. doi: 10.1126/SCIENCE.1101485.
- Reviews, Source, No Jul Aug, Orin S. Levine, Myron M. Levine, Vaccine Development, and Division Geographic. 2016. "Houseflies ( Musca Domestica ) as Mechanical Vectors of Shigellosis Author ( s ): Orin S . Levine and Myron M . Levine Published by : Oxford University Press Stable URL : Http://Www.Jstor.Org/Stable/4456042 Accessed : 18-08-2016 12 : 38 UTC Your Use of Th." 13(4):688–96.
- Rodríguez-Rubio, Lorena, Beatriz Martínez, David M. Donovan, Ana Rodríguez, and Pilar García. 2013. "Bacteriophage Virion-Associated Peptidoglycan Hydrolases: Potential New Enzybiotics." *Critical Reviews in Microbiology* 39(4):427–34. doi: 10.3109/1040841X.2012.723675.

- Rohou, Alexis, and Nikolaus Grigorieff. 2015. “CTFFIND4: Fast and Accurate Defocus Estimation from Electron Micrographs.” *Journal of Structural Biology* 192(2):216–21. doi: 10.1016/J.JSB.2015.08.008.
- Rolfo, Florencia, Gustavo Horacio Marin, Martin Silberman, Jorgelina Pattin, Silvina Giugno, Blanca Gatti, Marisa Bettiol, and Ana Rigoni. 2012. “Epidemiological Study of Shigellosis in an Urban Area of Argentina.” *Journal of Infection in Developing Countries* 6(4):324–28. doi: 10.3855/JIDC.1977.
- Roseman, A. M. 2004. “FindEM--a Fast, Efficient Program for Automatic Selection of Particles from Electron Micrographs.” *Journal of Structural Biology* 145(1–2):91–99. doi: 10.1016/J.JSB.2003.11.007.
- Rosenthal, Peter B. 2015. “From High Symmetry to High Resolution in Biological Electron Microscopy: A Commentary on Crowther (1971) ‘Procedures for Three-Dimensional Reconstruction of Spherical Viruses by Fourier Synthesis from Electron Micrographs.’” *Philosophical Transactions of the Royal Society B: Biological Sciences* 370(1666). doi: 10.1098/RSTB.2014.0345.
- De Rosier, D. J., and A. Klug. 1968. “Reconstruction of Three Dimensional Structures from Electron Micrographs.” *Nature* 217(5124):130–34. doi: 10.1038/217130A0.
- Roux, Simon, Jennifer R. Brum, Bas E. Dutilh, Shinichi Sunagawa, Melissa B. Duhaime, Alexander Loy, Bonnie T. Poulos, Natalie Solonenko, Elena Lara, Julie Poulain, Stéphane Pesant, Stefanie Kandels-Lewis, Céline Dimier, Marc Picheral, Sarah Searson, Corinne Cruaud, Adriana Alberti, Carlos M. Duarte, Josep M. Gasol, Dolors Vaqué, Peer Bork, Silvia G. Acinas, Patrick Wincker, and Matthew B. Sullivan. 2016. “Ecogenomics and Potential Biogeochemical Impacts of Globally Abundant Ocean Viruses.” *Nature* 537(7622):689–93. doi: 10.1038/NATURE19366.
- Roux, Simon, Mart Krupovic, Rebecca A. Daly, Adair L. Borges, Stephen Nayfach, Frederik Schulz, Jan-Fang Cheng, Natalia N. Ivanova, Joseph Bondy-Denomy, Kelly C. Wrighton, Tanja Woyke, Axel Visel, Nikos C. Kyrpides, and Emiley A. Elie-Fadrosh. 2019. “Cryptic Inoviruses Are Pervasive in Bacteria and Archaea across Earth’s Biomes.” *BioRxiv* 548222. doi: 10.1101/548222.
- Russel, M., and P. Model. 1981. “A Mutation Downstream from the Signal Peptidase Cleavage Site Affects Cleavage but Not Membrane Insertion of Phage Coat Protein.” *Proceedings of the National Academy of Sciences of the United States of America* 78(3):1717–21. doi: 10.1073/PNAS.78.3.1717.
- Sakaguchi, Takanori, Henrik Köhler, Xiubin Gu, Beth A. McCormick, and Hans Christian Reinecker. 2002. “Shigella Flexneri Regulates Tight Junction-Associated Proteins in Human Intestinal Epithelial Cells.” *Cellular Microbiology* 4(6):367–81. doi: 10.1046/J.1462-5822.2002.00197.X.
- Salmond, George P. C., and Peter C. Fineran. 2015. “A Century of the Phage: Past, Present and Future.” *Nature Reviews. Microbiology* 13(12):777–86. doi: 10.1038/NRMICRO3564.
- Samsygina, G. A., and E. G. Boni. 1984. “[Bacteriophages and Phage Therapy in Pediatric Practice].” *Pediatrriia* (4):67–70.

- Sanger, F., G. M. Air, B. G. Barrell, N. L. Brown, A. R. Coulson, J. C. Fiddes, C. A. Hutchison, P. M. Slocombe, and M. Smith. 1977. "Nucleotide Sequence of Bacteriophage Phi X174 DNA." *Nature* 265(5596):687–95. doi: 10.1038/265687A0.
- Sansonetti, P. J., J. Arondel, M. Huerre, A. Harada, and K. Matsushima. 1999. "Interleukin-8 Controls Bacterial Transepithelial Translocation at the Cost of Epithelial Destruction in Experimental Shigellosis." *Infection and Immunity* 67(3):1471. doi: 10.1128/IAI.67.3.1471-1480.1999.
- Sansonetti, Philippe J. 2004. "War and Peace at Mucosal Surfaces." *Nature Reviews. Immunology* 4(12):953–64. doi: 10.1038/NRI1499.
- Sansonetti, Philippe J., Josette Arondel, J. Robert Cantey, Marie Christine Prévost, and Michel Huerre. 1996. "Infection of Rabbit Peyer's Patches by *Shigella Flexneri*: Effect of Adhesive or Invasive Bacterial Phenotypes on Follicle-Associated Epithelium." *Infection and Immunity* 64(7):2752–64. doi: 10.1128/IAI.64.7.2752-2764.1996.
- Sansonetti, Philippe J., Josette Arondel, Jean Marc Cavaillon, and Michel Huerre. 1995. "Role of Interleukin-1 in the Pathogenesis of Experimental Shigellosis." *The Journal of Clinical Investigation* 96(2):884–92. doi: 10.1172/JCI118135.
- Sansonetti, Philippe J., Armelle Phalipon, Josette Arondel, Kavitha Thirumalai, Subhashis Banerjee, Shizuo Akira, Kiyoshi Takeda, and Arturo Zychlinsky. 2000. "Caspase-1 Activation of IL-1beta and IL-18 Are Essential for *Shigella Flexneri*-Induced Inflammation." *Immunity* 12(5):581–90. doi: 10.1016/S1074-7613(00)80209-5.
- Sansonetti, Philippe J., Antoinette Ryter, Philippe Clerc, Anthony T. Maurelli, and Joelle Mounier. 1986. "Multiplication of *Shigella Flexneri* within HeLa Cells: Lysis of the Phagocytic Vacuole and Plasmid-Mediated Contact Hemolysis." *Infection and Immunity* 51(2):461–69. doi: 10.1128/IAI.51.2.461-469.1986.
- Scallan, Elaine, Robert M. Hoekstra, Frederick J. Angulo, Robert V. Tauxe, Marc Alain Widdowson, Sharon L. Roy, Jeffery L. Jones, and Patricia M. Griffin. 2011. "Foodborne Illness Acquired in the United States--Major Pathogens." *Emerging Infectious Diseases* 17(1):7–15. doi: 10.3201/EID1701.P11101.
- Schattner, Peter, Angela N. Brooks, and Todd M. Lowe. 2005. "The TRNAscan-SE, Snoscan and SnoGPS Web Servers for the Detection of tRNAs and snoRNAs." *Nucleic Acids Research* 33(Web Server issue). doi: 10.1093/NAR/GKI366.
- Scheres, Sjors H. W. 2012a. "A Bayesian View on Cryo-EM Structure Determination." *Journal of Molecular Biology* 415(2):406–18. doi: 10.1016/J.JMB.2011.11.010.
- Scheres, Sjors H. W. 2012b. "A Bayesian View on Cryo-EM Structure Determination." *Journal of Molecular Biology* 415(2):406–18. doi: 10.1016/J.JMB.2011.11.010.
- Scheres, Sjors H. W. 2012c. "RELION: Implementation of a Bayesian Approach to Cryo-EM Structure Determination." *Journal of Structural Biology* 180(3):519–30. doi: 10.1016/J.JSB.2012.09.006.

- Scheres, Sjors H. W., Mikel Valle, and José María Carazo. 2005. "Fast Maximum-Likelihood Refinement of Electron Microscopy Images." *Bioinformatics (Oxford, England)* 21 Suppl 2(SUPPL. 2). doi: 10.1093/BIOINFORMATICS/BTI1140.
- Scheres, Sjors H. W., Mikel Valle, Rafael Nuñez, Carlos O. S. Sorzano, Roberto Marabini, Gabor T. Herman, and Jose Maria Carazo. 2005. "Maximum-Likelihood Multi-Reference Refinement for Electron Microscopy Images." *Journal of Molecular Biology* 348(1):139–49. doi: 10.1016/J.JMB.2005.02.031.
- Schmelcher, Mathias, David M. Donovan, and Martin J. Loessner. 2012. "Bacteriophage Endolysins as Novel Antimicrobials." *Future Microbiology* 7(10):1147–71. doi: 10.2217/FMB.12.97.
- Schroeder, Gunnar N., and Hubert Hilbi. 2008. "Molecular Pathogenesis of Shigella Spp.: Controlling Host Cell Signaling, Invasion, and Death by Type III Secretion." *Clinical Microbiology Reviews* 21(1):134–56. doi: 10.1128/CMR.00032-07.
- la Scola, Bernard, Stéphane Audic, Catherine Robert, Liang Jungang, Xavier de Lamballerie, Michel Drancourt, Richard Birtles, Jean Michel Claverie, and Didier Raoult. 2003. "A Giant Virus in Amoebae." *Science (New York, N.Y.)* 299(5615):2033. doi: 10.1126/SCIENCE.1081867.
- Seaman, Paul F., and Martin J. Day. 2007. "Isolation and Characterization of a Bacteriophage with an Unusually Large Genome from the Great Salt Plains National Wildlife Refuge, Oklahoma, USA." *FEMS Microbiology Ecology* 60(1):1–13. doi: 10.1111/J.1574-6941.2006.00277.X.
- Von Seidlein, Lorenz, Ryun Kim Deok, Mohammad Ali, Hyejon Lee, Xuan Yi Wang, Dinh Thiem Vu, Gia Canh Do, Wanpen Chaicumpa, Magdarina D. Agtini, Anowar Hossain, Zulfiqar A. Bhutta, Carl Mason, Ornthipa Sethabutr, Kaiser Talukder, G. B. Nair, Jacqueline L. Deen, Karen Kotloff, and John Clemens. 2006. "A Multicentre Study of Shigella Diarrhoea in Six Asian Countries: Disease Burden, Clinical Manifestations, and Microbiology." *PLoS Medicine* 3(9):1556–69. doi: 10.1371/JOURNAL.PMED.0030353.
- Sen, D., P. Dutta, B. C. Deb, and S. C. Pal. 1988. "NALIDIXIC-ACID RESISTANT SHIGELLA DYSENTERIAE TYPE 1 IN EASTERN INDIA." *The Lancet* 332(8616):911. doi: 10.1016/S0140-6736(88)92515-9.
- Senior, Andrew W., Richard Evans, John Jumper, James Kirkpatrick, Laurent Sifre, Tim Green, Chongli Qin, Augustin Židek, Alexander W. R. Nelson, Alex Bridgland, Hugo Penedones, Stig Petersen, Karen Simonyan, Steve Crossan, Pushmeet Kohli, David T. Jones, David Silver, Koray Kavukcuoglu, and Demis Hassabis. 2020. "Improved Protein Structure Prediction Using Potentials from Deep Learning." *Nature* 2020 577:7792 577(7792):706–10. doi: 10.1038/s41586-019-1923-7.
- Shahin, Khashayar, Mohadeseh Barazandeh, Lili Zhang, Abolghasem Hedayatkah, Tao He, Hongduo Bao, Mojtaba Mansoorianfar, Maoda Pang, Heye Wang, Ruicheng Wei, and Ran Wang. 2021. "Biodiversity of New Lytic Bacteriophages Infecting Shigella Spp. in Freshwater Environment." *Frontiers in Microbiology* 12. doi: 10.3389/FMICB.2021.619323.

- Shahin, Khashayar, Majid Bouzari, and Ran Wang. 2018. "Isolation, Characterization and Genomic Analysis of a Novel Lytic Bacteriophage VB\_SsoS-ISF002 Infecting *Shigella* Sonnei and *Shigella* Flexneri." *Journal of Medical Microbiology* 67(3):376–86. doi: 10.1099/JMM.0.000683.
- Shan, Jinyu, Ananthi Ramachandran, Anisha M. Thanki, Fatima B. I. Vukusic, Jakub Barylski, and Martha R. J. Clokie. 2018. "Bacteriophages Are More Virulent to Bacteria with Human Cells than They Are in Bacterial Culture; Insights from HT-29 Cells." *Scientific Reports* 2018 8:1 8(1):1–8. doi: 10.1038/s41598-018-23418-y.
- Sharma, Sonika, Sibnarayan Datta, Soumya Chatterjee, Mohan G. Vairale, Rajesh Kumar Prasad, Bidisha Das, and Vanlalhmuaka. 2020. "Isolation and Characterization of Lytic Bacteriophages from Wastewater and Its Application in Pathogen Reduction." *Defence Life Science Journal* 5(2):80–86. doi: 10.14429/DLSJ.5.15599.
- Shiferaw, Beletshachew, Suzanne Solghan, Amanda Palmer, Kevin Joyce, Ezra J. Barzilay, Amy Krueger, and Paul Cieslak. 2012. "Antimicrobial Susceptibility Patterns of *Shigella* Isolates in Foodborne Diseases Active Surveillance Network (FoodNet) Sites, 2000–2010." *Clinical Infectious Diseases : An Official Publication of the Infectious Diseases Society of America* 54 Suppl 5(SUPPL.5). doi: 10.1093/CID/CIS230.
- SHIGA, KIYOSHI. 1936. "The Trend of Prevention, Therapy and Epidemiology of Dysentery since the Discovery of Its Causative Organism." *New England Journal of Medicine* 215(26):1205–11. doi: 10.1056/nejm193612242152602.
- Shkoporov, Andrey N., Adam G. Clooney, Thomas D. S. Sutton, Feargal J. Ryan, Karen M. Daly, James A. Nolan, Siobhan A. McDonnell, Ekaterina V. Khokhlova, Lorraine A. Draper, Amanda Forde, Emma Guerin, Vimalkumar Velayudhan, R. Paul Ross, and Colin Hill. 2019. "The Human Gut Virome Is Highly Diverse, Stable, and Individual Specific." *Cell Host & Microbe* 26(4):527–541.e5. doi: 10.1016/J.CHOM.2019.09.009.
- Sigworth, F. J. 1998. "A Maximum-Likelihood Approach to Single-Particle Image Refinement." *Journal of Structural Biology* 122(3):328–39. doi: 10.1006/JSBI.1998.4014.
- Silva, Yolanda J., Liliana Costa, Carla Pereira, Ângela Cunha, Ricardo Calado, Newton C. M. Gomes, and Adelaide Almeida. 2014. "Influence of Environmental Variables in the Efficiency of Phage Therapy in Aquaculture." *Microbial Biotechnology* 7(5):401–13. doi: 10.1111/1751-7915.12090.
- Singer, Monique, and Philippe J. Sansonetti. 2004. "IL-8 Is a Key Chemokine Regulating Neutrophil Recruitment in a New Mouse Model of *Shigella*-Induced Colitis." *The Journal of Immunology* 173(6):4197–4206. doi: 10.4049/JIMMUNOL.173.6.4197.
- Skurnik, Mikael, Reija Venho, Paavo Toivanen, and Ayman Al-Hendy. 1995. "A Novel Locus of *Yersinia Enterocolitica* Serotype O:3 Involved in Lipopolysaccharide Outer Core Biosynthesis." *Molecular Microbiology* 17(3):575–94. doi: 10.1111/J.1365-2958.1995.MMI\_17030575.X.
- Slopek, S., I. Durlakowa, B. Weber-Dabrowska, A. Kucharewicz-Krukowska, M. Dabrowski, and R. Bisikiewicz. 1983. "Results of Bacteriophage Treatment of Suppurative Bacterial

- Infections. II. Detailed Evaluation of the Results.” *Archivum Immunologiae et Therapiae Experimentalis* 31(3):293–327.
- Smith, Douglas E., Sander J. Tans, Steven B. Smith, Shelley Grimes, Dwight L. Anderson, and Carlos Bustamante. 2001. “The Bacteriophage Straight Phi29 Portal Motor Can Package DNA against a Large Internal Force.” *Nature* 413(6857):748–52. doi: 10.1038/35099581.
- Soffer, Nitzan, Joelle Woolston, Manrong Li, Chythanya Das, and Alexander Sulakvelidze. 2017. “Bacteriophage Preparation Lytic for Shigella Significantly Reduces Shigella Sonnei Contamination in Various Foods.” *PloS One* 12(3). doi: 10.1371/JOURNAL.PONE.0175256.
- Spellberg, Brad, Robert Guidos, David Gilbert, John Bradley, Helen W. Boucher, W. Michael Scheld, John G. Bartlett, and John Edwards. 2008. “The Epidemic of Antibiotic-Resistant Infections: A Call to Action for the Medical Community from the Infectious Diseases Society of America.” *Clinical Infectious Diseases* 46(2):155–64. doi: 10.1086/524891/2/46-2-155-FIG002.GIF.
- Steffen, Robert, David R. Hill, and Herbert L. DuPont. 2015. “Traveler’s Diarrhea: A Clinical Review.” *JAMA* 313(1):71–80. doi: 10.1001/JAMA.2014.17006.
- Stevens, Joanne M., Edouard E. Galyov, and Mark P. Stevens. 2006. “Actin-Dependent Movement of Bacterial Pathogens.” *Nature Reviews. Microbiology* 4(2):91–101. doi: 10.1038/NRMICRO1320.
- Stone, Edel, Katrina Campbell, Irene Grant, and Olivia McAuliffe. 2019. “Understanding and Exploiting Phage-Host Interactions.” *Viruses* 11(6). doi: 10.3390/V11060567.
- Stothard, Paul, and David S. Wishart. 2005. “Circular Genome Visualization and Exploration Using CGView.” *Bioinformatics (Oxford, England)* 21(4):537–39. doi: 10.1093/BIOINFORMATICS/BTI054.
- Subramanian, Sundharraman, Kristin N. Parent, and Sarah M. Doore. 2020. “Ecology, Structure, and Evolution of Shigella Phages.” *Annual Review of Virology* 7(1):121–41. doi: 10.1146/ANNUREV-VIROLOGY-010320-052547.
- Sulakvelidze, A., Z. Alavidze, and Jr Morris. 2001. “Bacteriophage Therapy.” *Antimicrobial Agents and Chemotherapy* 45(3):649–59. doi: 10.1128/AAC.45.3.649-659.2001/ASSET/65EA6D0A-84FC-43AC-B12C-CD6CC793B377/ASSETS/GRAPHIC/AC0310583003.JPEG.
- Sullivan, Mitchell J., Nicola K. Petty, and Scott A. Beatson. 2011. “Easyfig: A Genome Comparison Visualizer.” *Bioinformatics (Oxford, England)* 27(7):1009–10. doi: 10.1093/BIOINFORMATICS/BTR039.
- Suloway, Christian, Jian Shi, Anchi Cheng, James Pulokas, Bridget Carragher, Clinton S. Potter, Shawn Q. Zheng, David A. Agard, and Grant J. Jensen. 2009. “Fully Automated, Sequential Tilt-Series Acquisition with Leginon.” *Journal of Structural Biology* 167(1):11–18. doi: 10.1016/J.JSB.2009.03.019.
- Summers, W. C. 2001. “Bacteriophage Therapy.” *Annual Review of Microbiology* 55:437–51. doi: 10.1146/ANNUREV.MICRO.55.1.437.

- Summers, William C. 1999. "Félix d'Herelle and the Origins of Molecular Biology." 230.
- Sunagawa, Shinichi, Daniel R. Mende, Georg Zeller, Fernando Izquierdo-Carrasco, Simon A. Berger, Jens Roat Kultima, Luis Pedro Coelho, Manimozhiyan Arumugam, Julien Tap, Henrik Bjørn Nielsen, Simon Rasmussen, Søren Brunak, Oluf Pedersen, Francisco Guarner, Willem M. de Vos, Jun Wang, Junhua Li, Joël Doré, S. Dusko Ehrlich, Alexandros Stamatakis, and Peer Bork. 2013. "Metagenomic Species Profiling Using Universal Phylogenetic Marker Genes." *Nature Methods* 2013 10:12 10(12):1196–99. doi: 10.1038/nmeth.2693.
- Sur, Dipika, Swapan K. Niyogi, Shravani Sur, Kamal K. Datta, Yoshifumi Takeda, Gopinath Balakrish Nair, and Sujit K. Bhattacharya. 2003. "Multidrug-Resistant Shigella Dysenteriae Type 1: Forerunners of a New Epidemic Strain in Eastern India? - Volume 9, Number 3—March 2003 - Emerging Infectious Diseases Journal - CDC." *Emerging Infectious Diseases* 9(3):404–5. doi: 10.3201/EID0903.020352.
- Suttle, Curtis A. 2005. "Viruses in the Sea." *Nature* 437(7057):356–61. doi: 10.1038/NATURE04160.
- Taneja, Neelam, and Abhishek Mewara. 2016. "Shigellosis: Epidemiology in India." *The Indian Journal of Medical Research* 143(5):565–76. doi: 10.4103/0971-5916.187104.
- Tang, Guang, Liwei Peng, Philip R. Baldwin, Deepinder S. Mann, Wen Jiang, Ian Rees, and Steven J. Ludtke. 2007. "EMAN2: An Extensible Image Processing Suite for Electron Microscopy." *Journal of Structural Biology* 157(1):38–46. doi: 10.1016/J.JSB.2006.05.009.
- Tang, Swee Seong, Sudhangshu Kumar Biswas, Wen Siang Tan, Ananda Kumar Saha, and Bey Fen Leo. 2019. "Efficacy and Potential of Phage Therapy against Multidrug Resistant Shigella Spp." *PeerJ* 7(4). doi: 10.7717/PEERJ.6225.
- Tavares, Paulo, Rudi Lurz, Asita Stiege, Beate Rückert, and Thomas A. Trautner. 1996. "Sequential Headful Packaging and Fate of the Cleaved DNA Ends in Bacteriophage SPP1." *Journal of Molecular Biology* 264(5):954–67. doi: 10.1006/JMBI.1996.0689.
- Taylor, David N., Peter Echeverria, Tibor Pál, Orntipa Sethabutr, Somsri Saiborisuth, Sumale Sricharmorn, Bernard Rowe, and John Cross. 1986. "The Role of Shigella Spp., Enteroinvasive Escherichia Coli, and Other Enteropathogens as Causes of Childhood Dysentery in Thailand." *The Journal of Infectious Diseases* 153(6):1132–38. doi: 10.1093/INFDIS/153.6.1132.
- Ter-Pogossian, Michel M. 1984. "Image Reconstruction from Projections, The Fundamentals of Computerized Tomography by G. T. Herman." *Medical Physics* 11(1):90–90. doi: 10.1118/1.595466.
- Tey, Beng Ti, Shin Tean Ooi, Khang Chi Yong, Michelle Yeen, Tan Ng, Tau Chuan Ling, and Wen Siang Tan. 2009. "Production of Fusion M13 Phage Bearing the Di-Sulphide Constrained Peptide Sequence (C-WSFFSNI-C) That Interacts with Hepatitis B Core Antigen." *African Journal of Biotechnology* 8(2):268–73.

- The, Source, British Medical, and No Sep. 2017. "The Etiology Of Tropical Dysentery Author (s): Simon Flexner Stable URL : <http://www.jstor.org/stable/20265833>." 2(2074):917–20.
- Tiemann, Bernd, Reinhard Depping, Egle Gineikiene, Laura Kaliniene, Rimas Nivinskas, and Wolfgang Rüger. 2004. "ModA and ModB, Two ADP-Ribosyltransferases Encoded by Bacteriophage T4: Catalytic Properties and Mutation Analysis." *Journal of Bacteriology* 186(21):7262–72. doi: 10.1128/JB.186.21.7262-7272.2004.
- Topka-Bielecka, Gracja, Sylwia Bloch, Bożena Nejman-Faleńczyk, Michał Grabski, Agata Jurczak-Kurek, Marcin Górniak, Aleksandra Dydecka, Agnieszka Necel, Grzegorz Węgrzyn, and Alicja Węgrzyn. 2020. "Characterization of the Bacteriophage VB\_EfaS-271 Infecting *Enterococcus Faecalis*." *International Journal of Molecular Sciences* 21(17):1–27. doi: 10.3390/IJMS21176345.
- Torres-Barceló, Clara, and Michael E. Hochberg. 2016. "Evolutionary Rationale for Phages as Complements of Antibiotics." *Trends in Microbiology* 24(4):249–56. doi: 10.1016/J.TIM.2015.12.011.
- Trofa, Andrew F., Hannah Ueno-Olsen, Ruiko Oiwa, and Masanosuke Yoshikawa. 1999. "Dr. Kiyoshi Shiga: Discoverer of the Dysentery Bacillus." *Clinical Infectious Diseases* 29(5):1303–6. doi: 10.1086/313437.
- Tu, Anh Hue T., Le Roy L. Voelker, Xuejun Shen, and Kevin Dybvig. 2001. "Complete Nucleotide Sequence of the Mycoplasma Virus P1 Genome." *Plasmid* 45(2):122–26. doi: 10.1006/PLAS.2000.1501.
- Tunyasuvunakool, Kathryn, Jonas Adler, Zachary Wu, Tim Green, Michal Zielinski, Augustin Židek, Alex Bridgland, Andrew Cowie, Clemens Meyer, Agata Laydon, Sameer Velankar, Gerard J. Kleywegt, Alex Bateman, Richard Evans, Alexander Pritzel, Michael Figurnov, Olaf Ronneberger, Russ Bates, Simon A. A. Kohl, Anna Potapenko, Andrew J. Ballard, Bernardino Romera-Paredes, Stanislav Nikolov, Rishub Jain, Ellen Clancy, David Reiman, Stig Petersen, Andrew W. Senior, Koray Kavukcuoglu, Ewan Birney, Pushmeet Kohli, John Jumper, and Demis Hassabis. 2021. "Highly Accurate Protein Structure Prediction for the Human Proteome." *Nature* 2021 596:7873 596(7873):590–96. doi: 10.1038/s41586-021-03828-1.
- Twort, F. W. 1915. "AN INVESTIGATION ON THE NATURE OF ULTRA-MICROSCOPIC VIRUSES." *The Lancet* 186(4814):1241–43. doi: 10.1016/S0140-6736(01)20383-3.
- Ud-Din, Abu I. M. S., Syeda U. H. Wahid, Hasan A. Latif, Mohammad Shahnaij, Mahmuda Akter, Ishrat J. Azmi, Trisheet N. Hasan, Dilruba Ahmed, Mohammad A. Hossain, Abu S. G. Faruque, Shah M. Faruque, and Kaisar A. Talukder. 2013. "Changing Trends in the Prevalence of Shigella Species: Emergence of Multi-Drug Resistant Shigella Sonnei Biotype g in Bangladesh." *PLOS ONE* 8(12):e82601. doi: 10.1371/JOURNAL.PONE.0082601.
- Valegård, Karin, Lars Liljas, Kerstin Fridborg, and Torsten Unge. 1990. "The Three-Dimensional Structure of the Bacterial Virus MS2." *Nature* 345(6270):36–41. doi: 10.1038/345036A0.



- Valpuesta, Jose M., and Jose L. Carrascosa. 1994. "Structure of Viral Connectors and Their Function in Bacteriophage Assembly and DNA Packaging." *Quarterly Reviews of Biophysics* 27(2):107–55. doi: 10.1017/S0033583500004510.
- Valpuesta, JoséMaría, Hisao Fujisawa, Sergio Marco, JoséMaría Carazo, and JoséL L. Carrascosa. 1992. "Three-Dimensional Structure of T3 Connector Purified from Overexpressing Bacteria." *Journal of Molecular Biology* 224(1):103–12. doi: 10.1016/0022-2836(92)90579-9.
- Vidaver, Anne K., R. K. Koski, and J. L. Van Etten. 1973. "Bacteriophage  $\Phi 6$ : A Lipid-Containing Virus of *Pseudomonas Phaseolicola*." *Journal of Virology* 11(5):799–805. doi: 10.1128/JVI.11.5.799-805.1973.
- Viertel, Tania Mareike, Klaus Ritter, and Hans Peter Horz. 2014. "Viruses versus Bacteria- Novel Approaches to Phage Therapy as a Tool against Multidrug-Resistant Pathogens." *The Journal of Antimicrobial Chemotherapy* 69(9):2326–36. doi: 10.1093/JAC/DKU173.
- Wang, Jia, Feiyang Zhao, Huzhi Sun, Qian Wang, Can Zhang, Wenhua Liu, Ling Zou, Qiang Pan, and Huiying Ren. 2019. "Isolation and Characterization of the *Staphylococcus Aureus* Bacteriophage VB\_SauS\_SA2." *AIMS Microbiology* 5(3):285–307. doi: 10.3934/MICROBIOL.2019.3.285.
- Wassef, J. S., D. F. Keren, and J. L. Mailloux. 1989. "Role of M Cells in Initial Antigen Uptake and in Ulcer Formation in the Rabbit Intestinal Loop Model of Shigellosis." *Infection and Immunity* 57(3):858–63. doi: 10.1128/IAI.57.3.858-863.1989.
- Watanabe, Ryohei, Tetsuya Matsumoto, Go Sano, Yoshikazu Ishii, Kazuhiro Tateda, Yoshinobu Sumiyama, Jumpei Uchiyama, Shingo Sakurai, Shigenobu Matsuzaki, Shosuke Imai, and Keizo Yamaguchi. 2007. "Efficacy of Bacteriophage Therapy against Gut-Derived Sepsis Caused by *Pseudomonas Aeruginosa* in Mice." *Antimicrobial Agents and Chemotherapy* 51(2):446. doi: 10.1128/AAC.00635-06.
- Way, Sing Sing, Alain C. Borczuk, Rene Dominitz, and Marcia B. Goldberg. 1998. "An Essential Role for Gamma Interferon in Innate Resistance to *Shigella Flexneri* Infection." *Infection and Immunity* 66(4):1342–48. doi: 10.1128/IAI.66.4.1342-1348.1998.
- Webb, Benjamin, and Andrej Sali. 2016. "Comparative Protein Structure Modeling Using MODELLER." *Current Protocols in Bioinformatics* 54:5.6.1-5.6.37. doi: 10.1002/CPBI.3.
- Weber-Dąbrowska, B., M. Dabrowski, and S. Šlopek. 1987. "Studies on Bacteriophage Penetration in Patients Subjected to Phage Therapy." *Archivum Immunologiae et Therapiae Experimentalis*.
- Weber-Dabrowska, Beata, Ewa Jończyk-Matysiak, Maciej Zaczek, Małgorzata Łobocka, Marzanna Łusiak-Szelachowska, and Andrzej Górski. 2016. "Bacteriophage Procurement for Therapeutic Purposes." *Frontiers in Microbiology* 7(AUG). doi: 10.3389/FMICB.2016.01177.
- Weill, François Xavier, Elisabeth Njamkepo, Nizar Fawal, Alicia Tran-Dien, Jane Hawkey, Nancy Strockbine, Claire Jenkins, Kaisar A. Talukder, Raymond Bercion, Konstantin Kuleshov, Renáta Kolínská, Julie E. Russell, Lidia Kaftyreva, Marie Accou-Demartin,

- Andreas Karas, Olivier Vandenberg, Alison E. Mather, Carl J. Mason, Andrew J. Page, Thandavarayan Ramamurthy, Chantal Bizet, Andrzej Gamian, Isabelle Carle, Amy Gassama Sow, Christiane Bouchier, Astrid Louise Wester, Monique Lejay-Collin, Marie Christine Fonkoua, Simon Le Hello, Martin J. Blaser, Cecilia Jernberg, Corinne Ruckly, Audrey Mérens, Anne Laure Page, Martin Aslett, Peter Roggentin, Angelika Fruth, Erick Denamur, Malabi Venkatesan, Hervé Bercovier, Ladaporn Bodhidatta, Chien Shun Chiou, Dominique Clermont, Bianca Colonna, Svetlana Egorova, Gururaja P. Pazhani, Analia V. Ezernitchi, Ghislaine Guigon, Simon R. Harris, Hidemasa Izumiya, Agnieszka Korzeniowska-Kowal, Anna Lutyhska, Malika Gouali, Francine Grimont, Céline Langendorf, Monika Marejková, Lorea A. M. Peterson, Guillermo Perez-Perez, Antoinette Ngandjio, Alexander Podkolzin, Erika Souche, Mariia Makarova, German A. Shipulin, Changyun Ye, Helena Žemličková, Mária Herpay, Patrick A. D. Grimont, Julian Parkhill, Philippe Sansonetti, Kathryn E. Holt, Sylvain Brisse, and Nicholas R. Thomson. 2016. “Global Phylogeography and Evolutionary History of *Shigella Dysenteriae* Type 1.” *Nature Microbiology* 2016 1:4 1(4):1–10. doi: 10.1038/nmicrobiol.2016.27.
- WHO. 2014. “Antimicrobial Resistance. Global Report on Surveillance.” *World Health Organization* 61(3):12–28. doi: 10.1007/s13312-014-0374-3.
- WHO Technical Report Series. 2011. “The Selection and Use of Essential Medicines: Report of the WHO Expert Committee, 2011.” *World Health Organization - Technical Report Series* 1006:1–268.
- Wiese, Sebastian, Thomas Gronemeyer, Rob Ofman, Markus Kunze, Cláudia P. Grou, José A. Almeida, Martin Eisenacher, Christian Stephan, Heiko Hayen, Lukas Schollenberger, Thomas Korosec, Hans R. Waterham, Wolfgang Schliebs, Ralf Erdmann, Johannes Berger, Helmut E. Meyer, Wilhelm Just, Jorge E. Azevedo, Ronald J. A. Wanders, and Bettina Warscheid. 2007. “Proteomics Characterization of Mouse Kidney Peroxisomes by Tandem Mass Spectrometry and Protein Correlation Profiling.” *Molecular & Cellular Proteomics* 6(12):2045–57. doi: 10.1074/MCP.M700169-MCP200.
- Williams, David B., and C. Barry Carter. 2009. “Transmission Electron Microscopy: A Textbook for Materials Science.” *Transmission Electron Microscopy: A Textbook for Materials Science* 1–760. doi: 10.1007/978-0-387-76501-3/COVER.
- Williams Smith, H., and M. B. Huggins. 1983. “Effectiveness of Phages in Treating Experimental *Escherichia Coli* Diarrhoea in Calves, Piglets and Lambs.” *Journal of General Microbiology* 129(8):2659–75. doi: 10.1099/00221287-129-8-2659.
- Williamson, Kurt E., Jeffry J. Fuhrmann, K. Eric Wommack, and Mark Radosevich. 2017. “Viruses in Soil Ecosystems: An Unknown Quantity Within an Unexplored Territory.” *Annual Review of Virology* 4(1):201–19. doi: 10.1146/ANNUREV-VIROLOGY-101416-041639.
- Wilson, John H. 1973. “Function of the Bacteriophage T4 Transfer RNA’s.” *Journal of Molecular Biology* 74(4). doi: 10.1016/0022-2836(73)90065-X.
- Wittebole, Xavier, and Steve Opal. 2020. “Phage therapy: Clinical Applications - Critical Appraisal of Randomized Controlled Trials.” *Biocommunication of Phages* 371–83. doi: 10.1007/978-3-030-45885-0\_18/COVER.

- Wright, Andrew, Michael McConnell, and Shiro Kanegasaki. 1980. "Lipopolysaccharide as a Bacteriophage Receptor." *Virus Receptors* 27–57. doi: 10.1007/978-94-011-6918-9\_3.
- Xu, Jingwei, Nir Dayan, Amir Goldbourt, and Ye Xiang. 2019. "Cryo-Electron Microscopy Structure of the Filamentous Bacteriophage IKE." *Proceedings of the National Academy of Sciences of the United States of America* 116(12):5493–98. doi: 10.1073/PNAS.1811929116.
- Xue, Min Quan, and Lindsay W. Black. 1990. "Role of the Major Capsid Protein of Phage T4 in DNA Packaging from Structure-Function and Site-Directed Mutagenesis Studies." *Journal of Structural Biology* 104(1–3):75–83. doi: 10.1016/1047-8477(90)90060-P.
- Yan, Jianlong, Jiaoxiao Mao, and Jianping Xie. 2014. "Bacteriophage Polysaccharide Depolymerases and Biomedical Applications." *BioDrugs : Clinical Immunotherapeutics, Biopharmaceuticals and Gene Therapy* 28(3):265–74. doi: 10.1007/S40259-013-0081-Y.
- Yap, Moh Lan, Thomas Klose, Fumio Arisaka, Jeffrey A. Speir, David Veesler, Andrei Fokine, and Michael G. Rossmann. 2016. "Role of Bacteriophage T4 Baseplate in Regulating Assembly and Infection." *Proceedings of the National Academy of Sciences of the United States of America* 113(10):2654–59. doi: 10.1073/PNAS.1601654113/SUPPL\_FILE/PNAS.1601654113.SM03.MP4.
- Yap, Moh Lan, and Michael G. Rossmann. 2014. "Structure and Function of Bacteriophage T4." *Future Microbiology* 9(12):1319–37. doi: 10.2217/FMB.14.91.
- Yazdi, Mahsa, Majid Bouzari, and Ezzat Allah Ghaemi. 2018. "Isolation and Characterization of a Lytic Bacteriophage (VB\_PmiS-TH) and Its Application in Combination with Ampicillin against Planktonic and Biofilm Forms of *Proteus Mirabilis* Isolated from Urinary Tract Infection." *Journal of Molecular Microbiology and Biotechnology* 28(1):37–46. doi: 10.1159/000487137.
- Young, Ry. 2013. "Phage Lysis: Do We Have the Hole Story Yet?" *Current Opinion in Microbiology* 16(6):790–97. doi: 10.1016/J.MIB.2013.08.008.
- Yuan, Yihui, and Meiyong Gao. 2017. "Jumbo Bacteriophages: An Overview." *Frontiers in Microbiology* 8(MAR). doi: 10.3389/FMICB.2017.00403.
- Yuan, Yihui, Qin Peng, Dandan Wu, Zheng Kou, Yan Wu, Pengming Liu, and Meiyong Gao. 2015. "Effects of Actin-like Proteins Encoded by Two *Bacillus Pumilus* Phages on Unstable Lysogeny, Revealed by Genomic Analysis." *Applied and Environmental Microbiology* 81(1):339–50. doi: 10.1128/AEM.02889-14/SUPPL\_FILE/ZAM999105913SO1.PDF.
- Zhang, Hui, Ran Wang, and Hongduo Bao. 2013. "Phage Inactivation of Foodborne *Shigella* on Ready-to-Eat Spiced Chicken." *Poultry Science* 92(1):211–17. doi: 10.3382/PS.2011-02037.
- Zhang, Kai. 2016. "Gctf: Real-Time CTF Determination and Correction." *Journal of Structural Biology* 193(1):1–12. doi: 10.1016/J.JSB.2015.11.003.
- Zhang, Yang, and Jeffrey Skolnick. 2004. "Scoring Function for Automated Assessment of Protein Structure Template Quality." *Proteins* 57(4):702–10. doi: 10.1002/PROT.20264.

- Zheng, Weili, Fengbin Wang, Nicholas M. I. Taylor, Ricardo C. Guerrero-Ferreira, Petr G. Leiman, and Edward H. Egelman. 2017. “Refined Cryo-EM Structure of the T4 Tail Tube: Exploring the Lowest Dose Limit.” *Structure (London, England : 1993)* 25(9):1436-1441.e2. doi: 10.1016/J.STR.2017.06.017.
- Zhu, Hui, Shenmin Yin, and Stewart Shuman. 2004. “Characterization of Polynucleotide Kinase/Phosphatase Enzymes from Mycobacteriophages Omega and Cjw1 and Vibritophage KVP40.” *Journal of Biological Chemistry* 279(25):26358–69. doi: 10.1074/jbc.M403200200.
- Zurawski, Daniel V., Chieko Mitsuhashi, Karen L. Mumy, Beth A. McCormick, and Anthony T. Maurelli. 2006. “OspF and OspC1 Are Shigella Flexneri Type III Secretion System Effectors That Are Required for Postinvasion Aspects of Virulence.” *Infection and Immunity* 74(10):5964–76. doi: 10.1128/IAI.00594-06/ASSET/0DB54473-6B28-420B-BA26-DE1C9938B804/ASSETS/GRAPHIC/ZII0100662140006.JPEG.
- Zychlinsky, Arturo, Catherine Fitting, Jean Marc Cavaillon, and Philippe J. Sansonetti. 1994. “Interleukin 1 Is Released by Murine Macrophages during Apoptosis Induced by Shigella Flexneri.” *The Journal of Clinical Investigation* 94(3):1328–32. doi: 10.1172/JCI117452.
- Zychlinsky, Arturo, Marie Christine Prevost, and Philippe J. Sansonetti. 1992. “Shigella Flexneri Induces Apoptosis in Infected Macrophages.” *Nature* 358(6382):167–69. doi: 10.1038/358167A0.
- Zychlinsky, Arturo, Kavitha Thirumalai, Josette Arondel, J. Robert Cantey, Antonlos O. Allprantis, and Philippe J. Sansonetti. 1996. “In Vivo Apoptosis in Shigella Flexneri Infections.” *Infection and Immunity* 64(12):5357. doi: 10.1128/IAI.64.12.5357-5365.1996.



# CHAPTER 14

**Publications**

**&**

**Conferences**



### 14.1 PUBLICATIONS

- **Mallick, B.**, Mondal, P. & Dutta, M. Morphological, biological, and genomic characterization of a newly isolated lytic phage Sfk20 infecting *Shigella flexneri*, *Shigella sonnei*, and *Shigella dysenteriae*1. **Sci Rep** 11, 19313 (2021). <https://doi.org/10.1038/s41598-021-98910-z>.
- Mondal, P., **Mallick, B.**, Dutta, M. & Dutta, S. Isolation, characterization, and application of a novel polyvalent lytic phage STWB21 against typhoidal and nontyphoidal *Salmonella* spp. **Front. Microbiol.** 13, 980025 (2022). <https://doi.org/10.3389/fmicb.2022.980025>.

### 14.2 CONFERENCES

- **Mallick, B.**; Mondal, P. and Dutta, M. (2020). Participated and presented orally on a topic entitled **“Isolation and Structural Characterization of a Lytic *Shigella* Phage by Transmission Electron Microscopic study”** at 12<sup>th</sup> Asia-Pacific Microscopy Conference (APMC) from 3<sup>rd</sup> to 7<sup>th</sup> February, 2020 by the Committee of Asia Pacific Societies for Microscopy, Electron Microscope Society of India and Indian Institute of Technology Hyderabad, held in Hyderabad, India.
- **Mallick, B.**; Mondal, P., Dutta, A and Dutta, M. (2022). Participated and presented a poster on a topic entitled **“Isolation and characterization of a novel lytic bacteriophage Sfk20 infecting *Shigella flexneri*, *Shigella sonnei*, and *Shigella dysenteriae* I”** at 16<sup>th</sup> Asian Conference on diarrhoeal disease and Nutrition (ASCODD) from 11<sup>th</sup> to 13<sup>th</sup> November 2022 by ICMR-National Institute of Cholera and Enteric Diseases, Kolkata, India.
- **Mallick, B.**; Mondal, P.; Dutta, A and Dutta, M. (2023). Participated and presented a poster on a topic entitled **“Isolation and characterization of a novel lytic bacteriophage Sfk20 infecting *Shigella flexneri* and its synergistic effect in combination with ampicillin against biofilm”** at the **International Conference on Electron Microscopy & XLI annual meeting of Electron Microscopy Society of India (EMSI)** from 8<sup>th</sup> to 10<sup>th</sup> February, 2023 by Electron Microscope Society of India & University of Delhi, Delhi, India.



OPEN

## Morphological, biological, and genomic characterization of a newly isolated lytic phage Sfk20 infecting *Shigella flexneri*, *Shigella sonnei*, and *Shigella dysenteriae*1

Bani Mallick, Payel Mondal & Moumita Dutta✉

Shigellosis, caused by *Shigella* bacterial spp., is one of the leading causes of diarrheal morbidity and mortality. An increasing prevalence of multidrug-resistant *Shigella* species has revived the importance of bacteriophages as an alternative therapy to antibiotics. In this study, a novel bacteriophage, Sfk20, has been isolated from water bodies of a diarrheal outbreak area in Kolkata (India) with lytic activity against many *Shigella* spp. Phage Sfk20 showed a latent period of 20 min and a large burst size of 123 pfu per infected cell in a one-step growth analysis. Phage-host interaction and lytic activity confirmed by phage attachment, intracellular phage development, and bacterial cell burst using ultrathin sectioning and TEM analysis. The genomic analysis revealed that the double-stranded DNA genome of Sfk20 contains 164,878 bp with 35.62% G + C content and 241 ORFs. Results suggested phage Sfk20 to include as a member of the T4 myoviridae bacteriophage group. Phage Sfk20 has shown anti-biofilm potential against *Shigella* species. The results of this study imply that Sfk20 has good possibilities to be used as a biocontrol agent.

*Shigella* species, one of the most common causes of diarrheal diseases in developing and underdeveloped countries, affects mostly children below 5 years<sup>1,2</sup>. Annually 188 million *Shigella* infection causes around 164,000 deaths worldwide<sup>3</sup>. *Shigella* transmitted primarily through the fecal–oral route and a very low number (10–100) of bacteria is sufficient to cause the infection<sup>2</sup>. In developing countries, outbreaks happen mainly due to contaminated food and water, poor hygiene, malnutrition, and lack of awareness<sup>4</sup>. *Shigella* spp. is gram-negative, non-motile, non-spore-forming, rod-shaped bacteria belonging to the family Enterobacteriaceae. There are four different serogroups: *S. flexneri*, *S. sonnei*, *S. boydii* and *S. dysenteriae*1 that causes the outbreaks. Among them, *S. flexneri* and *S. dysenteriae*1 were the causative agents of diarrheal cases predominantly in the developing world<sup>5</sup>. *Shigella* dysentery used to be controlled by antibiotic therapy. Recently, overuse and misuse of antibiotics have increased the number of multidrug-resistant strains of pathogenic bacteria that include *Shigella*<sup>6</sup>. Although there is some progress in vaccine development but an effective vaccine for *Shigella* spp. is yet to achieve<sup>7</sup>. The World Health Organization (WHO) has included *Shigella* in the list of priority pathogens in search of new antibiotics<sup>8</sup>.

Bacteriophages are bacterial viruses that infect specific host bacterial strains without affecting other bacteria. They are abundantly spread in all ecosystems wherever bacteria present<sup>9</sup> and survive through replicating inside the host cell by controlling its cellular components and releasing mature phage particles by host cell lysis<sup>10</sup>. Phage virulence was found to increase in the presence of human cells than in laboratory bacterial culture<sup>11</sup>. Lytic bacteriophages can infect and kill bacteria within a short period. Therefore, lytic phages are useful bio-control agents and provide a potential alternative treatment to conventional antibiotic therapy to treat bacterial diseases<sup>12</sup>. The first bacteriophage was isolated at almost the same time but independently by Twort<sup>13</sup> and Felix d'Herelle<sup>14</sup>. Immediately after the discovery, this phage was used to treat children suffering from severe *S. dysenteriae* infection<sup>15</sup>. So far, around 78 lytic *Shigella* phages have been isolated from environmental samples and

Division of Electron Microscopy, ICMR-National Institute of Cholera and Enteric Diseases, P-33, C.I.T. Road, Scheme XM, Beliaghata, Kolkata, WB 700010, India. ✉email: moumita.dutta@icmr.gov.in



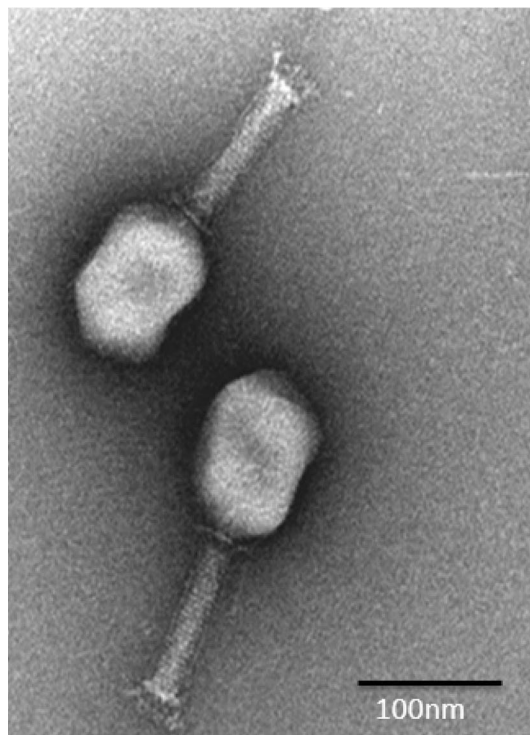


**Figure 1.** Negatively stained image of bacteriophage particles showing a prolate head, long contractile tail and a baseplate. Scale bar-100 nm.

showed effectiveness to control shigellosis<sup>16</sup>. But the discovery of antibiotics has pushed the phage treatment in the back foot. Recently certain drug-resistant strains have made treatment of some bacterial infections extremely difficult. In the search for alternative therapy, phage research has regained its importance<sup>17–19</sup>. To qualify as a potential therapeutic candidate, only the killing ability of newly isolated environmental phages is not sufficient<sup>20</sup>. A broad host range, large burst size, and production and storage stability are common characteristics to study. The absence of any toxin or lysogeny gene is also an important determinant to confirm by genome sequencing for therapeutic purposes<sup>21</sup>.

Understanding the phage-host interaction and exploiting the same will gradually increase our understanding to apply them in various medical and biotechnological purposes. Most of the known phages are long-tailed and belongs to the Caudovirales order<sup>22</sup>. The receptor-binding protein present in the phage tail machinery is the main component that initiates the attachment to a specific receptor in the host bacterial cell surface and begins the infection process<sup>23</sup>. Therefore, visualization study of phage-host interaction and a complete lytic cycle of phage provide valuable information. The aim of this study was the morphological, biological, and genomic characterization of a newly isolated lytic *Shigella* bacteriophage to use as a potential biocontrol agent for shigellosis. The interaction of host bacteria and bacteriophage was studied by TEM and SEM to elucidate the lytic cycle.

## Results

**Determination of morphology of phage Sfk20.** A lytic bacteriophage, Sfk20 was isolated from environmental water of a diarrheal outbreak area in Kolkata using *Shigella flexneri* 2a 2457T as host strain. TEM analysis revealed that the phage Sfk20 had a prolate head of  $91.08 \pm 4.92$  nm (length),  $62.34 \pm 4.82$  nm (width),  $n = 20$ , and a long contractile tail with  $99.59 \pm 4.92$  nm (length)  $18.66 \pm 2.52$  nm width,  $n = 20$  (Fig. 1). Based on the morphology, bacteriophage Sfk20 was classified as a member of the Myoviridae family, Caudovirales order<sup>22</sup>.

**Host range.** Host range analysis revealed that Sfk20 could infect *Shigella flexneri* serotypes 1b, 2a, 3a, *Shigella sonnei*, *Shigella dysenteriae* 1 but not *Shigella flexneri* serotypes 4,6 and *Shigella boydii* (Table 1). Phage Sfk20 could form clear plaques infecting *Salmonella typhimurium*, *Salmonella enteritidis* but not the *Salmonella typhi* strains. The EOP values obtained for the phage-sensitive *Shigella* strains were much higher compared to the non-typhoidal *Salmonella* strains. However, phage Sfk20 was unable to infect the *E. coli* and *V. cholera* strains used in this study.

**Phage stability.** Phage Sfk20 was tested at wide temperatures and pH values. The thermal stability showed that phage Sfk20 is most stable at 4 °C but decreases rapidly after 37 °C. Phage activity significantly reduced at 50 °C and completely inactivated at 70 °C (Fig. 2A). Phage Sfk20 was found most stable at pH 7–9 range indicating that neutral to slightly alkaline pH is suitable for the activity of phages (Fig. 2B). Phages were completely

Bacterial species	Strain No	Infectivity	EOPs
<i>Shigella flexneri</i> 2a	2457T	+	1
<i>Shigella flexneri</i> 3a	UB811	+	0.80
<i>Shigella flexneri</i> 1b	03075/19	+	0.79
<i>Shigella flexneri</i> 4	C2529	–	–
<i>Shigella flexneri</i> 6	UB812	–	–
<i>Shigella sonnei</i>	IDH00968	+	0.62
<i>Shigella dysenteriae</i> 1	NT4907	+	0.61
<i>Shigella boydii</i> 1	NK02379	–	–
<i>Salmonella enteritidis</i>	520833	+	0.000192
<i>Salmonella typhimurium</i>	PH-94	+	0.000296
<i>Salmonella typhi</i>	KOL 551	–	–
ETEC	IDH07942	–	–
<i>Vibrio cholerae</i> O1	MAK757	–	–

**Table 1.** Host range analysis of phage Sfk20. + = lysis; – = no lysis.

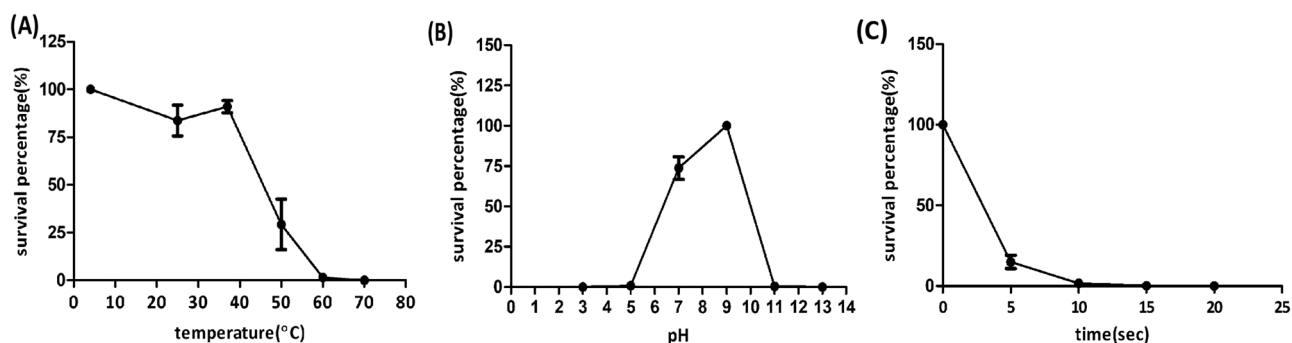


**Figure 2.** Stability of phage Sfk20: (A) Phage thermal stability at different temperature range. (B) Phage stability at different pH range, (C) Phage stability after UV irradiation.

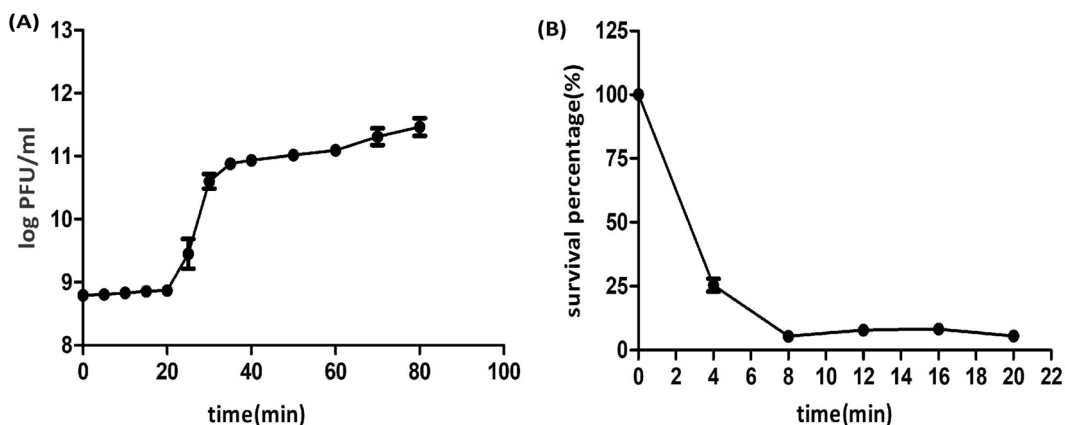


**Figure 3.** Growth characteristics of phage Sfk20; (A) One step growth experiment and (B) adsorption kinetics.

inactivated below pH 5 and above pH 11. Phage Sfk20 was highly sensitive to UV irradiation and completely inactivated after 15 s (Fig. 2C).

**One-step growth analysis and adsorption rate.** The one-step growth curve experiment was performed to calculate the latent period and burst size of the isolated phage Sfk20. As a result, a triphasic curve was obtained with the typical lag phase, burst phase, and stationary phase. A latent period of 20 min and an average burst size of 123 PFU per infected cell was shown in Fig. 3A. Around 94% of bacteriophage particles were adsorbed within the first 8 min. After that, the adsorption rate was very slow shown in Fig. 3B.

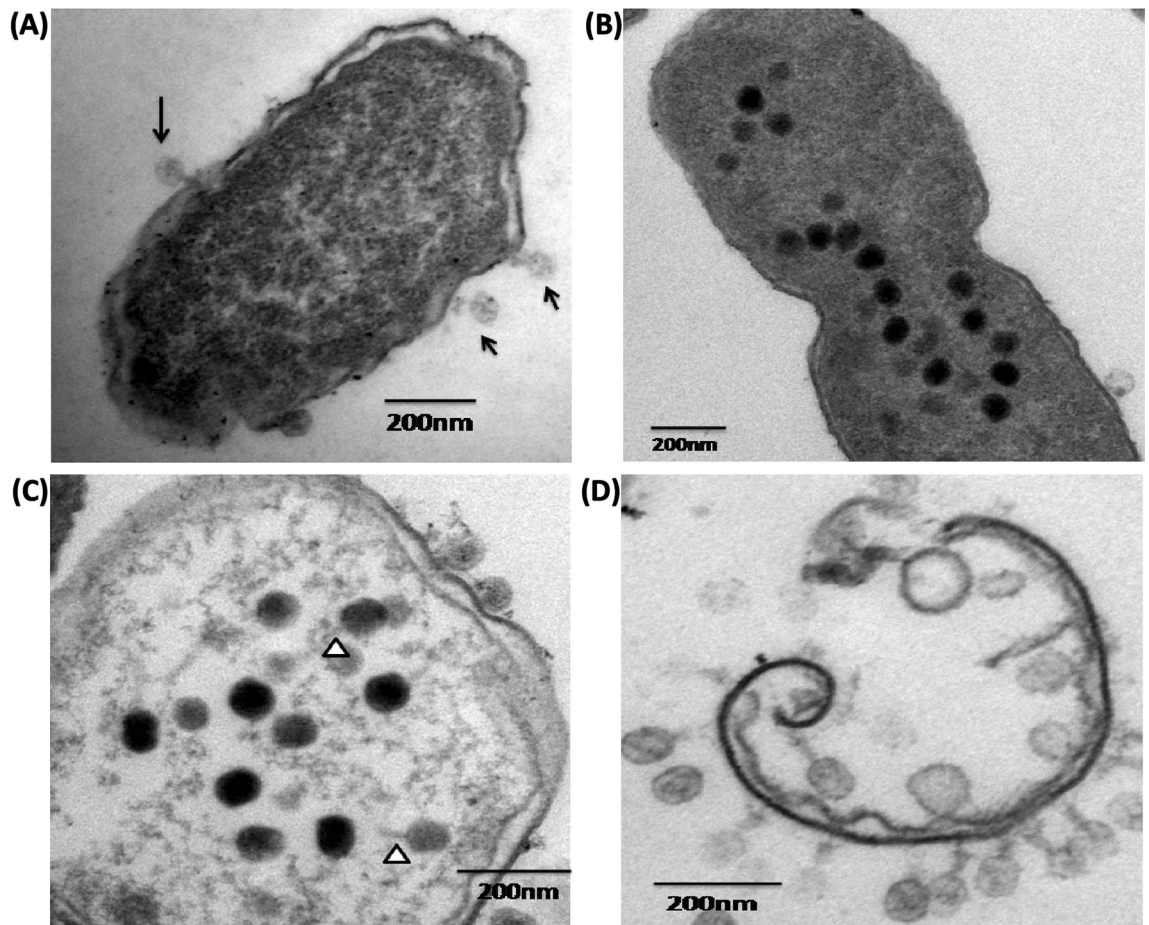


**Figure 4.** TEM images of ultrathin section of *Shigella flexneri* 2a infected with isolated host specific bacteriophage at different time points: (A) Bacteriophage attachment started at 15 min (black arrow indicates phage particles), (B) TEM image of 30 min shows intracellular phage development started, (C) Intracellular phage, loss of internal material and membrane disorganization is also shown. White arrowheads indicate phage tail. (D) Complete lysis of bacteria cell clearly shown at 60 min. Scale bar-200 nm.

**Electron Microscopy of bacteria-bacteriophage interaction.** Host bacteria *Shigella flexneri* 2a was infected with bacteriophage Sfk20 to visualize the intermediate steps at an ultrastructural level under TEM (Fig. 4). Few bacteriophages are attached to the bacterial cell after 15 min of infection shown in Fig. 4A. The intracellular phage development is visualized at 30 min in Fig. 4B, the loss of internal material and intactness of membrane shown in Fig. 4C. Finally, Fig. 4D showed the complete lysis of the bacterial cell wall around 60 min of infection.

Scanning electron microscopy of bacteria-bacteriophage interaction reveals the different stages of the lytic cycle. Supplementary Fig. S1A shows intact phage Sfk20 particles, followed by the initial step of phage attachment to bacteria (S1B), several phages attached to the bacterial cell surface at a later stage shown in S1C. Finally, disruption of a cell and progeny phages are out around the bacteria are captured in S1D.

**Biofilm degradation study.** *Shigella flexneri* 2a bacterial biofilm grown in a controlled manner on a coverslip was treated with phage Sfk20 alone and a combination of Sfk20 and ampicillin to show its ability to degrade biofilm and results were observed by scanning electron microscopy. Figure 5A and D showed the 24 and 48 h biofilm respectively. The biofilm of 48 h displayed a highly structured matrix formation to which bacteria adhered close to each other compared to 24 h. The phage Sfk20-treated biofilm showed the degradation of the background matrix that results in the more scattered bacterial distribution in Fig. 5B and E. Figure 5C and F showed that the combination of phage Sfk20 and ampicillin reduced the biofilm more significantly and changes were seen in bacterial appearance. The differences between the control biofilm and Sfk20-treated, and Sfk20-ampicillin treated biofilm showed the efficacy of phage Sfk20 in the application of biofilm removal. The Sfk20-ampicillin combination exerted better removal activity than Sfk20 alone.

A quantitative assay of biofilm degradation activity revealed that phage Sfk20 ( $10^{10}$  pfu/ml) and ampicillin (256  $\mu$ g/ml) alone caused ~40% ( $p < 0.001$ ) and ~31% ( $p < 0.001$ ) reduction in biofilm respectively when compared to the control (without phage). However, the effect of the Sfk20-ampicillin combination showed a higher reduction (~47%,  $p < 0.01$ ) in biofilm than that of Sfk20 and ampicillin alone. Also, each pair of combinations



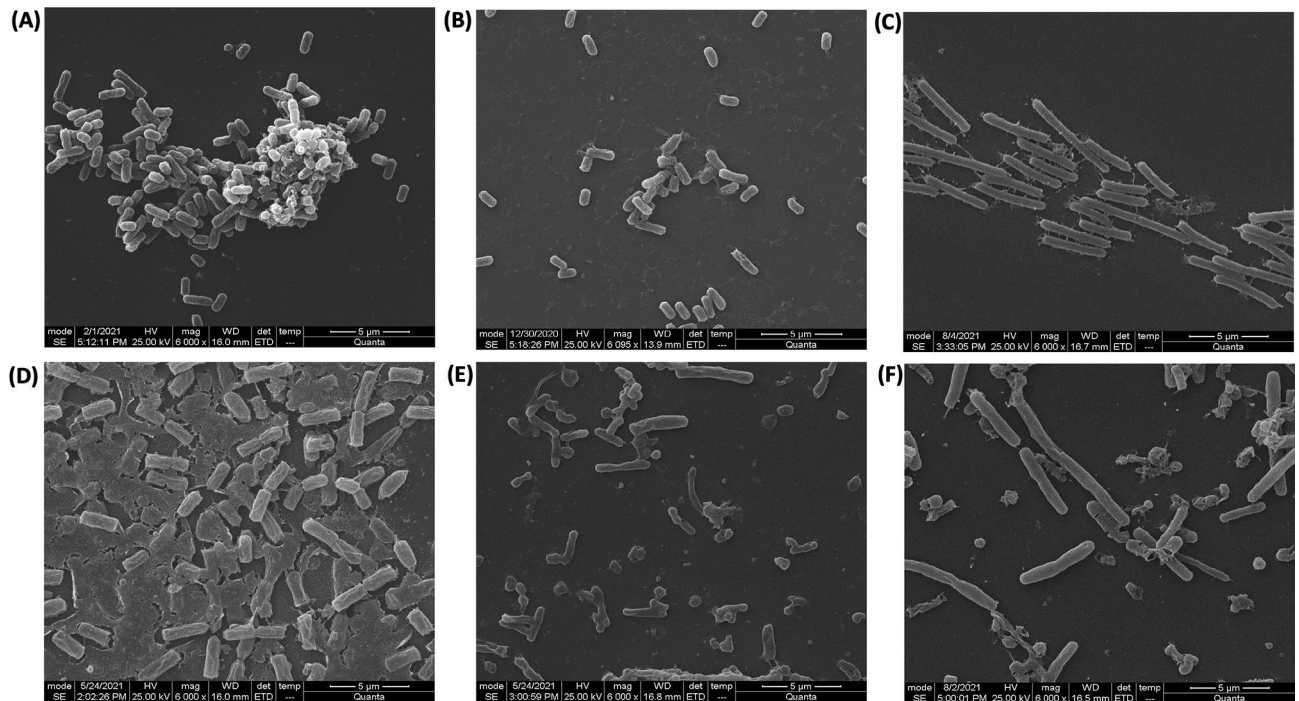


**Figure 5.** Scanning electron micrograph of biofilm formation and degradation assay. (A) 24 h untreated control, (B) 24 h biofilm treated with phage Sfk20, (C) 24 h biofilm treated with the combination of phage Sfk20 and ampicillin, (D) 48 h untreated control, (E) 48 h biofilm treated with phage Sfk20, (F) 48 h biofilm treated with the combination of phage Sfk20 and ampicillin.

showed a statistically significant reduction in biofilm (Supplementary Fig. S2). Therefore, a considerable synergistic effect was observed when biofilm was subjected to phage Sfk20 and ampicillin combination.

**Protein profile.** The structural protein profile of the bacteriophage Sfk20 were analyzed by 12.5% SDS-PAGE (Supplementary Fig. S3). The two major bands appeared at 53 kDa and 70 kDa. The other lighter bands appeared approximately at 13, 76, 100, and 155 kDa respectively.

**Restriction enzyme digestion of the phage genomic DNA.** The restriction digestion pattern is a quick and cost-effective method to detect differences among new phages. Supplementary Fig. S4 showed the pattern of restriction digestion of the phage Sfk20 DNA. Based on this result, the genome of phage Sfk20 carries double-stranded DNA. The phage DNA was cut by EcoRV only but resistant to EcoRI, BamHI, HindIII, PstI, BglII, and MluI restriction enzymes. *Shigella flexneri* phage vB\_SflS-ISF001 was also reported resistant to EcoRI and BamHI but sensitive to EcoRV<sup>24</sup>. *Shigella* phages vB\_SflM\_004 and vB\_SsoS\_008 were also found digested with only EcoRV<sup>25</sup>.

**Genome sequencing and comparative genomic analysis of Sfk20.** Phage Sfk20 genome has been sequenced and deposited in GenBank with accession number: MW341595. Genome analysis showed that the phage Sfk20 genome consists of 164,878 bp with a 35.62% total G + C content. Figure 6 represents the schematic genome map of phage Sfk20 drawn using the CG view server. The inner ring represents coding sequence locations (CDS) colored in blue; tRNA in this ring is marked in pink color. The ORFs were mainly annotated as structural proteins, genome packaging proteins, and lysis proteins. Further analysis identified 241 open reading frames (ORFs) and the predominant start codon was ATG (97%). GTG is an uncommon start codon for six ORF such as ORF19, ORF68, ORF76, ORF89, ORF104, and ORF118. Concrete gene information such as the positions, directions, amino acid range, putative function of each ORFs, and their function in phage life cycle was mentioned in Supplementary Table S1. The longest ORF of phage Sfk20 was ORF36 (protein-id: QPP47031) which was placed in the morphogenesis cluster. ORF36 encoded a gene that was very similar to the large distal long tail fiber subunit of Myoviridae *Shigella* phage SH7. ORF166 (protein\_id: QPP47161) represents the phage-encoded enzyme lysozyme/endolysin and ORF38 (protein\_id: QPP47033) encodes the protein holin responsible for bacterial lysis. These genes are crucial for host cell destruction during the burst phase of the phage life cycle. They are also called host lysis proteins. The DNA packaging genes such as large terminase subunit, small terminase protein, and putative terminase subunit located in ORF163, ORF198, and ORF199 respectively. Phage morphogenesis genes such as head completion protein, baseplate wedge subunit, neck protein, tail sheath stabilizer, and completion protein, prohead core protein, capsid and scaffold protein, prohead assembly protein, major capsid protein and baseplate hub subunit are located in ORF186, ORF189, ORF195, ORF197, ORF203,

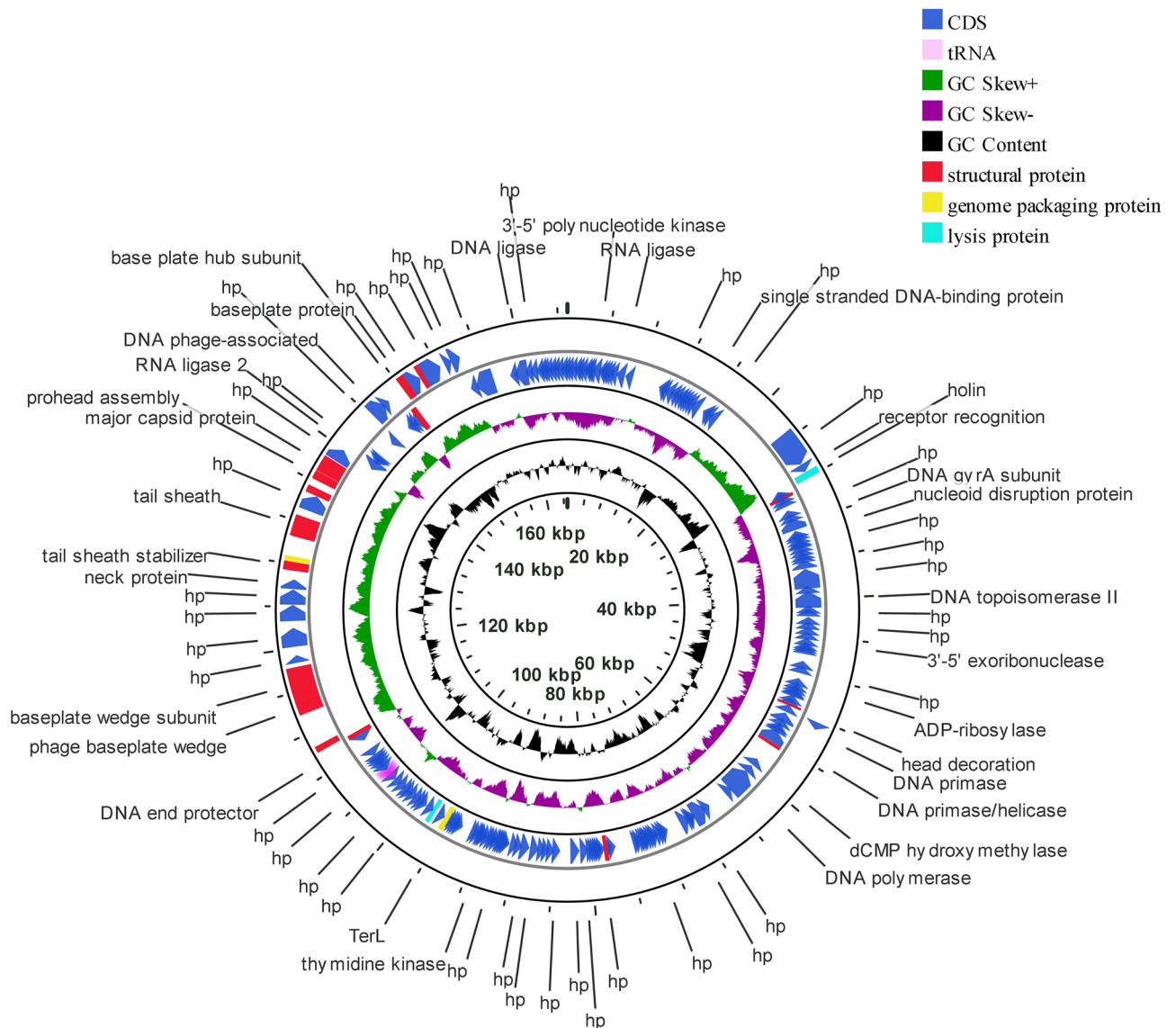


**Figure 6.** Schematic map of phage Sfk20 genome prepared using CGView. Outer ring represents coding sequence locations (CDS) in blue color; tRNA was marked in pink color. Hypothetical proteins were denoted as hp. The different functional ORFs were indicated in different colors. Red ORFs represent the structural proteins, yellow ORFs represent the genome packaging proteins and the cyan ORFs represent lysis proteins.

ORF204, ORF206, ORF207, and ORF219 respectively. Most of the packaging and morphogenesis genes are located in the middle and end of the genome. In addition, proteins responsible for phage nucleotide metabolism are DNA gyrase subunit, DNA endonuclease IV, DNA topoisomerase II, DNA primase, DNA polymerase, and endonuclease located in ORF46, ORF53, ORF59, ORF84, ORF96, and ORF122 respectively. The presence of nucleotide metabolism-associated genes in this phage indicates that the Sfk20 genome might reduce the dependence of phage DNA metabolism on the host bacteria. A total of 10 tRNA genes were identified in phage Sfk20. The functions of tRNA in the phage genome are still not clear though a widely accepted fact is phage tRNA gives considerable independence from host translational machinery<sup>26</sup>. A Megablast search of phage Sfk20 genome indicated it has a 95–97% sequence similarity to *Shigella* phage pSs-1, SH7, SfPhi01, Sf21, Sf23 (Supplementary Table S2). According to Megablast results, Sfk20 was classified as a member of the T4-like virus genus and myoviridae family. The alignment of phage Sfk20 genome with closely related five other myoviridae *Shigella* phages was represented by Easyfig (Fig. 7). The green arrows represent the coding sequence locations and blue shaded lines reflect the degree of homology between Sfk20 and other phages.

**Phylogenetic position of phage Sfk20.** Based on the base plate wedge protein sequences and terminase large subunits (TerL), the phylogenetic trees were generated to find the phylogenetic position of phage Sfk20 in this study (Supplementary Fig. S5). From the NCBI database, the reference sequences were collected. According



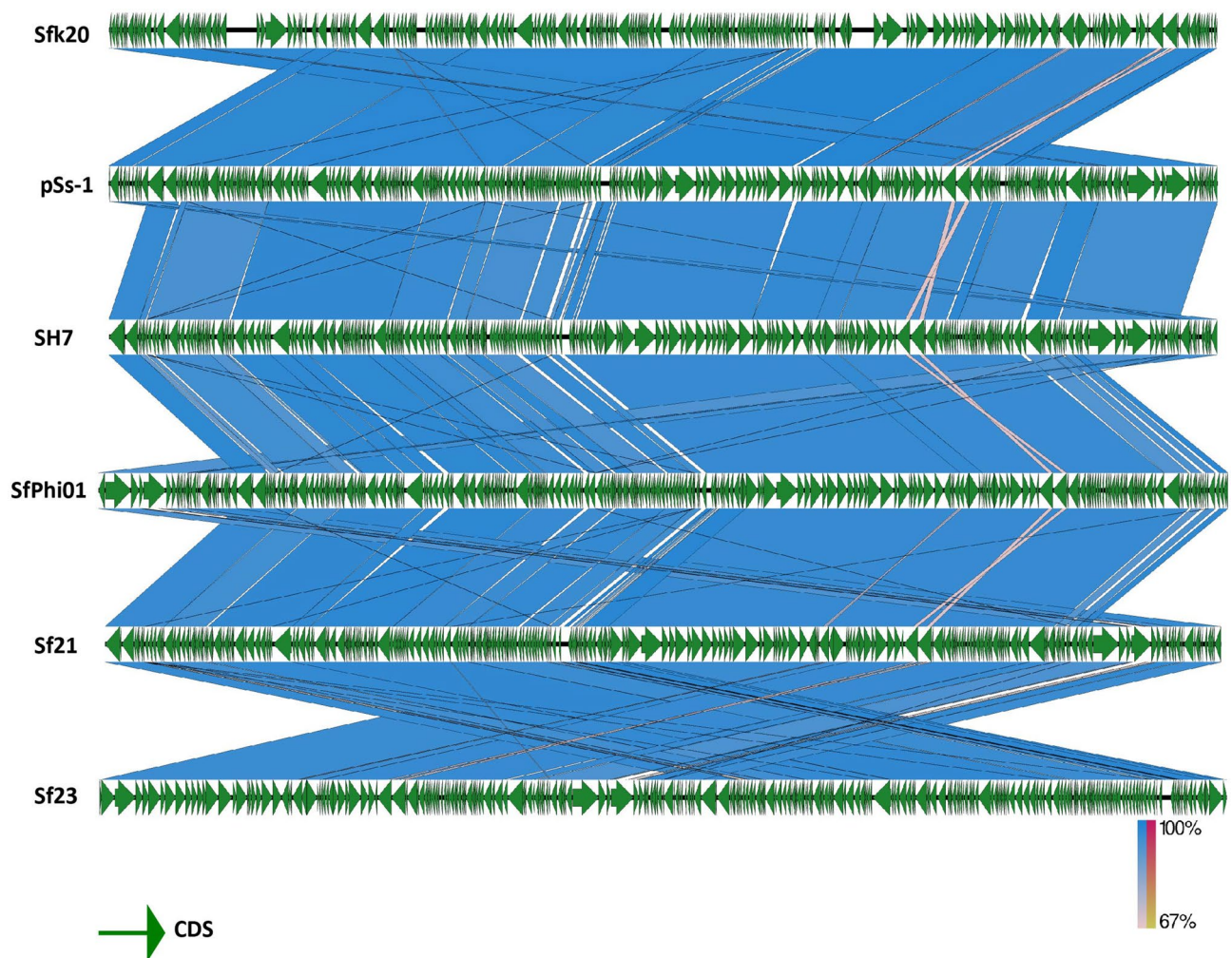


**Figure 7.** Easyfig schematic alignment of phage Sfk20 genome with five closely related phages using BLASTn program. Green arrows indicate the coding sequence location shaded blue lines indicate degree of homology between pairs.

to Phylogeny.fr dendrogram (<http://www.phylogeny.fr/>), phage Sfk20 belongs to T4-like virus genus, myoviridae family and caudovirales order.

## Discussion

The rapid increase of multidrug-resistant *Shigella* strains has become a global burden in diarrheal diseases. Virulent lytic phages can selectively infect and destroy the bacterial population including drug-resistant strains, using a mechanism distinct from antibiotics. Therefore, there is a renewed interest to control the MDR *Shigella* strains using phages as an alternative to antibiotic treatment. The Myoviridae bacteriophage Sfk20 used in this study appeared as a promising biocontrol candidate against shigellosis.

Studies have been reported to show the in vitro antimicrobial activity of many isolated phages and successful application of phage therapy since the early nineteenth century in a staggered manner. Many promising laboratory studies have failed to show positive outcomes in the recent controlled human trial<sup>27</sup>. Early phage therapy mostly failed due to inadequate knowledge of the fundamental phage biology and unsophisticated purification and storage procedure. Phages have beneficial characteristics but with some restrictions. Unknown gene function of phages, CRISPR-cas, phage stability, host immune responses, and scarcity of pharmacokinetic and pharmacodynamics models for dose optimization are some genuine concerns to implement phage therapy as an approved alternative. Also, the low pH sensitivity, enzymatic degradation, phage loss, and phage-neutralizing antibodies are some of the big concerns in human phage therapy. Meanwhile, compassionate phage therapy is in limited use in cases when all available therapeutic options are exhausted<sup>28</sup>.

In this study, the water sample was collected from a diarrheal outbreak area and *Shigella flexneri* 2a bacteria was the host for phage propagation. Host range analysis and high EOP values showed *Shigella flexneri* serotypes 1b, 2a, 3a are sensitive towards phage Sfk20 whereas *Shigella flexneri* serotypes 4 and 6 are resistant towards phage Sfk20. In developing countries, the predominant serotypes of *Shigella flexneri* are 1b, 2a, 3a, 4a, and 6 though serotype 2a is predominant in industrialized countries including India<sup>29</sup>. *Shigella flexneri* has been reported to progressively developing antibiotic resistance<sup>30</sup>. So we have chosen this as the host strain in our study. *Shigella*

*boydii* was rarely reported worldwide compared to other *Shigella* spp.<sup>31,32</sup> and there are limited studies published on *S. boydii*<sup>33</sup>. The Global Enteric Multicenter Study (GEMS) reported that only 5.4% of 1130 *Shigella* isolates were identified as *S. boydii*<sup>34</sup>. One study from India reported *S. flexneri* (60%) as the prevalent serogroup followed by *S. sonnei* (23.8%), *S. dysenteriae* (9.8%), and *S. boydii* (5.7%)<sup>35</sup>. *S. boydii* has been reported one of the prevalent serotypes only in Bangladesh<sup>36</sup>.

The stability of phages at varying temperatures and pH can be considered to make them suitable candidates for therapeutic purposes. Phage Sfk20 was found quite stable in the range 4–37 °C and for at least up to six months without losing viability in the usual storage temperature of 4 °C. It showed maximum stability in the range of pH 7–9 that is neutral to slightly alkaline. This information is valuable to consider the administration of phages through the oral route for therapeutic purposes. The acidic environment of the gastrointestinal tract is one of the major challenges for phage therapy during phage administration<sup>37</sup>. Most of the bacteriophages are found sensitive towards low pH. Phage Sfk20 also showed complete inactivity at pH < 5. Therefore, various methods and technologies have been developed to protect the therapeutic phages. Oral applications of phages predated by gastric neutralization are a practice in few European countries where phage therapy has always received substantial consideration<sup>38</sup>. Also, encapsulation of phages in liposomes or biopolymeric microparticles is another highly accepted technology to enhance phage survival while passing through the gut<sup>39</sup>. However, the selection of biopolymer is not so easy and the synthesis process has to satisfy certain features. To overcome this limitation, an alternative has been developed based on genetic engineering by displaying phospholipids on the surface of the phages. This natural coating process not only protects from the acidic pH of the GI tract but also maintains the infection ability of phages<sup>40</sup>. Previously the genetic engineering was quite difficult but with the development of a new technique Bacteriophage Recombineering of Electroporated DNA (BRED)<sup>41</sup>, the coating has become easy and cheaper than encapsulation. Therefore, the sensitivity of Sfk20 at low pH could be controlled during its trial in future phage therapy.

The one-step growth curve of phage Sfk20 suggests a latent period (20 min) and a large burst size of 123 pfu per cell. A large burst size favours this phage's application in phage therapy. Earlier reports on T4 revealed that if tRNA genes were deleted the burst size and protein synthesis rate eventually lowered down<sup>42</sup>. But some reports revealed that bacterial physiological states could affect the burst size of phages<sup>43</sup>.

In this study, we have used early log phase bacterial culture of *S. flexneri* 2a strain. Understanding the interaction of the bacteria-bacteriophage system is an approach to consider bacteriophages as biocontrol agents. Ultrastructural analysis of phage-infected bacteria and intracellular development of phages by transmission and scanning electron microscopic images interpret the morphogenetic pathway of phage Sfk20 and further showed similarities with T4 phage<sup>44</sup>. Further, the different forms of the infected cells in Figs. 4B and C indicated that the extent of intracellular phage development depends on the multiplicity of infection of an individual particle.

Biofilm degradation activity of phage Sfk20 alone and in combination with ampicillin was analyzed by scanning electron microscopy (SEM) (Fig. 5). Penetration, diffusion, and propagation are three important criteria to use single phages or phage cocktails to remove biofilms<sup>45</sup>. The results show phage Sfk20 could fulfil the criteria to a significant extent by degrading the biofilm of its host indicator bacteria *Shigella flexneri* 2a. Phage-ampicillin combination showed a synergistic effect (Fig. 5E) in the removal of *Shigella* biofilm though not complete removal. To the best of our knowledge, Sfk20 is one of the first lytic, tailed *Shigella* phages capable of degrading the biofilm formed by *Shigella flexneri* 2a strain in laboratory conditions. The bacterial biofilm has an extracellular matrix that acts as a physical barrier to the phage. Tailed phages can invade the matrix layer by the hydrolytic activity of depolymerase enzymes present in their tail spike proteins<sup>46</sup>. After that probably phages diffuse through the biofilm to infect and destroy bacteria in the deeper layer<sup>47</sup>. Sfk20 with its long contractile tail might help to remove the external matrix by its enzymatic activity. The other possible reasons for Sfk20 efficacy in biofilm removal are the presence of endolysins and virion-associated peptidoglycan hydrolases (VAPGHs) that either disrupt or make a small hole in the cell<sup>48,49</sup>. Moreover, a small percentage of stress-tolerant cells are usually present in biofilm and a recent study suggests phage lytic proteins can remove that cells<sup>50</sup>. It could probably facilitate the dispersion of the biofilm matrix. This study indicated structural characteristics and spatial information of the bacterial biofilm and qualitative observation of the disruption of the biofilm through direct imaging. The biofilm degradation capacity of Sfk20 revealed that it could be used in the future as a single phage or in a phage cocktail or phage-antibiotic combination as a therapeutic candidate for biofilm-mediated diseases.

We have also done a quantitative experiment to address the eradication efficacy. The use of bacteriophage Sfk20 (10<sup>10</sup> pfu/ml) with ampicillin at a high concentration (256 µg/ml) exhibited a better biofilm removal activity compared to the phage or antibiotic alone (Supplementary Fig. S2). This could be due to the presence and enzymatic activity of depolymerase in the phage tail. It might have degraded the extracellular capsular polysaccharide and phages could diffuse easily inside the biofilm to target bacteria in the deeper layer creating a hassle-free path for a higher dose of antibiotics to reach inside the biofilm. Thus a combination of phage plus antibiotic showed faster destruction of biofilm matrix and the associated bacteria. Similar results were observed in other phage-antibiotic combination therapy<sup>51,52</sup>. Phage-antibiotic synergism is observed in most of the infections caused by biofilm-producing bacteria<sup>53</sup>. Phage Sfk20 alone can remove at least 40% of the total biofilm and in combination with ampicillin, the removal percentage of biofilm was 47%. It confirmed the synergistic effect of the Sfk20-ampicillin combination.

Genome sequencing, analysis, and complete annotation provide sufficient information on the phage Sfk20 genome. Analysis of phage Sfk20 genome confirmed the presence of lytic proteins and absence of any lysogenic, toxin, or antibiotic resistance genes suggesting that the phage could be used as a safe biocontrol agent for host enteric bacteria. Holin and endolysin genes encode proteins responsible for progeny phage release at the end of a lytic cycle. The presence of both genes in the sequence of phage Sfk20 genome can confirm the lytic nature of this phage.

According to the mega blast search result, Sfk20 belongs to the genus T4-like viruses; order caudovirales; family myoviridae; subfamily Tevenvirinae. Recently a total of 78 isolated *Shigella* phages were grouped according to family and genome size and phage Sfk20 falls in the largest T4 like myoviridae family with a genome size 164.0–176.0 kbp<sup>16</sup>. Comparative genome analysis and biological properties suggested that phage Sfk20 has the highest similarity with pSs-1 [Supplementary Table S3].

Phylogenetic tree analysis of Sfk20 based on base plate wedge subunit and terminate large subunit with other related phages suggested that Sfk20 was closely related to other *Shigella* and *E. coli* phages and they probably evolved from a common ancestor.

In conclusion, a constant search for novel lytic bacteriophages during a seasonal upsurge of a diarrheal outbreak will indicate the presence of related virulent bacteria in the environment. Characterization of those phages will facilitate understanding phage biology and the strategy development for effective therapeutic applications.

## Materials and methods

**Isolation, purification and enrichment of bacteriophage.** *Shigella flexneri* 2a-specific bacteriophage was isolated from the water sample of a diarrheal outbreak area in Kolkata. A mixture of 25 ml water sample, 25 ml 10× phage broth media and 5 ml of log phase *Shigella flexneri* 2a culture was incubated at 37 °C for 24 h in shaking condition. After this incubation the suspension was centrifuged for 10 min at 10,000 rpm to remove the bacterial cells and the collected supernatant was filtered with a 0.22 µm membrane filter. Spot assay was performed initially to evaluate the presence of shigella phage testing on *Shigella flexneri* 2a 2457T using the double layer agar method. The single plaque isolation procedure was performed thrice by plaque assay to obtain the purified phage plaque. The phage suspension was concentrated and purified by ultracentrifugation (25,000 rpm, 1:30 h and 4 °C) and sucrose step-gradient ultracentrifugation (30,000 rpm, 2 h and 4 °C) respectively<sup>54</sup>. The purified high titre phage Sfk20 phage stock was stored at 4 °C for further studies.

**Transmission electron microscopy.** Purified high titre bacteriophage was negatively stained with 2% (w/v) uranyl acetate. The sample was examined under FEI Tecnai 12 BioTwin transmission electron microscope at an operating voltage 100 kV. Detailed morphology that includes the shape and size of bacteriophage particles are studied.

**Host range determination and efficiency of plating (EOP).** The infectivity of Sfk20 was tested against many bacterial strains as determined by standard spot assay<sup>55</sup>. Infectivity was tested on different enteric bacteria present in the laboratory. Briefly, 10 µl of phage ( $1.8 \times 10^{11}$  pfu/ml) sample was spotted onto the middle of bacterial lawn and the plate was incubated overnight at 37 °C and checked for the presence visible lysis zone. The EOP values are calculated as the ratio of the PFU value of phage with susceptible bacterial strain and the phage with indicator (*Shigella flexneri* 2a, 2457 T) bacterial strain.

**Phage stability assay.** To evaluate the heat resistant capacity of phage Sfk20, thermal stability was performed. The phage suspension (diluted in Tris MgCl<sub>2</sub> buffer) was incubated at different temperatures (4 °C, 25 °C, 37 °C, 50 °C, 60 °C, and 70 °C respectively) for 1 h and phage suspension was titred by soft agar over layer method<sup>56</sup>. For pH stability test, phage Sfk20 was examined by preincubating the phage suspensions ranging from pH 3–13 at 37 °C for 1 h. After the incubation period, the phage titre was determined by double agar layer method. To evaluate the phage stability under UV light, the phage suspension was kept at a different time interval of 5, 10, 15, and 20 s adapted and modified from elsewhere<sup>54</sup>. After that, the survival percentage of bacteriophage tested by the soft agar overlay method. All experiments were performed in triplicate.

**One-step growth analysis of bacteriophage and adsorption kinetics.** An early exponential phase culture (20 ml) of *Shigella flexneri* 2a 2457T (OD<sub>600</sub> = 0.5) was harvested by centrifugation (5000×g at 4 °C for 10 min). The pellet was resuspended in around 1 ml Luria broth followed by the addition of bacteriophage at an MOI 0.1. The mixture was incubated for adsorption at 37 °C for 5 min and diluted in Luria broth with a maximum volume of 10 ml and reincubated at 37 °C. Aliquots were taken out at different time intervals up to 80 min to calculate the phage titer by the soft agar layer method.

**Bacteriophage infection and intracellular development of phage.** *Shigella flexneri* 2a bacterial culture was mixed with Sfk20 bacteriophage and incubated at 37 °C. Samples were taken out at around 15, 30, and 60 min respectively and were immediately centrifuged at 7000 rpm for 5 min. In the next step, cell pellets resuspended in 3% glutaraldehyde in 0.1 M sodium cacodylate buffer to fix the cells<sup>57</sup>.

**Ultrathin sectioning of the bacterial cell.** In this experiment, cacodylate buffered glutaraldehyde was used as a primary fixative. After that, secondary fixation was done in 1% OsO<sub>4</sub> followed by dehydration with a series of ascending concentrations of ethanol. Then the samples were embedded in resin Agar100 and polymerization was done overnight at 60 °C. The ultrathin sections (40–50 nm) of the control and infected cells are cut with a Leica Ultracut UCT ultramicrotome (Leica Microsystems, Germany). The sections were picked up in nickel or copper grids, dual-stained with 2% aqueous uranyl acetate and 0.2% lead citrate, and grids were air-dried. The grids with sections were either stored or immediately examined under an FEI Tecnai 12 Biotwin TEM (FEI, Netherlands) at an accelerating voltage of 100 kV.



**Scanning electron microscopy.** For SEM analyses, to visualize the bacteriophage lytic cycle, samples were taken out from bacteria-bacteriophage mixture at early, mid, and late phase in Eppendorf tubes. Then samples were fixed with 3% glutaraldehyde in 0.1 M sodium cacodylate buffer and left overnight. After that, samples were dehydrated with ascending concentration of alcohol up to 100%. All dehydrated samples were treated with hexamethyldisilazane (HMDS) for chemical drying by increasing HMDS concentration stepwise up to 100% HMDS. The tubes were left in a fume hood overnight to evaporate HMDS completely. Samples mounted on specimen stubs, sputter-coated with gold, and images captured on an FEI Quanta 200 scanning electron microscope (FEI, Netherlands).

**Biofilm degradation assay and visualization with SEM.** A qualitative biofilm degradation activity of Sfk20 on *Shigella flexneri* 2a 2457T strain was determined following a previous method with some modification<sup>58</sup>. Cover slips were used for the formation of biofilm. Briefly 10 µl of overnight culture of *Shigella flexneri* 2a was incubated on coverslips submerged in LB media in 6-well plates and incubated at 37 °C for 24 h and 48 h respectively. The biofilm was then treated with phage Sfk20 ( $10^{10}$  PFU/ml), ampicillin (256 µg/ml) and a combination of both at same individual concentration. All treated samples were further incubated at 37 °C for overnight. After that, planktonic cells were removed and the coverslips were processed for SEM analysis as mentioned in visualization of bacteria-phage interaction method.

**Quantitative assay of biofilm degradation.** The quantitative experiment on the ability of Sfk20 to degrade the biofilm alone or in combination with antibiotic was also performed. Briefly, matured biofilm was grown on microtitre plate<sup>58</sup>, planktonic cells were removed and the biofilm was treated with phage Sfk20, ampicillin and their combination<sup>59</sup>. After the treatment the plates were incubated at 37 °C for overnight. Next day the phage and antibiotic were removed and the wells were rinsed with 1× PBS twice and stained with crystal violet. The total biomass of the biofilm was measured by plate reader at the absorbance of 595 nm (iMark Microplate Reader S/N 21673). Statistical analysis of the data was performed by two-way ANOVA with Graph-Pad Prism 5.00.

**SDS-PAGE analysis.** Phage suspension was boiled for 5 min and the structural proteins were extracted. The denatured proteins were separated by 12.5% SDS–polyacrylamide gel as described by Laemmli<sup>60</sup> with Mini-PROTEAN TGX Precast gels (Biorad, USA).

**Phage DNA extraction and restriction endonuclease digestion.** Bacteriophage DNA was isolated from the purified phage suspension using the DNA isolation kit (NorgenBiotek Corp., Canada) according to the instruction from the manufacturer. Phage genomic DNA was digested with the restriction endonuclease enzymes (EcoRI, BamHI, HindIII, PstI, EcoRV, BglII, and MluI) according to the supplier's protocols. DNA fragments were separated by electrophoresis at 100 V for 1 h on a 1% agarose gel and stained with ethidium bromide. DNA molecular marker (high range DNA ladder, HiMedia) ranging from 250 bp to 25 kbp was used.

**Genome sequencing of phage Sfk20.** Phage genome DNA was sequenced by Xcelris (Ahmedabad, India) using Next Generation Sequencing on an Illumina Platform and the sequencing end data was assembled with CLC Genomics Workbench v.6.0.5 with reads map back option. After that, the obtained sequencing results were analyzed for similarity search against nucleotide by BLASTN, NCBI program. Potential open reading frames (ORFs) were predicted using Genemark and Prokaryotic GeneMark.hmm version 3.25 respectively. The putative functions of those ORFs were analyzed by BLASTP, NCBI program. Using the BLASTP and PSI-BLAST programs against the non-redundant databases; the predicted ORFs were queried from translated sequences. The genome map of phage Sfk20 was drawn using the CG viewer server (<http://cgview.ca/>)<sup>61</sup>. The genomic comparison of phage Sfk20 with closely related myoviridae *Shigella* phages was illustrated in the form of a linear figure using Easyfig application (<http://mjsull.github.io/Easyfig/files.html>)<sup>62</sup>. In addition, tRNAs were predicted using ARAGORN (<http://130.235.244.92/ARAGORN/>)<sup>63</sup> and tRNAscan-SE (<http://lowelab.ucsc.edu/tRNAscan-SE/>)<sup>64</sup>. For phylogenetic analysis two predicted ORFs were selected based on their amino acid sequences. We have chosen the amino acid sequence of baseplate wedge protein (ORF189, protein\_id: QPP47184) and terminase large subunits (ORF163, protein\_id: QPP47158). The amino acid sequences of Sfk20 were aligned with those of other reference Myoviridae bacteriophages using MUSCLE and then the phylogenetic tree was constructed using “ONE CLICK” at Phylogeny.fr.

**Nucleotide sequence accession number.** The complete genome sequence of phage Sfk20 has been deposited in GenBank (Accession No. MW341595).

Received: 9 June 2021; Accepted: 7 September 2021

Published online: 29 September 2021

## References

1. DuPont, H. L. *Shigella* species (bacillary dysentery). In *Principles and Practice of Infectious Diseases* (eds Mandell, G. L. et al.) 2905–2910 (Churchill Livingstone Elsevier, 2010).
2. Niyogi, S. K. Shigellosis. *J. Microbiol.* **43**, 133–143 (2005).

3. Kotloff, K. L., Riddle, M. S., Platts-Mills, J. A., Pavlinac, P. & Zaidi, A. K. M. Shigellosis. *Lancet* **391**, 801–812 (2018).
4. Taneja, N. & Mewara, A. Shigellosis: Epidemiology in India. *Indian J. Med. Res.* **143**, 565–576 (2016).
5. Zaidi, M. B. & Estrada-García, T. Shigella: A highly virulent and elusive pathogen. *Curr. Trop. Med. Rep.* **1**, 81–87 (2014).
6. Williams, P. C. M. & Berkley, J. A. Guidelines for the treatment of dysentery (shigellosis): A systematic review of the evidence. *Paediatr. Int. Child Health* **38**, 50–65 (2018).
7. Levine, M. M., Kotloff, K. L., Barry, E. M., Pasetti, M. F. & Sztein, M. B. Clinical trials of Shigella vaccines: Two steps forward and one step back on a long, hard road. *Nat. Rev. Microbiol.* **5**, 540–553 (2007).
8. World Health Organization. *Global Priority List of Antibiotic-Resistant Bacteria to Guide Research, Discovery, and Development of New Antibiotics* 1–7 (WHO Press, 2017).
9. Clokie, M. R. J., Millard, A. D., Letarov, A. V. & Heaphy, S. Phages in nature. *Bacteriophage* **1**, 31–45 (2011).
10. Ofir, G. & Sorek, R. Contemporary phage biology: From classic models to new insights. *Cell* **172**, 1260–1270 (2018).
11. Shan, J. *et al.* Bacteriophages are more virulent to bacteria with human cells than they are in bacterial culture; Insights from HT-29 cells. *Sci. Rep.* **8** (2018).
12. Nagel, T. E. *et al.* The developing world urgently needs phages to combat pathogenic bacteria. *Front. Microbiol.* **7**, 1–4 (2016).
13. Twort, F. W. An investigation on the nature of ultra-microscopic viruses. *Lancet* **186**, 1241–1243. [https://doi.org/10.1016/s0140-6736\(01\)20383-3](https://doi.org/10.1016/s0140-6736(01)20383-3) (1915).
14. d’Herelle, F. Le bacteriophage. *La Nature* (1921).
15. d’Herelle, F. bacteriophages as a treatment in acute medical and surgical infections (1931).
16. Subramanian, S., Parent, K. N. & Doore, S. M. Ecology, structure, and evolution of *Shigella* phages. *Annu. Rev. Virol.* **7**(1), 121–141 (2020).
17. Kutter, E. *et al.* Phage therapy in clinical practice: Treatment of human infections. *Curr. Pharm. Biotechnol.* **11**, 1169–1186 (2010).
18. Kakasis, A. & Panitsa, G. Bacteriophage therapy as an alternative treatment for human infections. A comprehensive review. *Int. J. Antimicrob. Agents* **53**, 16–21 (2019).
19. Górski, A. *et al.* Phage therapy: Beyond antibacterial action. *Front. Med.* **5**, 1–8 (2010).
20. Gill, J. & Hyman, P. Phage choice, isolation, and preparation for phage therapy. *Curr. Pharm. Biotechnol.* **11**, 2–14 (2010).
21. Merabishvili, M. *et al.* Quality-controlled small-scale production of a well-defined bacteriophage cocktail for use in human clinical trials. *PLoS ONE* **4**, e4944 (2009).
22. Ackermann, H. W. 5500 phages examined in the electron microscope. *Arch. Virol.* **152**, 227–243 (2007).
23. Bertozzi Silva, J., Storms, Z. & Sauvageau, D. Host receptors for bacteriophage adsorption. *FEMS Microbiol. Lett.* **363**, 1–11 (2016).
24. Shahin, K. & Bouzari, M. Bacteriophage application for biocontrolling *Shigella flexneri* in contaminated foods. *J. Food Sci. Technol.* **55**, 550–559 (2018).
25. Shahin, K. *et al.* Biodiversity of new lytic bacteriophages infecting *Shigella* spp in freshwater environment. *Front. Microbiol.* **12**, 619323 (2021).
26. Albers, S. & Czech, A. Exploiting tRNAs to boost virulence. *Life (Basel)* **6**(1), 4 (2016).
27. Wittebole, X., Opal, S. & Witzany, G. Phagetherapy: Clinical applications – critical appraisal of randomized controlled trials. In: *Biocommunication of Phages*. 371–383 (Springer International Publishing, 2020).
28. World Medical Association Declaration of Helsinki. ethical principles for medical research involving human subjects. *World Med. Assoc. JAMA* **310**, 2191–2194 (2013).
29. Kotloff, K. L. *et al.* Global burden of Shigella infections: Implications for vaccine development and implementation of control strategies. *Bull. World Health Organ.* **77**, 651 (1999).
30. Ashkenazi, S., Levy, I., Kazaronovski, V. & Samra, Z. Growing antimicrobial resistance of *Shigella* isolates. *J. Antimicrob. Chemother.* **51**, 427–429 (2003).
31. Bratoeva, M. P., John, J. F. & Barg, N. L. Molecular epidemiology of trimethoprim-resistant *Shigella boydii* serotype 2 strains from Bulgaria. *J. Clin. Microbiol.* **30**, 1428–1431 (1992).
32. Ranjbar, R., Mammina, C., Pourshafie, M. R. & Soltan-Dallal, M. M. Characterization of endemic *Shigella boydii* strains isolated in Iran by serotyping, antimicrobial resistance, plasmid profile, ribotyping and pulsed-field gel electrophoresis. *BMC Res. Notes* **1**, 74 (2008).
33. Kania, D. A., Hazen, T. H., Hossain, A., Nataro, J. P. & Rasko, D. A. Genome diversity of *Shigella boydii*. *Pathog. Disease* **74**, ftw027 (2016).
34. Livio, S. *et al.* Shigella isolates from the global enteric multicenter study inform vaccine development. *Clin. Infect. Diseases Off. Publ. Infect. Diseases Soc. Am.* **59**, 933–941 (2014).
35. Pazhani, G. P., Ramamurthy, T., Mitra, U., Bhattacharya, S. K. & Niyogi, S. K. Species diversity and antimicrobial resistance of *Shigella* spp. isolated between 2001 and 2004 from hospitalized children with diarrhoea in Kolkata (Calcutta), India. *Epidemiol. Infect.* **133**, 1089–1095 (2005).
36. Akter, M. *et al.* Prevalence of *Shigella boydii* in Bangladesh: Isolation and characterization of a rare phage MK-13 that can robustly identify Shigellosis caused by *Shigella boydii* type 1. *Front. Microbiol.* **10** (2019).
37. Ly-Chatain, M. The factors affecting effectiveness of treatment in phages therapy. *Front. Microbiol.* **5**, 51 (2014).
38. Slopek, S. *et al.* Results of bacteriophage treatment of suppurative bacterial infections. I. General evaluation of results. *Arch. Immunol. Ther. Exp. (Warsz)* **31**, 267–291 (1983).
39. Malik, D. J. *et al.* Formulation, stabilisation, and encapsulation of bacteriophage for phage therapy. *Adv. Colloid Interface Sci.* **249**, 100–133 (2017).
40. Nobrega, F. L. *et al.* Genetically manipulated phages with improved pH resistance for oral administration in veterinary medicine (2016).
41. Marinelli, L., Hatfull, G. & Piuri, M. Recombineering: A powerful tool for modification of bacteriophage genomes. *Bacteriophage* **2**, 5–14 (2012).
42. Docking, R. E. Role of emerging technologies in geriatric pain management. *Clin. Geriatr. Med.* **32**(4), 787–795 (2016).
43. Bolger-Munro, M., Cheung, K., Fang, A. & Wang, L. T4 Bacteriophage average burst size varies with *Escherichia coli* B23 cell culture age. *J. Exp. Microbiol. Immunol.* **17**, 115–119 (2013).
44. Kellenberger, E. & Wunderli-Allenspach, H. Electron microscopic studies on intracellular phage development—history and perspectives. *Micron (Oxford, England)* **26**(3), 213–245 (1995).
45. Ferriol-González, C. & Domingo-Calap, P. Phages for biofilm removal. *Antibiotics (Basel, Switzerland)* **9**, 268 (2020).
46. Pires, D. P., Oliveira, H., Melo, L. D., Sillankorva, S. & Azeredo, J. Bacteriophage-encoded depolymerases: Their diversity and biotechnological applications. *Appl. Microbiol. Biotechnol.* **100**, 2141–2151 (2016).
47. Parasion, S., Kwiatek, M., Gryko, R., Mizak, L. & Malm, A. Bacteriophages as an alternative strategy for fighting biofilm development. *Pol. J. Microbiol.* **63**, 137–145 (2014).
48. Fischetti, V. A. Bacteriophage lysins as effective antibacterials. *Curr. Opin. Microbiol.* **11**, 393–400 (2008).
49. Rodríguez-Rubio, L., Martínez, B., Donovan, D. M., Rodríguez, A. & García, P. Bacteriophage virion-associated peptidoglycan hydrolases: potential new enzybiotics. *Crit. Rev. Microbiol.* **39**, 427–434 (2013).
50. Gutiérrez, D., Ruas-Madiedo, P., Martínez, B., Rodríguez, A. & García, P. Effective removal of staphylococcal biofilms by the endolysin LysH5. *PLoS ONE* **9**, e107307 (2014).

51. Bedi, M. S., Verma, V. & Chhibber, S. Amoxicillin and specific bacteriophage can be used together for eradication of biofilm of *Klebsiella pneumoniae* B5055. *World J Microbiol Biotechnol.* **25**, 1145–1151 (2009).
52. Harper, D. R. *et al.* Bacteriophages and biofilms. *Antibiotics* **3**, 270–284 (2014).
53. Chaudhry, W. N. *et al.* Synergy and order effects of antibiotics and phages in killing *Pseudomonas aeruginosa* biofilms. *PLoS ONE* **12**, e0168615 (2017).
54. Dutta, M. & Ghosh, A. N. Physicochemical Characterization of El Tor Vibriophage S20. *Intervirology* **50**, 264–272 (2007).
55. Kutter, E. Phage host range and efficiency of plating. *Methods Mol. Biol.* **501**, 141–149 (2009).
56. Yuan, Y. *et al.* Effects of actin-like proteins encoded by two *Bacillus pumilus* phages on unstable lysogeny revealed by genomic analysis. *Appl. Environ. Microbiol.* **81**, 339–350 (2015).
57. Majumdar, S., Dey, S. N., Chowdhury, R., Dutta, C. & Das, J. Intracellular development of cholera phage  $\Phi$ 149 under permissive and nonpermissive conditions: An electron microscopic study. *Intervirology* **29**, 27–38 (1988).
58. Nickerson, K. P. *et al.* Analysis of *Shigella flexneri* resistance, biofilm formation, and transcriptional profile in response to bile salts. *Infect. Immun.* **85**, e01067–e1116 (2017).
59. Yazdi, M., Bouzari, M. & Ghaemi, E. A. Isolation and characterization of a lytic bacteriophage (vB\_PmIS-TH) and its application in combination with ampicillin against planktonic and biofilm forms of *Proteus mirabilis* isolated from urinary tract infection. *J. Mol. Microbiol. Biotechnol.* **28**, 37–46 (2018).
60. Laemmli, U. K. Cleavage of Structural Proteins during the Assembly of the Head of Bacteriophage T4. *Nature* **227**, 680–685 (1970).
61. Stothard, P. & Wishart, D. S. Circular genome visualization and exploration using CGView. *Bioinformatics* **21**, 537–539 (2005).
62. Sullivan, M. J., Petty, N. K. & Beatson, S. A. Easyfig: A genome comparison visualizer. *Bioinformatics* **27**, 1009–1010 (2011).
63. Laslett, D. & Canback, B. ARAGORN, a program to detect tRNA genes and tmRNA genes in nucleotide sequences. *Nucl. Acids Res.* **32**, 11–16 (2004).
64. Schattner, P., Brooks, A. N. & Lowe, T. M. The tRNAscan-SE, snoscan and snoGPS web servers for the detection of tRNAs and snoRNAs. *Nucl. Acids Res.* **33**, 686–689 (2005).

## Acknowledgements

We gratefully acknowledge Dr. Shanta Dutta, Director, ICMR-NICED, for her advice and support throughout this work and for providing some bacterial strains. We would very much like to thank and acknowledge Dr. Hemanta Koley and Dr. Asish Mukhopadhyay, ICMR-NICED for providing some of the bacterial strains. We also thank Mrs Arpita Sarbajna for technical assistance in ultramicrotomy. We thankfully acknowledge Dr. Sayani Das for sharing her knowledge of phage isolation and purification. We would like to thank Dr. Sibnarayan Datta (DRDO) for guidance on genome sequence submission at NCBI. We would also extend our thanks to Dr. Amar Nath Ghosh for his valuable suggestions in this work. BM is financially supported by UGC-Junior Research Fellowship, Govt. of India. PM is financially supported by CSIR-Junior Research Fellowship, Govt. of India.

## Author contributions

B.M. and M.D. designed the concept of experimental work; B.M. performed the experiments on phage characterization, data analysis, and interpretation. P.M. and B.M. performed the genomic sequence data analysis, interpretation, and representation; B.M. and P.M. helped in manuscript writing; M.D. supervised the project as a principal investigator and prepared the manuscript. All authors reviewed and approved the final manuscript.

## Funding

This work was funded by ICMR (Indian Council of Medical Research)-NICED Institutional grant.

## Competing interests

The authors declare no competing interests.

## Additional information

**Supplementary Information** The online version contains supplementary material available at <https://doi.org/10.1038/s41598-021-98910-z>.

**Correspondence** and requests for materials should be addressed to M.D.

**Reprints and permissions information** is available at [www.nature.com/reprints](http://www.nature.com/reprints).

**Publisher's note** Springer Nature remains neutral with regard to jurisdictional claims in published maps and institutional affiliations.



**Open Access** This article is licensed under a Creative Commons Attribution 4.0 International License, which permits use, sharing, adaptation, distribution and reproduction in any medium or format, as long as you give appropriate credit to the original author(s) and the source, provide a link to the Creative Commons licence, and indicate if changes were made. The images or other third party material in this article are included in the article's Creative Commons licence, unless indicated otherwise in a credit line to the material. If material is not included in the article's Creative Commons licence and your intended use is not permitted by statutory regulation or exceeds the permitted use, you will need to obtain permission directly from the copyright holder. To view a copy of this licence, visit <http://creativecommons.org/licenses/by/4.0/>.

© The Author(s) 2021



## OPEN ACCESS

## EDITED BY

Alicja Wegrzyn,  
Institute of Biochemistry and Biophysics  
(PAN), Poland

## REVIEWED BY

Ahmed Askora,  
Zagazig University,  
Egypt  
Josefina León-Félix,  
Centro de Investigación en Alimentación y  
Desarrollo (CIAD), Mexico

## \*CORRESPONDENCE

Moumita Dutta  
moumita.dutta@icmr.gov.in;  
mdutta16@gmail.com

## SPECIALTY SECTION

This article was submitted to  
Phage Biology,  
a section of the journal  
Frontiers in Microbiology

RECEIVED 28 June 2022

ACCEPTED 25 July 2022

PUBLISHED 22 August 2022

## CITATION

Mondal P, Mallick B, Dutta M and  
Dutta S (2022) Isolation, characterization,  
and application of a novel polyvalent lytic  
phage STWB21 against typhoidal and  
nontyphoidal *Salmonella* spp.  
*Front. Microbiol.* 13:980025.  
doi: 10.3389/fmicb.2022.980025

## COPYRIGHT

© 2022 Mondal, Mallick, Dutta and Dutta.  
This is an open-access article distributed  
under the terms of the [Creative Commons  
Attribution License \(CC BY\)](#). The use,  
distribution or reproduction in other  
forums is permitted, provided the original  
author(s) and the copyright owner(s) are  
credited and that the original publication in  
this journal is cited, in accordance with  
accepted academic practice. No use,  
distribution or reproduction is permitted  
which does not comply with these terms.

# Isolation, characterization, and application of a novel polyvalent lytic phage STWB21 against typhoidal and nontyphoidal *Salmonella* spp.

Payel Mondal<sup>1</sup>, Bani Mallick<sup>1</sup>, Moumita Dutta<sup>1\*</sup> and  
Shanta Dutta<sup>2</sup>

<sup>1</sup>Division of Electron Microscopy, ICMR-National Institute of Cholera and Enteric Diseases, Kolkata, West Bengal, India, <sup>2</sup>Division of Bacteriology, ICMR-National Institute of Cholera and Enteric Diseases, Kolkata, West Bengal, India

*Salmonella* is one of the common causal agents of bacterial gastroenteritis-related morbidity and mortality among children below 5 years and the elderly populations. Salmonellosis in humans is caused mainly by consuming contaminated food originating from animals. The genus *Salmonella* has several serovars, and many of them are recently reported to be resistant to multiple drugs. Therefore, isolation of lytic *Salmonella* bacteriophages in search of bactericidal activity has received importance. In this study, a *Salmonella* phage STWB21 was isolated from a lake water sample and found to be a novel lytic phage with promising potential against the host bacteria *Salmonella typhi*. However, some polyvalence was observed in their broad host range. In addition to *S. typhi*, the phage STWB21 was able to infect *S. paratyphi*, *S. typhimurium*, *S. enteritidis*, and a few other bacterial species such as *Sh. flexneri* 2a, *Sh. flexneri* 3a, and *ETEC*. The newly isolated phage STWB21 belongs to the *Siphoviridae* family with an icosahedral head and a long flexible non-contractile tail. Phage STWB21 is relatively stable under a wide range of pH (4–11) and temperatures (4°C–50°C) for different *Salmonella* serovars. The latent period and burst size of phage STWB21 against *S. typhi* were 25 min and 161 plaque-forming units per cell. Since *Salmonella* is a foodborne pathogen, the phage STWB21 was applied to treat a 24 h biofilm formed in onion and milk under laboratory conditions. A significant reduction was observed in the bacterial population of *S. typhi* biofilm in both cases. Phage STWB21 contained a dsDNA of 112,834 bp in length, and the GC content was 40.37%. Also, genomic analysis confirmed the presence of lytic genes and the absence of any lysogeny or toxin genes. Overall, the present study reveals phage STWB21 has a promising ability to be used as a biocontrol agent of *Salmonella* spp. and proposes its application in food industries.

## KEYWORDS

*Salmonella*, lytic, bacteriophage, biofilm, onion